TECHNISCHE UNIVERSITÄT MÜNCHEN
TUM School of Life Sciences

Characterising prevailing hydrogenotrophic denitrifiers performing *in situ* nitrate remediation

Clara Maria Duffner

Vollständiger Abdruck der von der TUM School of Life Sciences der Technischen Universität München zur Erlangung des akademischen Grades einer

Doktorin der Naturwissenschaften (Dr. rer. nat.)

genehmigten Dissertation.

Vorsitzender:	Prof. Dr. Wolfgang Liebl
Prüfer der Dissertation:	1. Hon. Prof. Dr. Michael Schloter
	2. Prof. Dr. Florian Einsiedl
	3. Prof. Dr. Lars Bakken

Die Dissertation wurde am 11.04.2022 bei der Technischen Universität München eingereicht und durch die TUM School of Life Sciences am 16.09.2022 angenommen.

Foreword of the Author

Many important processes depend on a multitude of microbes, we would be foolish not to study the abundance of skills they posses. For our health, our planets health and for the sheer excitement of discovering something new. Through this research I had the pleasure of studying the unknown and I hope the findings will be helpful to some readers and maybe also to the groundwater.

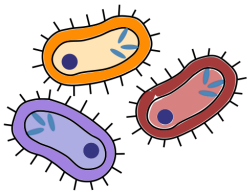

This work was funded by the Deutsche Forschungsgemeinschaft (DFG) through the International Graduate School of Science and Engineering (IGSSE), part of the Technical University Munich. Together with the Chair of Hydrogeology, we are grateful that we were given the opportunity to work on this interdisciplinary project 'Healthy Water'.
My special thanks goes to **Prof. Dr. Michael Schloter** for proposing this project together with **Prof. Dr. Florian Einsiedl** and for his scientific guidance. Equally important for the success of this thesis was the supervision by **Dr. Stefanie Schulz**, who gave me valuable support, critical feedback and trust in my ideas. Further, I would like to thank all members of the Research Unit Comparative Microbiome Analyses where I learned and laughed a lot. A special thanks goes to **Dr. Bärbel Fösel** for her support on the isolation and cultivation of autotrophic denitrifiers, **Susanne Kublik** for her expertise in sequencing as well as **Dr. Silvia Geschwendtner** for her advice on the sequencing data analyses. For moral support and much needed chats after long lab days I would like to thank my wonderful office pals: **Akane Chiba**, **Yvonne Bigott**, **Dr. Antonis Michas** and **Lisa Streb**.
I appreciate the collaboration with the Chair of Hydrogeology. The ideas of **Prof. Florian Einsiedl**, the structuring meetings with **Dr. Anja Wunderlich** and the team work on the microcosm experiment with **Sebastian Holzapfel**.
Very importantly, I would like to thank **Prof. Lars Bakken** and **Prof. Åsa Frostegård** for the opportunity to determine the denitrification phenotypes of my isolates in their laboratory at the Norwegian University of Life Sciences. I highly appreciate their expertise on denitrifier metabolism and the valuable discussions. I was warmly welcomed in their research group and received a lot of help from **Elisabeth Gautefall Hiis**, **Lars Molstad**, **Kjell Rune Jonassen**, **Ricarda Kellermann**, **Rannei Tjåland**, **Elsa Aasen**, **Linda Bergaust**, **Dr. Silas Vick**, **Yuan Gao** and **Marte Mølsæter Maråk**.

Finally, I would like to thank my wonderful parents for their continuous encouragement, my husband for being the best IT support and companion during home-office times, and my son for being pure joy during the finalisation of this thesis.

Contents

Summary

Groundwater is feeding rivers, lakes, and oceans and is thus an important part of the water cycle. It also serves as a source of drinking water for many municipalities. Pollution with nitrate; however, continuously increases due to human activities. It stems from excessive fertilizer application, manure deposited on fields, decomposing plant residues, and human waste leaking from the sewage system. Groundwater nitrate pollution endangers the stability of water ecosystems, the safety of our drinking water, and the climate. In anoxic aquifers with sufficient electron donors, nitrate reduction occurs naturally though microbial denitrification. Denitrification includes four reduction steps from nitrate via nitrite, nitric oxide and nitrous oxide to harmless N_2 gas. Other aquifers; however, contain low concentrations of electron donors in combination with the presence of oxygen, which makes denitrification inefficient. In such aquifers local nitrate remediation may be achieved by stimulating litho-autotrophic denitrifiers through the addition of the electron donor hydrogen. Yet, research investigating this strategy has encountered the problems of incomplete denitrification and the transient accumulation of the cytotoxic intermediate nitrite as well as the greenhouse gas nitrous oxide. We hypothesised that the hydrogenotrophic denitrifier community only comprises few taxa, which differ in their denitrification phenotypes. In such small communities the individual phenotypes and their proportion of the total community would largely impact the overall metabolism. This thesis therefore aims at defining the prevailing hydrogenotrophic denitrifying taxa in a nitrate polluted oxic model aquifer and investigates the individual contribution of these taxa to incomplete denitrification and the accumulation of intermediates. Furthermore, we hypothesised a link between genetic features and the denitrification phenotypes. Thus, besides characterising the phenotypes the genomes were also analysed.

Several microcosm and column experiments with groundwater sediment were performed, analysing the bacterial community composition by 16S rRNA gene amplicon sequencing after stimulation with hydrogen. Additionally, bacterial taxa belonging to the prevailing genera detected in the community analyses were isolated, their genomes were sequenced, and their denitrification phenotypes were characterised. The prevailing genus in the hydrogen treated microcosms was *Dechloromonas*, while *Hydrogenophaga* was most abundant in the column experiment. Species of both genera, *D. denitrificans* and *H. taeniospiralis*, as well as *Ferribacterium limneticum*, were isolated and proven to completely reduce nitrate to N_2 when stimulated with hydrogen under autotrophic conditions. Differences in the overall intermediate accumulation among communities therefore likely stem from the timing of reduction steps in individual taxa rather than from different proportions of truncated denitrifiers. Through detailed denitrification kinetics analyses we could show that the three complete hydrogenotrophic denitrifiers differed in their denitrification phenotypes. The largest difference among the three species was the transient nitrite accumulation, which was significantly larger in *H. taeniospiralis*, as it accumulated nitrite until all nitrate had been reduced, compared to the two *Rhodocyclaceae* isolates, which performed all steps simultaneously. Three possible genetic-based links to these denitrification phenotypes have been identified: First, the type of nitrate reductase gene, because *H. taeniospiralis* harboured *narG* and the other two *napA*.

Second, the genomes of *D. denitrificans* and *F. limneticum* harboured the *regAB* genes coding for a redox-sensing global regulator and *F. limneticum* harboured extra hydrogenase genes. Both *regAB* and the extra hydrogenase genes are likely involved in further reducing intermediate accumulation.

The obtained findings highlight the importance of determining the hydrogenotrophic denitrifier community in an aquifer in order to decide whether it can be remediated with hydrogen. Further, parameters specifically stimulating the *napA*-containing taxa with the least intermediate accumulation must be investigated to enable targeted stimulation.

Zusammenfassung

Grundwasser speist Flüsse, Seen und Ozeane und ist somit ein wichtiger Teil des Wasserkreislaufs. Gleichzeitig dient es als eine wichtige Trinkwasserquelle für zahlreiche Gemeinden. Grundwasserverschmutzung mit Nitrat steigt jedoch kontinuierlich an. Nitrat gelangt durch das Ausbringen von Düngemitteln und Gülle sowie kompostierenden Pflanzenresten aufs Feld und sickert in die Grundwasserleiter. Die Verschmutzung des Grundwassers durch Nitrat gefährdet sowohl die Stabilität der Wasserökosysteme, die Sicherheit von Trinkwasser als auch das Klima. In anoxischen Grundwasserleitern mit ausreichend Elektronen-Donatoren kommt Nitratreduktion durch mikrobielle Denitrifikation natürlicherweise vor. Die Denitrifikation besteht aus vier Reduktionsschritten von Nitrat über Nitrit, Stickoxid und Distickstoffoxid zu ungefährlichem N_2 Gas. Andere Grundwasserleiter sind jedoch oxisch und enthalten kaum Elektronen-Donatoren, wodurch Denitrifikation wenig effizient ist. Lokale Nitrat-Sanierung in solchen Grundwasserleitern könnte durch die Stimulation litho-autotropher Denitrifizierern mit Wasserstoff gelingen. Bei Untersuchungen dieser Sanierungsstrategie verlief die Denitrifikation jedoch häufig unvollständig oder es trat eine vorübergehende Akkumulation des zytotoxisch wirkenden Nitrits und/oder des Treibhausgases N_2O auf. Wir stellten die Hypothesen auf, dass die Gemeinschaft der hydrogenotropher Denitrifizierer nur aus wenigen Taxa besteht, die sich zudem in ihren Denitrifikationsphänotypen unterscheiden. In solchen kleinen Gemeinschaften haben die individuellen Phänotypen und deren Anteil an der Gesamtgemeinschaft einen großen Einfluss auf den Gesamtmetabolismus. Diese Doktorarbeit hat somit das Ziel die vorherrschenden hydrogenotrophen Denitrifizierer in einem mit Nitrat verschmutzten, oxischen Modellgrundwasserleiter zu bestimmen. Zudem wurde der individuelle Beitrag zu unvollständiger Denitrifikation und der Akkumulation von Zwischenprodukten dieser Bakterienarten untersucht. Außerdem nahmen wir einen Zusammenhang zwischen genetischen Eigenschaften und dem Denitrifikationsphänotypen an. Deshalb wurden neben der Charakterisierung der Phänotypen auch die Genome der Bakterienisolate analysiert.

Es wurden mehrere Mikrokosmos- und Säulenexperimente mit Grundwassersediment durchgeführt, bei denen die bakterielle Gemeinschaft nach Stimulation mit Wasserstoff mittels 16S rRNA Amplikon-Sequenzierung untersucht wurde. Bakterientaxa, die zu den vorherrschenden Gattungen der analysierten Gemeinschaften gehören, wurden isoliert, ihre Genome sequenziert und die Denitrifikationsphänotypen bestimmt. Die vorherrschende Gattung in den mit Wasserstoff behandelten Mikrokosmen war *Dechloromonas*, wohingegen *Hydrogenophaga* die höchste Abundanz im Säulenexperiment aufwies. Die Arten *D. denitrificans* und *H. taeniospiralis* dieser beiden Gattungen, sowie *Ferribacterium limneticum*, wurden isoliert und es konnte gezeigt werden, dass alle Nitrat vollständig zu N_2 reduzieren wenn sie unter autotrophen Bedingungen mit Wasserstoff stimuliert wurden.

Die Akkumulation von Zwischenprodukten liegt demnach eher an unterschiedlichen Abläufen der Reduktionsschritte in den dominierenden Bakterientaxa, als an unvollständiger Denitrifikation. Detailierte Analysen der Denitrifikationskinetiken zeigten, dass sich die drei Arten in ihren Denitri-

fikationsphänotypen stark unterscheiden. Der größte Unterschied zeigte sich bei der Akkumulation von Nitrit, die bei *H. taeniospiralis* signifikant höher war als bei den beiden Isolaten der Gattung *Rhodocyclaceae*. *H. taeniospiralis* akkumulierte Nitrit bis alles Nitrat verbraucht war, wohingegen die anderen Isolate alle Denitrifikationsschritte gleichzeitig durchführten. Es wurden drei mögliche Zusammenhänge der Phänotypen mit genetischen Eigenschaften identifiziert. Zum einen besteht ein Zusammenhang mit dem Gen der Nitratreduktase, da das *H. taeniospiralis* Genom *narG* aber die *Rhodocyclaceae* Genome *napA* aufwiesen. Desweiteren enthielten die Genome von *D. denitrificans* und *F. limneticum* die regAB Gene, die für einen globalen Regulator kodieren, der Änderungen des Redoxpotentials registriert und das *F. limneticum* Genom enthielt zusätzliche Hydrogenasegene. Sowohl bei regAB, als auch den zusätzlichen Hydrogenasegenen besteht ein möglicher Zusammenhang mit der weiteren Verringerung der Zwischenproduktakkumulation.

Die Ergebnisse zeigen auf, wie wichtig es ist die hydrogenotrophe Denitrifizierergemeinschaft im Grundwasserleiter zu untersuchen bevor eine Sanierung mit Wasserstoff durchgeführt wird. Außerdem ist es wichtig, dass Bedingungen identifiziert werden unter denen spezifisch *napA*-Denitrifizierer mit der niedrigsten Akkumulation von Zwischenprodukten stimuliert werden.

List of Abbreviations

16S rRNA gene gene coding for a RNA of the small ribosomal subunit of prokaryotes
anammox anaerobic ammonium oxidation
ASV amplicon sequence variant
atm atmospheric pressure
bp base pairs
BSA bovine serum albumine
°C degree Celsius
CBB Calvin-Benson-Basham cycle
CDD Conserved Domain Database
cDNA complementary deoxyribonucleic acid
cnorB Bc-heme containing nitric oxide reductase gene
cNorB Bc-heme containing nitric oxide reductase enzyme
dDDH digital DNA-DNA hybridisation
DEPC-MiliQ diethyl pyrocarbonate treated ultrapure water
DNA deoxyribonucleic acid
DNRA dissimilatory nitrate reduction to ammonium
dNTP deoxyribonucleotide triphosphate
DOC dissolved organic carbon
DRP Denitrification Regulatory Phenotype
EI first enrichment and isolation process
EII second enrichment and isolation process
ENS effective number of species
fixLJ O_2 sensing two-component system genes
FixLJ O_2 sensing two-component system
GC content guanine-cytosine content
gDNA genomic deoxyribonucleic acid
GW groundwater
HD hydrogenotrophic denitrifier
He helium
HMM Hidden Markov Model
kb kilobases
MB megabases
MM mineral medium
n number of replicates
napA periplasmic nitrate reductase gene
NapA periplasmic nitrate reductase enzyme
narG cytoplasmic nitrate reductase gene
NarG cytoplasmic nitrate reductase enzyme
narXL NO_3^- sensing two component system genes
NarXL NO_3^- sensing two component system

nirK Cu nitrite reductase gene

NirK Cunitrite reductase enzyme

nirS Cd_1 nitrite reductase gene

NirS Cd_1 nitrite reductase enzyme

nosZ nitrous oxide reductase gene

NosZ nitrous oxide reductase enzyme

OTU operational taxonomic unit

PO 'progressive onset' denitrification phenotype

ppmv parts per million volume

qnorB b-heme containing nitric oxide reductase gene

qNorB b-heme containing nitric oxide reductase enzyme

qPCR quantitative polymerase chain reaction

R2A Reasoner's 2A medium

RCO 'rapid complete onset' denitrification phenotype

regAB redox sensing two-component signal transduction system genes

RegAB redox sensing two-component signal transduction system

RNA ribonucleic acid

rpm revolutions per minute

rRNA ribosomal ribonucleic acid

RT-qPCR reverse transcription quantitative polymerase chain reaction

RubisCO ribulose-1,5-bisphosphate carboxylase-oxygenase

RQN RNA quality number

SED sediment

SRA Sequence Read Archive

SMRT single molecule real time

TSB Tryptic Soy Broth medium

U enzymatic unit

UC untreated control

v/v volume per volume

w/v weight per volume

x g times gravity

List of Publications included in this Thesis

Publication I (PI) - Research Article
C. Duffner, S. Holzapfel, A. Wunderlich, F. Einsiedl, M. Schloter and S. Schulz. "*Dechloromonas* and close relatives prevail during hydrogenotrophic denitrification in stimulated microcosms with oxic aquifer material". In: FEMS Microbiology Ecology 97 (3) (2021).
DOI: https://doi.org/10.1093/femsec/fiab004.

Publication II (PII) - Research Article
C. Duffner, S. Kublik, B. Fösel, Å. Frostegård, M. Schloter, L. Bakken and S. Schulz. "Genotypic and phenotypic characterization of hydrogenotrophic denitrifiers". In: Environmental Microbiology (online version) (2022). DOI: https://doi.org/10.1111/1462-2920.15921.

Publication III (PIII) - Perspective Article
C. Duffner, A. Wunderlich, M. Schloter, S. Schulz and F. Einsiedl. "Strategies to Overcome Intermediate Accumulation During *in situ* Nitrate Remediation in Groundwater by Hydrogenotrophic Denitrification". In: Frontiers in Microbiology 12 (2021).
DOI: https://doi.org/10.3389/fmicb.2021.610437.

Further publications mentioned in this thesis:

- E. Harris, E. Diaz-Pines, E. Stoll, M. Schloter, S. Schulz, **C. Duffner**, K. Li, K. L. Moore, J. Ingrisch, D. Reinthaler, S. Zechmeister-Boltenstern, S. Glatzel, N. Brüggemann and M. Bahn. "Denitrifying pathways dominate nitrous oxide emissions from managed grassland during drought and rewetting". In: Science Advances 7 (6) (2021).
  DOI: https://doi.org/10.1126/sciadv.abb7118.
- K. R. Jonassen, I. Ormåsen, **C. Duffner**, T. R. Hvidsten, Å. Frostegård, L. R. Bakken and S. H. W. Vick. "A novel dual enrichment strategy provides soil and digestate competent N2O-reducing bacteria for mitigating climate forcing in agriculture". In: bioRxiv (preprint) (2021).
  DOI: https://doi.org/10.1101/2021.05.11.443593.
- **C. Duffner**, S. Kublik, B. Fösel, M. Schloter, S. Schulz and J. A. Maresca. "Complete Genome Sequences of Hydrogenotrophic Denitrifiers". In: Microbiology Resource Announcements 11 (1) (2022). DOI: https://doi.org/10.1128/mra.01020-21.
- A. Peña Sanchez, **C. Duffner**, A. Wunderlich, B. Mayer, S. Schulz, M. Schloter and F. Einsiedl. "Seasonal dynamics of anaerobic oxidation of ammonium and denitrification in a dimictic lake during the stratified spring–summer period". In: Limnology and Oceanography (online version) (2022). DOI: https://doi.org/10.1002/lno.12067.

Publication I

Dechloromonas and close relatives prevail during hydrogenotrophic denitrification in stimulated microcosms with oxic aquifer material

Clara Duffner, Sebastian Holzapfel, Anja Wunderlich, Florian Einsiedl, Michael Schloter and Stefanie Schulz

Brief description:

Most hydrogenotrophic denitrifier communities have been analysed in H_2-based reactor experiments. The aim of this study was therefore to determine denitrifiers stimulated by H_2 addition that occur in nitrate polluted aquifers. We performed a microcosm experiment with groundwater and sediment from a porous nitrate polluted, oxic model aquifer located in the Hohenthann region north of Munich, Germany. The atmosphere of the sealed vials containing the collected sediment and groundwater was thus exchanged with 100% H_2 gas and the vials were incubated at 16°C. Every 10 hours four vials were sacrificed to determine the NO_3^-, NO_2^-, and ammonium concentrations as well as the bacterial community composition and the quantity of the denitrification reductase genes and transcripts.

Concurrent with the decreasing NO_3^- concentration, the relative abundance of the genus *Dechloromonas* increased significantly from less than 1% to approximately 24% after 80 h. Interestingly, out of 37 detected amplicon sequence variants (ASVs) assigned to *Dechloromonas*, only six ASVs increased significantly over the period of NO_3^- and NO_2^- reduction. Besides the prevalence of *Dechloromonas*, the results indicate species- or even strain-level differences in their hydrogenotorphic denitrifying abilities. Of the analysed denitrification reductase genes *napA*, *nirS* and clade I *nosZ* increased significantly over the observed period.

Contributions:

- Contributed to the experimental planning and design
- Performed the microcosm experiment together with Sebastian Holzapfel
- Performed sample preparation and 16S rRNA gene amplicon sequencing
- Performed RNA extraction, reverse transcription and qPCRs
- Performed data analysis and visualisation
- Wrote the manuscript

Publication II

Genotypic and phenotypic characterization of hydrogenotrophic denitrifiers

Clara Duffner, Susanne Kublik, Bärbel Fösel, Åsa Frostegård, Michael Schloter, Lars Bakken and Stefanie Schulz

Brief description:

The microcosm experiment (PI) indicated that the community of hydrogenotrophic denitrifiers comprises only few species. Based on these results we aimed at isolating the prevailing hydrogenotrophic denitrifier species from the same aquifer material and characterising their genotype and phenotype through whole genome sequencing as well as kinetics analyses of the denitrification regulatory phenotypes. Two enrichment and isolation attempts were performed with different outcomes. While the first isolation mainly led to taxa belonging to the familiy *Burkholderiaceae* such as *Hydrogenophaga*, the second isolation mainly resulted in taxa belonging to the family *Rhodocyclaceae*, such as *Dechloromonas*, *Ferribacterium* and *Quatrionicoccus*.

Eleven isolates of the mentioned genera were analysed. Eight thereof were able to perform complete hydrogenotrophic denitrification from NO_3^- to N_2. The genomes of these complete denitrifiers harboured at least one denitrification reductase gene for each of the four reduction steps, a RubisCO form II gene and at least three [NiFe]-hydrogenase genes. The three closely related non-hydrogenotrophic denitrifiers, which served as a control group, were either lacking a nitrite reductase gene (*Quatrionicoccus*) or a RubisCO gene (closest relative was *Dechloromonas*).

The denitrification regulatory phenotypes were determined by pure culture kinetics analyses in NO_3^- containing mineral medium under a H_2/CO_2 atmosphere. The incubations were placed inside a robotised incubation system and O_2, NO, N_2O, N_2, and NO_2^- were measured regularly. The biggest difference in the denitrification phenotypes was visible between the *Rhodocyclaceae* isolates *D. denitrificans* as well as *F. limneticum* and the *Burkholderiaceae* isolate *H. taeniospiralis*, who also differed in the type of nitrate and nitrous oxide reductase gene. While the *narG* and clade I *nosZ* harbouring *H. taeniospiralis* isolate accumulated all given NO_3^- as NO_2^- until all NO_3^- was gone, the *napA* and clade II *nosZ* harbouring *D. denitrificans* and *F. limneticum* isolates only accumulated small amounts or no NO_2^- at all.

Contributions:

- Experimental planning and design together with the other authors
- Performed isolation, Sanger sequencing and gDNA extraction for genome sequencing
- Performed endpoint and kinetics analyses to determine the denitrification phenotypes
- Performed data analysis and visualisation
- Wrote the manuscript

Publication III

Strategies to Overcome Intermediate Accumulation During *in situ* Nitrate Remediation in Groundwater by Hydrogenotrophic Denitrification

Clara Duffner, Anja Wunderlich, Michael Schloter, Stefanie Schulz and Florian Einsiedl

Brief description:

The perspective article reflects upon different approaches to minimize intermediate accumulation during hydrogenotrophic denitrification. These include the optimal H_2 delivery to reach sufficiently high H_2 concentrations, the role of community composition of hydrogenotrophic denitrifiers with regards to different denitrification phenotypes, and the potential of additionally implementing abiotic nitrate reduction through the addition of iron compounds. Due to the multiple factors contributing to intermediate accumulation and incomplete denitrification, we concluded that different approaches must be combined. Additionally, it is important that the nitrate polluted aquifers are investigated initially on their suitability for H_2-based *in situ* nitrate remediation. Parameters therefore include sufficient inorganic carbon, relatively low oxygen concentrations and a community of hydrogenotrophic denitrifiers that favours least intermediate accumulation.

Contributions:

- Conceptual planning together with Michael Schloter
- Performed literature research
- Wrote the manuscript

1. Introduction

1.1. Groundwater as a microbial habitat

Groundwater represents a very different habitat compared to soil. Whilst conditions in soil are quite heterogeneous, groundwater ecosystems are rather homogenous as they are are dark, poor in nutrients and carbon sources, and exhibit stable temperatures of around 10°C [1]. Due to these extreme conditions bacterial activity is substantially lower. Consequently bacterial doubling times can last from several to thousands of days [1]. In shallow aquifers annual recharge processes add oxygen (O_2) and agricultural amendments, such as nitrate (NO_3^-), into the groundwater ecosystem. Conversely deeper and older groundwater are more isolated ecosystems that rely on Fe(II)/Fe(III) and SO_4^{2-}/H_2S redox cycling [2]. Even though bacteria are the dominating microorganisms, groundwater ecosystems are also inhabited by archaea, protozoa and some fungi [3]. Each cm³ of groundwater contains between 10^2 and 10^6 bacterial cells and the same volume of aquifer sediment contains between 10^4 and 10^8 [1]. In soils the number of bacteria per gramm dry soil rather ranges between 10^8 and 10^{10} [4]. Recent cultivation-independent metagenomics analyses of aquifer sediment and groundwater, performed by Anantharaman et al. 2016 [5], discovered a total of 47 new bacterial phylum level lineages. These findings imply that the subsurface still holds a widely unknown microbial diversity.

Ecosystem properties, such as pore size, availability of nutrients and electron donors/acceptors, as well as the attachment surface areas, determine microbial community composition, abundance, and activity [3]. For example, in a study on hard-rock aquifers by Ben Maamar et al. 2015 [6] shallow groundwater with high NO_3^- concentrations (47-53 mg L^{-1}) was dominated by β-*Proteobacteria* (26-57%) [*Burkholderiaceae* (19-53%), and *Rhodocyclaceaea* (1-4%)], whereas deep groundwater, containing much less NO_3^-, was dominated by *Gallonellaceae* (25-44%). Interestingly, the community composition also differs between sediment attached and suspended bacteria [7]. Iron- and sulfate reducers are more often attached to the sediment, whereas α-, β- and, γ-*Proteobacteria* occur more frequently suspended in the groundwater.

1.2. Nitrate pollution in groundwater

The main component of the earths atmosphere, making up approximately 78.1%, is nitrogen (N) in the form of di-nitrogen (N_2). Nevertheless, the earths N-cycle has been largely impacted by a surplus of nitrogen input through industrial and intentional biological N-fixation. While a limit of 62 Tg N input per year has been determined as a safe operating space by Vries et al. 2013 [8], approx. 150 Tg N are actually still added each year [9]. This surplus of nitrogen eventually leads to climatic changes by increased emissions of the greenhouse gas nitrous oxide (N_2O), acidification of soil, the destruction of ecosystems through eutrophication, and poses direct and indirect risks to

human health [10, 11]. The major contributions of N originate from a few regions with intensive agriculture in North America, Europe, and Asia with high N application rates [9].

Fertilizer application has increased drastically since the invention of the Haber-Bosch process in 1910, which enabled the conversion of atmospheric N_2 to ammonia, and has been used increasingly year after year [10, 11]. It it therefore nowadays the largest source of nitrogen compounds to the global N-cycle [11]. Further, manure containing ammonia and organic nitrogen, is applied to fields in excess in areas with extended livestock production (Figure 1). In soils, ammonia is frequently converted to nitrate (NO_3^-) through nitrification [12]. Due to its high solubility, NO_3^- leaches from the soil to the groundwater whereby it is lost to the crops and pollutes the groundwater.

Between 2019 and 2021 alone 827 publications were assessing and investigating groundwater nitrate pollution in many regions across the globe (Web of Science, Search term: "nitrate contamination","groundwater", 3rd of August 2021). The majority of studies detected nitrate concentrations exceeding the World Health Organization (WHO) threshold for drinking water of 50 mg L^{-1} in a large fraction of analysed wells and boreholes [13, 14, 15, 16]. In these studies isotopic signature approaches detected manure and sewage as the main source of groundwater nitrate pollution. It is also an urgent problem in Germany, as 28% of analysed wells below agricultural land had nitrate concentrations above the WHO threshold [17]. Because of these high levels of NO_3^-, Germany was found guilty of having insufficient measures to combat NO_3^- pollution in groundwater in June 2018 by the European Court of Justice. This could result in the European Union imposing fines on Germany for breaching EU law.

Nitrogen leaching into groundwater can be reduced by applying fertilizer or manure only at times of lower risk, for example when plant-uptake is high and rainfall scarce, and by adapting the fertilizer application to the plant‘s demand [18]. A comparison by Dobermann 2005 [19] of more than 800 experiments showed that the nitrogen fertilizer use efficiency, meaning the proportion of recovered fertilizer-N in the above-ground biomass, was on average only 51%. Other protective agricultural practices have been analysed, such as replacing crops of a high nitrogen demand with low NO_3^- leaching crops, improving nutrient management, and using stored flood water to recharge the groundwater on suitable fields during the winter [20]. These measures have the potential to lower the NO_3^- levels by 80% within the next 40 years compared to business as usual scenarios [20].

1.2.1. Consequences of elevated nitrate input

Through the water cycle groundwater eventually flows to other aquatic ecosystems, such as rivers, lakes, and oceans. As a component of all amino acids, nitrogen is one of the main essential nutrients. An increase in nitrogen thus leads to enhanced primary production that is associated with eutrophication. Elevated NO_3^- levels in oligotrophic aquatic ecosystems therefore cause some species to thrive while others, adapted to low nutrient conditions, are suppressed and disappear

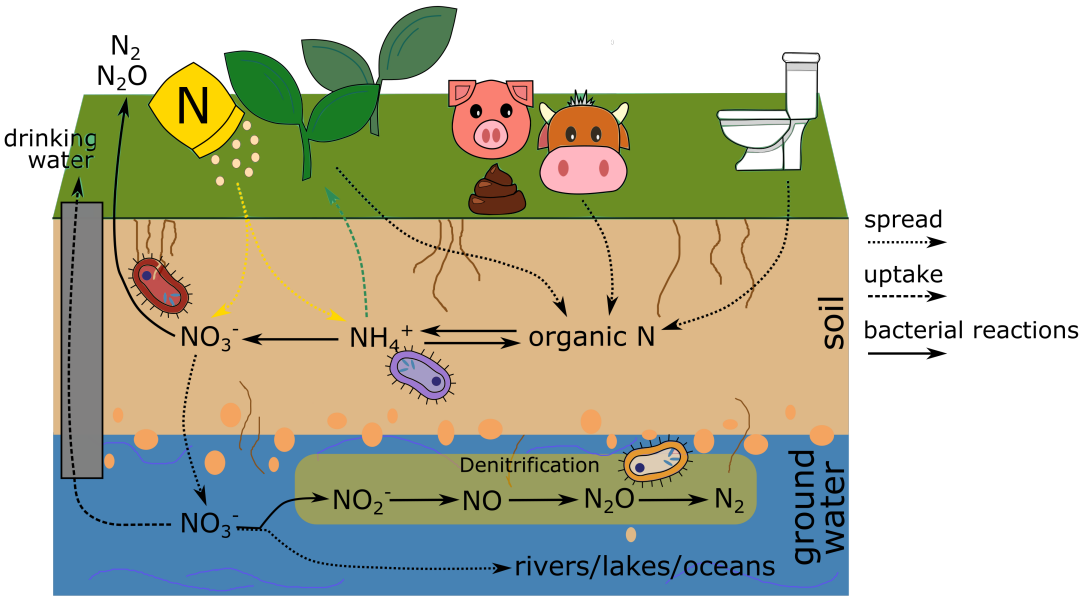

Figure 1 Causes of nitrate pollution in groundwater, which may spread to rivers lakes and oceans but is also naturally attenuated through denitrification if the conditions are right (based on graphic by [21]).

[22, 23]. The resulting algal blooms are depleting O_2 and consequently cause "dead-zones" for aquatic life [10, 11]. Additionally, NO_3^- is converted by bacteria to nitrite (NO_2^-) and N_2O, which may accumulate [24]. Elevated NO_2^- concentrations are toxic to fish and crayfish [25]. NO_2^- is blocking O_2-carriers leading to hypoxia. It is also causing an electrolyte imbalance, impairing neurotransmission, repressing the immune system and forming carcinogenic compounds. Emission of N_2O are mainly a threat to the climate as N_2O promotes the building of ground-level ozone, acts as a potent greenhouse gas and leads to acid rain [24]. In soil, N_2O emissions mainly stem from denitrifying activity during re-wetting events [26].

Besides the harm to aquatic ecosystems and the climate, elevated NO_3^- concentrations in groundwater also impact its use as drinking water. Above a concentration of 50 mg L^{-1} the European Union and the WHO consider water unsafe for drinking [24]. In the human gastrointestinal tract bacteria also convert NO_3^- to NO_2^-. The later binds to heamoglobin instead of O_2 and thus causes methemoglobinemia, a condition where the O_2-binding capacity of hemoglobin is impaired [27]. This binding is irreversible in infants below 6 months, wherefore elevated NO_3^- levels above 50 mg L^{-1} can be fatal for them [28]. Further, increased risks of cancer development and reproductive problems due to the consumption of NO_3^--enriched water have been reported [11]. A population wide health register data analysis by Schullehner et al. 2018 [29] showed a significantly increased risk of colorectal cancer development in people living in areas with drinking water NO_3^- concentrations above 3.87 mg L^{-1}. Such studies indicate that even the current drinking water standard is far too high to prevent negative long term health effects on the public. To deliver drinking water with NO_3^- concentrations below the maximum allowable threshold of 50 mg L^{-1}, waterworks are required to blend more contaminated water with clean water, relocate wells, and set up protected

areas [30]. However, if the pollution further increases costly measures for water purification have to be implemented.

1.2.2. Natural nitrate attenuation and its limitations

The dominant natural nitrate attenuation process in groundwater is microbial denitrification [24]. A large range of bacteria are able to denitrify, reducing NO_3^- to N_2 [31]. However, as facultative anaerobes denitrifiers only switch from aerobic respiration to denitrification when O_2 concentrations fall below approx. 62.5 µM whereby denitrification becomes energetically favourable [24, 32]. O_2 limiting conditions are reached in micro-scale anaerobic sites in organic rich patches or biofilms [24]. For denitrification to occur, also NO_3^- and electron donors must be sufficiently available, and favourable conditions regarding pH, temperature, nutrients and trace elements are required [24]. Most denitrifiers are heterotrophic, which means that they use organic carbon as the electron donor [31]. According to a review by Rivett et al. 2008 [24], lack of organic carbon was determined as the major factor limiting denitrification rates in aquifers. In many regions, such as the Kano Plains in Kenya, the Arborea region in Italy and the Pearl River Delta in China, isotopic signature approaches have detected mostly heterotrophic denitrifying activity in NO_3^- polluted aquifers [14, 15, 16]. The lowest measured O_2 concentrations in these investigated aquifers were between 0.55-2 mg L^{-1}, thus denitrification occurred also slightly above 1 mg-O_2 L^{-1}. Nonetheless, several recent publications detected litho-autotrophic denitrification through the oxidation of pyrite and sulfide as the main nitrate attenuation process in the investigated aquifers [33, 34, 35]. For example, in the Osona region north of Barcelona that has been declared vulnerable to NO_3^- pollution, approximately 25% of the polluting NO_3^- in the groundwater is naturally attenuated through litho-autotrophic denitrification coupled to pyrite oxidation [33, 35].

NO_3^- and O_2 levels are generally higher in shallow aquifers compared to deep aquifers [13, 14]. The elevated O_2 concentration minimizes natural NO_3^- attenuation in such vulnerable aquifers. For example in porous aquifers found in Southeast Germany, denitrification is therefore not a significant NO_3^- removal process [13]. The time until the present O_2 is sufficiently reduced for denitrification to commence was calculated to be over 100 years [13]. NO_2^-, the reduction product of NO_3^-, may also be reduced abiotically by Fe(II) species, located on mineral surfaces, in a process termed chemo-denitrification. The process is only relevant in the interface of anoxic and oxic redox zones, where Fe(II) and NO_3^-/NO_2^- co-occur [36].
Dissimilatory nitrate reduction to ammonium (DNRA), performed by strict anaerobes, exists under the same conditions as denitrification but it is observed rarely in groundwater and solely under NO_3^--limitation and high carbon availability [24, 37, 38].

1.3. Denitrification

The N-cycle consists of six processes: denitrification, N-fixation, nitrification, nitrate assimilation, DNRA, and anaerobic ammonium oxidation (anammox). Most substrates and intermediates of

denitrification are also involved in other processes of the N-cycle (Figure 2). For example, NO_3^- and NO_2^- can be produced by nitrification and they are both also used as a substrate in DNRA and nitrate assimilation. While NO_3^- reduction during DNRA is also performed by Nap and Nar reductases, nitrate assimilation requires a Nas reductase [39]. NO_2^- is also reduced to NO by Nir as the first step of the strictly anaerobic process anammox [40]. Further, NO_2^- can also be reduced to ammonium during DNRA and nitrate assimilation. While nitrification requires strictly oxic conditions, denitrification, DNRA and anammox are only performed under anoxic conditions.

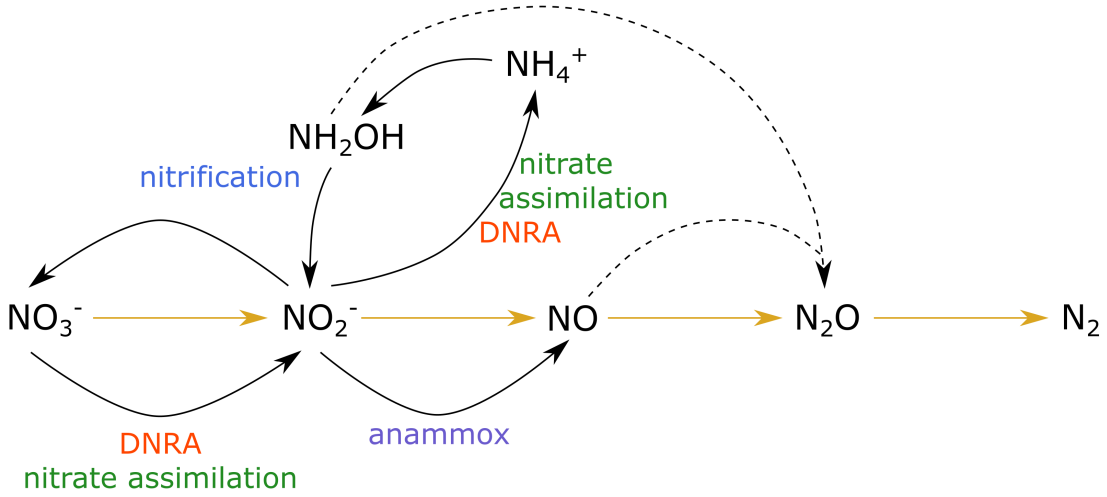

Figure 2 Reactions of denitrification and other N-cycle processes (nitrification, DNRA, anammox, and nitrate assimilation) which include the substrates and intermediates of denitrification. During nitrification ammonium (NH_4^+) is first oxidized to hydroxylamine (NH_2OH) and then further to nitrite. Hydroxylamine may be converted to N_2O by Cytochrome P460.

Denitrification is an energy conserving process that includes four redox reactions from NO_3^- (redox state +V) to atmospheric N_2 (redox state 0) (Equation 1.1), each catalysed by multisite metalloenzymes [41].

$$NO_3^-(+V) \rightarrow NO_2^-(+III) \rightarrow NO(+II) \rightarrow N_2O(+I) \rightarrow N_2(0) \tag{1.1}$$

In a strict sense denitrification includes only NO_2^-, NO and N_2O respiration [39], because the first step, NO_3^- to NO_2^-, is also performed in other metabolic pathways (Figure 2). The nitrite reductase catalyses the first committed step to a gaseous product and is thus considered to be the key enzyme of denitrification. However; in this thesis complete denitrification refers to the complete reduction of NO_3^- to N_2, as these are the required steps for nitrate attenuation to a harmless product. The denitrification pathway is modular with individual induction, except for NO_2^- and NO reduction. Those two steps are controlled interdependently to prevent the accumulation of the toxic NO radical [39].

The ability to denitrify is found among a range of bacterial and archaeal taxa [39, 42]. The widespread occurrence suggests that this trait emerged before prokaryotes split into two domains

[39]. Closely related genes involved in denitrification are found between distantly related bacterial taxa [43], at the same time closely related taxa can differ greatly in their ability to denitrify. These findings are consistent with the disagreement of phylogenetic trees from denitrification and 16S rRNA genes and suggest horizontal gene transfer and gene loss during evolution [42]. Also most genes involved in denitrification exhibit frequent substitutions due to their long evolutionary history [44]. Because of this high substitutional load, currently no optimal universal primer pair with full taxonomic range exists [44].

1.3.1. Genes and enzymes involved in denitrification

For every one of the four reduction reactions of denitrification at least two different enzymes or two different enzyme lineages are known [41]. Dissimilatory NO_3^- reduction is catalysed either by Nar, a membrane-bound nitrate reductase located in the cytoplasm that is encoded by *narG*, or by Nap, a periplasmic nitrate reductase encoded by *napA*. The two enzymes evolved separately [41]. Nar couples the NO_3^- reduction to proton translocation across the plasma membrane, whereas Nap dissipates the energy of the reaction [45]. The *nap* gene expression in *Paracoccus pantotrophus* is higher under aerobic growth, which is further evidence for its role in redox balancing rather than in energy conservation [45]. Dissimilatory NO_2^- reduction, which occurs in the periplasm, can be catalysed also by two non-homologous enzymes with either haem (cd1Nir, encoded by *nirS*) or copper (CuNir, encoded by *nirK*) as a cofactor [41, 46]. The taxonomic and environmental distribution of these two reductases differs greatly, which indicates that their genes must have arisen separately during evolution [44]. The long-prevailing assumption that these genes do not co-occur has; however, been recently refuted by Graf et al. 2014 [47] who detected some denitrifier genomes with both *nirS* and *nirK* genes. NO reduction can be catalysed by the nitric oxide reductase Nor, of which two classes are known. The quinol-oxidizing single-subunit class, encoded by *qnorB*, and the cytochrome bc-type complex class, encoded by *cnorB*. While both classes are occurring in denitrifiers, the *qnorB* type is also detected frequently in non-denitrifying strains who use the NO reductase for detoxification [48]. Similarly, N_2O reduction can be catalysed by two classes of nitrous oxide reductases (Nos), termed clade I and clade II. The latter has been described only recently in detail and half of the organisms possessing clade II *nosZ* are non-denitrifying N_2O reducers [49]. According to the study of Yoon et al. [50] the two clades of nitrous oxide reductases seem to confer certain physiological properties to its carrier. Clade II *nosZ* organisms displayed a higher affinity for N_2O while also producing 1.5 times more biomass per mol of N_2O consumed in an analysis comparing clade I and clade II *nosZ* harbouring pure cultures [50]. Measurements of the N_2O sink capacity correlating with the diversity and abundance of clade II *nosZ* bacteria [51] are supporting these results. Conversely, Conthe et al. 2018 [52] analysed continuous cultures enriched from a natural community in which clade I *nosZ* organisms still dominated even under N_2O limiting conditions. The maturation of both Nos enzymes is pH dependent. At a pH of 6.5 or lower the enzyme's maturation is impaired [53, 54], which explains why numerous studies observed an increase in N_2O emission in acidic soils [55].

Several other proteins, besides denitrifying reductases, are necessary for a functional electron transfer coupled to energy-generating proton translocation. These include chaperonins and metal

processing proteins for the maturation of the reductases, as well as electron carriers and regulatory proteins [43]. The genes encoding the proteins involved in each denitrification step are arranged in gene clusters. These clusters differ largely among bacterial and archaeal genomes, because only some arrangements are conserved [43]. Several evolutionary drivers, including horizontal gene transfer, convergent evolution of different structural types, as well as gene duplication and loss, are likely causes of the variation observed today [42]. The diversity in gene cluster organisation among denitrifiers is large; however, the extent of this diversity and the implications of different gene cluster organisations on the denitrification phenotypes are unknown, as most studies on the regulation of denitrification have been conducted with model organisms, such as *Paracoccus denitrificans* [32, 56].

Even though complete denitrification comprises the four reaction steps, only approximately one third of bacteria harbouring denitrification genes posses the complete set [32, 47]. The denitrification pathway is, in fact, vastly versatile, as shown by a genome comparison study by Graf et al. 2014 [47] that included 652 genomes harbouring at least one denitrification gene. Besides displaying the vast abundance of truncated denitrifying pathways, they also detected co-occurrence patterns of denitrification reductase genes across the different taxa. Only 27% of bacteria with a *nirK* gene had the potential to reduce NO_2^- up to N_2O, whereas 76% of *nirS* gene carriers had so [47]. Thus, *nirS* co-occurred much more frequently with *norB* and *nosZ* genes compared to *nirK*. However, *nirK* co-occurred more often with clade I *nosZ*.

1.3.2. Denitrification phenotypes

Alike the diverse combinations of denitrification reductase genes in denitrifier genomes, also a variety of denitrification phenotypes exist [32, 57]. These denitrification phenotypes not only differ in the presence or absence of denitrification steps but also in the transient accumulation of the intermediates NO_2^-, NO and N_2O, the O_2 concentration at the initiation of denitrification, the anoxic growth rate in relation to the oxic growth rate and the electron flow patterns [57]. Bergaust et al. 2011 [57] therefore established a standardised method to determine a set of basic characteristics of denitrification phenotypes during the transition from aerobic to anaerobic respiration. Liquid pure cultures are therefore grown tempered and stirred in sealed vials with initially approximately 1% O_2 in the headspace. NO, N_2O, N_2, and O_2 gases in the headspace are measured for each vial at regular intervals, as well as the NO_2^- concentrations in the liquid medium. The resulting characteristics from the standardised measurements enable the comparison of diverse denitrification phenotypes. The set of phenotypic characteristics was termed 'Denitrification Regulatory Phenotype' (DRP).

With this standardised method Lycus et al. 2017 [32] analysed the DRP of 70 isolates which performed at least one step of denitrification. 40 of those 70 isolates performed truncated denitrification, which was also visible in the genetic constitution of most of them but not in all. An analysis of the DRPs from eight *Thaurea* strains separated them into two groups. The first group displayed a 'rapid, complete onset' (RCO) of all denitrification reactions without NO_2^- accumulation. The

second group; however, displayed a 'progressive onset' (PO) of the transcription of denitrification genes and thus also the denitrification reactions, which lead to the transient accumulation of NO_2^- as long as NO_3^- was present [58]. Lycus et al. 2017 [32] observed the RCO DRP also in a *Bradyrhizobium* isolate and the PO DRP in a *Hydrogenophaga* isolate. Other DRPs that were observed include a *Pseudomonas* isolate which accumulated 100% of the given nitrogen oxides as N_2O before reducing it further to N_2 and a *Polaromonas* isolate which accumulated significant amounts of NO (max. 150 nM) as well as 80% of the given nitrogen oxides as N_2O. The latter DRP is unusual because the transient NO concentration is generally kept at 5-20 nM to avoid self-intoxication [32, 58]. Besides the accumulation of intermediates, also the O_2 concentration at which NO_3^- reduction is initiated varies among denitrifiers. NO_3^- reduction is mostly initiated when O_2 concentrations fall as low as 5 µM, but in some denitrifiers NO_3^- reduction already starts at 16-17 µM O_2 or it is initiated when O_2 is completely depleted [32].

For another phenotypic phenomenon of some denitrifiers, called bet-hedging, only a fraction of the population's cells commit to switch to denitrification and express the nitrite reductase [59]. This phenotypic diversification may reduce the metabolic investment under O_2 limiting conditions, in case of a brief anoxic spell. The electron flow pattern in such denitrifier populations displays a large drop in the total electron flow after the depletion of O_2 [32, 59]. On the contrary, isolates without such phenotypic diversification display a smooth pattern of total electron flow.

1.3.3. Regulation of denitrification

The expression of denitrification enzymes and thus the initiation of denitrification must be tightly regulated with regard to the available O_2, as denitrification is only energetically favourable when O_2 becomes too limited for aerobic respiration. On the one hand cells should not switch too early to avoid wasting resources in case of a merely temporary drop in the O_2 concentration. On the other hand, a delayed switch may lead to entrapment in anoxia, a state where all energy resources are depleted so that a functional denitrification respiratory chain cannot be expressed any more [59, 60]. Further, denitrification should only be initiated in the presence of sufficient NO_3^-. Besides the right starting conditions, it is also important that the NO production and consumption is co-regulated to avoid accumulation of the toxic intermediate. Consequently, denitrification regulatory proteins are mainly responding to lowering O_2, as well as the NO_3^- and NO concentrations [39, 61].

Several denitrification regulators and their role are known while others are still unidentified. Many studies on the regulation of denitrification focus on the best studied denitrifier *Paracoccus denitrificans*. As the combination and network of regulators differ among denitrifiers [62], the details of the network of transcriptional regulators and the influence of environmental signals in other taxa are often still unknown [56]. Important regulatory proteins sensing lowering O_2 concentrations are the two-component systems FixLJ and RegAB, both histidine kinases [62]. FixLJ is active in the absence of O_2 and is thereby a major regulator of the O_2 limitation response [63]. RegAB is indirectly activated by lowering O_2 concentrations, because as a redox sensor it becomes switched on when the bacterial cell is in a reduced state. It regulates energy generating

and consuming processes such as denitrification [62]. These two regulators are examples of global regulators which may induce all four steps of denitrification. Another two-component system, NarXL (ortholog of NarQP), specifically regulates the NO_3^- reductase expression upon activation by elevated NO_3^- and NO_2^- concentrations [62]. The tight regulation necessary for NO production and consumption requires several regulators responding to NO concentrations, which are activating or inhibiting the expression of the NO_2^- or NO reductases [62]. These include NNR, NsrR and NorR. Contrary to the other denitrification intermediates, elevated N_2O is not known to be perceived by denitrification regulatory proteins [62].

1.4. Hydrogenotrophic denitrification

Hydrogenotrophic denitrifiers couple the oxidation of hydrogen (H_2) to denitrification. They are autotrophic organisms, utilizing carbon dioxide (CO_2) or bicarbonate (HCO^{3-}) as their carbon source [27]. Equation 1.2 shows the overall stoichiometry of the full hydrogenotrophic denitrification reaction from NO_3^- to gaseous N_2. Each mole of NO_3^- also consumes one mole of the acid equivalent H^+, resulting in an increased pH [27].

$$2\,NO_3^- + 5\,H_2 + 2\,H^+ \rightarrow N_{2(g)} + 6\,H_2O \tag{1.2}$$

1.4.1. Hydrogen oxidation

Even though the Earth‘s atmosphere only contains 0.55 ppm (0.000055%) H_2 nowadays [64], it is hypothesised that during the development of life, H_2 played a major role as the first electron donor [65]. Sediments still contain larger amounts locally, as H_2 is produced during fermentation processes [66]. H_2 rarely accumulates because it is constantly depleted by H_2-consuming microorganisms. The oxidation of H_2 can be coupled to the reduction of several electron acceptors, such as O_2, NO_3^-, Fe(III), SO_4^{2-} and CO_2 [67]. Thereof, the two groups comprising the most important H_2-consuming prokaryotes are methanogenic archaea and sulfate-reducing bacteria [66]. However, hydrogenase genes, coding for the enzymes catalysing H_2-oxidation, occur in a wide range of bacterial and archaeal taxa [67]. Greening et al. 2016 [68] detected hydrogenase genes in 51 bacterial and archaeal phyla including lithotrophs, phototrophs, respirers and fermenters.
Hydrogenase enzymes are functionally and structurally diverse. They can be attributed to three unrelated classes which differ in the metal at the H_2-binding site: [NiFe]-, [FeFe]- and [Fe]-hydrogenases [67, 68]. The class of [NiFe]-hydrogenase is the best studied and contains the most known hydrogenases [67], which is why the focus of the following section is thereon. The class of [NiFe]-hydrogenases can be divided into 4 groups that entail a total of 22 subgroups [68]. Group 1 comprises respiratory hydrogenases which oxidise H_2 and reduce quinones in the respiratory chain, where H_2 oxidation is coupled to the reduction of electron acceptors [67]. They are connected directly to the quinone pool inside the respiratory chain by a cytochrome b at the periplasmic side of the membrane [69]. The subgroups included in the group of respiratory hydrogenases suggest that that the evolution of this enzyme was driven by the O_2 partial pressure [68]. The enzymes of subgroup 1a and 1b are O_2 sensitive, whereas the enzymes of subgroups 1d and 1h are

O_2 tolerant [68]. Group 2 comprises H_2-sensing hydrogenases performing regulatory functions that control the expression of respiratory hydrogenases in response to H_2 [67]. Group 3 includes redox-balancing or bidirectional hydrogenases that are able to reoxidise soluble cofactors, such as F_{420}, NAD or NADP, when reducing equivalents are needed by other proteins [67, 68]. Lastly, group 4 contains H_2 evolving hydrogenases that can dispose reducing equivalents by transferring electrons to protons from water [67].

1.4.2. CO_2 assimilation

Autotrophic bacteria obtain their carbon by fixing CO_2 into organic carbon, which is an energy-consuming process. Of the six currently known autotrophic CO_2 assimilation pathways, the Calvin-Benson-Basham (CBB) cycle is the most abundant; found in plants, algae, cyanobacteria as well as aerobic and anaerobic *Proteobacteria* of the α, β, and γ-subgroups [70]. The CBB cycle is also the most frequent CO_2 fixation pathway in chemo-litho-autotrophic *Proteobacteria* [71, 72]. Its widespread occurrence is likely due to the O_2 tolerance of its two main enzymes, the ribulose-1,5-biphosphate carboxylase (RubisCO) and the phosphoribulokinase [70]. Other CO_2 assimilation pathways, like the reductive citric acid cycle and the reductive acetyl-CoA pathway, are rather adapted to anoxic habitats and life at the thermodynamical limit [70]. Due to the relevance of the CBB cycle, this section will further focus on its key enzyme: RubisCO. Several forms of the RubisCO enzyme have evolved due to selective pressure of changing conditions regarding the CO_2 and O_2 level [70, 71]. The three forms, IA, IC, and II, exist in *Proteobacteria* [72]. Form II RubisCO has the highest turnover rate and is adapted to environments with low O_2 and high CO_2 [71]. It may bring its carrier an advantage in ecosystems with varying O_2 and CO_2 concentrations and is therefore often found in facultative autotrophs or mixotrophs [72]. Form IA and IC mostly occur in strictly chemo-litho-autotrophic bacteria and they are adapted to higher O_2 concentrations [71]. Alfreider et al. 2012 [72] detected distinct expression patterns of the different RubisCO forms in polluted groundwater depending on the redox conditions. While form IA and IC were expressed only in groundwater containing O_2, form II RubisCO transcripts were mostly stemming from denitrifiers [72].

1.4.3. Parameters influencing hydrogenotrophic denitrification

Several studies have investigated parameters influencing the turnover rates and the accumulation of intermediates during hydrogenotrophic denitrification, such as pH [73, 74, 75, 76], temperature [73, 76, 77], dissolved H_2 concentration [76, 78, 79, 80], NO_3^- concentration [81] and the ratio of inorganic carbon to nitrogen [74, 76].

Most studies determined the optimal **pH** for highest hydrogenotrophic denitrifying rates to range between 7.6 and 8.6 [27, 74]. Rezania et al. 2005 [73]; however, detected a temperature dependent pH optimum, which was 9.5 at 25°C and 8.5 at 12°C. The pH range 7.5-8.0 seems to enable the highest turnover rate, and it restrains NO_2^- accumulation. NO_2^- accumulation increases above pH 8.0 as well as at a slightly acidic pH, such as pH 6.5 and lower [76]. N_2O accumulation is lowest at the pH range 7.0-9.0 and also increases at pH 6.0 or lower [76]. The optimal **temperature** for the highest NO_3^- reduction rate is between 30-40°C [76, 77]; however, the least NO_2^- accumulation is reached at temperatures between 20-35°C. At temperatures below 15°C,

which occur in groundwater, intermediate accumulation increases. In a microcosm experiment containing activated sludge from an aerobic tank by Li et al. 2017 [76] both NO_2^- and N_2O concentration were significantly increased at 15°C. Rezania et al. 2005 [73] also observed significantly increased NO_2^- at 12°C compared to 25°C. **Dissolved H_2 concentrations** should be above 0.2 mg L^{-1} for hydrogenotrophic denitrification. In an experiment with mixed cultures of denitrifying bacteria, the nitrate reductase was inhibited below 0.1 mg-H_2 L^{-1} and the nitrite reductase was already inhibited below 0.2 mg-H_2 L^{-1} [81]. Several studies achieved optimal NO_3^- removal rates at H_2 concentrations between 0.4-0.8 mg L^{-1}; however, sufficient results were also obtained with higher H_2 concentrations [27]. Schnobrich et al. 2007 [80] could improve NO_3^- reduction by increasing the H_2 lumen pressure. Conversely, Li et al. 2017 [76] observed NO_2^- accumulation at 0.17 and 0.4 mg-H_2 L^{-1} but not at 0.02 mg-H_2 L^{-1}. Optimal **NO_3^- concentrations** for hydrogenotrophic denitrification are still under debate. While Vasiliadou et al. 2006 [81] observed an inhibition of NO_3^- removal rates above 40 mg-NO_3^- L^{-1}, others did not observe such inhibition at increasing NO_3^- concentrations, only a slight increase in NO_2^- accumulation [27]. Wang et al. 2015 even reached optimal performance of the hydrogenotrophic denitrification reactor at a NO_3^- loading of 105 mg L^{-1} [82]. Available **inorganic carbon** is essential for hydrogenotrophic denitrification to occur as the bacteria rely on CO_2 assimilation for their cellular carbon [83]. The optimal C/N ratio was 30 in the reactor experiment by Wang et al. 2015 [82]. Further, controversy remains on the effect of phosphate addition on NO_3^- reduction rates. Some studies [80, 84] achieved higher NO_3^- reduction rates following phosphate addition. It is overall noticeable that the different studies obtained varying results regarding the optimal conditions of hydrogenotrophic denitrification. Possibly, the optimal conditions also depend on the composition of the hydrogenotrophic denitrifier community.

1.4.4. Diversity and taxonomy of hydrogenotrophic denitrifiers

The majority of hydrogenotrophic denitrifiers belong to the phylum *Proteobacteria*, mainly β-*Proteobacteria* [27, 85]. The bacterial diversity in hydrogenotrophic denitrifier consortia is generally low due to the highly selective environmental conditions that the metabolism requires [27, 86]. The taxonomy and diversity of such consortia has mostly been studied in samples from H_2-based bioreactors or from H_2-based enrichments of sludge. *Acidovorax sp., Paracoccus sp., Acinetobacter sp.* and *Pseudomonas sp.* were isolated by Vasiliadou et al. 2006 [81] and verified as hydrogenotrophic denitrifiers as they grew in NO_3^--enriched synthetic groundwater with a H_2 and CO_2 atmosphere. Other potential hydrogenotrophic denitrifier genera were detected by 16S rRNA gene sequencing; such as *Hydrogenophaga* [86, 87, 88], *Rhodocyclus* [86], *Dechloromonas* [88, 89], *Azonexus* [88], *Propionivibrio* [89], *Sulfuricurvum* [88, 89] and *Rhodobacter* [89].
Kumar et al. 2018 [90] analysed an enrichment culture from groundwater of an oligotrophic aquifer stimulated with a combination of thiosulfate and H_2 as electron donors. They detected *Thiobacillus*, *Sulfuricella*, *Sulfuritalea*, *Dechloromonas* as well as *Hydrogenophaga* as the dominant genera. The genus *Dechloromonas* was also the prevailing taxa in a microcosm experiment of perchlorate contaminated soil with NO_3^- and H_2 addition [91]. In the field of perchlorate remediation much research has been conducted analysing bacterial consortia reducing NO_3^- and perchlorate with H_2 [88, 91, 92]. These consortia generally prefer NO_3^- over perchlorate [91] and are thus also possible hydrogenotrophic denitrifiers. In biofilms of a H_2-based membrane biofilm reactor *Dechloromonas*

was the dominant litho-autotrophic genus besides *Sulfuricurvum* and *Hydrogenophaga* [88]. According to functional-gene and pyrosequencing assays, *Dechloromonas* was mainly responsible for perchlorate-reduction, while the other two taxa reduced NO_3^- [88].

1.5. *In situ* nitrate remediation in groundwater

Local *in situ* remediation strategies are, besides reducing NO_3^- input to groundwater, an important strategy to protect drinking water wells or nature reserves. The most promising method to locally attenuate NO_3^- in aquifers is to stimulate denitrifying activity by creating anoxic conditions and providing an electron donor (Figure 3).

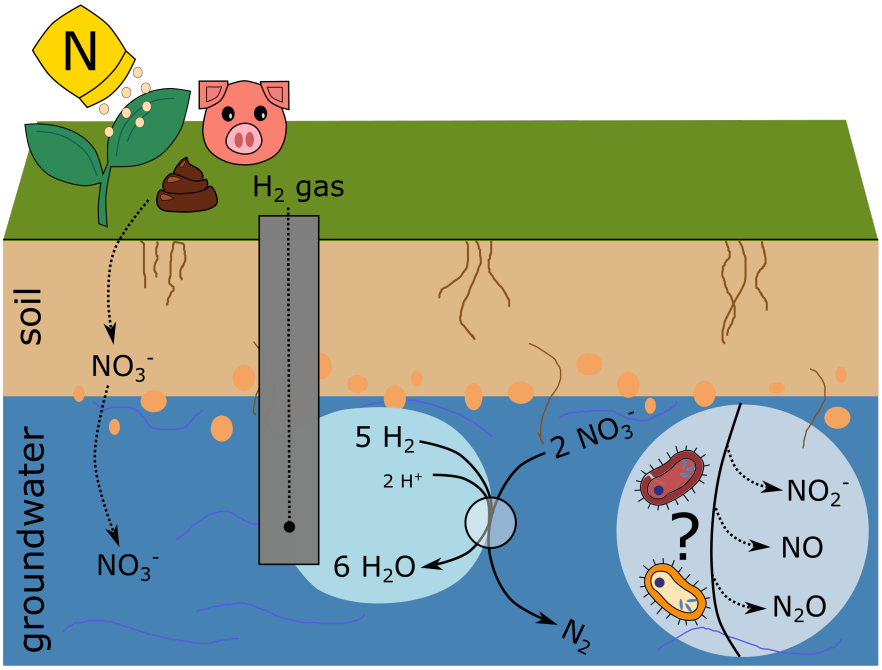

Figure 3 *In situ* nitrate remediation strategy with H_2 addition via semi-permeable membranes extending into the groundwater through a well. The strategy involves bacteria that are able to couple H_2 oxidation to denitrification, which are thereby growing and forming a biofilm on the H_2-releasing membrane. Their denitrifying activity should result in a significant reduction of the nitrate pollution downstream, where drinking water could be obtained.

1.5.1. Different electron donors

Stimulating heterotrophic denitrification by the addition of organic carbon leads to high denitrifying rates but at the same time to excessive bacterial growth that could congest aquifer pores. Further, the residual carbon may impede drinking water treatment [27, 80]. The addition of inorganic electron donors stimulating litho-autotrophic denitrifiers provides an alternative with lower denitrifying rates; however, without the risk of bio-clogging. Possible electron donors are for example sulfur and iron compounds, as well as H_2. The latter has the advantage over the other two that its oxidation does not form unwanted side-products that would require post-treatment. Many studies have proven H_2 as a good lithotrophic electron donor choice which is also least expensive per electron-equivalent [27, 81]. The downsides of H_2 gas are its low solubility of 1.6 mg L^{-1} at 20°C

in water and that it can create an explosive atmosphere in contact with O_2.

1.5.2. Delivery of the electron donor

An important factor for successful *in situ* nitrate remediation with H_2 is a safe and efficient way to deliver the gas into the groundwater and to achieve its maximum utilization by the hydrogenotrophic denitrifying bacteria. A large area of gas exchange is advantageous due to the low solubility of H_2 gas, and it additionally provides space for denitrifying bacteria to form a biofilm within the anoxic zone [93]. One method is to use semi-permeable membranes, for example gas-permeable silicon tubes, which was successfully tested by Ho et al. 2001 [94]. This method requires H_2 gas from external sources. Another method, called microbial electrolysis cells, generates H_2 itself from organic waste that could be delivered to the hydrogenotrophic denitrifiers via a gas diffusion membrane [95]. Similarly, microbial electrolysis cells could also directly deliver electrons [96]. While these approaches were able to achieve almost complete NO_3^- removal at relevant NO_3^- concentrations under laboratory conditions, its application *in situ* still needs to overcome technical challenges.

1.5.3. Challenges of *in situ* nitrate remediation by hydrogenotrophic denitrification

The main challenge of *in situ* NO_3^- remediation, besides technical issues of H_2 delivery, lie in incomplete denitrification and the transient accumulation of the harmful intermediates NO_2^- and N_2O. As mentioned previously, denitrification comprises four reduction steps. While some bacteria perform all, others may only perform a part of them. An imbalance in the microbial community composition, such as more N_2O producers than N_2O reducers, may therefore result in incomplete denitrification or transient intermediate accumulation. Another possible reason thereof lies in the denitrifier‘s physiology and influencing environmental factors.

Several experiments that have investigated hydrogenotrophic denitrification in microcosms [76, 84, 90] observed transient NO_2^- accumulation. In the microcosms of Chaplin et al. 2009 [84] NO_2^- remained untouched until all NO_3^- had been reduced; however, the H_2 gas volume percentage in the microcosms of this study was only 10%. This could have impacted the intermediate accumulation, as the H_2 concentration was shown to be an important factor. 100% NO_3^- removal was reached in several flow-through reactor experiments when the H_2 pressure was increased [75, 79]. Incomplete denitrification also occurs in natural environments [33, 97], which illustrates the generic nature of incompleteness of the denitrification process. Flint et al. 2021 [98] analysed carbonate karst aquifers, which are especially prone to NO_3^- pollution as well as groundwater surface mixing due to their structure. They found that incomplete denitrification to N_2O occurred more frequently in recharge water with residence times of several days, while complete denitrification was more prominent in aquifers with residence times of months and years.

1.6. Isolation of groundwater bacteria

Over 70% of bacteria in groundwater and sediment belong to clades that have not been cultivated yet [99]. This problem of non-cultivable bacteria is observed in most environments and was termed "the great plate count anomaly", due to the disparity between the number of cultivable bacteria on plates and the total number of cells detected under the microscope. Recently the number of cultivable bacteria could be increased in numerous studies by choosing adequate growth media and cultivation conditions that resemble the natural environment and growth conditions of the targeted taxa [100, 101]. Components of the growth medium that need to be considered include the concentration of macronutrients (C, O, H, N, S, P, K, Mg, Fe, Ca), micronutrients (Mn, Co, Cu, Mo, Zn, Ni, V, B), growth factors (amino acids, purines and pyrimidines, vitamins), pH, osmolarity, temperature as well as the hydrostatic pressure [100].

The amount of carbon has a large effect on the growth of oligotrophic bacteria. Reducing the organic carbon concentration from 0.25 g L^{-1}, present in yeast extract and peptone medium, to less than 5 mg L^{-1} generally increase the isolation outcome of oligotrophic bacteria by up to 20-60% [100]. Another strategy for the isolation of oligotrophic bacteria from freshwater or groundwater is the use of filter-sterilized and autoclaved water samples as the medium [102]. The preparation of the growth medium is just as important as its components. Tanaka et al. 2014 [103] observed that when phosphate was autoclaved separately from the agar, the total colony counts were significantly higher and the grown taxa were more reflective of the actual community structure compared to plates prepared with agar and phosphate autoclaved together. Also sugars autoclaved together with salts may form sugar phosphates that inhibit bacterial growth [100]. Separate sterilization of different components is therefore recommended. For the cultivation of diverse denitrifiers, Heylen et al. 2006 [104] tested 60 different combinations of 11 varying medium parameters including: pH, temperature, carbon source, molar C/N ratio, N-source, NaCl, as well as vitamin, riboflavin, thiamine and cobalamin solutions. They reached the highest number and diversity of isolated denitrifiers with following values for the five parameters: pH 7.0, nitrate concentration of 3 mM, 1 mL vitamin solution and no NaCl and riboflavin solution. The other parameters did not influence the isolation outcome as much. Implementing an enrichment step with specific conditions adapted to the metabolism of the target organisms prior to isolation on solid growth medium is also a common and promising step in isolation to initially increase the share of the targeted bacteria. For example Jonassen et al. 2021 [105] successfully isolated strong N_2O-reducing bacteria with growth in both soil and digestate by seven rounds of enrichment cultures alternating between γ-radiated soil and autoclaved digestate.

2. Aims and Hypotheses

Groundwater nitrate remediation with H_2 provides a promising strategy to locally minimize nitrate pollution and its impact on the ecosystem and drinking water quality. Despite numerous studies, actual *in situ* application is; however, still a long way to go. Pressing obstacles include the implementation of efficient and wide-ranging H_2 delivery to the groundwater as well as understanding the hydrogenotrophic denitrifier community compositions and its influence on the accumulation of unintended intermediates. This thesis, part of the "Healthy Water" (12.08) project funded by the International Graduate School for Science and Engineering (IGSSE) from the Technical University Munich, includes research on the microbiological part. The aim of this thesis therefore is the determination and characterisation of prevailing hydrogenotrophic denitrifier species occurring in NO_3^- polluted oxic aquifers which could be remediated by H_2 addition. Their denitrification regulatory phenotypes and genetic features were investigated and compared to detect prevailing hydrogenotrophic denitrifiers with least intermediate accumulation. Another aim was to possibly link genetic features of desired hydrogenotrophic denitrifiers to certain phenotypes. These genetic features could be used as marker genes to determine the applicability of *in situ* nitrate remediation with H_2 in a potential aquifer.

Hypothesis 1: Hydrogenotrophic denitrification is performed by few bacterial taxa.

We expected to find a specific community of few hydrogenotrophic denitrifiers due to the highly selective environmental conditions and because less than twenty bacterial genera have been detected in H_2-based environments. So far, the community of hydrogenotrophic denitrifiers was mainly determined in H_2-based bioreactors, thus the dominating taxa in NO_3^- polluted oxic aquifers are still largely unknown. Hypothesis 1 was mainly examined by bacterial community analyses using 16S rRNA gene amplicon sequencing over the course of a microcosm experiment (PI) and at the end of a flow-through column experiment. The results thereof were validated by the enrichment and isolation of hydrogenotrophic denitrifiers under selective conditions (PIIa).

Hypothesis 2: Hydrogenotrophic denitrifiers differ in their denitrification phenotypes. Intermediate accumulation of NO_2^- and N_2O is therefore influenced by the bacterial community composition.

Since we expected the hydrogenotrophic denitrifier community to comprise only a limited number of species, we aimed at determining the denitrification phenotypes of the prevailing species in pure cultures under standardised conditions (PIIb). We also expected hydrogenotrophic denitrifiers to entail different phenotypes, because heterotrophic denitrifiers are known to posses diverse denitrifier phenotypes. Observed differences in intermediate accumulation among studies on hydrogenotrophic denitrification are another indication of the existence of diverse hydrogenotrophic denitrifier phenotypes.

Hypothesis 3: The genetic features of hydrogenotrophic denitrifiers shape their denitrification phenotype and thus their tendency to accumulate intermediates.

Due to the numerous observations of a discrepancy between denitrification phenotypes and genotypes, the phenotype cannot solely be predicted by the set of denitrification reductase genes carried by a species. However, if we expand the set of analysed genes to hydrogenase, RubisCO and denitrification regulatory genes as well, we may identify certain genes harboured by species with less intermediate accumulation. Hypothesis 3 was analysed by comparing the determined phenotypes to the results of whole genome analyses (PIIb).

3. Materials and Methods

3.1. Experimental descriptions

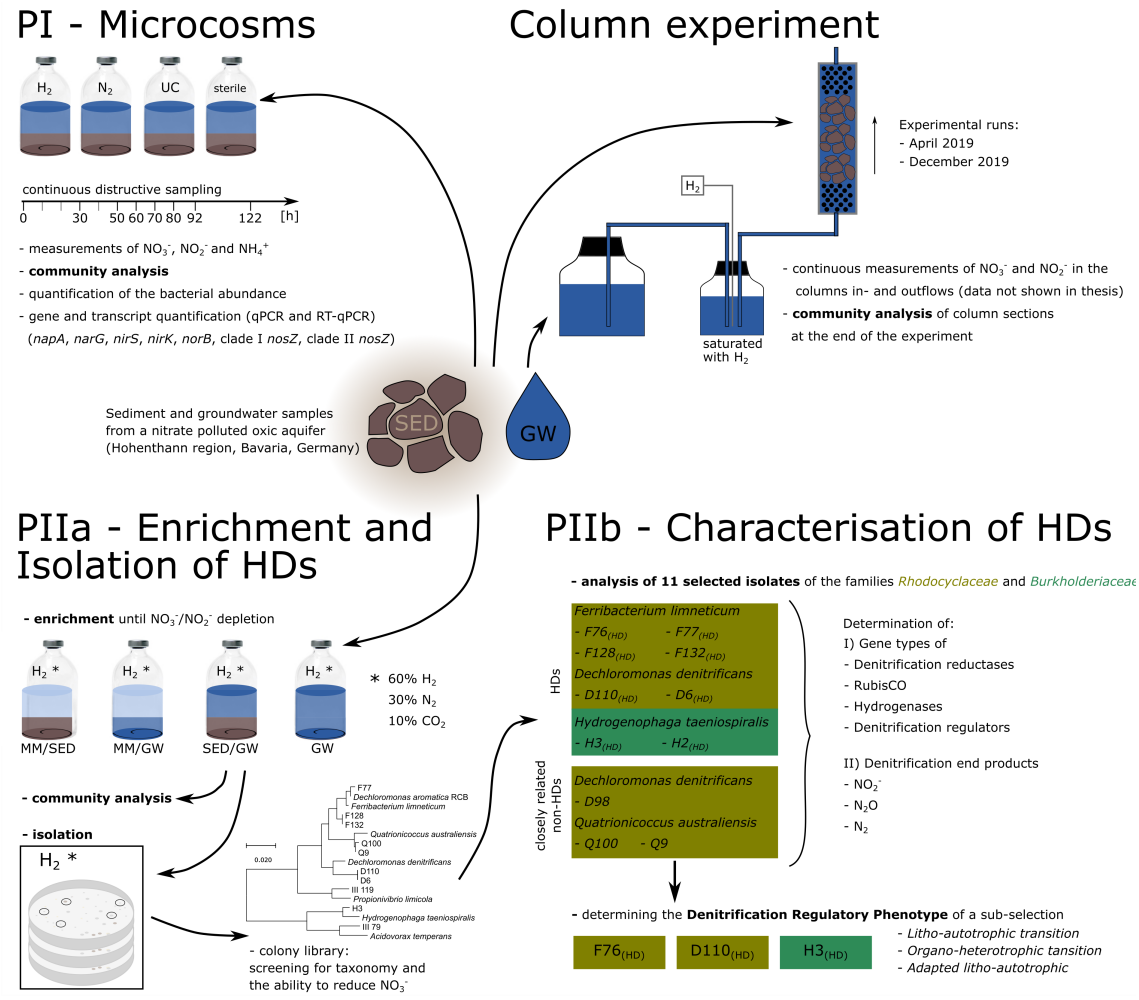

Figure 4 Overview of the experimental procedures of experiments PI, PII and the column experiment. Sediment (SED) and groundwater (GW) were sampled for the three experiments from an aquifer located in the Hohenthann region, north-east of Munich, Germany. PI analysed the changing bacterial community composition over time in microcosms containing SED and GW and a 100% H_2 atmosphere. Microcosms with N_2 gas or atmospheric air (UC) as well as autoclaved microcosms with a H_2 atmosphere (sterile) served as controls. Besides determining the community composition, the NO_3^-, NO_2^- and ammonium concentrations as well as the bacterial abundance and denitrification reductase genes and transcripts were quantified. Similar enrichment cultures were set up for PIIa containing either mineral medium (MM) and SED, MM and GW, SED and GW or solely GW and a 60% H_2 atmosphere with additional 10% CO_2 and 30% N_2. Once NO_3^- and NO_2^- were depleted the enrichments were diluted and spread onto MM or GW agar plates and incubated with the same H_2 containing atmosphere inside anaerobic pots. The bacterial communities of the enrichments were analysed and a colony library was prepared of which the taxonomy was determined via full 16S rRNA gene Sanger sequencing. The genomes of a selection of 11 isolated of the families *Rhodocyclaceae* and *Burkholderiaceae* were sequenced and the presence and gene types of the denitrification reductases, RubisCO, hydrogenases and denitrification regulators were determined. Further, their denitrification end products were analysed, whereby they could be categorized into two groups; complete hydrogenotrophic denitrifiers (HDs) and closely related non-hydrogenotrophic denitrifiers (non-HDs). The Denitrification Regulatory Phenotypes of a sub-selection including one member of each phylogenetic group of HDs was determined under three conditions; *Litho-autotrophic transition, Organo-heterotrophic transition* and *Adapted litho-autotrophic*. The column experiment was performed to determine the bacterial community in a flowing system with added H_2, containing the same sediment and groundwater. The bacterial community was determined at the end of the experimental run. In all three experiments, the bacterial communities were determined by 16S rRNA gene amplicon sequencing.

3.1.1. Sampling site

Samples for all experiments were collected in the Hohenthann area, 90 km north-east of Munich in Germany [Figure 5 (A)]. The area is part of the Bavarian Tertiary Molasse-Hills, comprising limestone and sandstone debris deposited by the rising alps. Maize cultivation and hog farming dominate the landscape causing nitrate pollution in a main porous aquifer and several perched aquifers [13]. Additionally, the aquifers are largely electron donor limited and oxic. The main aquifer has a median O_2 concentration of 198.8 µM and the perched aquifer of 249.1 µM, while the median dissolve organic carbon (DOC) is 11.8 µM in the main and 33.3 µM in the perched aquifer [13]. The pH ranges between 7.2-7.4 and the temperature between 10.8-10.9 °C. Sediment samples were collected from the main porous aquifer below a fallow field (GPS: 48°42‘01.2"N 12°00‘10.2"E) by drilling a hole with an auger up to the saturated zone of the aquifer at a depth of 2-2.5 m [Figure 5 (B) & (C)]. The groundwater was collected from a spring discharging from one of the small, perched aquifers. The sampling for the microcosm experiment (PI) was done in August 2018, for the enrichment and isolation (PIIa) in February and October 2019, and for the column experiments in October 2018. The sediment and groundwater were transported to the laboratory at < 10°C and stored at 4°C prior to the experiments. The enrichments of PIIa were started directly on the following day.

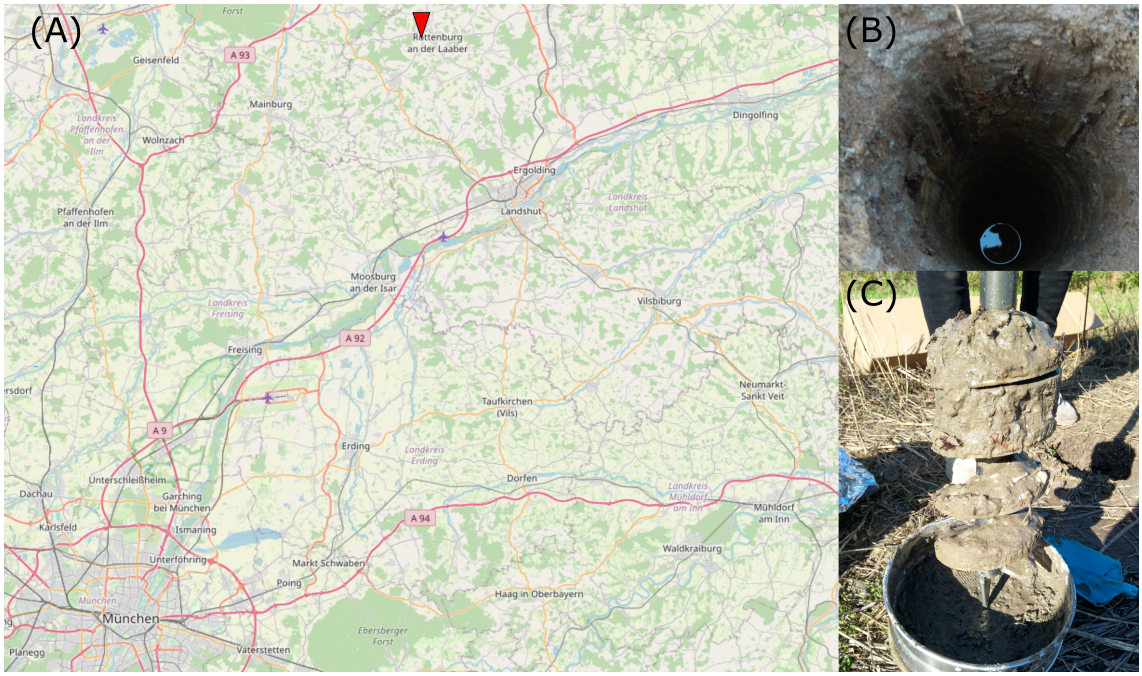

Figure 5 (A) Map (© OpenStreetMap-Mitwirkende, www.openstreetmap.org/copyright) indicating the location of the sampling site 90 km north-east of Munich. (B) The hole was approximately 2-2.5 m deep and (C) was drilled with a manual auger.

3.1.2. Microcosms (PI)

The microcosm experiment was performed to verify that the aquifer material of the Hohenthann area comprises hydrogenotrophic denitrifiers reducing nitrate and its products when given H_2 under anoxic conditions. Therefore NO_3^-, NO_2^- and ammonium were measured over the course of the microcosm incubations. In order to detect prevailing hydrogenotrophic denitrifiers, changes in the bacterial community composition and the quantity of the denitrification reductase genes

and transcripts were determined at the same time points by 16S rRNA amplicon sequencing and (RT)-qPCR (Figure 4).

Initially, large gravel was removed by sieving the wet sediment through a 2 mm sieve and particles were removed from the groundwater by passing it through a filter with a 20 µm pore size. Each incubation consisted of 30 g sieved sediment and 85 mL groundwater inside a 120 mL vial closed hermetically with a butyl rubber septum and an aluminium crimp cap. In total 69 vials were prepared in this manner and were treated as well as sampled in the following way: Four vials, representing the initial bacterial community, were sampled at the beginning of the experiment (0 h) when the treatments were applied. Forty vials were sparged with circa 1 L H_2 gas produced by a hydrogen generator (Precision series, Peak Scientific, Scotland) of which four vials were sampled respectively in 10 h intervals. Serving as an anaerobic control (N_2) without an electron donor, eight vials were sparged with N_2 gas, whereof four vials were sampled after 77 h and another four after 126 h. Of further eight vials, with ambient air serving as an untreated control (UC), four vials were sampled after 76 h and the other four after 125 h. Nine vials were autoclaved prior to the H_2 sparging serving as a sterile control (sterile). Three vials of the nine were sampled respectively at 0 h, 72 h and 128 h. In order to confirm that the applied gas sparging was sufficient, four exemplary H_2- and N_2-treated microcosms contained an O_2 sensor spot that was measured non-invasive with an O_2 sensor (Fibox 4 trace, PreSens, Germany).
All vials were incubated on a rotary shaker at 220 rpm at 16°C and were sampled destructively, so that each microcosm remained undisturbed until its sampling time. At the sampling time individual samples were taken for the chemical analysis and for the microbiological analyses (16S rRNA gene amplicon sequencing and (RT)-qPCR). For the former approximately 10 mL mixed sediment-groundwater suspension was filtered (0.22 µm PES) to remove bacteria and to analyse nitrate, nitrite and ammonium. For the microbiological analyses two times 15 mL of the suspension were centrifuged for 10 min at 7700 x g and 4°C, the supernatant was discarded, and the pellets frozen at -80°C until nucleic acid extraction. The samples from the H_2-treated microcosms sacrificed at 40 h, 100 h and 114 h, as well as the samples from the sterile microcosms were not included in the 16S rRNA amplicon sequencing because no changes in the bacterial community composition was expected according to the NO_3^-/NO_2^- measurements and because this method cannot discriminate between living and dead cells in the sterile control samples.

3.1.3. Isolation of hydrogenotrophic denitrifiers (PIIa)

Hydrogenotrophic denitrifiers were enriched and isolated to detect complete hydrogenotrophic denitrifiers and to characterise their individual denitrification genotypes and phenotypes (Figure 4). Based on the results of PI, the focus was on hydrogenotrophic denitrifiers from the *Rhodocyclaceae* family, as these had been shown to enrich over time in the microcosm incubations with H_2. The enrichment and isolation process was performed twice, termed EI and EII, because EI resulted in little isolates assigned to the family *Rhodocyclaceae*. For EII the use of mineral medium (MM) was dispensed during the enrichment, and it was diluted in the preparation of the agar plates used for isolation.

Enrichments and isolation

The enrichments were set up inside 200 mL vials containing approx. 100 mL of either groundwater (GW), sediment and groundwater (SED/GW), mineral medium and groundwater (MM/GW), or mineral medium and sediment (MM/SED). EI comprised two replicates per setup (GW, SED/GW, MM/GW, MM/SED) and EII four replicates per setup (GW, SED/GW). The bottles were sealed with a rubber septum fastened by an aluminium crimp cap. Nitrate concentrations were approx. 1.13 mM (70 mg L^{-1}) in the MM, as well as in the GW and SED samples. The exact GW, SED, and MM volumes are specified in ([106], Table S4). The MM included following minerals: 1 g L^{-1} NaCl, 0.188 g L^{-1} $MgCl_2$, 0.2 g L^{-1} KH_2PO_4, 0.25 g L^{-1} NH_4Cl, 0.5 g L^{-1} KCl, and 0.15 g L^{-1} $CaCl_2$ * 2 H_2O (basal medium of [107]). It additionally contained separately autoclaved 30 mM $NaHCO_3$ buffer and 1.5-2 mM $NaNO_3$, as well as filter-sterilized 0.2% (v/v) trace element solution (DSMZ Mineral Medium 461) and 0.1% (v/v) vitamin solution [108] (compositions listed in Table 1), as well as 0.1% (v/v) selenite tungsten solution [107]. All components were added to the basal medium after autoclaving and lastly the pH was adjusted to 7.2 with 1M HCl. Sealed vials were flushed with a gas mixture of 60% H_2, 10% CO_2, and 30% N_2 for approx. 15 minutes until the outflowing air contained 0% O_2 (digital oximeter, Greisinger Electronic, Germany) and were thereafter incubated at 14-20°C. NO_3^- and NO_2^- concentrations were quantified every two to five days over the enrichment period. The complete consumption of NO_3^- and NO_2^- took between six and 46 days, depending on the composition of the enrichment setup. Afterwards the enriched cultures were serially diluted (10^{-2} - 10^{-4}) and plated onto agar plates. The agar plates used during EI consisted of the described MM and 1.5% (w/v) purified agar (Oxoid Thermo Fisher, USA). The plates used during EII were prepared either with diluted MM (10% of the original salts, trace elements, and vitamins) or with filtered (0.2 µm) autoclaved groundwater as well as 1.5% purified agar. For one replicate per setup three transfers of 10% (v/v) to fresh MM (EI) and to 0.2 µm filtered and autoclaved GW (EII) were performed upon NO_3^- and NO_2^- depletion. These transferred enrichments were plated as described above on agar plates for the isolation of hydrogenotrophic denitrifiers. The agar plates were placed in anoxic pots, flushed with the same 60% H_2, 10% CO_2, and 30% N_2 gas mixture for over one hour, and incubated subsequently for approximately 6 weeks at 14–20°C.

solution	compound	concentration
trace element SL-10	$FeCl_2 * 4 H_2O$	3 mg L^{-1}
	$ZnCl_2$	0.14 mg L^{-1}
	$MnCl_2 * 4 H_2O$	0.1 mg L^{-1}
	$CoCl_2 * 6 H_2O$	0.19 mg L^{-1}
	$CuCl_2 * 2 H_2O$	0.002 mg L^{-1}
	$NiCl_2 * 6 H_2O$	0.024 mg L^{-1}
	$Na_2MoO_4 * 2 H_2O$	0.036 mg L^{-1}
	H_3BO_3	0.006 mg L^{-1}
	HCl (25%)	0.02 ml
vitamin	folic acid	2 µg L^{-1}
	p-aminobezoic acid	5 µg L^{-1}
	D(+) biotin	2 µg L^{-1}
	nicotinic acid	5 µg L^{-1}
	vitamin B5	5 µg L^{-1}
	pyridoxine hydrochloride	10 µg L^{-1}
	thiamine hydrochloride	5 µg L^{-1}
	riboflavin	5 µg L^{-1}
	vitamin B12	0.1 µg L^{-1}
	lipoic acid	5 µg L^{-1}

Table 1 Composition of the trace element solution SL-10 (DSMZ Mineral Medium 461) and the vitamin solution [108] used to prepare the mineral medium.

Colony Screening and Taxonomic Assignment of Isolates

In total 300 colonies were screened taxonomically by full length 16S rRNA gene Sanger sequencing. A large fraction of the colonies resembled the colony morphology of *Dechloromonas denitrificans* [109]: round, < 0.5 mm in diameter, white/transparent with smooth edges (Figure 6).

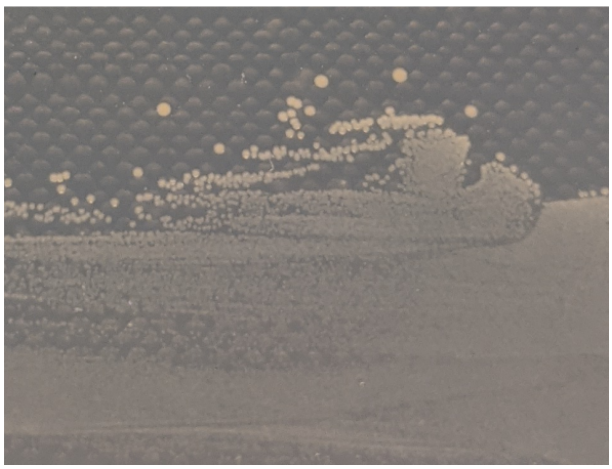

Figure 6 Colony morphology of a *Dechloromonas denitrificans* isolate.

Forty-five different isolates of the 300 screened colonies, including several assigned to the species *D. denitrificans*, *F. limneticum*, *Q. australiensis* and *H. taeniospiralis*, were further individually tested for their ability to reduce NO_3^- in liquid MM with a H_2 containing atmosphere. The isolates able to reduce at least 35% of the initial NO_3^- were assigned to the species *F. limneticum*, *D. denitrificans*, and *H. taeniospiralis* according to their 16S rRNA gene sequences ([106] Table S3). The isolates with the following abbreviations were chosen to be analysed genotypically and phenotypically: $F76_{(HD)}$, $F77_{(HD)}$, $F128_{(HD)}$, $F132_{(HD)}$ (*F. limneticum*), $D110_{(HD)}$, $D6_{(HD)}$ (*D. denitrificans*), and $H3_{(HD)}$, $H2_{(HD)}$ (*H. taeniospiralis*). As these were later proven to be complete hydrogenotrophic denitrifiers they are marked with HD hereafter. Additionally, three taxa, whose closest relatives were *D. denitrificans* and *Q. australiensis*, without the ability to reduce NO_3^- with H_2, were also selected for further characterisation. They were given the following abbreviations: D98 (*D. denitrificans*) and Q9/Q100 (*Q. australiensis*).

Bacterial Community Analysis of Enrichment Cultures

Additionally, samples of the final enrichments and of the original sediment and groundwater samples were taken to determine their bacterial community. For the enrichments with sediment (SED/GW, MM/SED) 2 mL was sufficient, whereas 10 mL were required of the other enrichments. These were pelleted and frozen for the analysis. For the original groundwater sample, 3 L groundwater material were collected on a 0.22 µm filter. The DNA of these samples was extracted with the NucleoSpin Soil Kit (Macherey Nagel, Germany) and subsequently the bacterial community composition was determined by 16S rRNA gene amplicon sequencing.

3.1.4. Genotypic and phenotypic characterisation of the isolates (PIIb)

The overall goal of the isolate characterisation was to determine in what way the individual taxa were contributing to intermediate accumulation during denitrification and whether these phenotypes could be attributed to certain genetic features (Figure 4).

Genotypic characterisation

The genomes of the 11 isolates $F76_{(HD)}$, $F77_{(HD)}$, $F128_{(HD)}$, $F132_{(HD)}$, $D110_{(HD)}$, $D6_{(HD)}$, $H3_{(HD)}$, $H2_{(HD)}$, D98, Q100, and Q9 were sequenced with the PacBio SMRT long-read technology. Genes coding for enzymes required during hydrogenotrophic denitrification, such as denitrification reductases, denitrification regulators, hydrogenases and RubisCO, were determined and specified.

Phenotypic characterisation

Initially, the end product during hydrogenotrophic autotrophic denitrifying growth was determined for all 11 isolates. The respective experiment was termed 'Endpoint analysis'. Therefore NO_3^-, NO_2^-, NO, N_2O, N_2 and CO_2 concentrations were quantified at the end of the incubation period. The final pH and pressure inside the incubation vials were determined as well.

Further, the denitrification kinetics of a sub-selection of three isolates, comprising one isolate of each phylogenetically distinct hydrogenotrophic denitrifier group ($F76_{(HD)}$, $D110_{(HD)}$, $H3_{(HD)}$), were analysed over time under three different conditions. The kinetics were investigated when the cells were depleting O_2 and transitioning to the anaerobic reduction of NO_3^- to N_2. These transition experiments were conducted under litho-autotrophic conditions with H_2 as the sole electron donor and CO_2 as the carbon source (*Litho-autotrophic transition*), as well as with an organic carbon containing medium (*Organo-heterotrophic transition*). Differences between these two transition experiments indicate whether intermediate accumulation or other denitrification characteristics differ depending on the electron donor. Another litho-autotrophic kinetics experiment was performed with bacteria already adapted to denitrification, thus with cells equipped with a fully expressed denitrification proteome (*Adapted litho-autotrophic*). Differences between the *Litho-autotrophic transition* and *Adapted litho-autotrophic* experiments indicate whether intermediate accumulation is caused by either delayed gene expression of some denitrification reductase genes during the transition phase or by the kinetics of the different denitrification reductases and the respective electron pathway. The anoxic batch cultures containing the medium and atmosphere of the respective experiment were placed inside a robotised incubation system with a constant temperature of 18°C and stirring. They were auto-sampled in parallel on a regular basis to measure the gases NO, N_2O, N_2, and O_2 via gas chromatography. Concurrently the liquid NO_2^- concentration was determined in manually taken small liquid samples.

3.1.5. Column experiment

The columns were prepared with quartz sand (∅ 0.7 cm) at the influent and effluent segment (5 cm each) and with collected sediment in the middle part (40 cm). Collected groundwater, containing 65-70 mg L^{-1} NO_3^-, was first saturated with N_2 and circulated through the column to make it anoxic. After approximately 80 h, the groundwater was saturated with H_2 gas with a hydrogen generator, whereby hydrogenotrophic denitrification was stimulated. Initially, a strong decrease in NO_3^- was observed concurrent with a peak in NO_2^-. An equilibrium at 45-50 mg L^{-1} NO_3^- and approximately 15 mg L^{-1} NO_2^- was reached after further 125 h. The same experiment was

performed in April and December of 2019. These measurements cannot be shown in this thesis as they will be published by our collaborator. At the end of the experimental run sediment samples for microbiological analysis were taken from 2 cm sections of each 50 cm long column. The samples were frozen until a selection of the samples (sections 6-12 cm, 24-30 cm, and 38-44 cm) was subjected to DNA extraction and 16S rRNA gene amplicon sequencing. A negative extraction control was run alongside the samples. The average and standard deviation of the 12 samples of each column were calculated.

3.2. Chemical analyses

3.2.1. Nitrate, nitrite and ammonium measurements

Nitrate and nitrite were determined for all experiments; however, they were quantified for the different experiments in different laboratories. Therefore, and because the different experiments did not require the same level of accuracy, different methods of nitrate and nitrite determination were used.

PI and column experiment:

The NO_3^- and NO_2^- concentrations were quantified in the filtered liquid samples with ion chromatography (DIONEX ICS-1100, Thermo Fisher Scientific, Waltham, USA). The detection limits were 0.008 mM for NO_3^- and 0.007 mM for NO_2^-. The NO_3^- and NO_2^- concentrations were measured for all vials of PI, while the NH_4^+ concentrations were determined only for one representative replicate, as no changes were expected. The detection limit was 0.013 mM for NH_4^+.

PIIa:

The NO_3^- and NO_2^- concentrations of the enrichments were determined in a fast manner using spectrophotometry. The monitoring of the NO_3^- and NO_2^- reduction did not require high accuracy; however, results were needed instantly. NO_3^- was quantified by adding 50 µL of 5% resorcinol and 1.3 mL 36N sulphuric acid to 1 mL sample. The absorption at 360 nm wavelength was measured in a spectrophotometer after the mixture had cooled down, and it was compared to a standard curve (Velghe & Claeys, 1985). NO_2^- was quantified according to Tsikas et al. (1997), where 100 µL 37.5 mM sulfanilic acid and 100 µL 20% acetic acid were added to 1 mL sample, which was then incubated for 10 minutes in the dark. Afterwards 100 µL 12.5 mM N-(1-naphtyl)ethylendiamine dihydrochloride was added and the mixture was again incubated in the dark for 20 minutes. Finally, the absorption was measured at 540 nm wavelength and compared to a standard curve.

PIIb:

The NO_3^- and NO_2^- measurements for the denitrification phenotype analyses required high accuracy. Thus, both were quantified by converting NO_3^- and NO_2^- to NO and then analysing the NO concentrations with a chemiluminescence NOx analyser (Sievers 280i, GE Analytical Instruments) (Cox, 1980, Braman & Hendrix, 1989, MacArthur et al., 2007). Therefore, 10 µL bacterial suspension was added to a triiodide (I_3^-) solution, converting NO_2^- to NO, thereby determining the NO_2^- concentration. An additional 10 µL of bacterial suspension was added to a heated 1M vanadium(III) chloride ($VaCl_3$) solution (95°C), which converted both NO_3^- and NO_2^- to NO. The NO_3^- concentrations thus resulted from the difference in the NO_2^- and NO_3^-/NO_2^- measurements. The detection limits were approx. 0.002 mM for both methods.

3.2.2. Gas measurements

Gas concentrations in the headspace of the anaerobic incubations were determined for the denitrification phenotype analyses of PIIb. The prepared vials were therefore placed inside the 18°C water bath with continuous stirring at 600 rpm of the robotised incubation system [110, 111]. The headspace gas of each incubation vial was automatically sampled every two to four hours, depending on the length of the experiment. Per measurement 1.9 mL headspace gas was sampled and injected into a gas chromatography (CP4900 microGC, Varian (now Agilent Technologies)) to quantify O_2, N_2, N_2O, CO_2 and CH_4 concentrations. The samples were additionally injected into a chemiluminescence NOx analyser (Model 200A, Advanced Pollution Instrumentation, USA) to quantify the NO concentrations. Further details on the instruments and method are given in Bergaust et al. 2008 [112]. The sampling volume was replaced in the headsapce after each measurement by an equal volume of helium gas, whereby the headspace pressure was maintained at approximately 1 atm. Three standard gas mixtures, containing 25 ppmv NO in N_2, 150 ppmv N_2O and 1 % CO_2 in He, and 21 % O_2 in N_2, were measured alongside for every time point in order to calibrate the gas concentrations and to capture the dilution of the headspace gases due to the sampling as well as leakage over time. In the continuous litho-autotrophic incubations with H_2 and CO_2 gas, the pressure in the headspace was reduced as the bacteria were consuming both H_2 and CO_2. To improve the accuracy of the measured gases, the pressure loss was estimated and integrated into calculating the gas concentrations and parameters derived thereof. The stoichiometry for the hydrogenotrophic denitrifying incubations was therefore not as accurate as described for heterotrophic incubations in Molstad et al. 2007 [110]).

The chromatography output (ppmv) was converted to µM in liquid for O_2, nM in liquid for NO, and µmol $vial^{-1}$ for N_2O-N and N_2-N. The gas solubility of the measured gases at the condition of the incubations (18°C and pH 7.1) as well as the measurements of the standard gas mixtures were therefore considered. In the kinetics analyses NO_2^- was measured at different time points than the gases, thus the concentrations at the gas measurement time points were interpolated using the SRS1 Cubic Spline Software (http://www.srs1software.com) and converted to µmol $vial^{-1}$. Additionally, the electron flow [µmol e^- h^{-1}] to terminal oxidases and the denitrification reductases (Nar/Nap, Nir, Nor, Nos) was calculated with the gross rates of each denitrification step [113].

3.3. Molecular analyses

3.3.1. DNA extraction

Several different DNA extraction methods were applied depending on the amount of DNA present in the samples and the required intactness of the DNA for the intended use.

PI and column experiment:

The DNA of the microcosm samples (PI) was extracted from a complete pellet, comprising 15 mL pelleted groundwater-sediment suspension, and the DNA of the column sections was extracted from 0.45-0.75 g sediment. A phenol-chloroform based protocol described in Lüders et al. 2004 [114] and Töwe et al. 2011 [115] was used therefore. A negative extraction control, without sample

material, was performed concurrently for every new extraction run. For the phenol-chloroform based method, samples were bead-beaten for 30 s at 5.5 m s^{-1} together with $NaPO_4$ buffer and a SDS-containing solution. The following centrifugation step for 10 min at 14 000 x g and the subsequent transfer of the supernatant removed solid particles in the sample and freed the DNA from histones and the lipid membrane. The DNA containing suspension was then mixed with phenol/chloroform/isoamylalcohol and centrifuged to separate the DNA-containing upper aqueous phase from the protein and lipid containing lower organic phase. This step was repeated twice with chloroform/isoamylalcohol to enhance the purification of the DNA. After an incubation with PEG-solution, the DNA was precipitated and washed with 70% ethanol before it was eluted in DEPC-MiliQ water.

PIIa:

The DNA from the enrichments and the original sediment and groundwater samples was isolated with the NucleoSpin Soil Kit (Macherey Nagel, Düren, Germany). The kit was chosen for this purpose due to the limited amount of sample material. Recommended procedures of the manufacturer's protocol were followed, with the lysis buffer SL2 and 30 s 5.5 m s^{-1} bead beating.

PIIb:

The 11 isolates were grown under oxic conditions for two to four days in R2A medium at 30°C up to late exponential phase. A suitable volume was harvested to obtain approx. 4.5 x 10^9 cells, which is the recommended input amount for the QIAGEN Genomic-tip protocol. The genomic DNA of the isolates was then extracted with the QIAGEN Genomic-tip (20/G) procedure (QIAGEN, Hilden, Germany) because the gDNA for PacBio single molecule real time (SMRT) long read sequencing requires intact DNA with as little fragmentation as possible. The protocol of the manufacturer was followed. The kit's procedure does not require a beating step in order to extract the gDNA gently.

3.3.2. RNA extraction and reverse transcription

The RNA of the microcosm samples from PI was extracted from pellets of 15 mL sediment-groundwater suspension, identical to the ones used for the DNA extraction. The extraction was performed with the RNeasy Power Soil Total RNA Kit (QIAGEN, Hilden, Germany) according to the manufacturer's manual. The small amount of residual DNA in the extracts was digested with DNase (TURBO DNase, Invitrogen, Waltham, USA) using 1 µg RNA as input. The RNA was thereafter purified with the RNA Clean & Concentrator-5 Kit (Zymo Research, Irvine, USA). In order to validate the absence of DNA in the RNA extracts, a *nirS* based qPCR was performed as described in section 3.4. A *nirS* gene based PCR was favoured over a 16S rRNA gene based PCR to avoid complications due to DNA contamination in laboratory reagents (Salter et al., 2014). Moreover, the *nirS* gene was highly abundant in the DNA extracts of all samples, according to the previously performed *nirS* qPCRs with DNA. The integrity of the extracted RNA was determined with a Fragment Analyzer (Agilent Technologies, Santa Clara, USA) and the standard sensitivity RNA analysis kit (DNF-471, Agilent Technologies), because reverse transcription requires RNA of high quality. The ProSize data analysis software determines the RNA quality number (RQN) by capillary electrophoresis, where 1 represents completely degraded RNA, and 10 undamaged RNA (ProSize 3.0.1.6, Advanced Analytical Technologies, USA). The RNA of one H_2-treated vial from time point 30 h had a RQN of only 3.5, which was considerably lower compared to the rest of the

samples with an average RQN of 7.12 (SD 0.77). The outlier sample with a RQN of 3.5 was thus omitted from further analyses.

The reverse transcription reaction contained 40 ng RNA, 1X RT buffer, 1X dNTPs, 1X RT random primers, and 50 U MultiScribe reverse transcriptase from the High-Capacity cDNA Reverse Transcription Kit (Applied Biosystems, Waltham, MA, USA). It contained additionally 20 U RNase inhibitor (Thermo Fisher Scientific, Waltham, USA) to avoid RNA degradation during the reaction. With the purpose of detecting contamination extraction controls without sample input and DNase reaction controls were run alongside of the samples.

3.3.3. DNA and RNA quantification

DNA and RNA were quantified spectrophotometrically and fluorometrically. The examination of the nucleic acids with a nanodrop based spectrophotometer [PEQLAB (now VWR), Pensylvania, USA]; however, mainly served as an indicator of the extract's purity, based on the absorption ratios A_{260}/A_{280} and A_{260}/A_{230}. When an exact quantification was required, for example to calculate the input for the amplicon PCR and the reverse transcription steps, a fluorometric quantification method was performed. The PicoGreen dsDNA Assay Kit (Thermo Fisher Scientific, Waltham, USA) was used for the quantification of DNA and the RiboGreen RNA Assay Kit (Thermo Fisher Scientific, Waltham, USA) was used for the quantification of RNA , both according to the manufacturer's protocol.

3.4. Quantitative real-time PCR

The genes and transcripts of all denitrification reductases (*narG*, *napA*, *nirS*, *nirK*, *qnorB*, *cnorB*, clade I *nosZ*, and clade II *nosZ*) as well as the 16S rRNA gene (Table 2) were quantified by real-time PCR on a 7300 Real-Time PCR System (Applied Biosystems, Waltham, USA) for PI. To avoid PCR inhibition, the optimal dilutions of the DNA and cDNA extracts were determined initially. A dilution series of exemplary samples was therefore subjected to *nirS* and 16S rRNA gene qPCR to obtain the dilution at which inhibition is no longer observed. For the DNA extracts a dilution of 1:25 was needed for the functional genes and a dilution of 1:500 for the 16S rRNA gene. For the cDNA extracts a dilution of 1:8 was sufficient for the functional genes except for the RT-qPCR of clade II *nosZ*, which did not require any dilution at all.

The standards of all genes, except for clade II *nosZ*, were composed of the respective gene fragment inserted into a plasmid. The origin of the inserted gene fragments are stated in table 2. In the case of the clade II *nosZ* standard, the plasmid backbone seemed to inhibit the gene amplification, thus another approach was implemented. The clade II *nosZ* gene of *D. denitrificans* DNA was therefore amplified, purified, quantified, and then used as a linear standard. The preparation of the standard was performed prior to the (RT)-qPCR to avoid degradation. All standards were serially diluted with copy numbers ranging from 10^7 to 10 gene copies per reaction.

Gene	Thermal profile & cycles	Primer pair	[µM]	Standard
16S rRNA	(95°C-15",58°C-30",72°C-30") x40	FP 16S, RP 16S [116]	0.2	*P. putida*
napA	(95°C-30",60°C-30",72°C-30") x5a	V17m	0.4	*P. fluorescens*
	(95°C-30",55°C-30",72°C-30") x40	napA4r [117]		
narG	(95°C-30",63°C-30",72°C-30") x5[a]	narG-f	0.2	*P. stutzeri*
	(95°C-30",58°C-30",72°C-30") x40	narG-r [117]		
nirS	(95°C-45",57°C-45",72°C-45") x40	Cd3aF [118]	0.2	*P. stutzeri*
		R3cd [119]		
nirK	(95°C-30",63°C-30",72°C-30") x5[a]	nirK876 [120]	0.2	*A. irakense*
	(95°C-30",58°C-30",72°C-30 s) x40	nirK5R [121]		
qnorB	(95°C-15",60°C-30",72°C-30") x5[a]	qnorB2F	0.4	*S. meliloti*
	(95°C-15",55°C-30",72°C-30") x40	qnorB5R [48]		
cnorB	(95°C-15",60°C-30",72°C-30") x5[a]	cnorB2F	0.4	*P. putida*
	(95°C-15",55°C-30",72°C-30") x40	cnorB6R [48]		
clade I	(95°C-15",65°C-30",72°C-30") x5[a]	nosZ2F	0.4	*P. fluorescens*
nosZ	(95°C-15",60°C-30",72°C-30") x40	nosZ2R [121]		
clade II	(95°C-30",59°C-30",72°C-45") x5[a]	nosZII-F	1	*D. denitrificans*
nosZ	(95°C-30",54°C-30",72°C-45",80°C-30") x40	nosZII-R [122]		

Table 2 Thermal profiles for the 16S rRNA and denitrification reductase gene qPCRs, the primer pair and their input concentration as well as the origin of the inserted gene of the standard.

Each qPCR reaction contained 1X Power Sybr Green Master Mix (Applied Biosystems, Waltham, USA), 0.2-1 µM forward and reverse primer (Table 2), and 2 µL diluted DNA/cDNA. For stabilization, the qPCR reactions of most genes contained 0.06% BSA, only the qPCR reaction of clade II *nosZ* required 0.25 µg T4 Gene 32 protein . The qPCRs cycling conditions (Table 2) were adjusted to the respective primer pair; however, they were all initiated with a 10 s denaturation step and were finalized with a melting curve. The melting curve results were used to validate the specificity of the amplified products. When the results of the melting curve were imprecise, an additional agarose gel of exemplary samples was performed. The R^2 of all standard curves was above 0.99 and the efficiencies at least above 70% (Table 3). The efficiencies were calculated using the slope of the standard curve with the equation Eff = $10^{(-1/\text{slope})}$-1 [115]. The gene and transcript copy numbers were calculated per mL sediment-groundwater suspension and were displayed as connected dot plots including the standard deviation.

Gene	Efficiency [%] of qPCR	Efficiency [%] of RT-qPCR
16S rRNA	80.55	-
napA	71.26	72.79
narG	77.93	81.89
nirS	99.37	92.82
nirK	98.35	99.66
qnorB	88.57	77.57
cnorB	70.51	78.08
clade I *nosZ*	89.51	94.17
clade II *nosZ*	70.40	72.79

Table 3 Efficiencies of the performed qPCRs and RT-qPCRs from PI.

3.5. DNA sequencing and data processing

3.5.1. Sanger sequencing

The full 16S rRNA genes of the obtained isolates (PIIa) were amplified with the primer pair 27F and 1429R [123]. Therefore, one colony was added to 50 µL PCR reaction mixture, that included 1X PCR buffer, 0.2 mM dNTPs, 1.5 mM $MgCl_2$, 0.1 mg BSA, 0.2 µM forward and reverse primer, as well as 3 U Taq DNA polymerase (Thermo Fisher - Invitrogen, Waltham, USA). The PCR was initiated by denaturing the DNA at 94°C for 10 min, followed by 30 cycles of 94°C 1 min - 56°C 1 min - 72°C 1.5 min, and finalized with an elongation step at 72°C for 5 min. The PCR reaction products were purified with the Nucleo-Spin Gel and PCR Clean-up Kit (Macherey-Nagel, Düren, Germany). The obtained 16S rRNA gene fragments were then sequenced with the Sanger method using BigDye Terminator v3.1 sequencing chemistry on an ABI 3730 capillary sequencer (Thermo Fisher Scientific, Waltham, USA). Afterwards, the sequencing chromatograms were manually reviewed and amended if necessary. After the forward and reverse reads were merged, the taxonomy was assigned by aligning the sequences against the rRNA/ITS databases of the nucleotide Basic Local Alignment Search Tool (nblast) (NCBI: https://blast.ncbi.nlm.nih.gov/Blast.cgi).

3.5.2. MiSeq 16S rRNA amplicon sequencing

The bacterial community composition of PI, PIIa and the column experiment was determined by 16S rRNA gene-targeted amplicon sequencing with an Illumina MiSeq sequencer (Illumina, San Diego, USA). The library preparation and sequencing was performed for each experiment individually. Approximately 300 base pairs of the 16S rRNA gene were therefore amplified; however, different primer pairs were used due to changes in the research unit‘s standardised protocol for amplicon sequencing analyses of environmental samples. Primer pair 0008f/0343r

[124], amplifying the V1 and V2 region, was used for PI, whereas primer pair 0515f/0806r of the earth microbiome project [125, 126], amplifying the V4 region, was used for PIIa and the column experiment (Table 4).

Each amplicon PCR reactions contained 0.2 µM forward and reverse primer, 1X NebNext High-Fidelity PCR Master Mix (New England BioLabs, Ipswich, USA) and 2-4 ng of DNA. The reaction mixtures were initially denatured for 1 min at 98°C, followed by 25-27 cycles of 98°C 10 s - 60°C 30 s - 72°C 30 s, and concluded with a final elongation step at 72°C for 5 min. Triplicates were pooled when the successful amplification was confirmed by an agarose gel and were further purified with magnetic beads (AMPure XP Beads, Beckman Coulter, Brea, USA or MagSi-NGSPREP Plus, magtivio, Nuth, Netherlands) at a volume ratio of 0.6:1 or 0.8:1 beads per sample. The ratio 0.6:1 was used when the amplification products contained recognisable primer-dimers on the agarose gel. This was the case for the 0515f/0806r primer pair, so the samples of PIIa and the column experiment were also purified twice. The purified products were run on a capillary fragment analyser (Agilent Technologies, Santa Clara, USA) to determine the amplicons' size, concentration, and purity.

The following indexing PCR reaction of total 25 µL contained 8-10 ng amplicon DNA, 1X NebNext High-Fidelity PCR Master Mix, and 2.5 µL of sample-specific forward and reverse indexing primer respectively (Nextera Dual Indexes Set, Illumina, San Diego, USA). The PCR started with 30 s of initial denaturation at 98°C, followed by 8-10 cycles of 98°C 10 s - 55°C 30 s - 72°C 30 s, again concluded by 72°C for 5 min. The indexed amplicons were purified and analysed by capillary electrophoresis as described above. Afterwards samples were diluted to 4 nM, pooled equimolar and then loaded on the Illumina MiSeq platform with 20% PhiX for paired-end sequencing with the Reagent Kit v3 (2x300 bp) (Illumina, San Diego, USA).

The sequenced reads were demultiplexed and processed with QIIME2 using the DADA2 plugin for denoising [127]. The N-terminal trimming was set to 10 bp in all experiments, while the C-terminal trimming was set to the basepair at which the quality score fell below 25. Forward reads were thus trimmed at 260-280 bp and reverse reads at 200-220 bp (Table 4). After the denoising step on average 44.7% of the reads remained in PI, 66.7% in experiment PIIa, and 57% in the column experiment. Thereafter three types of reads were removed. The removed reads included single reads, reads from non-bacterial domains and reads of ASVs with more than 9 reads detected in the negative extraction control sample. A classifier was pre-trained with the respective primer pair based on the SILVA 16S database release 132 [128] for the actual taxonomic assignment. Subsampling to the minimum number of reads per sample in the respective run was performed with the vegan package (version v2.4-2 and 2.5-7) [129] in R project (version 3.5.3 and 4.0.3) [130] to account for unequal sampling depth.

Experiment	DNA extraction	primer pair	C-terminal trimming	reads after denoising [%]	# reads after subsampling
PI	phenol-chloroform	0008f/0343r	f:260 r:220	44.70	17 515
PIIa	NucleoSpin Soil Kit	0515f/0806r	f:270 r:200	65.34 (EI)	35 921 (EI)
				68.04 (EII)	28 584 (EII)
column experiment	phenol-chloroform	0515f/0806r	f:280 r:200	57.00	36 752

Table 4 Differences in the 16S rRNA amplicon sequencing library preparation procedure between PI (microcosms), PII (enrichments of hydrogenotrophic denitrifiers), and the column experiment.

3.5.3. SMRT PacBio genome sequencing

The genomic DNA of the 11 selected isolates was sequenced using the PacBio SMRT long-read technology. SMRTbell libraries were prepared from the extracted gDNA with the SMRTbell Express Template Prep Kit 2.0 Part Number 101-696-100 Version 6 (March 2020) (PacBio, Menlo Park, USA) according to the manufacturer's protocol. The gDNA was sheared to 9-14 kb long fragments using g-TUBEs (Covaris, Woburn, USA) and then further processed without additional size selection. Each library, with a maximum expected genome size of 33 Mb, was sequenced separately. They were each loaded onto two SMRT cells at 3 and 6 pM, as recommended by the PacBio diffusion loading protocol. Initially the libraries were immobilized on the SMRT cells for 2 h, followed by 2 h of pre-extension. They were then sequenced on the Sequel System using 3.0 chemistry and a movie time of 10 h. The SMRT Link software (version 8.0.0.80529, PacBio) with the HGAP4 pipeline was used to assemble the genomes. The seed coverage was therefore set to 30. The sequences were circularised with the Circlator software v1.5.5 [131] in order to assess the completeness of the genomes. The genome sequence quality was additionally assessed with the CheckM software v1.1.2 [132].

3.6. Bioinformatics

3.6.1. Community analyses

The analyses of the 16S rRNA gene amplicon data were performed in R project with additional packages. The rarefaction curves, assessing the sequencing depth, were generated with the vegan package (version v2.4 2) [129]. The vegan package was also used to calculated the alpha diversity indices Shannon and Simpson, which were then converted to the effective number of species (ENS) by taking the exponent of the Shannon index and by dividing one by the complement of the Simpson index [133]. All stacked bar plots, showing the relative abundance on different taxonomic levels (phylum, family, ASV), were computed with the phyloseq package (version 1.30.0 and 1.34.0) [134]. The 40 most abundant ASVs of the phyla *Proteobacteria* and *Bacteroidetes* in

the H_2-treated microcosms (PI) were selected and depicted in a heatmap, generated with the ComplexHeatmap package [135].

Some ASVs which increasing in relative abundance in the H_2-treated microcosms of PI were not taxonomically assigned up to the genus level. To narrow down the taxonomy of these unassigned ASVs, their 324 bp long amplicon sequences were aligned against the rRNA/ITS databases (NCBI: https://blast.ncbi.nlm.nih.gov/Blast.cgi) with the nucleotide Basic Local Alignment Search Tool (nblast). As the resulting percentage identity was below 97%, maximum-likelihood phylogenetic trees were additionally created. The phylogenetic trees were generated with the software MEGA-X [136] including the amplicon sequences and trimmed 16S rRNA gene sequences of closely related type species downloaded from the SILVA database [128].

3.6.2. Genome analyses

Important genes of hydrogenotrophic denitrification were identified and their specific class was determined. Several methods were combined to avoid false annotations. These included genes coding for denitrification reductases, RubisCO, hydrogenases, and denitrification regulators. Initially, the circularized genomes were annotated with Prokka v1.13 [137] using blast v2.7 and a similarity e-value cut-off of 1e-05. The Prokka annotations of the **denitrification reductase genes** were additionally verified by determining their domain (Table 5). The annotated gene sequences were therefore searched against the conserved domain database (Lu et al., 2020) and the ones without the gene-specific domain accession were eliminated. The genes of the nitrate and nitrite reductases, which evolved separately (*napA*/*narG* and *nirS*/*nirK*) [41], could be differentiated by the the annotations. However, *qnorB*/*cnorB* and clade I nosZ/clade II *nosZ* are different classes of genes descending from a common ancestor, which could not differentiated by the Prokka annotation alone. Thus, the annotated *norB* gene sequences were incorporated in a maximum-likelihood phylogenetic tree with classified *cnorB* and *qnorB* sequences (Genbank AJ507329-AJ507380) from Braker and Tiedje 2003 [48] using MEGA-X [136]. Depending on the position of the respective annotated gene sequence within the phylogenetic tree, their affiliation with the *qnorB* or *cnorB* class could be determined. Clade I and clade II *nosZ* could be differentiated more easily, as they have different domains. Clade I *nosZ* contains the domain accession PRK02888 and clade I *nosZ* contains the domain accession TIGR04246 (Table 5). The **RubisCO genes** (*cbbM* and *cbbL*) were detected using a Hidden Markov Model (HMM) search (HMMER 3.3, http://hmmer.org/) with the Pfam HMMs PF00016 (large subunit) and PF00101 (small subunit) in addition to the te Prokka annotations. In order to identify the RubisCO form, the amino acid sequences of the HMM search hits were included in a maximum-likelihood tree together with the RubisCO partial sequences analysed by Alfreider et al. 2012 [72] (GenBank JF414941–JF415078). The position of the HMM search hits within the tree verified the RubisCO genes and assigned them to form IA, IC, and II. The Prokka annotations for the **hydrogenase genes** were inconclusive. Thus, known [NiFe]-, [FeFe]-, and [Fe]-hydrogenase sequences analysed by Greening et al. 2016 [68] were downloaded from NCBI and were used to detect and classify the hydrogenase genes in the genomes. An HMM specific for each metal-centre type hydrogenase was generated with HMMER 3.3 [138]. Hydrogenase genes in the isolate's genomes were searched using the generated

gene	KEGG	domain accession (CDD)
napA	K02567	PRK13532
narG	K00370	TIGR01580 or COG5013
nirS	K15864	pfam02239 or cl26549 & pfam13442 or COG2010
nirK	K00368	TIGR02376 (superfamily cl31204)
qnorB	K04561	cl00275
cnorB	"	"
clade I *nosZ*	K00367	PRK02888
clade II *nosZ*	"	TIGR04246

Table 5 KEGG numbers and domains accessions of the denitrification reductase genes.

HMMs. Furthermore, maximum-likelihood trees were generated for each metal-centre type with the HMM search hits and hydrogenase sequences from Greening et al. 2016 [68]. Greening et al. 2016 [68] also assigned information on the hydrogenase group and subgroup to the hydrogenase gene sequences. The location of the HMM hit sequences within the tree therefore enabled the verification and classification of the identified hydrogenase genes. Additionally, a manual revision of the L1/L2 metal centre motifs, specific to the respective hydrogenase group/subgroup, as shown in Table 2 of [68], was performed.

The position of these detected genes within the genomes of hydrogenotrophic denitrifiers were visualised for the three sub-selected isolates $F76_{(HD)}$, $D110_{(HD)}$, and $H3_{(HD)}$ with the DNAPlotter [139]. The circular genome representations additionally show the genes on the forward and on the reverse strand as well as the GC-content. If the genes of interest were in proximity, their gene neighbourhood was plotted with the web-based software Gene Graphics [140].

3.6.3. Data availability

The 16S rRNA gene amplicon sequencing dataset of PI is available as part of the BioProject PRJNA626487 in the Sequence Read Archive (SRA) repository under the BioSample accession numbers SAMN14610043-SAMN14610054. Further, the 16S rRNA gene amplicon sequencing dataset of the PIIa enrichments and the assembled genome sequences of the 11 isolates from PIIb are available under the BioProject PRJNA727717. The genome sequences are deposited at NCBI under the BioSample accessions SAMN19030600-SAMN19030611 and the 16S rRNA gene amplicon sequences of the enrichments are deposited in the SRA repository under the BioSample accession numbers SAMN19613689–SAMN19613703. The genomes of the sub-selected isolates with whom the 'Kinetics analyses' were performed were additionally published in a genome announcement [141].

3.7. Denitrification regulatory phenotype analyses

The analyses on the denitrification regulatory phenotypes of the selected isolates were performed in the laboratory of the Nitrogen Group, located at the Norwegian University of Life Sciences (NMBU), under the supervision of Prof. Lars Bakken and Prof. Åsa Frostegård. Initially, the denitrification end products under standard hydrogenotrophic autotrophic conditions were determined for 11 isolates ($F76_{(HD)}$, $F77_{(HD)}$, $F128_{(HD)}$, $F132_{(HD)}$, $D110_{(HD)}$, $D6_{(HD)}$, $H3_{(HD)}$, $H2_{(HD)}$, D98, Q100, and Q9) in an experiment called 'Endpoint analysis'. Thereafter, the denitrification regulatory phenotypes of a sub-selection ($F76_{(HD)}$, $D110_{(HD)}$, $H3_{(HD)}$) were determined by 'Kinetics analyses', whereby O_2, NO_2^-, NO, N_2O and N_2 were monitored over time during three experiments; *Litho-autotrophic transition*, *Heterotrophic transition* and *Adapted litho-autotrophic*.

3.7.1. Incubation setup

The 11 isolates were revived from glycerol stocks on R2A agar plates (1.5%) incubated at 30°C. Liquid pre-cultures were inoculated with single colonies and grown aerobically in complex organic medium, R2A or 20% TSB, to obtain higher cell density. The pre-cultures were washed for the litho-autotrophic experiments to remove the carbon-containing medium before being used as inocula. The cultures were therefore harvested at mid/late exponential phase, centrifuged, and washed with MM. Since the *F. limneticum* isolate $F77_{(HD)}$ did not grow at all aerobically in liquid culture, several colonies were scratched off an agar plate to be used as an inoculum for the 'Endpoint analysis'.

The incubations for the 'Endpoint analysis' and 'Kinetics analyses' were prepared inside 120 mL vials which contained 50 mL medium and a triangular magnetic stirring bar. The incubations of the 'Endpoint analysis' and the *Litho-autotrophic transition* and *Adapted litho-autotrophic* experiments contained the MM described in section 3.1.3, but without the selenite tungsten solution, and a H_2/CO_2 atmosphere. The heterotrophic incubations of the *Organo-heterotrophic transition* experiment contained complex organic medium, R2A for $F76_{(HD)}$ and $D110_{(HD)}$, and 20% TSB for $H3_{(HD)}$. Once the inocula were added to the medium, the vials were closed with rubber septa and aluminium crimp caps, and the headspace gas was exchanged with helium gas during six cycles of evacuation and helium addition under constant stirring (900 rpm) [110]. Each cycle comprised 180 s vacuum pumping, 40 s helium addition, and 30 s pause. Thereafter, the helium overpressure was released. 20 mL CO_2 and 40 mL H_2 were injected into the headspace of the litho-autotrophic incubations, whereas no additional gases were added to the organo-heterotrophic incubations.

3.7.2. Controls

Control vials with the same setup but without inoculum were measured alongside the inoculated vials during all experiments in order to detect potential contamination or leakage of N_2 gas. An additional control containing the same setup with inoculum but without H_2 gas was run for each isolate during the 'Endpoint analysis' as well. This control enabled the detection or exclusion of potential denitrification by carry-over carbon. To ensure that the cultures were pure and viable at

the beginning and the end of the incubations, the inoculum and the final cultures were streaked onto R2A agar plates, incubated at 30°C and examined two to three days later.

3.7.3. Endpoint analysis

The 'Endpoint analysis' was performed in triplicates for all 11 selected isolates. As inoculum, 1 mL pre-culture at an optical density (OD_{600}) of 0.3 was centrifuged at 4400 x g for 5 minutes, washed, and eluted in 1 mL MM. The inoculum was then added to 50 mL MM containing 1.5 mM $NaNO_3$ and 0.5 mM $NaNO_2$. The vials were helium flushed, the overpressure was released, and 40 mL H_2 and 20 mL CO_2 were added. Finally, 1.4 mL N_2O gas (approx. 50 µmol N_2O $vial^{-1}$) were added as well, so that the incubations initially contained all the NOx intermediates of denitrification, except for NO gas. The obtained overpressure of around 0.725 bar (C9555 pressure meter, Comark Instruments, UK) was kept over the incubation period of minimum 10 days at 18°C and 120 rpm inside a shaking incubator. At the end of the incubation period, all measurements took place immediately. Firstly, the overpressure was quantified with a pressure meter (C9555 pressure meter, Comark Instruments, UK), then it was released, and the vials were placed in the robotised incubation system, where the headspace gases were measured twice. Also, the NO_3^- and NO_2^- concentrations were determined, and the pH was measured directly after opening each vial. Growth of hydrogenotrophic denitrifying isolates was visible at the end of the incubations; however, especially the *Rhodocyclaceae* isolate cells were sticking together and were forming lumps, which made it impossible to determine the optical density reliably.

3.7.4. Kinetics analyses

The 'Kinetics analyses', determining the denitrification regulatory phenotypes, were performed for the sub-selection with minimum three replicates (n stated in Table 1 of [106]). Three different kinetics experiments were performed. These experiments varied in the state of the cells (transition to denitrification vs. adapted to denitrification) and in the electron donor and carbon availability (H_2 and CO_2 vs. organic carbon). For the two transition experiments O_2 gas was added to the headspace at the initiation of the incubation. In contrast, the adapted experiment contained cells already expressing the denitrification proteome at the beginning of the incubation, thus remained O_2 free. For the two litho-autotrophic experiments pre-cultures were washed to remove the carbon-containing medium. The vials were incubated and measured in the robotised incubation system until all given NO_3^- had been reduced to N_2. NO_3^- was quantified only initially, but NO_2^- was measured throughout the incubation, more frequently during its accumulation period.

For the ***Litho-autotrophic transition*** experiment pre-cultures were grown to mid/late exponential phase, which signified an OD_{600} of 0.11-0.16 for $D110_{(HD)}$ and $F76_{(HD)}$ and of 0.97-1.55 for $H3_{(HD)}$. 20-50 mL pre-culture were centrifuged at 8000 x g for 10 minutes, washed two times with 20 mL MM, and were then eluted in the same medium. The washing process of the inoculum was performed collectively for all replicates, so that the inoculum was the same within the same experimental run. 1 mL of the inoculum was added to each vial comprising 50 mL MM with 2 mM $NaNO_3$. The vials were helium flushed, H_2/CO_2 gas was added, and they were placed in the robotised incubation system. After acclimatisation to 18°C and stirring for improved gas

solubilization, the overpressure was released and 0.6 mL O_2 gas was added (approx. 26.5 µmol O_2 $vial^{-1}$). The headspace gases were measured in 4 h intervals over a 120 h period. At the end of the *Litho-autotrophic transition* experiment the vials were used for the ***Adapted litho-autotrophic*** experiment, because these cells were already adapted to denitrification. The vials were reconditioned by adding another 2 mM $NaNO_3$, flushing the headspace with helium gas and adding fresh H_2/CO_2 gas. After the release of the overpressure the experiment was started and gases were measured in 2 h intervals over a 24 h period. For the ***Heterotrophic transition*** experiment 1 mL pre-culture at an OD_{600} of 0.1 was added to 50 mL organic medium (R2A for $D110_{(HD)}$ and $F76_{(HD)}$, 20% TSB medium for $H3_{(HD)}$) with additional 2 mM $NaNO_3$. The vials were helium flushed, placed inside the robotised incubation system, and the overpressure was released before 0.6 mL O_2 gas was added. The headspace gases were sampled in 3 h intervals over a 45 h period for the *Rhodocyclaceae* isolates and over a 120 h period for the *H. taeniospiralis* isolate.

3.8. Statistical analyses

Comparisons were tested for statistical significance with a robust one-way ANOVA with trimmed means (t1way function) and the corresponding post-hoc test (lincon function), both from the package WRS2 [142]. This test was used for the amplicon sequencing results because such data is non-parametric. Due to the low number of replicates, the same functions were used to test for differences between isolates during the kinetics experiments (PIIb) and to test for differences in mean gene/transcript copy numbers during the microcosm experiment (PI). For all statistical tests performed, p-values <0.05 after Benjamini-Hochberg correction [143] were considered significant.

4. Results

4.1. Column Experiment

The column experiment was performed to examine the denitrification potential in sediment-groundwater material upon stimulation with H_2 in a flowing system. Since the genera *Dechloromonas, Ferribacterium* and *Hydrogenophaga* had been determined as important hydrogenotrophic denitrifiers in the microcosms (PI) and the isolation and characterisation experiment (PII), it was of interest whether their sequences would also account for a large share in the column experiment. The columns were therefore filled with sediment from the nitrate polluted sampling site in the Hohenthann region. Initially groundwater saturated with H_2 from the same site was flown through. Once the flow-though experiment had run for 330 h and a reduction equilibrium had been reached, the bacterial community composition of the column sediment was determined. The rarefaction analysis of the 16S rRNA gene amplicon data indicates a sufficient sequencing depth as all curves reach a plateau within the subsampled range (Figure 7).

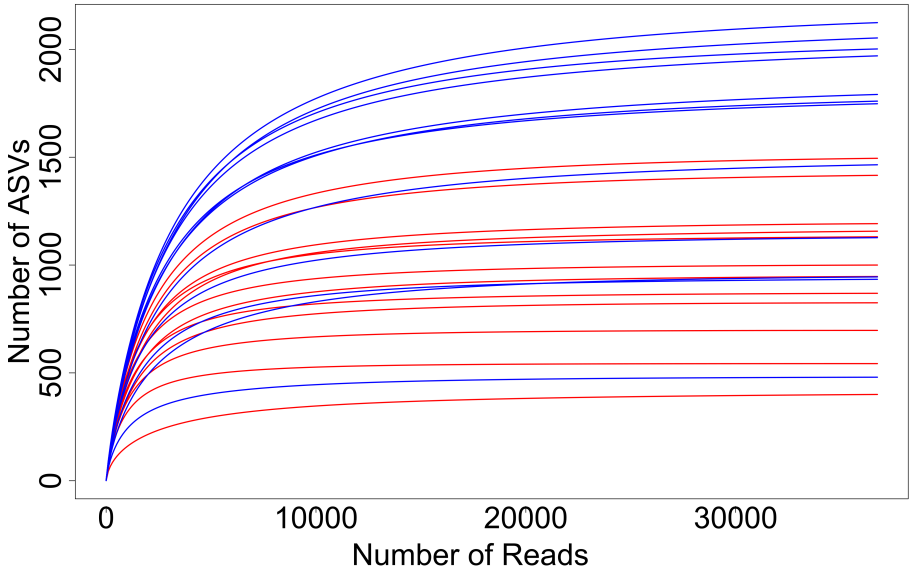

Figure 7 Rarefaction curves of the 16S rRNA gene sequencing results from the April (red) and December (blue) column experiment.

Both, *Dechloromonas* and *Hydrogenophaga*, were among the 20 genera with the highest relative abundance (Table 6). *Dechloromonas* had an average relative abundance of 2.6% in the April and of 2.3% in the December experiment. The average relative abundance of *Hydrogenophaga* was significantly higher with an average of 6.1% and 4.1% respectively (t1way, April $p = 0.01$, December $p = 0.0004$) (Figure 8). A large portion of *Burkholderiaceae* ASVs remained unclassified, 17.7% in the April and 17.3% in the December experiment, which in part may also belong to the genus *Hydrogenophaga*. The genus *Ferribacterium* was also detected but only 0.6% of of reads

were assigned to it in the April and and 0.1% in the December experiment.

Burkholderiaceae	unclassified	17.7 ± 8.8	17.3 ± 3.4
Anaerolineaceae	uncultured	2.0 ± 0.7	1.4 ± 0.5
Rhodocyclaceae	unclassified	1.9 ± 1.5	1.9 ± 0.9
unclassified *Bacillales*		2.0 ± 0.8	1.4 ± 0.3
Rhodocyclaceae	***Dechloromonas***	2.6 ± 1.4	2.3 ± 2.0
Gemmatimonadaceae	uncultured	1.5 ± 0.8	1.4 ± 0.6
Bacillaceae	*Bacillus*	2.3 ± 1.0	1.4 ± 0.4
Rhodocyclaceae	*Methyloversatilis*	0.1 ± 0.1	2.1 ± 1.2
Burkholderiaceae	***Hydrogenophaga***	6.1 ± 3.3	4.1 ± 0.9
unclassified *Chloroflexi*		3.0 ± 1.0	2.7 ± 0.5
Sphingomonadaceae	*Sphingopyxis*	0.1 ± 0.3	1.9 ± 2.1
Nitrospiraceae	*Nitrospira*	1.2 ± 0.5	1.6 ± 0.6
Gaillaceae	*Gaiella*	1.4 ±0.5	1.0 ± 0.3
Xanthobacteraceae	unclassified	1.7 ± 1.4	1.1 ± 0.2
Pseudomonadaceae	*Pseudomonas*	0.6 ± 0.2	2.1 ± 1.4
unclassified *Rokubacteriales*		1.6 ± 0.6	1.4 ± 0.6
Sphingomonadaceae	*Sphingomonas*	0.6 ± 0.8	1.8 ± 0.8
unclassified *Acidobacteria*		2.5 ± 1.0	2.5 ± 0.9
Chromobacteriaceae	*Vogesella*	1.8 ± 0.9	0.6 ± 0.2
Nitrosomonadaceae	MND1	1.0 ± 0.7	1.2 ± 0.5

Table 6 Average relative abundance and the respective standard deviation of the 20 most abundant genera detected in the columns of the April and December experiment.

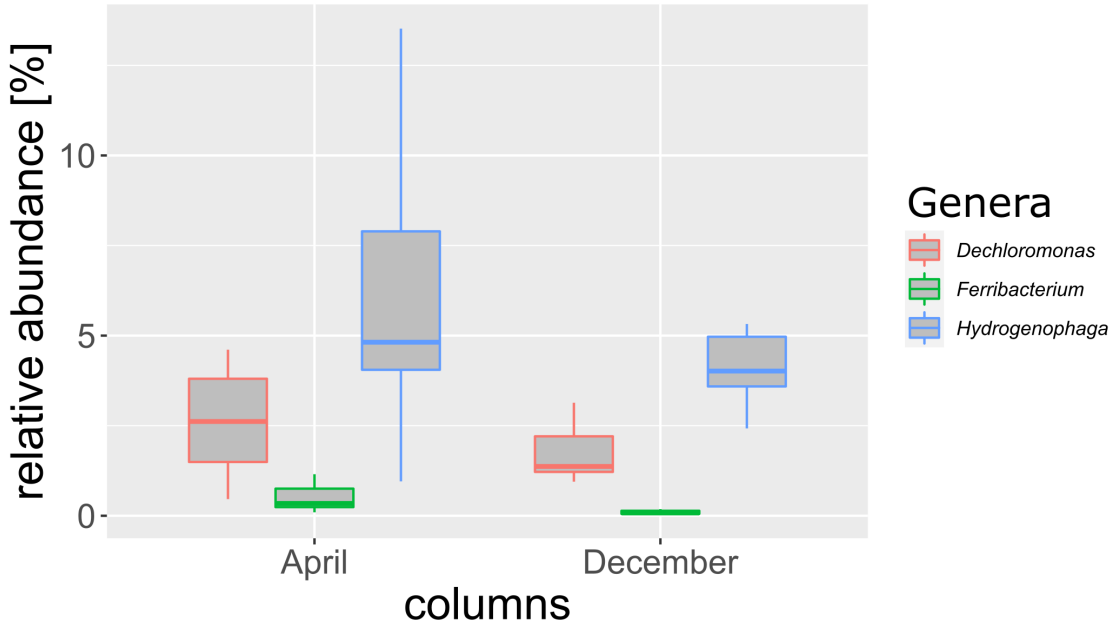

Figure 8 Boxplots showing the relative abundance of the the hydrogenotrophic denitrifier genera *Dechloromonas, Ferribacterium* and *Hydrogenophaga* in the columns of the April and December experiment.

5. Discussion

The research discussed in this thesis is part of the project 'Healthy Water', an interdisciplinary project that aims at understanding hydrogeological and microbiological processes during *in situ* nitrate remediation with H_2 in polluted oxic aquifers. A special focus was set on ways to prevent incomplete denitrification as well as transient accumulation of the intermediates NO_2^- and N_2O. These are known challenges during hydrogenotrophic nitrate remediation studies. This Ph.D. thesis defines the prevailing hydrogenotrophic denitrifying community in a model aquifer and displays the contribution of individual community members to incomplete denitrification and the accumulation of intermediates.

5.1. The few members of the hydrogenotrophic denitrifier community

Hydrogenotrophic denitrification requires the ability to use N-oxides as the electron acceptor, H_2 as the electron donor, and CO_2 as the carbon source. Due to these selective requirements, the hydrogenotrophic denitrifier community, as stated in Hypothesis 1, comprises only few taxa [27, 86]. This was also visible in the performed experiments with aquifer material from the Hohenthann region where only a limited number of bacteria seemed to perform hydrogenotrophic denitrification. All isolated complete hydrogenotrophic denitrifiers (PIIb) belonged to only three species of β-*Proteobacteria*: *Dechloromonas denitrificans*, *Ferribacterium limneticum*, and *Hydrogenophaga taeniospiralis*. The species *Quatrionicoccus australiensis* was also isolated numerously but only reduced NO_3^- to NO_2^- under the tested litho-autotrophic conditions. The low diversity of the hydrogenotrophic denitrifier community was also visible in the results of the microcosm experiment (PI), where the α-diversity, described by the effective number of species (ENS), dropped from 1000 at 30 h to 235 at 80 h. The small enriched community in the H_2-treated microcosms was dominated by the genus *Dechloromonas*, whose relative abundance increased 15.3-fold over the period of NO_3^- reduction. Further, only three unclassified ASVs of the family *Rhodocyclaceae*, likely belonging to the genera *Rhodocyclus, Azospira* or *Propionivibrio*, were additionally determined as part of this community. Both, *Rhodocyclus* and *Propionivibrio*, have been detected in H_2-based reactor experiments previously [86, 89]. Their relevance for *in situ* nitrate remediation with H_2 was; however, not proven within the work of this thesis. Even though one *Propionivibrio* isolate was obtained during PIIa, it only reduced insignificant amounts of NO_3^- in MM under a H_2/CO_2 atmosphere.

Of the total 37 ASVs assigned to *Dechloromonas* in the amplicon sequencing analysis of PI only six increased significantly. These six ASVs positioned in three clusters across the constructed phylogenetic tree, which included all 37 ASVs as well as *D. agitata, D. aromatica, D. hortensis, D. denitrificans*, *F. limneticum* and *Q. australiensis*. The later two are monospecific genera which position within the *Dechloromonas* subtree [144]. Thus, instead of representing three different *Dechloromonas* species, it is more likely that the three clusters represent the species *D. denitrificans*,

F. limneticum and *Q. australiensis*, the *Rhodocyclaceae* species that were numerously isolated in PIIa. Currently, the genus *Dechloromonas* includes three validly published species; *D. agitata, D. hortensis* and *D. denitrificans* (LPSN, https://lpsn.dsmz.de/genus/dechloromonas, 27.08.2021), of whom only *D. denitrificans* is known to perform complete denitrification [109, 145]. This further supports the speculation of the involvement of *F. limneticum* and *Q. australiensis* besides *D. denitrificans* in the H_2-treated microcosms of PI instead of species-specific differences among *Dechloromonas* species. Two of the six *Dechloromonas* ASVs increased in relative abundance only until 70-80 h, the time of nitrate depletion, while the other four increased further. These two ASVs may actually belong to *Q. australiensis* who only reduced NO_3^- to NO_2^- in the phenotypic analyses (PIIb). Also, the lack of ASVs assigned to *Ferribacterium* and *Quatrionicoccus* by the used bioinformatic pipeline was only observed in PI. Both were detected in the 16S rRNA gene amplicon sequencing analyses of the enrichments of PIIa and at least *Ferribacterium* was detected in the column experiment. This absence of ASVs assigned to *Ferribacterium* and *Quatrionicoccus* in the microcosms experiment (PI) may have been due to the usage of different primer pairs. While primer pair 0008f/0343r was used for PI, primer pair 0515f/0806r was used for PIIa and the column experiment. Due to the binding site of the forward primer 0008f at the very beginning of the 16S rRNA gene, 48.6-66.7% of the sequence accessions available in the used SILVA database of *Dechloromonas, Ferribacterium, Quatrionicoccus* and *Hydrogenophaga* do not contain sequence data at the position of the primer pair (according to a TestPrime 1.0 analysis, database SSU r138.1, taxonomy SILVA Ref NR) [124]. In contrast, there are no sequence accessions without data at the V4 region covered by the 0515f/0806r primer pair.

The genera *Dechloromonas* and *Hydrogenophaga* have both been identified as abundant OTUs in several H_2 based biofilm reactors [86, 87, 88, 89]. *Dechloromonas* was also an abundant clade II *nosZ* OTU in an enrichment culture based on acetate and N_2O and also enriched in environments containing environmental contaminants, such as BTEX [146] and perchlorate [147]. The respective families of these two genera have; however, not only been detected in artificial surroundings but also in aquifers comparable to the model aquifers in Hohenthann. For example, in an upper section aquifer in France, which is high in NO_3^- and O_2 but low in DOC [148], 26-57% of detected β-*Proteobacteria* in the groundwater samples were assigned to *Rhodocyclaceae* as well as *Comamonadaceae* and *Oxalobacteraceae* (these families are combined as *Burkholderiaceae* in the used SILVA database release 132). Further, a study that investigated a dynamic alpine oligotrophic porous aquifer found that in the samples collected in May 43% of sequences belonged to *Rhodocyclaceae* and 6% to *Comamonadaceae* whereas in July 16% belonged to *Rhodocyclaceae* and 54% to *Comamonadaceae* [149]. Among these, most *Rhodocyclaceae* sequences were related to the genera *Dechloromonas* and *Ferribacterium*. This widespread occurrence of *Dechloromonas, Ferribacterium* and *Hydrogenophaga* in aquifers suggests that the obtained results based on the model aquifer can be transferred to other comparable aquifers.

The observed phenotypes of the three analysed complete hydrogenotrophic denitrifiers (PIIb) differed in some aspects from the original species descriptions of *D. denitrificans* [109], *F. limneticum* [150] and *H. taeniospiralis* [151, 152]. While the *D. denitrificans* strain isolated from the gut of

an earthworm performs heterotrophic denitrification with acetate, butyrate, glutamate and lactate, among others, it does not oxidise H_2 [109]. Similarly, the *F. limneticum* strain Cda-1, isolated from a mining impacted freshwater lake, does not use H_2 as an electron donor, does not respire NO_2^-, and only grows strictly anaerobic [150]. Interestingly, two obtained *F. limneticum* isolates, $F76_{(HD)}$ and $F77_{(HD)}$, showed a different performance during aerobic cultivation. $F76_{(HD)}$ grew aerobically with carbon, even though slowly, in both R2A liquid culture and on agar plates, whereas $F77_{(HD)}$ only grew small colonies aerobically on R2A agar plates. With a dDDH value of 60.8%, $F76_{(HD)}$ and $F77_{(HD)}$ are likely different strains. It seems therefore, like there are strain-level differences regarding O_2 respiration among *F. limneticum* strains. In contrast to the other two original species descriptions, the original *H. taeniospiralis* strain, isolated from a soil near Barcelona, does grow chemolithoautotrophically with H_2 as an energy source and performs heterotrophic denitrification [151, 152]. However, in the experiments leading to the species description it was unable to combine these two metabolisms and did not perform autotrophic hydrogenotrophic denitrification.

Even though *D. denitrificans*, *F. limneticum* and *H. taeniospiralis* were the closest described relatives of the complete hydrogenotrophic denitrifier isolates, the mentioned phenotypic differences were observed compared to the original species description. The taxonomic assignment based on the 16S rRNA gene identity indicated the affiliation to the respective species, as it was above 98.9% for all *F. limneticum* isolates, 97.77% for all *D. denitrificans* isolates and above 99.3% for the two *H. taeniospiralis* isolates (PIIb). The whole genome-based comparison results of dDDH and GC-content difference were conflicting and in the case of *F. limneticum* unavailable as no whole-genome sequence was available at the time of analysis. However, based on their phenotypic characteristics, the isolated bacteria must be different strains compared to the strains originally described for the respective species. The hydrogenotrophic denitrifier isolates are niche generalists as they may perform many different metabolisms and adapt to changing environments. Among niche generalists large accessory genomes, dispensable genes occurring in only a subset of the species strains, are common [153]. Thus, such differences among strains of the same species are not surprising.

5.2. The different denitrification phenotypes and their impact on intermediate accumulation

Besides a large taxonomic diversity, denitrifying bacteria also comprise a range of different phenotypes [32]. The varying phenotypic traits include truncated and complete denitrification, differences in the timing of the four reduction reactions leading to transient accumulation of intermediates, varying O_2 levels at the initiation of denitrification, and other phenomena such as bet-hedging [32, 57, 60]. The denitrification phenotypes of the three analysed complete hydrogenotrophic denitrifiers were very distinct; especially *H. taeniospiralis* differed from the other two isolates, which confirms Hypothesis 2.

The transient intermediate accumulation of complete denitrifiers can be either temporary, meaning

solely during the initiation of denitrification or lasting. Temporary accumulation is caused by delayed gene expression. Lasting accumulation; however, is caused either by an unbalanced ratio of active enzymes of consecutive denitrification steps or by varying competitiveness of the electron pathways to the different denitrification reductases [154, 155]. The NO_2^- accumulation was lasting in all three analysed complete hydrogenotrophic denitrifier isolates (PIIb), because a similar amount of NO_2^- accumulated when the cells were transitioning from oxic respiration to denitrification as when they were already adapted. This lasting NO_2^- accumulation varied; however, among the three. The *H. taeniospiralis* isolate was transiently accumulating 100% of the given NO_3^- as NO_2^-, whereas *D. denitrificans* only accumulated approximately 20% and *F. limneticum* none at all. During the microcosms experiment (PI), which was dominated by the genus *Dechloromonas* according to the community analysis, the maximum measured NO_2^- was also approximately 20% of the initial NO_3^-. These results are thus in agreement with the pure culture 'Kinetics analyses' results of PIIb. The calculated electron flow of the 'Kinetics analyses' (PIIb) showed that after O_2 depletion electrons were simultaneously flowing to all denitrification reductases in *F. limneticum* and *D. denitrificans*. In *H. taeniospiralis* they were initially only flowing to the nitrate reductases until all NO_3^- had been reduced, which explains the 100% accumulation of the given NO_3^- as NO_2^-. Similar different phenotypes were observed by Liu et al. 2013 [58] when classifying several denitrifying *Thauera* strains. While the group of RCO isolates displayed a simultaneous electron flow to all denitrification reductases, the group of PO isolates was accumulating NO_2^- and did not transcribe *nirS* until the given NO_3^- was consumed [58]. The N_2O accumulation was, on the other hand, temporary in all three characterised isolates. It was clearly higher when the bacteria were transitioning from oxic respiration to denitrification as opposed to when they were already adapted and had expressed the denitrification proteome. A delayed expression of the nitrous oxide reductase genes in hydrogenotrophic denitrifiers could have been visible in the transcript quantification results of the microcosm experiment (PI). However, the transcript quantity of all denitrification reductase genes peaked simultaneously at 80 h. Likely, the measurements temporal resolution of 10 h was too low to detect such a delay in gene expression. In closed systems all transiently accumulated intermediates are eventually reduced to N_2. However, in open aqueous systems, like in flowing groundwater, transient intermediate accumulation becomes relevant, as intermediates may be carried away from the anoxic H_2-rich zone during slow sequential reduction. This would imply incomplete denitrification and therefore impede *in situ* nitrate remediation attempts. In flowing groundwater transient intermediate accumulation is therefore just as harmful to the success of nitrate remediation attempts as actual incomplete denitrification due to a lack of some denitrification genes.

The results of the experiments performed for this thesis collectively indicate that the most important members of hydrogenotrophic denitrifiers were the three analysed complete hydrogenotrophic denitrifier species. However, the abundance ratio of the three species seemed to differ between the experiments. The hydrogenotrophic denitrifier community was either dominated by *D. denitrificans* and *F. limneticum*, both belonging to the family *Rhodocyclaceae*, or by *H. taeniospiralis* of the *Burkholderiaceae* family. This can be observed in the following examples: The microcosm experiment (PI) was dominated by *Dechloromonas* whereas *Hydrogenophaga* was not detected at

all. Further, the EI enrichments (PIIa) were dominated by *Burkholderiaceae* ASVs, whereas the EII enrichments were dominated by *Rhodocyclaceae* ASVs, which was also reflected in the actual isolation output. While the EI enrichments led to a total of 19 isolates assigned to *Hydrogenophaga*, only one *Hydrogenophaga* isolate was isolated during the EII isolation. Inversely, the EII isolation led to a total of 18 *Dechloromonas* and *Ferribacterium* isolates, whereas none thereof were isolated during the EI isolation. Finally, during the column experiments, *Hydrogenophaga* had approximately double the relative abundance than the genus *Dechloromonas*.
The observed difference in dominance between *Dechloromonas* and*Ferribacterium* as well as *Hydrogenophaga* may be due to the slightly different incubation conditions among the performed experiments as well as due to the different sampling time points of the original sediment and groundwater material. Despite relatively stable conditions in aquifers, seasonal changes in the bacterial community compositions are observed, especially in shallow unconfined aquifers [156]. Chick et al. 2020 [156] detected significant seasonal variation in β-*Proteobacteria* sequences, with an elevated abundance during summer. This coincides with seasonal changes in groundwater NO_3^- concentrations which are reaching their highest levels from June to August [157]. The species *D. denitrificans*, *F. limneticum* and *H. taeniospiralis* may react differently to altering NO_3^- concentrations whereby their abundance undergoes different seasonal changes. Possibly other seasonal factors also play a role. The varying seasonal abundance of these prevailing hydrogenotrophic denitrifiers in such shallow unconfined aquifers should be further investigated.

It is generally challenging to prove a causal relationship between microbial community composition and an increased intermediate product ratio, because both measures are also linked to pH and other factors. Additionally, there are large differences in the hydrogenotrophic denitrifying abilities among different species of a genera, thus genus-level community analyses are imprecise. Ways in which the microbial community composition may alter the overall outcome of denitrification include an imbalance in denitrification reductase genes caused by truncated denitrifiers and different phenotypes of complete denitrifiers under the given conditions. The results of this thesis indicate that truncated denitrifiers do not seem to play a major role in hydrogenotrophic denitrifying communities, because most members of the isolated hydrogenotrophic denitrifies (PIIb) performed all four denitrification steps and also harboured the respective genes. In the microcosm experiment (PI), the quantity of the four denitrification reductase genes (*napA*, *nirS*, *cnorB* and clade I *nosZ*) increased within a similar range, indicating that most members of the enriched hydrogenotrophic denitrifier community harboured the genes to perform all four denitrification reactions. The phenotypes of the complete hydrogenotrophic denitrifiers, on the other side, differed substantially and therefore play a major role in affecting transient intermediate accumulation. A recent study by Highton et al. 2020 [158] was able to prove a sustained correlation between the microbial community composition and N_2O emissions in soil because they were able to exclude a pH effect due to the experimental setup. Similar to our results, Highton et al. 2020 [158] showed that in soils with a higher N_2O emission potential the bacterial community was not lacking reductase genes but showed a poor timing of N_2O reduction. Consequently, the N_2O emission potential was determined by different phenotypes that carried out N_2O production either more sequentially or more concurrently. The findings of Highton et al. 2020 support our results. This

signifies that a bacterial community dominated by *H. taeniospiralis* species would denitrify more sequentially, accumulating more NO_3^- and likely also N_2O, compared to a community dominated by *D. denitrificans* and *F. limneticum*.

5.3. Links between genetic features and the denitrification phenotypes

Agreement between the genotype and phenotype is observed in many denitrifiers but there are also numerous exceptions [32]. These exceptions arise from the interaction of the environmental conditions and the regulatory biology of denitrification. The kinetics analyses results revealed that the type of nitrate reductase impacts transient NO_2^- accumulation. This supports Hypothesis 3, stating that the genetic features of hydrogenotrophic denitrifiers shape their denitrification phenotypes.

The eleven analysed isolates (PIIb) were either complete hydrogenotrophic denitrifiers, NO_3^--reducers or non-hydrogenotrophic denitrifying organisms. The complete denitrifiers harboured the four required denitrification reductase genes, thus their genotypes and phenotypes agreed in that regard. The two NO_3^--reducers assigned to the species *Q. australiensis* harboured *napA, cnorB* and clade II *nosZ* genes but were missing a nitrite reductase gene. They reduced NO_3^- but refrained from using N_2O despite the presence of the necessary gene. Another example of a disagreement between the denitrification reductase genotype and phenotype was the isolate D98 which did not perform any steps of hydrogenotrophic denitrification despite possessing all denitrification reductase genes. Such cases may lead to varying results in studies correlating, for example *nosZ* gene abundance to the N_2O emission potential [51, 53, 159]. However, in our genomic analysis, we also considered other necessary genes for a hydrogenotrophic denitrifying lifestyle, such as RubisCO genes, hydrogenase genes and several denitrification regulatory genes. It was thereby observed that D98 was missing a RubisCO gene and thus likely lacks the ability to assimilate CO_2 under the tested conditions. Consequently it also did not denitrify under the hydrogenotrophic autotrophic conditions.

All analysed complete hydrogenotrophic denitrifiers harboured genes coding for one denitrification reductase type for each denitrification step, as well as a gene coding for RubisCO and at least three hydrogenase genes coding for a respiratory, H_2-sensing, and redox-balancing version. Likely this set of genes is required to perform hydrogenotrophic denitrification. The observations highlight the importance of examining the genetic potential of other capacities required to grow under the analysed conditions.

The 100% NO_2^- accumulating denitrification phenotype, as observed in *H. taeniospiralis*, may be linked to the nitrate reductase type, which is Nar as opposed to Nap in *D. denitrificans* and

F. limneticum. Mania et al. 2020 [154] and Gao et al. 2021 [155] observed a strong preference of N_2O reduction over NO_3^- reduction in *napA*-harbouring Bradyrhizobia strains which was abolished if the strain carried a *narG* gene. Based on these result they concluded that Nos is more competitive in recruiting electrons from the quinol pool compared to Nap. Gao et al. 2021 further excluded the alternative explanation of lower Nap than Nos abundance by proteomic analysis. The reduced competitiveness was not observed for strains with Nar [155], thus we can conclude that Nar is generally more competitive compared to Nap. Unfortunately the nitrate reductase type of the *Thauera* strains from Liu et al. 2013 [58] were not determined. However, in the study of Lycus et al. 2017 [32] the denitrification phenotypes and genotypes of numerous denitrifying isolates were determined. Several 'progressive onset' stains, closest related to *Hydrogenophaga* and *Polaromonas*, harboured a *narG* gene and a 'rapid complete onset' strain, closest related to *Bradyrhizobium*, harboured a *napA*.

The amount of temporary transient N_2O accumulation during the transition from oxic respiration to denitrification also differed most between the *Rhodocyclaceae* isolates and the *H. taeniospiralis* isolate. Again, the generally higher N_2O accumulation in *H. taeniospiralis* compared to the other two isolates may be linked to the respective reductase genes, because both $F76_{(HD)}$ and $D110_{(HD)}$ harboured two clade II *nosZ* genes, whereas the *H. taeniospiralis* isolate $H3_{(HD)}$ harboured a clade I *nosZ* gene. These results are in agreement with findings by Yoon et al. 2016 [50] which showed that clade II *nosZ* organisms posses a higher N_2O affinity. A higher affinity leads to a faster substrate turnover and thus less transient accumulation.

Besides the characteristics of the two nitrite and nitrous oxide reductases, an additional cause of the large phenotypic differences between the *H. taeniospiralis* isolate and the two *Rhodocyclaceae* isolates may be the global regulators controlling the shift between oxic respiration and denitrification, which also differed between the two groups. While *H. taeniospiralis* harboured the two-component system FixLJ, *D. denitrificans* and *F. limneticum* were equipped with the two-component system RegAB (PIIb). The two global regulator systems differ in their mechanism to detect lowering O_2 concentrations, as FixLJ is activated by the absence of O_2 [62] and RegAB senses the lowering ubiquinone redox state following decreasing O_2 concentrations inside the respiratory chain [160]. Due to the direct sensing of the ubiquinone redox state by RegB inside the denitrification respiratory membrane, *D. denitrificans* and *F. limneticum* may detect changing electron availability faster. This could result in a more efficient electron flow to the denitrification reductases compared with the *fixLJ*-carrying *H. taeniospiralis*.

All eight analysed complete hydrogenotrophic denitrifiers harboured genes coding for a RubisCO form II and for three [NiFe] hydrogenases. The hydrogenases included one respiratory hydrogenase from group 1d, one H_2-sensing hydrogenase from group 2b and one redox-balancing hydrogenase from group 3d (PIIb). As facultative anaerobes, hydrogenotrophic denitrifiers must contain O_2 tolerating enzymes that do not require O_2. Both, the RubisCO form II and the three hydrogenase types are O_2 tolerant [68, 71], which is necessary in the shallow model aquifers where samples

were taken for the experiments. The other RubsiCO forms, IA and IC, are adapted to high O_2 concentrations [71]. The three hydrogenase genes have different functions and are widely distributed, especially among *Proteobacteria* [161]. The group 1d respiratory hydrogenase is the only hydrogenase oxidising H_2 inside the periplasm and transferring electrons to the cytochrome bc_1 complex and quinones inside the respiratory chain (Figure 9) [161]. The group 2b H_2-sensing hydrogenase, quite differently, controls the expression of respiratory hydrogenases and group 3d generates reducing equivalents from NAD for hydrogenotrophic carbon fixation [161]. Three *F. limneticum* isolates, $F76_{(HD)}$, $F128_{(HD)}$ and $F132_{(HD)}$, were the only complete hydrogenotrophic denitrifiers isolated harbouring two additional hydrogenase genes including a O_2-sensitive group 1c respiratory hydrogenase and a group 2c H_2-sensing hydrogenase. This genotypic difference of additional hydrogenase genes between $F76_{(HD)}$ and $D110_{(HD)}$ may be the cause of even lower NO_2^- accumulation in $F76_{(HD)}$, as observed during the 'Kinetics analyses'.

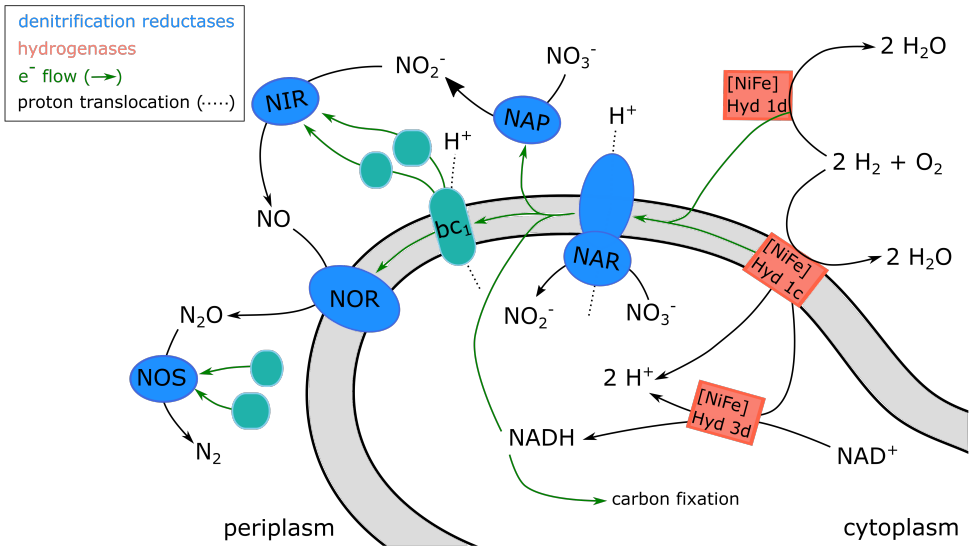

Figure 9 Potential electron transport chain of hydrogenotrophic denitrifiers (based on figure 2(A) in Duffner et al. 2021 [162]).

5.4. Recommendations to improve *in situ* nitrate remediation with hydrogen

Complete hydrogenotrophic denitrification is favoured under certain aquifer conditions while others make it more difficult to achieve complete reduction of NO_3^- to N_2. These favourable conditions include a pH between 6.5-8.6 and sufficient inorganic carbon for autotrophy as well as to buffer the pH. Also, the dissolved O_2 concentration and NO_3^- concentrations should not be too high because this would require even larger dissolved H_2 concentrations, which are generally difficult to achieve *in situ*. Local *in situ* nitrate removal approaches with H_2 should therefore only be attempted in aquifers with suitable conditions to avoid incomplete denitrification or transient intermediate accumulation (PIII). Additional to acquiring the above mentioned parameters, the prevailing hydrogenotrophic denitrifier community should also be determined to asses whether

an aquifer could be nitrate remediated. This could be achieved either through 16S rRNA gene-based community analyses in order to detect the genera that include complete hydrogenotrophic denitrifiers or through qPCR-based quantification of the nitrate reductase genes *narG* and *napA*. The second option is simpler and more economic. For both methods sediment and groundwater samples should be previously subjected to selective hydrogenotrophic denitrifier enrichment under a H_2/CO_2 atmosphere, as described for PIIa. The abundance of the hydrogenotrophic denitrifiers should thereby be increased to a level that can be clearly detected, as seen in PI and PIIa.

According to a review by Karanasios et al. 2010 [27] the optimal dissolved H_2 concentration for efficient hydrogenotrophic denitrification is between 0.4-0.8 mg L^{-1}. Below 0.2 mg H_2 L^{-1} the nitrate reductase is inhibited [163]. The dissolved H_2 concentration of 0.51 mg L^{-1} in the kinetics experiments (PIIb) was chosen accordingly and did result in complete hydrogenotrophic denitrification. Such dissolved H_2 concentrations can be easily reached in closed batch experiment; however, it is challenging to reach *in situ* due to the groundwater flow and the high diffusion coefficient of H_2 in water (PIII). For example, during an *in situ* experiment by Chaplin et al. 2009 [84] even a increase in the lumen pressure from 1.68 atm to 2.36 atm could not achieve a nitrate reduction above 50%. For *in situ* trials it is thus important to release the H_2 gas over a large exchange area which serves also as a surface area for biofilm formation. Lee and Rittmann 2002 achieved 95% nitrogen removal in a hollow fibre biofilm reactor, with a 1340 cm^2 surface area and 110 µm biofilm thickness, whereby 96% of the added H_2 was utilized. In their experiment H_2 was limiting the rate of nitrate reduction, thus as long as the denitrification capacity was below its maximum, almost all added H_2 was consumed inside the biofilm [78]. Their results highlight the importance of promoting biofilm formation to enhance bacterial growth and avoid the loss of H_2 gas by diffusion.

In order to prevent intermediate accumulation, we could further specifically promote the taxa with least intermediate accumulation, e.g. *napA*-carrying hydrogenotrophic denitrifiers (*D. denitrificans* and *F. limneticum*) or inoculate with such bacterial taxa. During the 'Kinetics analyses' of PIIb, growth differences based on the availability of O_2 and DOC were already observed. For example, the time to achieve complete reduction of NO_3^- to N_2 during the *Litho-autotrophic transition* experiment was between 80-100 h for all three analysed isolates. There was; however, a large difference among the isolates during organo-heterotrophic denitrification, as the *D. denitrificans* and *F. limneticum* isolates only took 35-40 h, whereas the *H. taeniospiralis* isolate needed 120 h. Contrary, the *H. taeniospiralis* cells were growing much faster and to a higher optical density under heterotrophic oxic conditions. This indicates that the *Rhodocyclaceae* isolates may have a selective advantage if the aquifer still contains relevant amounts of dissolved organic carbon under anoxic conditions, e.g. when H_2 has been added. Dissolved organic carbon in combination with increased O_2 concentrations; however, may give a selective advantage to *H. taeniospiralis* cells. Co-cultivation experiments with different combinations of *D. denitrificans*, *F. limneticum* and *H. taeniospiralis* under different conditions regarding pH, initial O_2, NO_3^- and DOC concentration thus are necessary to determine these conditions for the specific stimulation of desired

hydrogenotrophic denitrifiers.
Another option may be the inoculation with the desired taxa, for example by inoculating the H_2-releasing membrane before insertion into the aquifer. If a biofilm has been formed already prior to the insertion, the inoculated taxa rather remain on the membrane where they are needed, especially since a high cell density is required to obtain significant results. For example, Jonassen et al. 2021 [105] and Domeignoz-Horta et al. 2016 [164] were able to reduce N_2O accumulation from soil significantly by inoculating with 10^6-10^8 cells g^{-1} soil. However, currently there are still perceived limitations about bioremediation, such as questions regarding the required inoculation concentration, the final survival of the microbes as well as the effects on the ecology and the natural microbial community structure [165]. Thus, the impact of such microbial inoculants on the groundwater ecosystem must be evaluated initially.

A complementing approach to H_2 addition may be the application of reactive Fe(II)-containing minerals, such as siderite ($FeCO_{3(s)}$) (PIII), in order to reduce NO_2^- accumulation. The abiotic reduction of NO_2^- by Fe(II), called chemo-denitrification, occurs naturally under environmental conditions [166, 167] and could be enhanced by the injection of siderite particles into the H_2 plume. Nano-sized Fe(II)-containing minerals have a larger surface area, higher availability and a wider range of distribution [168]; however, they also entail possible risks regarding unknown long-term effects, transformation and eco-toxicity [169]. Further uncertainties about the general application of reactive Fe(II)-containing minerals exist, such as the possible reaction with sediment potentially clogging the aquifer [170], the possible increase of NO and N_2O accumulation [168] as well as the difficulties of efficient delivery of the Fe(II)-containing minerals to the anoxic H_2 plume. While the application of reactive Fe(II)-containing minerals is a promising way to alleviate NO_2^- accumulation during *in situ* nitrate remediation with H_2, many open questions remain before its application.

6. Conclusion and Outlook

The combination of community analyses and the genotypic and phenotypic characterisation of isolates enabled us to define the prevailing complete hydrogenotrophic denitrifiers in the analysed nitrate polluted oxic model aquifers and to determine the members with the least transient accumulation of nitrite or N_2O.

The results proved our hypotheses that hydrogenotrophic denitrifier communities consist of only few taxa (Hypothesis 1) and include different denitrification regulatory phenotypes (Hypothesis 2). Also, the different phenotypic characteristics could be linked to genetic features (Hypothesis 3). These findings imply, that even when the external parameters, such as pH, NO_3^-, O_2 and H_2 concentration as well as the groundwater flow, are the same, differences in NO_2^- accumulation still occur due to the composition of the bacterial community. It is therefore essential to investigate the hydrogenotrophic denitrifier community when examining whether a nitrate polluted aquifer is suited for such a remediation approach.

Further, it is of interest to understand the factors resulting in the dominance of either the *Rhodocyclaceae* isolates or *H. taeniospiralis*. Therefore, future work should include co-cultivation of *D. denitrificans*, *F. limneticum* and *H. taeniospiralis* under different conditions regarding pH, initial O_2, NO_3^- and DOC concentration and examine which species are more successful under the given conditions. This information may enable the targeted stimulation of the desired species with least intermediate accumulation. It is additionally important to examine the impact of H_2-based nitrate remediation on the aquifer‘s ecosystem with regards to other microbes. The sphere of influence of the added H_2 gas needs to be clarified, whether most of the H_2 is consumed inside the biofilm grown on the H_2-releasing membrane or whether it further diffuses into the water. It would be of interest to asses whether the added H_2, besides stimulating hydrogenotrophic denitrification, also leads to other functional changes in the groundwater bacterial community. A metagenomics analysis of samples from the biofilm and the surrounding groundwater/sediment from a large tank experiment could answer such questions.

As we obtained detailed knowledge on the individual prevailing hydrogenotrophic denitrifier species by analysing the behaviour of communities and pure cultures in batch experiments, future work must focus on the distribution of H_2 gas in an aquifer setting and how these bacteria grow and behave in such an environment. The knowledge obtained about the genotypic and phenotypic features of *D. denitrificans*, *F. limneticum* and *H. taeniospiralis* can help in doing so, as important and species-specific genes as well as characteristic phenotypic behaviour have been determined.

Bibliography

[1] Griebler, Christian. and Lueders, Tillmann. “Microbial biodiversity in groundwater ecosystems”. In: *Freshwater Biology* 54.4 (2009), pp. 649–677. DOI: https://doi.org/10.1111/j.1365-2427.2008.02013.x.

[2] Ayraud, Virginie et al. “Physical, biogeochemical and isotopic processes related to heterogeneity of a shallow crystalline rock aquifer”. In: *Biogeochemistry* 81.3 (2006), pp. 331–347. DOI: https://doi.org/10.1007/s10533-006-9044-4.

[3] Ghiorse, William C. and Wilson, John T. “Microbial Ecology of the Terrestrial Subsurface”. In: *Advances in Applied Microbiology*. Advances in Applied Microbiology 33 (1988). Ed. by Allen I. Laskin, pp. 107 –172. DOI: https://doi.org/10.1016/S0065-2164(08)70206-5.

[4] Zhang, Zhaojing et al. “Soil bacterial quantification approaches coupling with relative abundances reflecting the changes of taxa”. In: *Scientific Reports* 7.1 (2017), p. 4837. DOI: https://doi.org/10.1038/s41598-017-05260-w.

[5] Anantharaman, Karthik et al. “Thousands of microbial genomes shed light on interconnected biogeochemical processes in an aquifer system”. In: *Nature Communications* 7.13219 (2016).

[6] Ben Maamar, Sarah et al. “Groundwater Isolation Governs Chemistry and Microbial Community Structure along Hydrologic Flowpaths”. In: *Frontiers in Microbiology* 6 (2015), p. 1457. DOI: https://doi.org/10.3389/fmicb.2015.01457.

[7] Flynn, Theodore M. et al. “Functional microbial diversity explains groundwater chemistry in a pristine aquifer”. In: *BMC Microbiology* 13.1 (2013), p. 146. DOI: https://doi.org/10.1186/1471-2180-13-146.

[8] de Vries, Wim et al. “Assessing planetary and regional nitrogen boundaries related to food security and adverse environmental impacts”. In: *Current Opinion in Environmental Sustainability* 5.3 (2013), pp. 392–402. DOI: https://doi.org/10.1016/j.cosust.2013.07.004.

[9] Steffen, Will et al. “Planetary boundaries: Guiding human development on a changing planet”. In: *Science* 347.6223 (2015). DOI: 10.1126/science.1259855.

[10] Galloway, James N. et al. “Transformation of the Nitrogen Cycle: Recent Trends, Questions, and Potential Solutions”. In: *Science* 320.5878 (2008), pp. 889–892. DOI: https://doi.org/10.1126/science.1136674.

[11] Fields, Scott. “Global Nitrogen: Cycling out of Control”. In: *Environmental Health Perspectives* 112.10 (2004), pp. 556–563. DOI: https://doi.org/10.1289/ehp.112-a556.

[12] Beeckman, Fabian, Motte, Hans, and Beeckman, Tom. “Nitrification in agricultural soils: impact, actors and mitigation”. In: *Current Opinion in Biotechnology* 50 (2018), pp. 166–173. DOI: https://doi.org/10.1016/j.copbio.2018.01.014.

[13] Wild, Lisa, Mayer, Bernhard, and Einsiedl, Florian. “Decadal delays in groundwater recovery from nitrate contamination caused by low O_2 reduction rates”. In: *Water Resources Research* 54 (2018), pp. 9996–10012. DOI: https://doi.org/10.1029/2018WR023396.

[14] Nyilitya, Benjamin, Mureithi, Stephen, and Boeckx, Pascal. “Tracking Sources and Fate of Groundwater Nitrate in Kisumu City and Kano Plains, Kenya”. In: *Water* 12.2 (2020). DOI: https://doi.org/10.3390/w12020401.

[15] Biddau, R. et al. “Source and fate of nitrate in contaminated groundwater systems: Assessing spatial and temporal variations by hydrogeochemistry and multiple stable isotope tools”. In: *Science of The Total Environment* 647 (2019), pp. 1121–1136. DOI: https://doi.org/10.1016/j.scitotenv.2018.08.007.

[16] Zhu, Aiping et al. “Combined microbial and isotopic signature approach to identify nitrate sources and transformation processes in groundwater”. In: *Chemosphere* 228 (2019), pp. 721–734. ISSN: 0045-6535. DOI: https://doi.org/10.1016/j.chemosphere.2019.04.163.

[17] Umweltbundesamt. *FAQ zu Nitrat im Grund- und Trinkwasser (German)*. Sept. 2018.

[18] Cameron, K.C., Di, H.J., and Moir, J.L. “Nitrogen losses from the soil/plant system: a review”. In: *Annals of Applied Biology* 162.2 (2013), pp. 145–173. DOI: https://doi.org/10.1111/aab.12014.

[19] Dobermann, Achim R. “Nitrogen Use Efficiency - State of the Art”. In: *Agronomy and Horticulture, University of Nebraska - Faculty Publications* (2005).

[20] Bastani, Mehrdad and Harter, Thomas. “Source area management practices as remediation tool to address groundwater nitrate pollution in drinking supply wells”. In: *Journal of Contaminant Hydrology* 226 (2019), p. 103521. DOI: https://doi.org/10.1016/j.jconhyd.2019.103521.

[21] Uhlman, Kristine and Artiola, Janick. “Nitrate Contamination Potential in Arizona Groundwater: Implications for Drinking Water Wells”. In: *(Te University of Arizona Cooperative Extention* (July 2011).

[22] Stevens, Carly J. et al. “Impact of Nitrogen Deposition on the Species Richness of Grasslands”. In: *Science* 303.5665 (2004), pp. 1876–1879. DOI: https://doi.org/10.1126/science.1094678.

[23] Isbell, Forest et al. “Nutrient enrichment, biodiversity loss, and consequent declines in ecosystem productivity”. In: *Proceedings of the National Academy of Sciences* 110.29 (2013), pp. 11911–11916. DOI: https://doi.org/10.1073/pnas.1310880110.

[24] Rivett, Michael O. et al. “Nitrate attenuation in groundwater: A review of biogeochemical controlling processes”. In: *Water Research* 42.16 (2008), pp. 4215 –4232. DOI: https://doi.org/10.1016/j.watres.2008.07.020.

[25] Camargo, Julio A. and Alonso, Álvaro. “Ecological and toxicological effects of inorganic nitrogen pollution in aquatic ecosystems: A global assessment”. In: *Environment International* 32.6 (2006), pp. 831–849. DOI: https://doi.org/10.1016/j.envint.2006.05.002.

[26] Harris, Eliza et al. “Denitrifying pathways dominate nitrous oxide emissions from managed grassland during drought and rewetting”. In: *Science Advances* 7.6 (2021), eabb7118. DOI: https://doi.org/10.1126/sciadv.abb7118.

[27] Karanasios, K. A. et al. “Hydrogenotrophic denitrification of potable water: a review”. In: *Journal of hazardous materials* 180.1-3 (2010), pp. 20–37. DOI: https://doi.org/10.1016/j.jhazmat.2010.04.090.

[28] Ward, Mary H. et al. “Drinking Water Nitrate and Human Health: An Updated Review”. In: *International journal of environmental research and public health* 15.7 (2018), p. 1557. DOI: https://doi.org/10.3390/ijerph15071557.

[29] Schullehner, Jörg et al. “Nitrate in drinking water and colorectal cancer risk: A nationwide population-based cohort study”. In: *International Journal of Cancer* (2018). DOI: https://doi.org/10.1002/ijc.31306.

[30] Umweltbundesamt. *Fakten zur Nitratbelastung in Grund- und Trinkwasser (German)*. May 2018.

[31] Skiba, U. “Denitrification”. In: *Encyclopedia of Ecology*. Ed. by Sven Erik Jørgensen and Brian D. Fath. Oxford: Academic Press, 2008, pp. 866–871. ISBN: 978-0-08-045405-4. DOI: https://doi.org/10.1016/B978-008045405-4.00264-0.

[32] Lycus, Pawel et al. “Phenotypic and genotypic richness of denitrifiers revealed by a novel isolation strategy”. In: *The ISME journal* 11.10 (2017), 2219—2232. ISSN: 1751-7362. DOI: https://doi.org/10.1038/ismej.2017.82.

[33] Otero, N. et al. “Monitoring groundwater nitrate attenuation in a regional system coupling hydrogeology with multi-isotopic methods: The case of Plana de Vic (Osona, Spain)”. In: *Agriculture, Ecosystems and Environment* 133.1 (2009), pp. 103–113. DOI: https://doi.org/10.1016/j.agee.2009.05.007.

[34] Jahangir, M. M. R. et al. “Quantification of *In Situ* Denitrification Rates in Groundwater Below an Arable and a Grassland System”. In: *Water, Air, and Soil Pollution* 224 (2013), p. 1693. DOI: https://doi.org/10.1007/s11270-013-1693-z.

[35] Hernández-del Amo, Elena et al. “Isotope and microbiome data provide complementary information to identify natural nitrate attenuation processes in groundwater”. In: *Science of The Total Environment* 613-614 (2018), pp. 579–591. DOI: https://doi.org/10.1016/j.scitotenv.2017.09.018.

[36] Melton, Emily D. et al. “The interplay of microbially mediated and abiotic reactions in the biogechemical Fe cycle”. In: *Nature Reviews Microbiology* 12 (2014), pp. 797–808. DOI: https://doi.org/10.1038/nrmicro3347.

[37] Schmidt, Christoph S., Richardson, David J., and Baggs, Elizabeth M. “Constraining the conditions conducive to dissimilatory nitrate reduction to ammonium in temperate arable soils”. In: *Soil Biology and Biochemistry* 43.7 (2011), pp. 1607–1611. DOI: https://doi.org/10.1016/j.soilbio.2011.02.015.

[38] Tiedje J.M., Sexstone A.J. Myrold D.D. et al. “Denitrification: ecological niches, competition and survival”. In: *Antonie van Leeuwenhoek* 48 (1983), pp. 569–583. DOI: https://doi.org/10.1007/BF00399542.

[39] Zumft, W. G. “Cell biology and molecular basis of denitrification”. In: *Microbiology and molecular biology reviews* 61.4 (1997), pp. 533–616.

[40] Alejandra, Peña Sanchez et al. “Seasonal dynamics of anaerobic oxidation of ammonium and denitrification in a dimictic lake during the stratified spring–summer period”. In: *Limnology and Oceanography* n/a.n/a (). DOI: https://doi.org/10.1002/lno.12067.

[41] van Spanning, Rob J.M., Richardson, David J., and Ferguson, Stuart J. “Chapter 1 - Introduction to the Biochemistry and Molecular Biology of Denitrification”. In: *Biology of the Nitrogen Cycle*. Ed. by Hermann Bothe, Stuart J. Ferguson, and William E. Newton. Amsterdam: Elsevier, 2007, pp. 3–20. ISBN: 978-0-444-52857-5. DOI: https://doi.org/10.1016/B978-044452857-5.50002-3.

[42] Jones, Christopher M. et al. “Phylogenetic Analysis of Nitrite, Nitric Oxide, and Nitrous Oxide Respiratory Enzymes Reveal a Complex Evolutionary History for Denitrification”. In: *Molecular Biology and Evolution* 25.9 (2008), pp. 1955–1966. DOI: https://doi.org/10.1093/molbev/msn146.

[43] Philippot, Laurent. “Denitrifying genes in bacterial and Archaeal genomes”. In: *Biochimica et Biophysica Acta (BBA) - Gene Structure and Expression* 1577.3 (2002), pp. 355 –376. DOI: https://doi.org/10.1016/S0167-4781(02)00420-7.

[44] Bonilla-Rosso, German et al. “Design and evaluation of primers targeting genes encoding NO-forming nitrite reductases: implications for ecological inference of denitrifying communities”. In: *Scientific Reports* 6.39208 (2016).

[45] Gates, Andrew J., Richardson, David J., and Butt, Julea N. “Voltammetric characterization of the aerobic energy-dissipating nitrate reductase of *Paracoccus pantotrophus*: exploring the activity of a redox-balancing enzyme as a function of electrochemical potential”. In: *Biochemical Journal* 409.1 (2008), pp. 159–168. DOI: https://doi.org/10.1042/BJ20071088.

[46] Kuypers, Marcel M. M., Marchant, Hannah K., and Kartal, Boran. “The microbial nitrogen-cycling network”. In: *Nature Reviews Microbiology* 16 (2018), pp. 263–276.

[47] Graf, Daniel R. H., Jones, Christopher M., and Hallin, Sara. “Intergenomic Comparisons Highlight Modularity of the Denitrification Pathway and Underpin the Importance of Community Structure for N_2O Emissions”. In: *PLOS ONE* 9.12 (Dec. 2014), pp. 1–20. DOI: https://doi.org/10.1371/journal.pone.0114118.

[48] Braker, Gesche and Tiedje, James M. “Nitric Oxide Reductase (*norB*) Genes from Pure Cultures and Environmental Samples”. In: *Applied and Environmental Microbiology* 69.6 (2003), pp. 3476–3483. DOI: https://doi.org/10.1128/AEM.69.6.3476-3483.2003.

[49] Hallin, Sara et al. “Genomics and Ecology of Novel N_2O-Reducing Microorganisms”. In: *Trends in Microbiology* 26.1 (2018), pp. 43 –55. DOI: https://doi.org/10.1016/j.tim.2017.07.003.

[50] Yoon, Sukhwan et al. “Nitrous Oxide Reduction Kinetics Distinguish Bacteria Harboring Clade I NosZ from Those Harboring Clade II NosZ”. In: *Applied and Environmental Microbiology* 82.13 (2016), pp. 3793–3800. DOI: 10.1128/AEM.00409-16.

[51] Jones, Christopher M. et al. “Recently identified microbial guild mediates soil N_2O sink capacity”. In: *Nature Climate Change* 4 (2014), pp. 801–805. DOI: https://doi.org/10.1038/nclimate2301.

[52] Conthe, Monica et al. “Life on N_2O: deciphering the ecophysiology of N2O respiring bacterial communities in a continuous culture”. In: *The ISME Journal* 12.4 (2018), pp. 1142–1153. DOI: https://doi.org/10.1038/s41396-018-0063-7.

[53] Liu, Binbin et al. “Impaired Reduction ofN_2O to N_2 in Acid Soils Is Due to a Posttranscriptional Interference with the Expression of *nosZ*”. In: *mBio* 5.3 (2014), e01383–14. DOI: 10.1128/mBio.01383-14.

[54] Bergaust, Linda et al. “Denitrification response patterns during the transition to anoxic respiration and posttranscriptional effects of suboptimal pH on nitrous oxide reductase in *Paracoccus denitrificans*”. In: *Applied and environmental microbiology* 76.20709842 (2010), pp. 6387–6396.

[55] M Slmek, J E Cooper. “The influence of soil pH on denitrification: progress towards the understanding of this interaction over the last 50 years”. In: *European Journal of Soil Science* 53 (2002), pp. 345–354. DOI: https://doi.org/10.1046/j.1365-2389.2002.00461.x.

[56] Gaimster, Hannah et al. “Transcriptional and environmental control of bacterial denitrification and N_2O emissions”. In: *FEMS Microbiology Letters* 365.5 (Dec. 2017). DOI: https://doi.org/10.1093/femsle/fnx277.

[57] Bergaust, L., Bakken, L., and Frostegård, Å. “Denitrification regulatory phenotype, a new term for the characterization of denitrifying bacteria.” In: *Biochemical Society transactions* 39 1 (2011), pp. 207–212.

[58] Liu, Binbin et al. “Strains in the genus Thauera exhibit remarkably different denitrification regulatory phenotypes”. In: *Environmental Microbiology* 15.10 (Oct. 2013), pp. 2816–2828. DOI: https://doi.org/10.1111/1462-2920.12142.

[59] Lycus, Pawel et al. “A bet-hedging strategy for denitrifying bacteria curtails their release of N_2O ”. In: *Proceedings of the National Academy of Sciences* 115.46 (2018), pp. 11820–11825. DOI: https://doi.org/10.1073/pnas.1805000115.

[60] Hassan, Junaid et al. “Transient Accumulation of NO_2^- and N_2O during Denitrification Explained by Assuming Cell Diversification by Stochastic Transcription of Denitrification Genes”. In: *PLOS Computational Biology* 12.1 (Jan. 2016), pp. 1–24. DOI: https://doi.org/10.1371/journal.pcbi.1004621.

[61] Giannopoulos, Georgios et al. “Tuning the modular *Paracoccus denitrificans* respirome to adapt from aerobic respiration to anaerobic denitrification”. In: *Environmental Microbiology* 19.12 (2017), pp. 4953–4964. DOI: https://doi.org/10.1111/1462-2920.13974.

[62] Spiro, Stephen. “Nitrous oxide production and consumption: regulation of gene expression by gas-sensitive transcription factors”. In: *Philosophical Transactions of the Royal Society B: Biological Sciences* 367.1593 (2012), pp. 1213–1225. DOI: 10.1098/rstb.2011.0309.

[63] Sciotti, Michel-Angelo et al. “Disparate Oxygen Responsiveness of Two Regulatory Cascades That Control Expression of Symbiotic Genes in *Bradyrhizobium japonicum*”. In: *Journal of Bacteriology* 185.18 (2003), pp. 5639–5642. DOI: https://doi.org/10.1128/JB.185.18.5639-5642.2003.

[64] Schmidt, Ulrich. “Molecular hydrogen in the atmosphere”. In: *Tellus* 26.1-2 (1974), pp. 78–90. DOI: https://doi.org/10.1111/j.2153-3490.1974.tb01954.x.

[65] Nick Lane John F. Allen, William Martin. “How did LUCA make a living? Chemiosmosis in the origin of life”. In: *Bioessays* 32 (2010), pp. 271–280. DOI: https://doi.org/10.1002/bies.200900131.

[66] Schwartz, Edward, Fritsch, Johannes, and Friedrich, Bärbel. “H2-Metabolizing Prokaryotes”. In: *The Prokaryotes: Prokaryotic Physiology and Biochemistry*. Ed. by Eugene Rosenberg et al. Berlin, Heidelberg: Springer Berlin Heidelberg, 2013, pp. 119–199. DOI: https://doi.org/10.1007/978-3-642-30141-4_65.

[67] Vignais, Paulette M. and Billoud, Bernard. “Occurrence, Classification, and Biological Function of Hydrogenases: An Overview”. In: *Chemical Reviews* 107.10 (2007), pp. 4206–4272. DOI: https://doi.org/10.1021/cr050196r.

[68] Greening C., Biswas A. Carere C. et al. “Genomic and metagenomic surveys of hydrogenase distribution indicateH_2 is a widely utilised energy source for microbial growth and survival”. In: *ISME Journal* 10 (2016), pp. 761–777. DOI: https://doi.org/10.1038/ismej.2015.153.

[69] Pandelia, Maria-Eirini, Lubitz, Wolfgang, and Nitschke, Wolfgang. “Evolution and diversification of Group 1 [NiFe] hydrogenases. Is there a phylogenetic marker for O_2-tolerance?” In: *Biochimica et Biophysica Acta (BBA) - Bioenergetics* 1817.9 (2012), pp. 1565–1575. DOI: https://doi.org/10.1016/j.bbabio.2012.04.012.

[70] Berg, Ivan A. “Ecological Aspects of the Distribution of Different Autotrophic CO_2 Fixation Pathways”. In: *Applied and Environmental Microbiology* 77.6 (2011), pp. 1925–1936. DOI: {https://doi.org/10.1128/AEM.02473-10},.

[71] Badger, Murray Ronald and Bek, Emily Jane. “Multiple Rubisco forms in *Proteobacteria*: their functional significance in relation to CO_2 acquisition by the CBB cycle”. In: *Journal of Experimental Botany* 59.7 (Feb. 2008), pp. 1525–1541. DOI: https://doi.org/10.1093/jxb/erm297.

[72] Alfreider, Albin, Schirmer, Mario, and Vogt, Carsten. “Diversity and expression of different forms of RubisCO genes in polluted groundwater under different redox conditions”. In: *FEMS Microbiology Ecology* 79.3 (Mar. 2012), pp. 649–660. DOI: https://doi.org/10.1111/j.1574-6941.2011.01246.x.

[73] Rezania, B., Cicek, N., and Oleszkiewicz, J.A. “Kinetics of hydrogen-dependent denitrification under varying pH and temperature conditions”. In: *Biotechnology and Bioengineering* 92.7 (2005), pp. 900–906. DOI: https://doi.org/10.1002/bit.20664.

[74] Ghafari, Shahin, Hasan, Masitah, and Aroua, Mohamed Kheireddine. “A kinetic study of autohydrogenotrophic denitrification at the optimum pH and sodium bicarbonate dose”. In: *Bioresource Technology* 101.7 (2010), pp. 2236–2242. DOI: https://doi.org/10.1016/j.biortech.2009.11.068.

[75] Lee, Kuan-Chun and Rittmann, Bruce E. “Effects of pH and precipitation on autohydrogenotrophic denitrification using the hollow-fiber membrane-biofilm reactor”. In: *Water Research* 37.7 (2003), pp. 1551–1556. ISSN: 0043-1354. DOI: https://doi.org/10.1016/S0043-1354(02)00519-5.

[76] Li, Peng et al. “Nitrogen Removal and N_2O Accumulation during Hydrogenotrophic Denitrification: Influence of Environmental Factors and Microbial Community Characteristics”. In: *Environmental Science & Technology* 51.2 (2017), pp. 870–879. DOI: https://doi.org/10.1021/acs.est.6b00071.

[77] Zhou, Minghua et al. “Nitrate removal from groundwater by a novel three-dimensional electrode biofilm reactor”. In: *Electrochimica Acta* 52.19 (2007), pp. 6052–6059. DOI: https://doi.org/10.1016/j.electacta.2007.03.064.

[78] Lee, Kuan-Chun and Rittmann, Bruce E. “Applying a novel autohydrogenotrophic hollow-fiber membrane biofilm reactor for denitrification of drinking water”. In: *Water Research* 36.8 (2002), pp. 2040–2052. DOI: https://doi.org/10.1016/S0043-1354(01)00425-0.

[79] Haugen, K.S, Semmens, M.J, and Novak, P.J. “A novel *in situ* technology for the treatment of nitrate contaminated groundwater”. In: *Water Research* 36.14 (2002), pp. 3497–3506. DOI: https://doi.org/10.1016/S0043-1354(02)00043-X.

[80] Schnobrich, Matthew R. et al. “Stimulating hydrogenotrophic denitrification in simulated groundwater containing high dissolved oxygen and nitrate concentrations”. In: *Water Research* 41.9 (2007), pp. 1869 –1876. DOI: https://doi.org/10.1016/j.watres.2007.01.044.

[81] Vasiliadou, I.A., Pavlou, S., and Vayenas, D.V. “A kinetic study of hydrogenotrophic denitrification”. In: *Process Biochemistry* 41.6 (2006), pp. 1401 –1408. DOI: https://doi.org/10.1016/j.procbio.2006.02.002.

[82] Wang, Hongyu et al. “Microbial community in a hydrogenotrophic denitrification reactor based on pyrosequencing”. In: *Applied Microbiology and Biotechnology* 99.24 (2015), pp. 10829–10837. DOI: https://doi.org/10.1007/s00253-015-6929-y.

[83] Khanitchaidecha, Wilawan and Kazama, Futaba. “Hydrogenotrophic denitrification in an attached growth reactor under various operating conditions”. In: *Water Supply* 12.1 (2012), pp. 72–81. DOI: https://doi.org/10.2166/ws.2011.120.

[84] Chaplin, Brian P et al. “Stimulating *In Situ* Hydrogenotrophic Denitrification with Membrane-Delivered Hydrogen under Passive and Pumped Groundwater Conditions”. In: *Journal of Environmental Engineering* 135.8 (2009), pp. 666–676. DOI: https://doi.org/10.1061/(ASCE)EE.1943-7870.0000021.

[85] Wu, Jinling, Yin, Yanan, and Wang, Jianlong. “Hydrogen-based membrane biofilm reactors for nitrate removal from water and wastewater”. In: *International Journal of Hydrogen Energy* 43.1 (2018), pp. 1 –15. DOI: https://doi.org/10.1016/j.ijhydene.2017.10.178.

[86] Zhang, Yanhao et al. “Autohydrogenotrophic denitrification of drinking water using a polyvinyl chloride hollow fiber membrane biofilm reactor”. In: *Journal of Hazardous Materials* 170.1 (2009), pp. 203–209. DOI: https://doi.org/10.1016/j.jhazmat.2009.04.114.

[87] Park, Ho Il, Choi, Yong-Jin, and Pak, Daewon. “Autohydrogenotrophic Denitrifying Microbial Community in a Glass Beads Biofilm Reactor”. In: *Biotechnology Letters* 27.13 (2005), pp. 949–953. DOI: https://doi.org/10.1007/s10529-005-7654-x.

[88] Zhao, He-Ping et al. “Interactions between Perchlorate and Nitrate Reductions in the Biofilm of a Hydrogen-Based Membrane Biofilm Reactor”. In: *Environmental Science and Technology* 45.23 (2011). PMID: 22017212, pp. 10155–10162. DOI: https://doi.org/10.1021/es202569b.

[89] Zhao, He-Ping et al. “Using a Two-Stage Hydrogen-Based Membrane Biofilm Reactor (MBfR) to Achieve Complete Perchlorate Reduction in the Presence of Nitrate and Sulfate”. In: *Environmental Science & Technology* 47.3 (2013), pp. 1565–1572. DOI: https://doi.org/110.1021/es303823n.

[90] Kumar, Swatantar et al. “Thiosulfate- and hydrogen-driven autotrophic denitrification by a microbial consortium enriched from groundwater of an oligotrophic limestone aquifer”. In: *FEMS Microbiology Ecology* 94.10 (2018), fiy141. DOI: https://doi.org/10.1093/femsec/fiy141.

[91] Nozawa-Inoue, Mamie et al. “Effect of nitrate, acetate, and hydrogen on native perchlorate-reducing microbial communities and their activity in vadose soil”. In: *FEMS Microbiology Ecology* 76.2 (2011), pp. 278–288. DOI: https://doi.org/10.1111/j.1574-6941.2011.01045.x.

[92] Nerenberg, Robert, Kawagoshi, Yasunori, and Rittmann, Bruce E. “Microbial ecology of a perchlorate-reducing, hydrogen-based membrane biofilm reactor”. In: *Water Research* 42.4 (2008), pp. 1151 –1159. DOI: https://doi.org/10.1016/j.watres.2007.08.033.

[93] Chu, Libing and Wang, Jianlong. “Denitrification performance and biofilm characteristics using biodegradable polymers PCL as carriers and carbon source”. In: *Chemosphere* 91.9 (2013), pp. 1310–1316. DOI: https://doi.org/10.1016/j.chemosphere.2013.02.064.

[94] Ho, C.M., Tseng, S.K., and Chang, Y.J. “Autotrophic denitrification via a novel membrane-attached biofilm reactor”. In: *Letters in Applied Microbiology* 33.3 (2001), pp. 201–205. DOI: https://doi.org/10.1046/j.1472-765x.2001.00984.x.

[95] Liang, Dandan et al. “Remediation of nitrate contamination by membrane hydrogenotrophic denitrifying biofilm integrated in microbial electrolysis cell”. In: *Water Research* 188 (2021), p. 116498. DOI: https://doi.org/10.1016/j.watres.2020.116498.

[96] Cecconet, Daniele et al. “In situ groundwater remediation with bioelectrochemical systems: A critical review and future perspectives”. In: *Environment International* 137 (2020), p. 105550. DOI: https://doi.org/10.1016/j.envint.2020.105550.

[97] Barrett, Maria et al. “Abundance of denitrification genes under different peizometer depths in four Irish agricultural groundwater sites”. In: *Environmental Science and Pollution Research* 20.9 (2013), pp. 6646–6657. DOI: https://doi.org/10.1007/s11356-013-1729-3.

[98] Flint, Madison K. et al. “Nitrous oxide processing in carbonate karst aquifers”. In: *Journal of Hydrology* 594 (2021), p. 125936. DOI: https://doi.org/10.1016/j.jhydrol.2020.125936.

[99] Lloyd, Karen G. et al. “Phylogenetically Novel Uncultured Microbial Cells Dominate Earth Microbiomes”. In: *mSystems* 3.5 (2018), e00055–18. DOI: https://doi.org/10.1128/mSystems.00055-18.

[100] Overmann, Jörg. “Principles of Enrichment, Isolation, Cultivation and Preservation of Prokaryotes”. In: *The Prokaryotes: Volume 1: Symbiotic associations, Biotechnology, Applied Microbiology*. Ed. by Martin Dworkin et al. New York, NY: Springer New York, 2006, pp. 80–136. ISBN: 978-0-387-30741-1. DOI: 10.1007/0-387-30741-9_5. URL: https://doi.org/10.1007/0-387-30741-9_5.

[101] Wu, Xiaoqin et al. “Culturing of “Unculturable” Subsurface Microbes: Natural Organic Carbon Source Fuels the Growth of Diverse and Distinct Bacteria From Groundwater”. In: *Frontiers in Microbiology* 11 (2020), p. 3171. DOI: https://doi.org/10.3389/fmicb.2020.610001.

[102] Eguchi, Mitsuru et al. “*Sphingomonas alaskensis* Strain AFO1, an Abundant Oligotrophic Ultramicrobacterium from the North Pacific”. In: *Applied and Environmental Microbiology* 67.11 (2001), pp. 4945–4954. DOI: https://doi.org/10.1128/AEM.67.11.4945-4954.2001.

[103] Tanaka, Tomohiro et al. “A Hidden Pitfall in the Preparation of Agar Media Undermines Microorganism Cultivability”. In: *Applied and Environmental Microbiology* 80.24 (2014), pp. 7659–7666. DOI: 10.1128/AEM.02741-14.

[104] Heylen, Kim et al. “Cultivation of Denitrifying Bacteria: Optimization of Isolation Conditions and Diversity Study”. In: *Applied and Environmental Microbiology* 72.4 (2006), pp. 2637–2643. DOI: 10.1128/AEM.72.4.2637-2643.2006.

[105] Jonassen, Kjell Rune et al. “A novel dual enrichment strategy provides soil- and digestate-competent N2O-respiring bacteria for mitigating climate forcing in agriculture”. In: *bioRxiv (preprint)Pe* (2021). DOI: https://doi.org/10.1101/2021.05.11.443593.

[106] Duffner, Clara et al. “Genotypic and phenotypic characterization of hydrogenotrophic denitrifiers”. In: *Environmental Microbiology* n/a.n/a (2022). DOI: https://doi.org/10.1111/1462-2920.15921.

[107] Widdel, F and Bak, F. *The Prokaryotes: A Handbook on the Biology of Bacteria: Ecophysiology, Isolation, Identification, Applications (Chapter: Gram-Negative Mesophilic Sulfate-Reducing Bacteria)*. Springer New York, 1992. ISBN: 978-1-4757-2191-1.

[108] Balch, WE et al. “Methanogens: reevaluation of a unique biological group”. In: *Microbiological reviews* 43.2 (1979), 260—296. DOI: https://doi.org/10.1128/mr.43.2.260-296.1979.

[109] Horn, Marcus A. et al. “*Dechloromonas denitrificans* sp. nov., *Flavobacterium denitrificans* sp. nov., *Paenibacillus anaericanus* sp. nov. and *Paenibacillus terrae* strain MH72, N_2O-producing bacteria isolated from the gut of the earthworm *Aporrectodea caliginosa*”. In: *International Journal of Systematic and Evolutionary Microbiology* 55.3 (2005), pp. 1255–1265. DOI: https://doi.org/10.1099/ijs.0.63484-0.

[110] Molstad, Lars, Dörsch, Peter, and Bakken, Lars R. “Robotized incubation system for monitoring gases (O_2, NO, N_2O, N_2) in denitrifying cultures”. In: *Journal of Microbiological Methods* 71.3 (2007), pp. 202–211. DOI: https://doi.org/10.1016/j.mimet.2007.08.011.

[111] Molstad, Lars, Dörsch, Peter, and Bakken, Lars. *Improved robotized incubation system for gas kinetics in batch cultures*. Sept. 2016. DOI: https://doi.org/10.13140/RG.2.2.30688.07680.

[112] Bergaust, Linda et al. “Transcription and activities of NOx reductases in Agrobacterium tumefaciens: the influence of nitrate, nitrite and oxygen availability”. In: *Environmental Microbiology* 10.11 (2008), pp. 3070–3081. DOI: https://doi.org/10.1111/j.1462-2920.2007.01557.x.

[113] Bakken, Lars. *Spreadsheet for gas kinetics in batch cultures: KINCALC*. Jan. 2021. DOI: https://doi.org/10.13140/RG.2.2.19802.36809.

[114] Lueders, Tillmann, Manefield, Mike, and Friedrich, Michael W. “Enhanced sensitivity of DNA- and rRNA-based stable isotope probing by fractionation and quantitative analysis of isopycnic centrifugation gradients”. In: *Environmental Microbiology* 6.1 (2004), pp. 73–78. DOI: https://doi.org/10.1046/j.1462-2920.2003.00536.x.

[115] Töwe, Stefanie et al. “Improved protocol for the simultaneous extraction and column-based separation of DNA and RNA from different soils”. In: *Journal of Microbiological Methods* 84.3 (2011), pp. 406–412. DOI: https://doi.org/10.1016/j.mimet.2010.12.028.

[116] Bach, H.-J et al. “Enumeration of total bacteria and bacteria with genes for proteolytic activity in pure cultures and in environmental samples by quantitative PCR mediated amplification”. In: *Journal of Microbiological Methods* 49.3 (2002), pp. 235–245. DOI: https://doi.org/10.1016/S0167-7012(01)00370-0.

[117] Bru, D., Sarr, A., and Philippot, L. “Relative Abundances of Proteobacterial Membrane-Bound and Periplasmic Nitrate Reductases in Selected Environments”. In: *Applied and Environmental Microbiology* 73.18 (2007), pp. 5971–5974. DOI: https://doi.org/10.1128/AEM.00643-07.

[118] Michotey, Valérie, Méjean, Vincent, and Bonin, Patricia. “Comparison of Methods for Quantification of Cytochrome cd_1-Denitrifying Bacteria in Environmental Marine Samples”. In: *Applied and Environmental Microbiology* 66.4 (2000), pp. 1564–1571. DOI: https://doi.org/10.1128/AEM.66.4.1564-1571.2000.

[119] Throbäck, Ingela Noredal et al. “Reassessing PCR primers targeting *nirS*, *nirK* and *nosZ* genes for community surveys of denitrifying bacteria with DGGE”. In: *FEMS Microbiology Ecology* 49.3 (Sept. 2004), pp. 401–417. DOI: https://doi.org/10.1016/j.femsec.2004.04.011.

[120] Braker, Gesche, Fesefeldt, Andreas, and Witzel, Karl-Paul. “Development of PCR Primer Systems for Amplification of Nitrite Reductase Genes (*nirK* and *nirS*) To Detect Denitrifying Bacteria in Environmental Samples”. In: *Applied and Environmental Microbiology* 64.10 (1998), pp. 3769–3775. DOI: https://doi.org/10.1128/AEM.64.10.3769-3775.1998.

[121] Henry, Sonia et al. “Quantification of denitrifying bacteria in soils by nirK gene targeted real-time PCR”. In: *Journal of Microbiological Methods* 59.3 (2004), pp. 327–335. DOI: https://doi.org/10.1016/j.mimet.2004.07.002.

[122] Jones, C. M. et al. “The unaccounted yet abundant nitrous oxide-reducing microbial community: a potential nitrous oxide sink”. In: *ISME Journal* 7 (2013), pp. 417–426. DOI: https://doi.org/10.1038/ismej.2012.125.

[123] Lane, DJ. *16S/23S rRNA sequencing*. john Wiley and Sons, New York, 1991.

[124] Klindworth, Anna et al. “Evaluation of general 16S ribosomal RNA gene PCR primers for classical and next-generation sequencing-based diversity studies”. In: *Nucleic Acids Research* 41.1 (Aug. 2012). DOI: https://doi.org/10.1093/nar/gks808.

[125] Apprill A McNally S, Parsons R Weber L. “ Minor revision to V4 region SSU rRNA 806R gene primer greatly increases detection of SAR11 bacterioplankton”. In: *Aquatic Microbial Ecology* 75 (2015), pp. 129–137. DOI: https://doi.org/10.3354/ame01753.

[126] Parada, Alma E., Needham, David M., and Fuhrman, Jed A. “Every base matters: assessing small subunit rRNA primers for marine microbiomes with mock communities, time series and global field samples”. In: *Environmental Microbiology* 18.5 (2016), pp. 1403–1414. DOI: https://doi.org/10.1111/1462-2920.13023.

[127] Bolyen E., Rideout J.R. Dillon M.R. et al. “Reproducible, interactive, scalable and extensible microbiome data science using QIIME 2”. In: *Nature Biotechnology* 37 (2019), pp. 852–857. DOI: https://doi.org/10.1038/s41587-019-0209-9.

[128] Quast, Christian et al. “The SILVA ribosomal RNA gene database project: improved data processing and web-based tools”. In: *Nucleic Acids Research* 41.D1 (Nov. 2012), pp. D590–D596. DOI: https://doi.org/10.1093/nar/gks1219.

[129] Oksanen J Blanchet FG, Friendly M et al. “Vegan: Community Ecology Package”. In: *R Package Version. 2.0-10. CRAN* (2013).

[130] Team., R Development. “R: A Language and Environment for Statistical Computing”. In: *R Foundation for Statistical Computing* (2019).

[131] Hunt M., Silva N.D. Otto T.D. et al. “Circlator: automated circularization of genome assemblies using long sequencing reads”. In: *Genome Biology* 16 (2015), p. 294. DOI: https://doi.org/10.1038/s41587-019-0209-9.

[132] Parks DH Imelfort M, Skennerton CT Hugenholtz P Tyson GW. “CheckM: assessing the quality of microbial genomes recovered from isolates, single cells, and metagenomes”. In: *Genome Biology* 25 (2015), pp. 1043–1055. DOI: https://doi.org/10.1101/gr.186072.114.

[133] Hill, M. O. “Diversity and Evenness: A Unifying Notation and Its Consequences”. In: *Ecology* 54.2 (1973), pp. 427–432. DOI: https://doi.org/10.2307/1934352.

[134] McMurdie, Paul J. and Holmes, Susan. “phyloseq: An R Package for Reproducible Interactive Analysis and Graphics of Microbiome Census Data”. In: *PLOS ONE* 8.4 (Apr. 2013), pp. 1–11. DOI: https://doi.org/10.1371/journal.pone.0061217.

[135] Gu, Zuguang, Eils, Roland, and Schlesner, Matthias. “Complex heatmaps reveal patterns and correlations in multidimensional genomic data”. In: *Bioinformatics* 32.18 (May 2016), pp. 2847–2849. DOI: https://doi.org/10.1093/bioinformatics/btw313.

[136] Kumar, Sudhir et al. “MEGA X: Molecular Evolutionary Genetics Analysis across Computing Platforms”. In: *Molecular Biology and Evolution* 35.6 (May 2018), pp. 1547–1549. DOI: https://doi.org/10.1093/molbev/msy096.

[137] Seemann, Torsten. “Prokka: rapid prokaryotic genome annotation”. In: *Bioinformatics* 30.14 (Mar. 2014), pp. 2068–2069. DOI: https://doi.org/10.1093/bioinformatics/btu153.

[138] Finn, Robert D. et al. “HMMER web server: 2015 update”. In: *Nucleic Acids Research* 43.W1 (May 2015), W30–W38. DOI: https://doi.org/10.1093/nar/gkv397.

[139] Carver, Tim et al. “DNAPlotter: circular and linear interactive genome visualization”. In: *Bioinformatics* 25.1 (2008), pp. 119–120. DOI: https://doi.org/10.1093/bioinformatics/btn578.

[140] Harrison, Katherine J, Crécy-Lagard, Valérie de, and Zallot, Rémi. “Gene Graphics: a genomic neighborhood data visualization web application”. In: *Bioinformatics* 34.8 (2017), pp. 1406–1408. DOI: https://doi.org/10.1093/bioinformatics/btx793.

[141] Duffner, Clara et al. “Complete Genome Sequences of Hydrogenotrophic Denitrifiers”. In: *Microbiology Resource Announcements* 11.1 (2022), e01020–21. DOI: https://doi.org/10.1128/mra.01020-21.

[142] Mair P., Wilcox R. “Robust statistical methods in R using the WRS2 package”. In: *Behavior Research Methods* (2020). DOI: https://doi.org/10.3758/s13428-019-01246-w.

[143] Benjamini, Yoav and Hochberg, Yosef. “Controlling the False Discovery Rate: A Practical and Powerful Approach to Multiple Testing”. In: *Journal of the Royal Statistical Society: Series B (Methodological)* 57.1 (1995), pp. 289–300. DOI: https://doi.org/10.1111/j.2517-6161.1995.tb02031.x.

[144] Oren, Aharon. “The Family *Rhodocyclaceae*”. In: *The Prokaryotes: Alphaproteobacteria and Betaproteobacteria*. Ed. by Eugene Rosenberg et al. Berlin, Heidelberg: Springer Berlin Heidelberg, 2014, pp. 975–998. ISBN: 978-3-642-30197-1. DOI: 10.1007/978-3-642-30197-1_292. URL: https://doi.org/10.1007/978-3-642-30197-1_292.

[145] Achenbach, L A et al. “*Dechloromonas agitata* gen. nov., sp. nov. and *Dechlorosoma suillum* gen. nov., sp. nov., two novel environmentally dominant (per)chlorate-reducing bacteria and their phylogenetic position.” In: *International Journal of Systematic and Evolutionary Microbiology* 51.2 (2001), pp. 527–533.

[146] Bradford, Lauren M. et al. “Transcriptome-Stable Isotope Probing Provides Targeted Functional and Taxonomic Insights Into Microaerobic Pollutant-Degrading Aquifer Microbiota”. In: *Frontiers in Microbiology* 9 (2018), p. 2696. DOI: https://doi.org/10.3389/fmicb.2018.02696.

[147] Salinero, Kennan Kellaris et al. “Metabolic analysis of the soil microbe *Dechloromonas aromatica* str. RCB: indications of a surprisingly complex life-style and cryptic anaerobic pathways for aromatic degradation”. In: *BMC Genomics* 10.1 (2009), p. 351. DOI: https://doi.org/10.1186/1471-2164-10-351.

[148] Ben Maamar, Sarah et al. “Groundwater Isolation Governs Chemistry and Microbial Community Structure along Hydrologic Flowpaths”. In: *Frontiers in Microbiology* 6 (2015), p. 1457. DOI: https://doi.org/10.3389/fmicb.2015.01457.

[149] Zhou, Yuxiang, Kellermann, Claudia, and Griebler, Christian. “Spatio-temporal patterns of microbial communities in a hydrologically dynamic pristine aquifer”. In: *FEMS Microbiology Ecology* 81.1 (July 2012), pp. 230–242. DOI: https://doi.org/10.1111/j.1574-6941.2012.01371.x.

[150] Cummings, David E. et al. “*Ferribacterium limneticum*, gen. nov., sp. nov., an Fe(III)-reducing microorganism isolated from mining-impacted freshwater lake sediments”. In: *Archives of Microbiology* 171.3 (1999), pp. 183–188. DOI: https://doi.org/10.1007/s002030050697.

[151] Lalucat, J., Pares, R., and Schlegel, H. G. “*Pseudomonas taeniospiralis* sp. nov., an R-Body-Containing Hydrogen Bacterium”. In: *International Journal of Systematic and Evolutionary Microbiology* 32.3 (1982), pp. 332–338. DOI: https://doi.org/10.1099/00207713-32-3-332.

[152] Willems, A. et al. "*Hydrogenophaga*, a New Genus of Hydrogen-Oxidizing Bacteria That Includes *Hydrogenophaga flava* comb. nov. (Formerly *Pseudomonas flava*), *Hydrogenophaga palleronii* (Formerly *Pseudomonas palleronii*), *Hydrogenophaga pseudoflava* (Formerly *Pseudomonas pseudoflava* and "*Pseudomonas carboxydoflava*"), and *Hydrogenophaga taeniospiralis* (Formerly *Pseudomonas taeniospiralis*)". In: *International Journal of Systematic and Evolutionary Microbiology* 39.3 (1989), pp. 319–333. DOI: https://doi.org/10.1099/00207713-39-3-319.

[153] Brockhurst, Michael A. et al. "The Ecology and Evolution of Pangenomes". In: *Current Biology* 29.20 (2019), pp. 1094–1103. DOI: https://doi.org/10.1016/j.cub.2019.08.012.

[154] Mania, Daniel et al. "A common mechanism for efficient N_2O reduction in diverse isolates of nodule-forming bradyrhizobia". In: *Environmental Microbiology* 22.1 (2020), pp. 17–31. DOI: https://doi.org/10.1111/1462-2920.14731.

[155] Gao, Yuan et al. "Competition for electrons favours N2O reduction in denitrifying Bradyrhizobium isolates". In: *Environmental Microbiology* 23.4 (2021), pp. 2244–2259. DOI: https://doi.org/10.1111/1462-2920.15404.

[156] Chik, Alex H.S. et al. "Evaluation of groundwater bacterial community composition to inform waterborne pathogen vulnerability assessments". In: *Science of The Total Environment* 743 (2020), p. 140472. DOI: https://doi.org/10.1016/j.scitotenv.2020.140472.

[157] Gao, Yang et al. "Groundwater Nitrogen Pollution and Assessment of Its Health Risks: A Case Study of a Typical Village in Rural-Urban Continuum, China". In: *PLOS ONE* 7.4 (Apr. 2012), pp. 1–8. DOI: https://doi.org/10.1371/journal.pone.0033982.

[158] Highton, Matthew P. et al. "Soil N_2O emission potential falls along a denitrification phenotype gradient linked to differences in microbiome, rainfall and carbon availability". In: *Soil Biology and Biochemistry* 150 (2020), p. 108004. DOI: https://doi.org/10.1016/j.soilbio.2020.108004.

[159] Morales, Sergio E., Cosart, Theodore, and Holben, William E. "Bacterial gene abundances as indicators of greenhouse gas emission in soils". In: *The ISME Journal* 4 (2010), pp. 799–808. DOI: https://doi.org/10.1038/ismej.2010.8.

[160] Wu, Jiang, Bauer, Carl E., and Maloy, Stanley. "RegB Kinase Activity Is Controlled in Part by Monitoring the Ratio of Oxidized to Reduced Ubiquinones in the Ubiquinone Pool". In: *mBio* 1.5 (2010), e00272–10. DOI: https://doi.org/10.1128/mBio.00272-10.

[161] Søndergaard, Dan, Pedersen, Christian N. S., and Greening, Chris. "HydDB: A web tool for hydrogenase classification and analysis". In: *Scientific Reportsl* 6 (2016), p. 34212. DOI: https://doi.org/10.1038/srep34212.

[162] Duffner, Clara et al. "Strategies to Overcome Intermediate Accumulation During *in situ* Nitrate Remediation in Groundwater by Hydrogenotrophic Denitrification". In: *Frontiers in Microbiology* 12 (2021), p. 443. DOI: https://doi.org/10.3389/fmicb.2021.610437.

[163] Chang, Chih Cheng, Tseng, Szu Kung, and Huang, Hsien Kai. “Hydrogenotrophic denitrification with immobilized *Alcaligenes eutrophus* for drinking water treatment”. In: *Bioresource Technology* 69.1 (1999), pp. 53–58. DOI: https://doi.org/10.1016/S0960-8524(98)00168-0.

[164] Domeignoz-Horta, L.A. et al. “Non-denitrifying nitrous oxide-reducing bacteria - An effective N2O sink in soil”. In: *Soil Biology and Biochemistry* 103 (2016), pp. 376–379. DOI: https://doi.org/10.1016/j.soilbio.2016.09.010.

[165] Ahmad, Maqshoof et al. “Perspectives of Microbial Inoculation for Sustainable Development and Environmental Management”. In: *Frontiers in Microbiology* 9 (2018), p. 2992. DOI: https://doi.org/10.3389/fmicb.2018.02992.

[166] Grabb, Kalina C. et al. “A dual nitrite isotopic investigation of chemodenitrification by mineral-associated Fe(II) and its production of nitrous oxide”. In: *Geochimica et Cosmochimica Acta* 196 (2017), pp. 388–402. DOI: https://doi.org/10.1016/j.gca.2016.10.026.

[167] Jones, L. Camille et al. “Stable Isotopes and Iron Oxide Mineral Products as Markers of Chemodenitrification”. In: *Environmental Science & Technology* 49.6 (2015), pp. 3444–3452. DOI: https://doi.org/10.1021/es504862x.

[168] Margalef-Marti, Rosanna et al. “Nitrate and nitrite reduction by ferrous iron minerals in polluted groundwater: Isotopic characterization of batch experiments”. In: *Chemical Geology* 548 (2020), p. 119691. DOI: https://doi.org/10.1016/j.chemgeo.2020.119691.

[169] Crane, R.A. and Scott, T.B. “Nanoscale zero-valent iron: Future prospects for an emerging water treatment technology”. In: *Journal of Hazardous Materials* 211-212 (2012), pp. 112–125. DOI: https://doi.org/10.1016/j.jhazmat.2011.11.073.

[170] Strutz, Tessa J. et al. “Nanoscale zero-valent iron: Future prospects for an emerging water treatment technology”. In: *Journal of Hazardous Materials* 23 (2016), pp. 17200–17209. DOI: https://doi.org/10.1007/s11356-016-6814-y.

Attachments

Publication I

FEMS Microbiology Ecology, 97, 2021, fiab004

doi: 10.1093/femsec/fiab004
Advance Access Publication Date: 11 January 2021
Research Article

RESEARCH ARTICLE

Dechloromonas and close relatives prevail during hydrogenotrophic denitrification in stimulated microcosms with oxic aquifer material

Clara Duffner[1,2,†], Sebastian Holzapfel[3], Anja Wunderlich[3], Florian Einsiedl[3], Michael Schloter[1,2] and Stefanie Schulz[2,*]

[1]Chair of Soil Science, TUM School of Life Sciences Weihenstephan, Technical University Munich, Emil-Ramann-Straße 2, 85354 Freising, Germany, [2]Research Unit Comparative Microbiome Analysis, Helmholtz Zentrum München, Ingolstädter Landstr. 1, 85764 Neuherberg, Germany and [3]Chair of Hydrogeology, Technical University Munich, Arcisstraße 21, 80333 Munich, Germany

[*]**Corresponding author:** Research Unit Comparative Microbiome Analysis, Helmholtz Zentrum München, Ingolstädter Landstr. 1, 85764 Neuherberg, Germany. Tel: +49 89 3187 3054; E-mail: stefanie.schulz@helmholtz-muenchen.de

One sentence summary: Members of the bacterial family *Rhodocyclaceae*, especially *Dechloromonas*, were detected as the major denitrifiers under hydrogenotrophic conditions in a groundwater-sediment microcosm experiment.

Editor: Lee Kerkhof
[†]Clara Duffner, http://orcid.org/0000-0001-7517-8434

ABSTRACT

Globally occurring nitrate pollution in groundwater is harming the environment and human health. *In situ* hydrogen addition to stimulate denitrification has been proposed as a remediation strategy. However, observed nitrite accumulation and incomplete denitrification are severe drawbacks that possibly stem from the specific microbial community composition. We set up a microcosm experiment comprising sediment and groundwater from a nitrate polluted oxic oligotrophic aquifer. After the microcosms were sparged with hydrogen gas, samples were taken regularly within 122 h for nitrate and nitrite measurements, community composition analysis via 16S rRNA gene amplicon sequencing and gene and transcript quantification via qPCR of reductase genes essential for complete denitrification. The highest nitrate reduction rates and greatest increase in bacterial abundance coincided with a 15.3-fold increase in relative abundance of *Rhodocyclaceae*, specifically six ASVs that are closely related to the genus *Dechloromonas*. The denitrification reductase genes *napA*, *nirS* and clade I *nosZ* also increased significantly over the observation period. We conclude that taxa of the genus *Dechloromonas* are the prevailing hydrogenotrophic denitrifiers in this nitrate polluted aquifer and the ability of hydrogenotrophic denitrification under the given conditions is species-specific.

Keywords: nitrate pollution; remediation; *Rhodocyclaceae*; groundwater; hydrogen oxidation; denitrification genes

INTRODUCTION

Nitrate leaching into groundwater as a result of intensified nitrogen fertilization and animal farming has been a severe global environmental problem since the 1970s (Rivett *et al.* 2008). Monitoring of the nitrate levels in the upper aquifers in Germany (EEA monitoring network) showed that 18% of groundwater wells had nitrate concentrations above 0.8 mM (50 mg NO_3/L) (Keppner, Grimm and Fischer 2017) and are thereby classified as polluted according to the European nitrate directive

Received: 6 May 2020; **Accepted:** 8 January 2021

(91/676/EEC, 1991). In the aquatic environment and the gastrointestinal tract bacteria reduce nitrate to nitrite. The later binds to haemoglobin at its active site thus impairing the oxygen-binding capacity, which can be fatal for infants (Greer and Shannon 2005). Additionally, epidemiological studies reported significant correlations between increased occurrence of colorectal cancer and the consumption of nitrate-enriched drinking water, even at concentrations far below 0.8 mM (Schullehner *et al.* 2018; Ward *et al.* 2018). Thus, minimizing nitrate concentrations in groundwater, widely used as the main source of drinking water, is important to ensure human health in the long run.

Denitrification is the dominant nitrate transformation process in groundwater and thus a natural biotic process of nitrate remediation (Rivett *et al.* 2008). It is defined as an energy gaining dissimilatory transformation of nitrate or nitrite to a gas species (Zumft 1997). However, under aerobic conditions, the denitrification capacity is poor and microbial available electron donors such as dissolved organic carbon (DOC) or reduced sulphur are often limited in groundwater (Wild, Mayer and Einsiedl 2018). Thus, the *in situ* addition of an electron donor into groundwater, potentially stimulating oxygen consumption and subsequently denitrification, represents a powerful remediation strategy for nitrate polluted aquifers (Janda *et al.* 1988; Smith *et al.* 2001; Chaplin *et al.* 2009). Hydrogen was proven to be the most practical electron donor for this purpose because autotrophic hydrogenotrophic denitrification leads to less bioclogging as it only reaches 40% of the cell yield compared to heterotrophic denitrification (Ergas and Reuss 2001). Additionally, no by-products requiring post-treatment may be formed (Karanasios *et al.* 2010). Also it is likely that aquifers naturally harbor hydrogenotrophic chemolithoautotrophic bacteria because a large proportion of the bacterial population in aquifers holds the genetic potential to fix CO_2 via the Calvin cycle (Herrmann *et al.* 2015) and hydrogenase genes occur over a wide range of phyla and environments (Greening *et al.* 2015). Microcosm experiments with sediment stemming from nitrate polluted oxic aquifers and hydrogen addition showed complete nitrate removal but with transient nitrite accumulation (Schnobrich *et al.* 2007; Chaplin *et al.* 2009). However, to the best of our knowledge the only *in situ* experiment conducted so far reported incomplete nitrate reduction and no reduction of nitrite (Chaplin *et al.* 2009). While some denitrifiers perform four steps reducing nitrate to gaseous N_2, others may only perform a subset due to lack of genes or unfavorable environmental conditions (Graf, Jones and Hallin 2014; Lycus *et al.* 2017). Since the denitrification intermediate nitrite is toxic and nitrous oxide represents an potent greenhouse gas (Mosier 1998), it is important to understand which hydrogenotrophic denitrifiers perform complete denitrification.

Confirmed autotrophic hydrogenotrophic denitrifiers in pure cultures belong to the genera *Acidovorax*, *Paracoccus*, *Acinetobacter* and *Pseudomonas* (Szekeres *et al.* 2002; Vasiliadou *et al.* 2006b). Additionally, *Rhodocyclus*, *Sulfuricurvum*, *Hydrogenophaga* and *Dechloromonas* were detected by 16S rRNA gene sequencing of stable communities in hydrogen-based bioreactors (Zhang *et al.* 2009; Zhao *et al.* 2011). *Hydrogenophaga* and *Dechloromonas* as well as *Sulfuritalea* were also detected as dominant transcriptionally active hydrogenotrophic denitrifiers in a microcosm experiment with groundwater and crushed rock from a pristine aquifer (Kumar *et al.* 2018a). These results from hydrogen-based bioreactors and pristine groundwater enrichments indicate which bacterial taxa are capable of autotrophic hydrogenotrophic denitrification. However, it is unknown which taxa would dominate upon hydrogen addition in a nitrate polluted oxic porous aquifer where *in situ* remediation seems to be an effective tool to reduce nitrate below drinking-water maximum allowable concentrations of 0.8 mM. Therefore, a microcosm experiment with sediment and groundwater from a tertiary aquifer located in southeast Germany was conducted under a hydrogen atmosphere measuring microbial nitrate reduction over time. The sampling area is characterized by intensive pig farming with groundwater nitrate concentrations up to 1.61 mM, high median oxygen concentrations of up to around 200 μM and, median DOC of only 11.8 μM (Wild, Mayer and Einsiedl 2018). Based on modelling results, the same authors determined a denitrification lag time (time prior to commencement of denitrification) of approximately 114 years for this aquifer, which illustrates the need for bioremediation in addition to reducing nitrogen input into groundwater. Over the course of the experiment microcosms were sampled destructively at several timepoints to determine the microbial community composition with 16S rRNA gene amplicon sequencing. We hypothesized that if the community changes upon hydrogen addition, the relative abundance of the hydrogenotrophic denitrifying community should increase as nitrate concentrations decrease. Additionally, denitrification genes and transcripts were quantified via (RT)-qPCR. Due to the highly selective conditions the diversity of denitrifiers in such aquatic environments is generally low (Zhang *et al.* 2009; Karanasios *et al.* 2010) and therefore an increased abundance of reductase genes and their corresponding transcripts may reflect the hydrogenotrophic denitrifiers of this community. The goal was to determine the predominant members of hydrogenotrophic denitrifier communities and which genes involved in denitrification were most abundant in the stimulated microcosms with oxic aquifer material.

METHODS

Study site and sampling method

The Hohenthann area is located 90 km northeast of Munich (Germany) within the Bavarian Tertiary Molasse-Hills. Both a main porous aquifer and several perched aquifers are nitrate polluted, electron donor limited and oxic. Sediment samples were taken from the main porous aquifer, whereas groundwater was collected from a spring discharging from one of the small perched aquifers. More details concerning the physicochemical parameters of the area and the oxygen reduction rates can be found in Wild, Mayer and Einsiedl (2018). Sampling for this study was done in August 2018. The sediment samples were taken on a fallow field (GPS: 48°42′01.2″N 12°00′10.2″E) with an auger from the saturated zone of the aquifer at a depth between 2 and 2.5 m. The groundwater discharging from the spring has on average 100 μM DOC. The sediment and groundwater were transported to the laboratory at <10°C and stored at 4°C prior to the experiment.

Microcosm experiment set up and sampling

Prior to the experiment the collected wet sediment was sieved (2 mm) to remove larger gravel and the groundwater was filtered (pore size ~20 μm) to remove particles. A total of 30 g of sieved sediment and 85 mL groundwater were added to 120 mL vials closed with butyl rubber septa and aluminium crimp caps. Overall, 69 vials were prepared. A total of four vials were sampled at the start of the experiment (0 h), simultaneous to the treatment's application, to assess the initial community. A total of forty vials were sparged with approximately 1 L of hydrogen (H_2) using a hydrogen generator (Precision series, Peak Scientific, Scotland).

Another eight vials were sparged with nitrogen as an anaerobic control lacking an electron donor (N_2), while eight vials with ambient air served as an untreated control (UC) and nine vials autoclaved prior to hydrogen sparging served as an abiotic control (sterile). At each sampling point four vials were destructively sampled so that the remaining microcosms stayed undisturbed. The sampling timepoints, and applied analyses of each treatment and control are stated in Table 1. Some sampling timepoints of the hydrogen-treated samples were excluded from the microbial analysis because the results of the chemical analysis did not suggest changes in the microbial community composition. The sterile controls were also excluded from the microbial analysis since DNA sequencing cannot differentiate between living and dead bacteria. The absence of oxygen in the hydrogen- and the nitrogen-treated microcosms was confirmed in four vials with an oxygen sensor (Fibox 4 trace, PreSens, Germany). During the experiment, all microcosms were incubated at 16°C on a rotary shaker (220 rpm). For the microbiological analyses two times 15 mL mixed sediment-groundwater suspension were centrifuged for 10 min at 7700 × *g* and 4°C. The supernatant was discarded, the pellets shock-frozen in liquid nitrogen and stored at −80°C until further processing. The samples for the chemical analysis were filtered (0.22 μm PES) to remove bacteria and analysed via ion chromatography (DIONEX ICS-1100, Thermo Fisher Scientific, Waltham, MA, USA). Nitrate and nitrite were measured in all vials while ammonium was only measured in one replicate per timepoint. The concentration of each sample is the mean of three measurements and the detection limits are 0.008 mM for nitrate, 0.007 mM for nitrite and 0.013 mM for ammonium.

Nucleic acid extraction and reverse transcription

DNA was extracted from one complete pellet (15 mL groundwater-sediment suspension) using the phenol–chloroform based protocol described in Lueders, Manefield and Friedrich (2004) and Töwe *et al.* (2011) and quantified fluorometrically. Due to the overall low DNA output, the RNA was extracted separately with the RNeasy Power Soil Total RNA Kit (QIAGEN, Hilden, Germany) from the second pellet sampled and quantified spectrophotometrically. Residual DNA in the extracts was digested with DNase (TURBO DNase, Thermo Fisher Scientific (Invitrogen), Waltham, MA, USA) with 1 μg RNA as input. The RNA was purified (RNA Clean & Concentrator-5 Kit, Zymo Research, Irvina, CA, USA) and the absence of DNA in the samples was confirmed using a *nirS* based qPCR according to the protocol in Table S3 (Supporting Information). Confirmation with a 16S rRNA gene-based PCR was not considered as useful due to known DNA contamination in laboratory reagents (Salter *et al.* 2014). Instead *nirS* was chosen as a marker gene because quantification on the DNA level (Fig. 5A) showed a high abundance of *nirS* genes in all samples. Furthermore, the RNA's quality was determined with a Fragment Analyzer (DNF-471 Standard Sensitivity RNA Analysis Kit, Agilent Technologies, Santa Clara, CA, USA). The extracted RNA of one hydrogen-treated vial from timepoint 30 h had a noticeable lower RNA quality number (RQN) of 3.5 compared to the rest of the samples (RQN 7.12, SD: 0.77). The sample with the low RQN value was omitted from further analysis, however three replicates of the timepoint remained. The purified RNA was quantified fluorometrically so that consistently 40 ng RNA were added to the reverse transcription reaction (High-Capacity cDNA Reverse Transcription Kit, Thermo Fisher Scientific (Applied Biosystems), Waltham, MA, USA). The two negative extraction controls and two DNase reaction controls were run alongside the samples.

16S rRNA gene amplicon sequencing, data processing and statistical analysis

Bacterial community composition was determined by 16S rRNA gene-targeted Illumina MiSeq amplicon sequencing. The hypervariable regions V1 and V2 of the 16S rRNA gene were amplified over 25 cycles with the adapter containing primer pair S-D-Bact-0008-a-S-16 5′-AGAGTTTGATCMTGGC-3′ and S-D-Bact-0343-a-A-15 5′-CTGCTGCCTYCCGTA-3′ (Klindworth *et al.* 2013) in triplicates. Besides the primers, the PCR reaction contained the NebNext High-Fidelity 2X PCR Master Mix (New England BioLabs, Ipswich, MA, USA) and 2 ng/μL DNA. Triplicates were pooled when the successful amplification was confirmed by an agarose gel and purified (AMPure XP Beads, Beckman Coulter, Brea, CA, USA). The amplicon's size, concentration and purity were determined by capillary electrophoresis. A total of 10 ng DNA were used as input in the following index PCR which added sample-specific indices (Nextera Dual Indexes Set, Illumina, San Diego, CA, USA) to the adapters during eight cycles. The indexed amplicons were also purified and analysed by capillary electrophoresis as described above. Afterwards they were equalized to 4 nM, pooled and loaded on the Illumina MiSeq platform with 20% PhiX for paired-end sequencing with the Reagent Kit v3 (2 × 300 bp; Illumina).

The demultiplexed sequenced reads were processed with QIIME 2 (Bolyen *et al.* 2019). Denoising was performed with the DADA2 plugin whereby the N-terminal trimming was set to 10 bp and the C-terminal trimming to 260 bp for the forward and to 220 bp for the reverse reads. The amplified sequence variants (ASVs) with reads in the negative extraction control were removed from all samples. For the taxonomic assignment (*P*-confidence $\geq$ 0.9), a classifier was pre-trained with the primer pair 0008/0343 based on the SILVA 16S database release 132 (Quast *et al.* 2012). To compensate for unequal sampling depth subsampling to the minimum number of reads per sample (17 515) was performed using the vegan package (version v2.4–2; Oksanen *et al.* 2019) in R project (version 3.5.3; R Development Core Team 2019). Data analysis was performed in R project using additional packages. The alpha diversity indices (Shannon and Simpson) were calculated with the vegan package (version v2.4-2; Oksanen *et al.* 2019) and converted to the effective number of species (ENS) by taking the exponent of the Shannon index and by dividing one by the complement of the Simpson index (Hill 1973). The stacked bar plots were generated with the phyloseq package (version 1.30.0; McMurdie and Holmes 2013) and the heatmap with the ComplexHeatmap package (Gu, Eils and Schlesner 2016). Because relative abundances are non-parametric data, a robust one-way ANOVA with trimmed means (t1way function) and the corresponding post-hoc test lincon, both from the package WRS2 (Mair and Wilcox 2019), were used to test which taxa differed in relative abundance over time. Low abundant taxa were removed from the tests when the sum of reads of a given taxa in all samples was less than four. Differences were considered significant if p-values were <0.05 after Benjamini–Hochberg correction (Benjamini and Hochberg 1995). The closest relatives of unclassified ASVs which increased significantly over time were determined with the nucleotide Basic Local Alignment Search Tool (nblast) by aligning the ASV sequence against the rRNA/ITS databases (NCBI: https://blast.ncbi.nlm.nih.gov/Blast.cgi). Because the percentage identity was

Table 1. Description of the microcosms experiment set up including the sampling time points, number of replicates and the performed subsequent analyses (x) for the treatments (H_2 and N_2) and controls (UC and sterile).

Treatment	None	H_2										N_2		UC		Sterile + H_2		
Time [h]	0	30	40	50	60	70	80	92	100	114	122	77	126	76	125	0	72	128
Replicates	4	4	4	4	4	4	4	4	4	4	4	4	4	4	4	3	3	3
Chemical analysis	x	x	x	x	x	x	x	x	x	x	x	x	x	x	x	x	x	x
Microbial analysis	x	x		x	x	x	x	x			x	x	x	x	x			

below 97%, additionally maximum-likelihood phylogenetic trees were created using MEGA-X (Kumar *et al.* 2018b). The phylogenetic trees were generated with the 324 bp long amplicon sequences and trimmed 16S rRNA gene sequences of closely related type species downloaded from the SILVA database (Quast *et al.* 2012). The amplicon sequence dataset is available in the Sequence Read Archive (SRA) repository under the BioSample accession numbers SAMN14610043-SAMN14610054 as part of the BioProject PRJNA626487.

Quantification of denitrification genes and transcripts

The genes and transcripts of all relevant reductases (Table S2, Supporting Information) were quantified by qPCR on a 7300 Real-Time PCR System (Applied Biosystems). Additionally, the overall bacterial abundance was determined by quantifying the 16S rRNA gene. To avoid PCR inhibition the optimal dilutions were determined for DNA (denitrification genes 1:25, 16S rRNA gene 1:500) and cDNA (1:8, only for clade II *nosZ* undiluted) by a dilution series qPCR. The standards were serially diluted ranging from 10^7 to 10^1 gene copies/µL. The standards of all genes, except for clade II *nosZ*, consisted of the respective gene fragment (source bacteria stated in Table S3, Supporting Information) inserted into a plasmid. The plasmid backbone however inhibited the clade II *nosZ* gene amplification. Therefore, clade II *nosZ* was amplified, purified and quantified to be used as a linear standard prior to starting the qPCR run. The qPCR reactions, performed in 96-well plates, contained Power Sybr Green Master Mix (Applied Biosystems), 0.2–1 µM forward and reverse primer (Table S3, Supporting Information) and 2 µL diluted DNA/cDNA. Additionally, the qPCR reactions of all genes, except for clade II *nosZ*, contained 0.06% BSA while the reactions of the clade II *nosZ* qPCRs contained 0.25 µg T4 Gene 32 protein. The qPCRs had an initial 10 min denaturation step at 95°C followed by gene-specific cycling conditions listed in Table S3 (Supporting Information). The specificity of the amplified products was verified by a melting curve analysis and agarose gels of exemplary samples. The R^2 of all standard curves was above 0.99 and the efficiencies, listed in Table S4 (Supporting Information), were calculated as described in Töwe *et al.* (2010) with the equation Eff $= 10^{(-1/\text{slope})} - 1$. The gene and transcript copy numbers were calculated per mL sediment-groundwater suspension. The differences in mean gene/transcript copy numbers were statistically tested with a robust ANOVA from the R package WRS2 (Mair and Wilcox 2019). As done for the analysis of sequencing data, tests with *P*-values <0.05 after Benjamini–Hochberg correction (Benjamini and Hochberg 1995) were considered significant.

RESULTS

Chemical analysis

The groundwater and sediment sampled from a highly nitrate polluted oxic oligotrophic aquifer inside sealed microcosms was sparged with hydrogen gas to stimulate the hydrogenotrophic denitrifying bacteria. Figure 1 shows the measured nitrate, nitrite and ammonium concentrations over time. In contrast to the nitrogen-treatment and the untreated control, the hydrogen-treatment stimulated denitrification up to complete nitrate and nitrite reduction. The initial nitrate concentration was fully reduced within 80 h. At the beginning, nitrate was reduced at an average rate of 6.6 μM/h however between 60 and 80 h the nitrate reduction rate increased to more than 35.6 μM/h. During this exponential phase of nitrate reduction, the nitrite concentrations peaked with the highest measured concentration (0.252 mM) after 70 h. Nitrite was still measured when nitrate was below detection limit but was also fully reduced after at least 92 h. A small amount of nitrate was also reduced in the nitrogen-treated and untreated control microcosms, however at much lower average rates (N_2: 2.68 μM/h, UC: 0.88 μM/h) (Fig. 1). The sterile control microcosms, however, displayed no nitrate reduction at all. Throughout the experiment ammonium concentrations remained below 0.024 mM in the measured vials.

Community analysis

The bacterial community composition in the groundwater and sediment suspensions was determined by 16S rRNA gene amplicon sequencing. On average the samples contained 113 283 sequence reads of which 54.2% were lost during denoising (Table S1, Supporting Information). The sampling depth was sufficient as the rarefaction curves reached a plateau at the cut-off of 17 515 reads (Fig. S1, Supporting Information). The effective number of species (ENS; Fig. 2A) decreased by half in the hydrogen-treated microcosms from an initial average ENS of 2099 to 915 within the first 30 h. The ENS in the nitrogen-treated and untreated control microcosms also decrease to around 1000, so this early drop can be attributed to the incubation rather than to the treatment. However, contrary to the controls the ENS in the hydrogen-treated microcosms further decreased between 30 and 80 h to average 235. The ENS based on the Simpson index (Fig. S2, Supporting Information) shows comparable results. Concurrent, 16S rRNA gene copies increased significantly over time ($P = 0.002$, t1way), especially between 60 and 92 h ($P = 0.009$, lincon; Fig. 2B), while no significant changes over time were observed in the nitrogen-treated microcosms and the untreated control.

The phylum *Bacteroidetes* increased significantly from 5.76% mean relative abundance at the beginning to above 10% after 60 h in the hydrogen-treated microcosms ($P = 0.001$, lincon; Fig. 3A and Fig. S4, Supporting Information). A similar increase in relative abundance also occurred in the nitrogen-treated (77 h, $P = 0.0009$ and lincon), and in the untreated control microcosms (76 h, $P = 0.0002$, lincon). Notably the mean relative abundance did not increase further thereafter in either treatments or control. The significant increase in *Bacteroidetes* was mainly attributed to the families *Crocinitomicaceae* and *Prolixibacteraceae* which both increased significantly in the hydrogen-treated ($P = 0.00003$, $P = 0.0004$, t1way) and nitrogen-treated microcosms (*P*

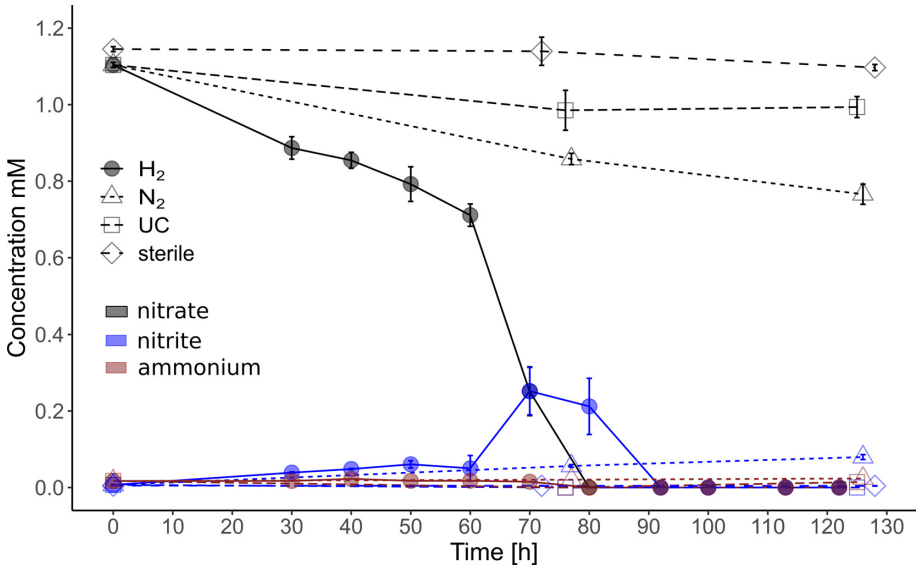

Figure 1. Nitrate, nitrite and ammonium concentrations over time in the hydrogen-treated (H_2), nitrogen-treated (N_2), untreated control (UC) and sterile microcosms. The data points for nitrate and nitrite are mean values from four replicates, except in the sterile control, where each data point is a mean value of three replicates. Error bars are SDs. The data points for ammonium are from one representative replicate.

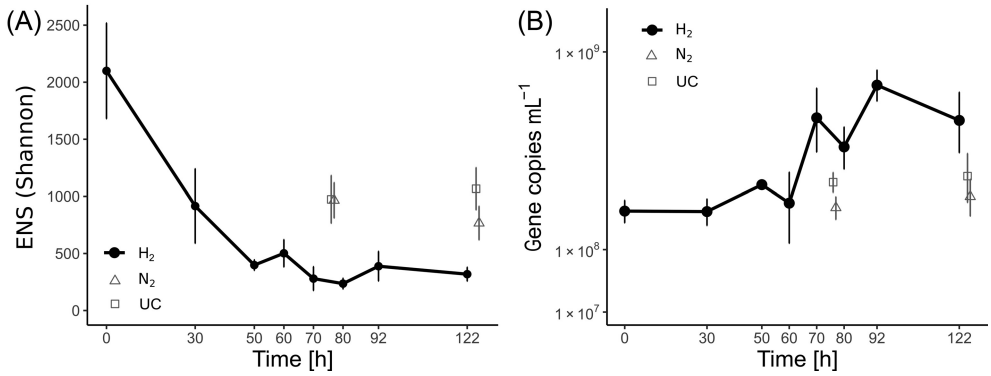

Figure 2. Changes in **(A)** the effective number of species (Shannon) based on the 16S rRNA gene amplicon sequencing data and **(B)** the bacterial abundance based on 16S rRNA gene quantification with qPCR in the hydrogen-treated, nitrogen-treated and untreated control microcosms over time. Timepoint 0 h represents the initial community independent from a treatment. The data points are mean values from four replicates; error bars are SDs.

= 0.047, P = 0.049, t1way; Fig. 3A). Also, in the untreated control, *Crocinitomicaceae* (P = 0.009, t1way) increased, however their relative abundance remained below 1.25% at all timepoints.

The second phylum which increased significantly over time was *Proteobacteria*. However, unlike *Bacteroidetes,* the increase was observed only in the hydrogen-treated microcosms (P = 0.00003, t1way; Fig. 3B and Fig. S4, Supporting Information). Its relative abundance rose from 37.9% at the beginning to 61.1% after 80 h, from then on it remained constant until the last measurement. A total of two families belonging to *Proteobacteria* contributed to the significant increase, namely *Rhodocyclaceae* (P = <0.00001, t1way) and *Burkholderiaceae* (P = 0.007, t1way). The former increased 15.3-fold in relative abundance from average 2 to 30.1% within the first 80 h while the later increased only 2.3-fold from average 5.8 to 13.5% within the same period. During the first 50 h, the relative abundance of *Rhodocyclaceae* increased at a rate of 0.1%/h which rose to 0.285%/h between 50 and 80 h, the period of the highest nitrate reduction rate and greatest increase in 16S rRNA copies. A first shift in the bacterial community composition of the hydrogen-treated microcosms between 30 and 50 h and a second shift after 60 h is visible in Fig. 3 and the heatmap (Fig. S3, Supporting Information), which includes the 40 most abundant ASVs of the phyla *Proteobacteria* and *Bacteroidetes* in the hydrogen-treated microcosms. In the hydrogen-treated microcosms, the significantly increased ASVs (t1way) of the first shift mostly belong to the family *Burkholderiaceae* e.g. *Rhodoferax*, as well as *Prolixibacteraceae* BSV13, *Fluviicola* and *Geobacter* (Fig. S3, Supporting Information). The genera *Curvibacter*, *Ramlibacter* and *Sulfuricella* also increased in relative abundance in the first 50 h however not statistically significant. Several ASVs which increased during the first community shift, including *Rhodoferax* and *Prolixibacteraceae,* also increased in relative abundance in the nitrogen-treated microcosms (Fig. S3, Supporting Information). However, these changes were not statistically significant. In contrast, the taxa belonging to the second shift, *Dechloromonas*, three unclassified *Rhodocyclaceae* ASVs (ii) and, two unclassified *Burkholderiaceae* ASVs (i), only enriched significantly in the hydrogen-treated microcosms but not in the nitrogen-treated nor in the untreated control (Fig. S3, Supporting Information). According to nblast and the created phylogenetic trees (Fig. S5, Supporting Information) the unclassified *Rhodocylcacea* ASVs (ii) are closely related to *Azospira*

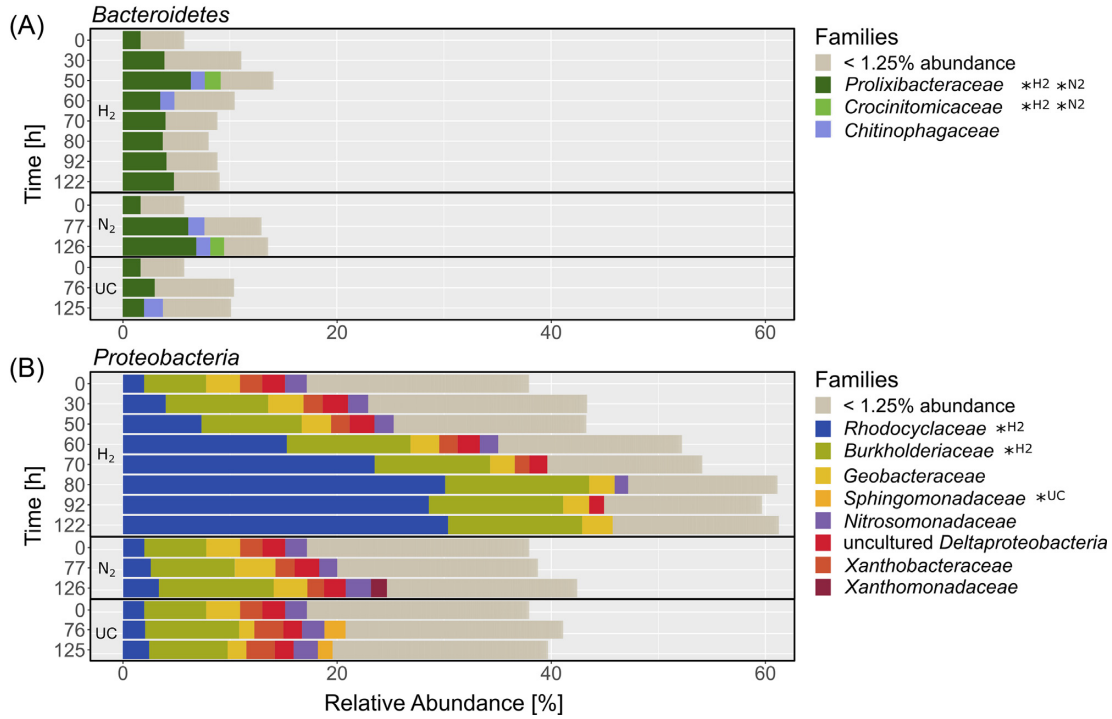

Figure 3. Changes in the bacterial community structure on the family level of the two phyla; **(A)** *Bacteroidetes* ($P = 0.00015$, t1way), and **(B)** *Proteobacteria* ($P = 0.00003$, t1way) which increased significantly in the hydrogen-treated microcosms over time. All significantly increased families (t1way) which reached at least 1.25% relative abundance at one timepoint are marked with an asterisk and the respective treatment/control it refers to (H_2: hydrogen, N_2: nitrogen, UC: untreated control). The stacked bars represent mean relative abundances of four replicates.

and *Rhodocyclus* and the unclassified *Burkholderiaceae* ASVs (i) are closely related to *Massilia*. *Sulfuritalea* increased in relative abundance within the first 50 h, like the taxa of the first community shift, and remained constant thereafter. The genus with the highest increase in relative abundance was *Dechloromonas* rising from on average 0.8% at the beginning to 24% after 80 h in the hydrogen-treated microcosms, while its relative abundance always remained below 1% in the nitrogen-treated microcosms and the untreated control (Fig. 4A). In the hydrogen-treated microcosms, 37 detected ASVs were assigned to the genus *Dechloromonas* of which only six increased significantly over time. Thereof, ASV15089, ASV5383 and ASV1396 were initially of such low abundance, that they remained below the detection limit even until 30 h. ASV15089 and ASV5383 increased in relative abundance until 92 h while ASV13899 and ASV9041 only increased until 70 to 80 h. A phylogenetic tree was constructed based on an alignment of the 324 bp long amplicon sequences of the 37 *Dechloromonas* ASVs and the trimmed 16S rRNA gene sequences of the type strains of all *Rhodocyclaceae* genera (Fig. 4B). It shows that the six *Dechloromonas* ASVs which increased significantly over time form three clusters within the *Dechloromonas* subtree. The monospecific genera *Ferribacterium* and *Quatrionicoccus* also position within the *Dechloromonas* subtree.

While the phyla *Bacteroidetes* and *Proteobacteria* increased significantly in relative abundance in the hydrogen-treated microcosms the phyla *Acidobacteria* ($P = 0.0003$, t1way), *Chloroflexi* ($P = 0.0005$, t1way), *Rokubacteria* ($P = 0.0005$, t1way) and *Nitrospirae* ($P = 0.02$, t1way) decreased significantly over time (Fig. S4, Supporting Information). No significant decrease in relative abundance of these phyla was observed in either the nitrogen-treated or the untreated control microcosms.

Denitrification genes and transcripts

In the hydrogen-treated microcosms the gene abundance of *napA* ($P = 0.001$, t1way), *nirS* ($P = <0.00001$, t1way), *qnorB* ($P = 0.045$, t1way) and clade I *nosZ* ($P = <0.00001$, t1way) increased significantly over time (Fig. 5A). Comparisons of all timepoints against each other using post-hoc test lincon showed significant differences between the timepoints 0–60 h and 70–122 h for the genes *napA*, *nirS* and clade I *nosZ* but not for *qnorB*. For *napA*, *nirS* and clade I *nosZ* the greatest increase was between 50 and 80 h while for *qnorB* only a slight gradual increase was measured. The mean gene abundance of *cnorB* also increased strongly between 60 and 92 h, however the variability between replicates was rather high. The copy number of most transcripts of the measured reductase genes increased from 60 to 80 h after which they decreased again (Fig. 5B). These changes were however mostly not significant. An exception were *nirK* transcripts, which did not increase at all, and clade I *nosZ* transcripts which started to increase in abundance earlier and peaked at 70 h. Significant changes in the abundance patterns of genes and transcripts of the analysed reductases over time were neither observed in the nitrogen treatment nor in the untreated control (Fig. 5).

DISCUSSION

In this study, we aimed to detect taxa stimulated under hydrogenotrophic denitrifying conditions, which were expected to increase in relative abundance during the period of greatest nitrate reduction activity. The maximum measured nitrate reduction rate of 35.6 μM/h, comparable with other studies on hydrogenotrophic denitrification (Ergas and Reuss 2001; Vasiliadou, Pavlou and Vayenas 2006a), was between 60 and 80 h. Con-

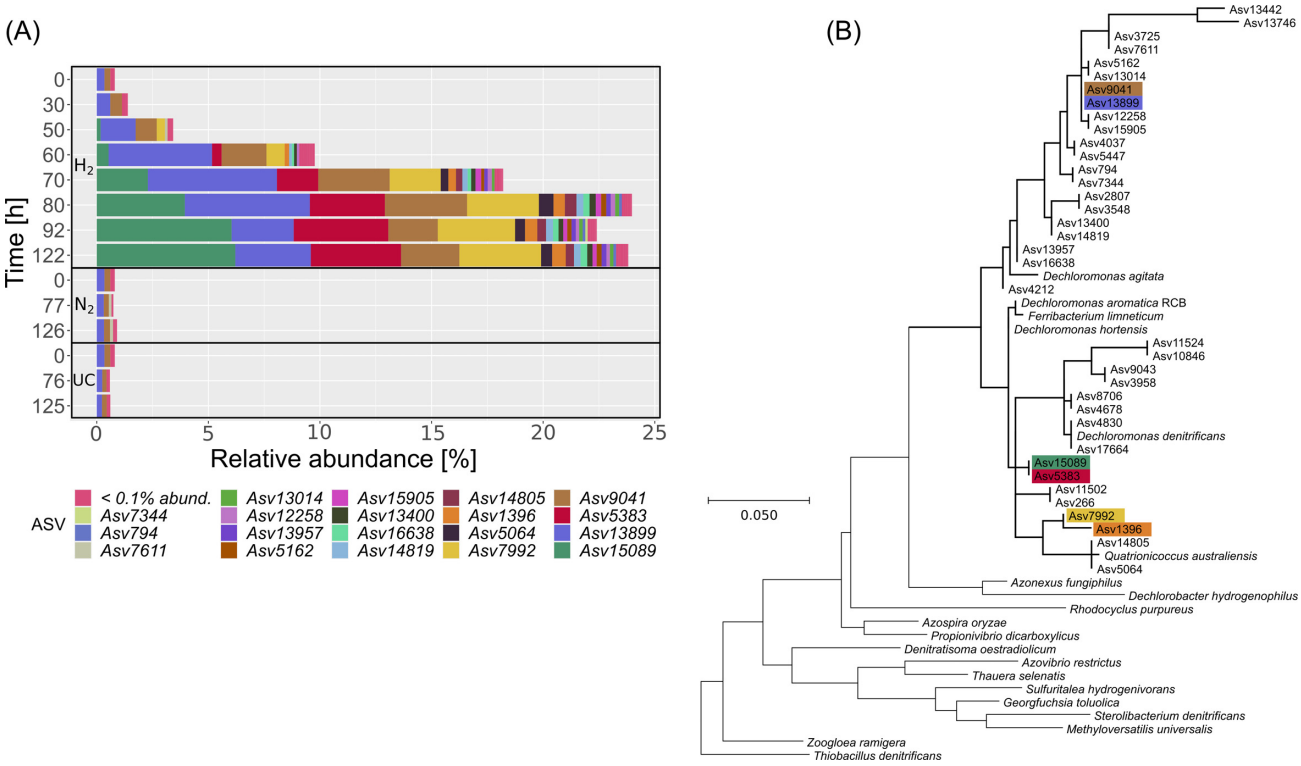

Figure 4. The stacked bar plot **(A)** shows the 37 detected ASVs assigned to the genus *Dechloromonas*. The stacked bars represent mean relative abundances of four replicates. Only six ASVs increased significantly in relative abundance in the hydrogen-treated microcosms. A phylogenetic tree **(B)** constructed with the amplicon sequences of the 37 detected *Dechloromonas* ASVs and 16S rRNA sequences of most type strains belonging to *Rhodocyclaceae*. The six ASVs which significantly increased over time (t1way) are marked with their respective color.

sequently, the highest energy gain and resulting greatest growth of bacteria utilizing hydrogen for denitrification is expected during this period. This is further corroborated by a decrease of ENS and a significant increase of 16S rRNA copies/mL between 60 and 92 h. The genera which increased greatest in relative abundance during this period were *Dechloromonas* and *Sulfuritalea* along with five unclassified ASVs which may belong to the genera *Azospira*/*Rhodocylcus* and *Massilia*. These taxa neither increased in the nitrogen-treated microcosms nor in the untreated control, which indicates that they were using hydrogen as the main electron donor. *Rhodocyclaceae*, the family with the greatest increase in relative abundance as it includes the genera *Dechloromonas*, *Azospira*/*Rhodocylcus*, *Sulfuritalea*, is known to contribute significantly to denitrification in wastewater treatment systems (Wang *et al.* 2020). The genera belonging to *Rhodocyclaceae* which increased significantly in relative abundance between 60 and 80h are all known hydrogenotrophic denitrifiers (Zhang *et al.* 2009; Zhao *et al.* 2011; Kumar *et al.* 2018a). Two unclassified ASVs likely belonging to the genus *Massilia* also increased in relative abundance between 60 and 80 h but contrary to the previous they belong to the family *Burkholderiaceae*. To our knowledge it has not been described as a hydrogenotrophic denitrifier yet whereby its role as such is questionable.

Dechloromonas was the genus with the greatest increase in relative abundance. Bacteria of this genus have been detected in many different environments and are known for their diverse abilities to degrade environmental contaminants such as aromatic hydrocarbons (BTEX; Bradford *et al.* 2018) and perchlorate (Salinero *et al.* 2009). They are also known to reduce nitrate, preferring it even over perchlorate, despite being energetically slightly less favorable (Nozawa-Inoue *et al.* 2011; Wang *et al.* 2018). Conthe *et al.* (2018) detected *Dechloromonas* as the most abundant clade II *nosZ* OTU in an enrichment culture grown on acetate and N_2O as the sole electron acceptor. This demonstrates the ability of *Dechloromonas* as a N_2O reducer. These qualities, which include wide occurrence, degradation of environmental contaminants as well as nitrate and strong N_2O reduction, are desirable traits in hydrogenotrophic denitrifiers for *in situ* remediation. The significant increase in relative abundance of only six out of 37 detected ASVs assigned to *Dechloromonas* implies species or even strain level differences in their hydrogenotrophic denitrifying abilitiy. This is further supported by differing behavior among these six *Dechloromonas* ASVs. While ASV13899 and ASV9041 increased in relative abundance only until 70–80 h, ASV15089 and ASV5383 continued, thereafter, when all nitrate had been reduced. Potentially ASV13899 and ASV9041 are incomplete denitrifiers, while ASV15089 and ASV5383 reduce all intermediates including nitrite, NO and N_2O as well. Generally, denitrification is a polyphyletic and ancient trait (Zumft 1997), so it is not unusual that even closely related taxa differ greatly in their denitrification characteristics (Liu *et al.* 2013) or in their genetic capability to denitrify (Jones *et al.* 2008; Graf, Jones and Hallin 2014). In the phylogenetic tree of *Rhodocyclaceae*, all 37 ASVs assigned to *Dechloromonas* clustered within the *Dechloromonas* subtree. The *Dechloromonas* subtree also includes the monospecific genera *Ferribacterium* and *Quatrionicoccus*, which can also be observed in other phylogenetic trees based on full 16S rRNA gene sequences (Oren 2014). Considering this, some ASVs which were assigned to the genus *Dechloromonas* by the used bioinformatic pipeline, could belong to the genera *Quatrionicoccus* or *Ferribacterium*. Of the six ASVs which seem to perform hydrogenotrophic

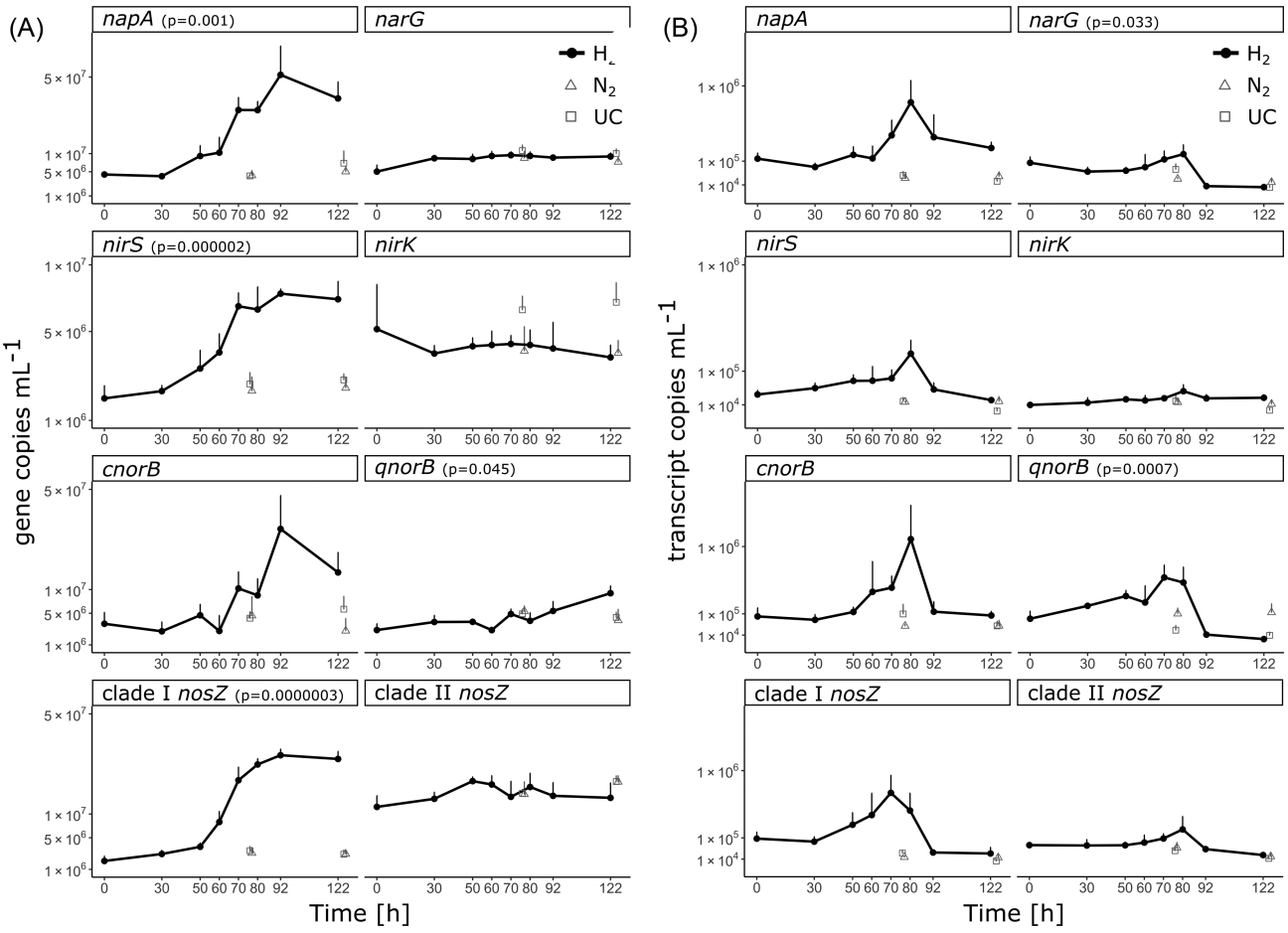

Figure 5. (A) Gene and **(B)** transcript abundance per mL sediment-groundwater suspension of the reductase genes *napA* and *narG* ($NO_3^- \rightarrow NO_2^-$), *nirS* and *nirK* ($NO_2^- \rightarrow NO$), *cnorB* and *qnorB* ($NO \rightarrow N_2O$), as well as clade I and clade II *nosZ* ($N_2O \rightarrow N_2$). The *y*-axes are square-root transformed, all data points are mean values of four replicates and error bars are SDs. Gene or transcript copy numbers differed significantly (t1way) only in the hydrogen-treated microcosms. The according *p*-values are stated. Timepoint 0 h represents the initial community independent from a treatment ($n = 4$).

denitrification, ASV7992 and ASV1396 clustered with *Quatrionicoccus australiensis* but none clustered with *Ferribacterium limneticum*. An identification beyond the genus level within the *Dechloromonas* subtree is however not feasible because the phylogenetic tree is only based on the 324 bp long amplicon sequences. These findings illustrate the need to isolate and analyse pure cultures of *Dechloromonas* and close relatives to elucidate the traits determining their hydrogenotrophic denitrification ability.

Clearly, the observed nitrate reduction in the hydrogen-treated microcosms was catalysed by microbiota because no nitrate reduction occurred in the sterile microcosms. Alternative metabolic pathways, such as dissimilatory nitrate reduction to ammonium (DNRA), are unlikely as denitrification may be favored over DNRA under carbon limitation and high nitrate availability in bacterial communities (Kraft *et al.* 2014). Also, throughout the experiment ammonium concentrations remained below 0.024 mM in all analysed microcosms. The increase in 16S rRNA gene copies in the hydrogen-treated microcosms, primarily between 60 and 92 h, confirms that the community composition changes resulted from an average 3.8-fold growth between 0 and 92 h rather than a partial decline due to death.

The gene copy numbers of *napA*, *nirS* and clade I *nosZ* increased significantly simultaneous from 50 h onwards. The amplicon sequencing results of the microcosm experiment confirmed the observation of other studies (Zhang *et al.* 2009; Karanasios *et al.* 2010) that hydrogenotrophic communities are stable and consist only of a few taxa. Consequently, *napA*, *nirS* and clade I *nosZ* are likely the pre-dominant denitrification reductases of the *Rhodocyclaceae* dominated community that increased in relative abundance in this study in parallel. Identification of the reductase genes in the genomes of three available *Dechloromonas* species (Table S5, Supporting Information) supports the obtained qPCR results of the nitrate and nitrite reductase, as all three analysed genomes contain one *napA* but no *narG* gene, and *nirS* but no *nirK* genes. While the nitric oxide reductase qPCR results were inconclusive, the qPCR results of *nosZ* indicate that clade I was the dominating nitrous oxide reductase. However, all three *Dechloromonas* genomes contain only clade II *nosZ* genes, thus we would have expected to see an increase in clade II *nosZ*, which was only the case on the transcript level. To check whether the observed increase in clade I *nosZ* can be attributed to another genus the available full genome sequences of *Azospira* and *Sulfuritalea* were also analysed (Table S5, Supporting Information), but either they contained clade II *nosZ* or no *nosZ* gene at all. Linking the qPCR results of the denitrification reductases to specific ASVs appears to be difficult as a direct proof of function and microbial identity is only possible with a metagenomics or amplicon sequencing

approach, which was beyond the scope of this study. Especially in the case of clade I and clade II *nosZ* the difference in the amplification products of the two qPCR makes a comparison difficult. The only published clade II *nosZ* qPCR amplifies a 690–720 bp long amplification product with a resulting low efficiency (Jones *et al.* 2013), while the clade I *nosZ* qPCR produces a 267 bp long amplification product (Henry *et al.* 2004). According to the RT-qPCR results, the expression of clade I *nosZ* began prior to the expression of the other reductases. Generally, the nitrate reductase is regulated separately and is expressed initially, while the other reductase genes share a common regulator in addition to individual ones (Bothe, Ferguson and Newton 2007). The temporal expression of the later differs between different species. When Bergaust *et al.* (2010) measured the gene expression in *Paracoccus denitrificans* every 2 h they found that the transcription of the *nosZ* gene started even some hours before the expression of *nirS* or *norB*. An early expression of *nosZ* gene is therefore not unlikely. However, a higher temporal resolution in the sampling timepoints would be required to detect a sequential expression.

The way each reductase type influences the phenotype is not fully understood. However, recent studies indicate advantageous attributes of *napA*, *nirS* and clade II *nosZ* type reductases, occurring in the detected dominant genera *Dechloromonas* and *Azospira*, for autotrophic hydrogenotrophic denitrifiers. For facultative bacteria switching from aerobic to anaerobic conditions and from organotrophy to lithotrophy a potential advantage of *napA* is its functional flexibility. Besides anaerobic respiration NapA can also perform redox-energy dissipation which is useful under sufficient carbon and oxygen conditions (Richardson *et al.* 2001). The multiple *nirS* gene copies detected in the *Dechloromonas* genomes (Table S5, Supporting Information; Wang *et al.* 2020), imply higher nitrite reduction rates due to increased transcription and subsequent protein production. An actual physiological advantage of clade II *nosZ* over clade I *nosZ* has been determined by Yoon *et al.* (2016). They could show that bacteria with known clade II *nosZ* had higher biomass yield and higher N_2O affinity compared to clade I *nosZ*. Additionally, clade II *nosZ* contains the signal peptide for Sec protein translocation into the periplasm while clade I *nosZ* contains the signal peptide for Tat protein translocation which requires substantially more energy (Lee, Tullman-Ercek and Georgiou 2006). The resulting higher metabolic efficiency of clade II NosZ reductases can be considered as a competitive advantage, especially in oligotrophic habitats.

The significantly increased taxa in the hydrogen-treated microcosms between 30 and 50 h, when the nitrate reduction rate was still low, receded once the second community shift emerged. These taxa, including *Rhodoferax* belonging to *Burkholderiaceae*, *Prolixibacteraceae* BSV13, *Fluviicola* and *Geobacter,* are not known as hydrogenotrophic denitrifiers. Some of these taxa increased in relative abundance, even though not significant, in the nitrogen-treated microcosms, which also displayed limited reduction of nitrate and steady increase in nitrite. Likely these taxa were growing on residual DOC from the sample material.

The initial bacterial community from the groundwater sediment suspension (0 h) was comparable to bacterial communities in similar upper section aquifers. For example, in an aquifer in France with high nitrate and oxygen concentrations in combination with low organic carbon (108 μM DOC; Ben Maamar *et al.* 2015) *Burkholderiaceae* was the dominating family and *Rhodocyclaceae* was also detected. *Burkholderiaceae* was also the family with the highest relative abundance at the beginning of this microcosm experiment. Notably, the taxa assigned to the family *Burkholderiaceae* in this study, according to the SILVA database release 132, were assigned to the families *Comamonadaceae* and *Oxalobacteraceae* in the study by Ben Maamar *et al.* (2015).

In conclusion, the present study revealed two community shifts. The first consisting of potential heterotrophic denitrifiers feeding on residual DOC and the second consisting of typical autotrophic hydrogenotrophic denitrifiers. Species of the genus *Dechloromonas*, and possibly also of their close relatives *Quatrionicoccus* and *Ferribacterium*, prevailed in the hydrogenotrophic denitrifier community and its members carry reductase genes, which likely favor facultative anaerobic lifestyle as well as high nitrite and N_2O reduction. The later suggests the genetic potential for complete denitrification which is additionally supported by the increased abundance of reductase genes involved in all four denitrification steps over time. The observed species- or even strain-level differences in the hydrogenotrophic denitrifying capabilities require isolation and analysis of isolates of the genera *Dechloromonas*, *Quatrionicoccus*, *Ferribacterium* as well as of close relatives from the family *Rhodocyclaceae* such as *Rhodocyclus* and *Azospira*.

ACKNOWLEDGMENT

We thank Susanne Thiemann from the Chair of Hydrogeology for the chemical analysis and Susanne Kublik from the Research Unit Comparative Microbiome Analysis for the MiSeq Illumina sequencing.

SUPPLEMENTARY DATA

Supplementary data are available at *FEMSEC* online.

FUNDING

Supported by Deutsche Forschungsgemeinschaft (DFG) through TUM International Graduate School of Science and Engineering (IGSSE), GSC 81.

Conflicts of Interest. None declared.

REFERENCES

Benjamini Y, Hochberg Y. Controlling the false discovery rate: a practical and powerful approach to multiple testing. *J R Stat Soc Ser B Methodol* 1995;**57**:289–300.

Ben Maamar S, Aquilina L, Quaiser A *et al.* Groundwater isolation governs chemistry and microbial community structure along hydrologic flowpaths. *Front Microbiol* 2015;**6**:1457.

Bergaust L, Mao Y, Bakken LR *et al.* Denitrification response patterns during the transition to anoxic respiration and post-transcriptional effects of suboptimal pH on nitrous oxide reductase in *Paracoccus denitrificans*. *Appl Environ Microbiol* 2010;**76**:6387–96.

Bolyen E, Rideout JR, Dillon MR *et al.* Reproducible, interactive, scalable and extensible microbiome data science using QIIME 2. *Nat Biotechnol* 2019;**37**:852–7.

Bothe H, Ferguson S, Newton W. *Biology of the Nitrogen Cycle*. Elsevier Science, 2007.

Bradford LM, Vestergaard G, Táncsics A *et al.* Transcriptome-stable isotope probing provides targeted functional and taxonomic insights into microaerobic pollutant-degrading aquifer microbiota. *Front Microbiol* 2018;**9**. DOI: 10.3389/fmicb.2018.02696.

Chaplin BP, Schnobrich MR, Widdowson M *et al.* Stimulating in situ hydrogenotrophic denitrification with membrane-delivered hydrogen under passive and pumped groundwater conditions. *J Environ Eng* 2009;**135**:666–76.

Conthe M, Wittorf L, Kuenen JG *et al.* Life on N2O: deciphering the ecophysiology of N2O respiring bacterial communities in a continuous culture. *ISME J* 2018;**12**:1142–53.

Ergas SJ, Reuss AF. Hydrogenotrophic denitrification of drinking water using a hollow fibre membrane bioreactor. *J Water Supply Res Technol Aqua* 2001;**50**:161–71.

Graf DRH, Jones CM, Hallin S. Intergenomic comparisons highlight modularity of the denitrification pathway and underpin the importance of community structure for N2O emissions. *PLoS One* 2014;**9**:1–20.

Greening C, Biswas A, Carere CR *et al.* Genomic and metagenomic surveys of hydrogenase distribution indicate H2 is a widely utilised energy source for microbial growth and survival. *ISME J* 2015;**10**:761.

Greer FR, Shannon M. Infant methemoglobinemia: the role of dietary nitrate in food and water. *Pediatrics* 2005;**116**:784–6.

Gu Z, Eils R, Schlesner M. Complex heatmaps reveal patterns and correlations in multidimensional genomic data. *Bioinformatics* 2016;**32**: 2847–9.

Henry S, Baudoin E, López-Gutiérrez JC *et al.* Quantification of denitrifying bacteria in soils by nirK gene targeted real-time PCR. *J Microbiol Methods* 2004;**59**:327–35.

Herrmann M, Rusznyák A, Akob DM *et al.* Large fractions of CO2-fixing microorganisms in pristine limestone aquifers appear to be involved in the oxidation of reduced sulfur and nitrogen compounds. *Appl Environ Microbiol* 2015;**81**:2384–94.

Hill MO. Diversity and evenness: a unifying notation and its consequences. *Ecology* 1973;**54**:427–32.

Janda V, Rudovský J, Wanner J *et al.* In situ denitrification of drinking water. *Water Sci Technol* 1988;**20**:215–9.

Jones CM, Graf DR, Bru D *et al.* The unaccounted yet abundant nitrous oxide-reducing microbial community: a potential nitrous oxide sink. *ISME J* 2013;**7**:417–26.

Jones CM, Stres B, Rosenquist M *et al.* Phylogenetic analysis of nitrite, nitric oxide, and nitrous oxide respiratory enzymes reveal a complex evolutionary history for denitrification. *Mol Biol Evol* 2008;**25**:1955–66.

Karanasios KA, Vasiliadou IA, Pavlou S *et al.* Hydrogenotrophic denitrification of potable water: a review. *J Hazard Mater* 2010;**180**:20–37.

Keppner L, Grimm F, Fischer D. *Nitratbericht 2016*, Bundesministerium für Umwelt, Naturschutz, Bau und Reaktorsicherheit (BMUB) & Bundesministeriumfür Ernährung und Landwirtschaft (BMEL), 2017.

Klindworth A, Pruesse E, Schweer T *et al.* Evaluation of general 16S ribosomal RNA gene PCR primers for classical and next-generation sequencing-based diversity studies. *Nucleic Acids Res* 2013;**41**:e1–e.

Kraft B, Tegetmeyer HE, Sharma R *et al.* The environmental controls that govern the end product of bacterial nitrate respiration. *Science* 2014;**345**:676–9.

Kumar S, Herrmann M, Blohm A *et al.* Thiosulfate- and hydrogen-driven autotrophic denitrification by a microbial consortium enriched from groundwater of an oligotrophic limestone aquifer. *FEMS Microbiol Ecol* 2018a;**94**:fiy141.

Kumar S, Stecher G, Li M *et al.* MEGA X: molecular evolutionary genetics analysis across computing platforms. *Mol Biol Evol* 2018b;**35**:1547–9.

Lee PA, Tullman-Ercek D, Georgiou G. The bacterial twin-arginine translocation pathway. *Annu Rev Microbiol* 2006;**60**:373–95.

Liu B, Mao Y, Bergaust L *et al.* Strains in the genus Thauera exhibit remarkably different denitrification regulatory phenotypes. *Environ Microbiol* 2013;**15**:2816–28.

Lueders T, Manefield M, Friedrich MW. Enhanced sensitivity of DNA- and rRNA-based stable isotope probing by fractionation and quantitative analysis of isopycnic centrifugation gradients. *Environ Microbiol* 2004;**6**:73–8.

Lycus P, Lovise Bøthun K, Bergaust L *et al.* Phenotypic and genotypic richness of denitrifiers revealed by a novel isolation strategy. *ISME J* 2017;**11**:2219–32.

Mair P, Wilcox R. Robust statistical methods in R using the WRS2 package. *Behav Res Methods* 2019, DOI: 10.3758/s13428-019-01246-w.

McMurdie PJ, Holmes S. phyloseq: an R package for reproducible interactive analysis and graphics of microbiome census data. *PLoS One* 2013;**8**. DOI: 10.1371/journal.pone.0061217.

Mosier AR. Soil processes and global change. *Biol Fertil Soils* 1998;**27**:221–9.

Nozawa-Inoue M, Jien M, Yang K *et al.* Effect of nitrate, acetate, and hydrogen on native perchlorate-reducing microbial communities and their activity in vadose soil. *FEMS Microbiol Ecol* 2011;**76**:278–88.

Oksanen J, Blanchet FG, Friendly M *et al.* vegan: community ecology package. 2019, https://CRAN.R-project.org/package=vegan (03 February 2020, date last accessed).

Oren A. The family Rhodocyclaceae. In: Rosenberg E, DeLong EF, Lory S, Stackebrandt E, Thompson F (eds.) *The Prokaryotes: Alphaproteobacteria and Betaproteobacteria*, Berlin Heidelberg: Springer, 2014, 975–98.

Quast C, Pruesse E, Yilmaz P *et al.* The SILVA ribosomal RNA gene database project: improved data processing and web-based tools. *Nucleic Acids Res* 2012;**41**:D590–D6.

R Development Core Team. R: a language and environment for statistical computing. *R Foundation for Statistical Computing*, 2019.

Richardson DJ, Berks BC, Russell DA *et al.* Functional, biochemical and genetic diversity of prokaryotic nitrate reductases. *Cell Mol Life Sci CMLS* 2001;**58**:165–78.

Rivett MO, Buss SR, Morgan P *et al.* Nitrate attenuation in groundwater: a review of biogeochemical controlling processes. *Water Res* 2008;**42**:4215–32.

Salinero KK, Keller K, Feil WS *et al.* Metabolic analysis of the soil microbe *Dechloromonas aromatica* str. RCB: indications of a surprisingly complex life-style and cryptic anaerobic pathways for aromatic degradation. *BMC Genomics* 2009; **10**:351.

Salter SJ, Cox MJ, Turek EM *et al.* Reagent and laboratory contamination can critically impact sequence-based microbiome analyses. *BMC Biol* 2014;**12**:87.

Schnobrich MR, Chaplin BP, Semmens MJ *et al.* Stimulating hydrogenotrophic denitrification in simulated groundwater containing high dissolved oxygen and nitrate concentrations. *Water Res* 2007;**41**:1869–76.

Schullehner J, Hansen B, Thygesen M *et al.* Nitrate in drinking water and colorectal cancer risk: a nationwide population-based cohort study. *Int J Cancer* 2018. DOI: 10.1002/ijc.31306. Epub 2018 Feb 23.

Smith RL, Miller DN, Brooks MH *et al.* In situ stimulation of groundwater denitrification with formate to remediate nitrate contamination. *Environ Sci Technol* 2001;**35**:196–203.

Szekeres S, Kiss I, Kalman M *et al.* Microbial population in a hydrogen-dependent denitrification reactor. *Water Res* 2002;**36**:4088–94.

Töwe S, Albert A, Kleineidam K *et al.* Abundance of microbes involved in nitrogen transformation in the rhizosphere of *Leucanthemopsis alpina* (L.) Heywood grown in soils from different sites of the Damma Glacier Forefield. *Microb Ecol* 2010;**60**:762–70.

Töwe S, Wallisch S, Bannert A *et al.* Improved protocol for the simultaneous extraction and column-based separation of DNA and RNA from different soils. *J Microbiol Methods* 2011;**84**:406–12.

Vasiliadou IA, Pavlou S, Vayenas DV. A kinetic study of hydrogenotrophic denitrification. *Process Biochem* 2006a;**41**:1401–8.

Vasiliadou IA, Siozios S, Papadas IT *et al.* Kinetics of pure cultures of hydrogen-oxidizing denitrifying bacteria and modeling of the interactions among them in mixed cultures. *Biotechnol Bioeng* 2006b;**95**:513–25.

Wang O, Melnyk RA, Mehta-Kolte MG *et al.* Functional redundancy in perchlorate and nitrate electron transport chains and rewiring respiratory pathways to alter terminal electron acceptor preference. *Front Microbiol* 2018; **9**:376.

Wang Z, Li W, Li H *et al.* Phylogenomics of rhodocyclales and its distribution in wastewater treatment systems. *Sci Rep* 2020;**10**:3883.

Ward MH, Jones RR, Brender JD *et al.* Drinking water nitrate and human health: an updated review. *Int J Environ Res Public Health* 2018;**15**:1557.

Wild L, Mayer B, Einsiedl F. Decadal delays in groundwater recovery from nitrate contamination caused by low O2 reduction rates. *Water Resour Res* 2018;**54**: 9996–10012.

Yoon S, Nissen S, Park D *et al.* Nitrous oxide reduction kinetics distinguish bacteria harboring Clade I NosZ from those harboring Clade II NosZ. *Appl Environ Microbiol* 2016;**82**:3793–800.

Zhang Y, Zhong F, Xia S *et al.* Autohydrogenotrophic denitrification of drinking water using a polyvinyl chloride hollow fiber membrane biofilm reactor. *J Hazard Mater* 2009;**170**:203–9.

Zhao HP, Van Ginkel S, Tang Y *et al.* Interactions between perchlorate and nitrate reductions in the biofilm of a hydrogen-based membrane biofilm reactor. *Environ Sci Technol* 2011;**45**:10155–62.

Zumft WG. Cell biology and molecular basis of denitrification. *Microbiol Mol Biol Rev* 1997;**61**:533–616.

Publication I Supplementary Materials

RESEARCH ARTICLE

Dechloromonas and close relatives prevail hydrogenotrophic denitrification in stimulated microcosms with oxic aquifer material

Clara Duffner[1,2], Sebastian Holzapfel[3], Anja Wunderlich[3], Florian Einsiedl[3], Michael Schloter[1,2], Stefanie Schulz[2,*]

[1] Chair of Soil Science, TUM School of Life Sciences Weihenstephan, Technical University Munich, Emil-Ramann-Straße 2, 85354 Freising, Germany, [2] Research Unit Comparative Microbiome Analysis, Helmholtz Center Munich, Ingolstädter Landstr. 1, 85764 Neuherberg, Germany, [3] Chair of Hydrogeology, Technical University Munich, Arcisstraße 21, 80333 Munich, Germany

*__Corresponding author:__ Phone: +49 89 3187 3054; E-Mail: stefanie.schulz@helmholtz-muenchen.de

One sentence summary: Members of the bacterial family *Rhodocyclaceae*, especially *Dechloromonas*, were detected as the major denitrifiers under hydrogenotrophic conditions in a groundwater-sediment microcosm experiment.

Keywords: nitrate pollution, remediation, *Rhodocyclaceae*, groundwater, hydrogen oxidation, denitrification genes

---

SUPPLEMENTARY MATERIALS

Table S1: Quality control statistics output from Qiime2 showing the loss of reads of each sample after filtering, denoising, merging of reads, and removal of chimeric reads.

sample ID	treatment	duration	input	filtered	denoised	merged	non-chimeric
CD1	initial sample	0	342273	241129	241129	175961	169441
CD2	initial sample	0	184170	129027	129027	87049	85006
CD3	initial sample	0	218855	152209	152209	108067	104226
CD4	initial sample	0	345100	232293	232293	173254	166379
CD5	UC	76	91206	63440	63440	41618	40008
CD6	UC	76	111861	76584	76584	50548	48478
CD7	UC	76	167153	119274	119274	84029	80599
CD8	UC	76	124124	85695	85695	58105	55526
CD9	UC	125	107612	75206	75206	49782	47713
CD10	UC	125	107547	75047	75047	49390	47174
CD11	UC	125	167561	117698	117698	81581	78001
CD12	UC	125	126474	85880	85880	57136	55259
CD13	N_2	77	136535	99045	99045	68000	64734
CD14	N_2	77	125989	89229	89229	60076	57576
CD15	N_2	77	120256	83594	83594	56569	53714
CD16	N_2	77	99615	69140	69140	45347	43022
CD17	N_2	126	75494	52875	52875	33973	32051
CD18	N_2	126	119868	76682	76682	52751	48607
CD19	N_2	126	131357	93979	93979	65318	60861
CD20	N_2	126	106543	72656	72656	48902	45994
CD21	H_2	30	125159	91774	91774	63394	59697
CD22	H_2	30	182188	129646	129646	92330	87180
CD23	H_2	30	90108	63876	63876	43363	41066
CD24	H_2	30	63185	43729	43729	27470	25997
CD29	H_2	50	47835	33474	33474	20533	19484
CD30	H_2	50	48129	33330	33330	20399	19261
CD31	H_2	50	41300	29530	29530	18694	17515
CD32	H_2	50	59518	48123	48123	27610	25195
CD33	H_2	60	75765	55035	55035	36593	34120
CD34	H_2	60	83631	58121	58121	39495	37147
CD35	H_2	60	75806	53091	53091	34345	32415

sample ID	treatment	duration	input	filtered	denoised	merged	non-chimeric
CD36	H_2	60	62310	41684	41684	27410	25192
CD37	H_2	70	85190	60767	60767	42419	39171
CD38	H_2	70	54741	39737	39737	27548	25553
CD39	H_2	70	41521	30296	30296	20872	19346
CD40	H_2	70	43967	30796	30796	20479	18841
CD41	H_2	80	49534	36938	36938	25289	22300
CD42	H_2	80	69249	50222	50222	34074	29032
CD43	H_2	80	60952	43898	43898	29563	26578
CD44	H_2	80	77060	55624	55624	39206	35169
CD45	H_2	92	190133	134818	134818	99655	90006
CD46	H_2	92	116630	83399	83399	62430	56126
CD47	H_2	92	128948	93957	93957	70625	63458
CD48	H_2	92	103872	70165	70165	51262	46494
CD57	H_2	122	133263	98202	98202	71301	62218
CD58	H_2	122	106289	76726	76726	55759	50793
CD59	H_2	122	98548	71664	71664	53428	46225
CD60	H_2	122	113135	81022	81022	58647	52150
CDNE	library-prep control		736	470	470	457	410
PCRneg1	library-prep control		693	473	473	362	362
PCRneg2	library-prep control		536	327	327	325	303
PCRneg3	library-prep control		8	0	0	0	0

Table S2: Known denitrification genes for the four steps of denitrification and their evolutionary relation (Bothe, et al. 2007).

Reaction	**Name**	**Abbreviations**	**Relation**
$NO_3^- \rightarrow NO_2^-$	membrane-bound nitrate reductase	*narG*	separate evolution
	periplasmic nitrate reductase	*napA*	
$NO_2^- \rightarrow NO$	Cd_1 nitrite reductase	*nirS*	separate evolution
	Cu nitrite reductase	*nirK*	
$NO \rightarrow N_2O$	Bc-heme containing nitric oxide reductase	*cnorB,*	common ancestor, different classes
	b-heme containing nitric oxide reductase	*qnorB*	
$N_2O \rightarrow N_2$	clade I nitrous oxide reductase	clade I *nosZ*	common ancestor, different classes
	clade II nitrous oxide reductase	clade II *nosZ*	

Table S3: qPCR protocols, primers and the source organism of the gene used to generate the standard for each analysed reductase gene. (a = touchdown).

Target gene	Thermal profile & cycles	Primer pair	[µM]	Source of standard
16S rRNA	(95°C-15 s/58°C-30 s/72°C-30 s) x40	FP 16S, RP 16S (Bach, et al. 2002)	0.2	*Pseudomonas putida*
napA	(95°C-30 s/60°C-30 s/72°C-30 s) x5[a] (95°C-30 s/55°C-30 s/72°C-30 s) x40	V17m, napA4r (Bru, et al. 2007)	0.4	*Pseudomonas fluorescens*
narG	(95°C-30 s/63°C-30 s/72°C-30 s) x5[a] (95°C-30 s/58°C-30 s/72°C-30 s) x40	narG-f, narG-r (Bru, et al. 2007)	0.2	*Pseudomonas stutzeri*
nirS	(95°C-45 s/57°C-45 s/72°C-45 s) x40	Cd3aF (Michotey, et al. 2000), R3cd (Throbäck, et al. 2004)	0.2	*Pseudomonas stutzeri*
nirK	(95°C-30 s/63°C-30 s/72°C-30 s) x5[a] (95°C-30 s/58°C-30 s/72°C-30 s) x40	nirK876 (Braker, et al. 1998), nirK 5R (Henry, et al. 2004)	0.2	*Azospirillum irakense*
qnorB	(95°C-15 s/60°C-30 s/72°C-30 s) x5[a] (95°C-15 s/55°C-30 s/72°C-30 s) x40	qnorB2F, qnorB5R (Braker and Tiedje 2003)	0.4	*Sinorhizobium meliloti*
cnorB	(95°C-15 s/60°C-30 s/72°C-30 s) x5[a] (95°C-15 s/55°C-30 s/72°C-30 s) x40	cnorB2F, cnorB6R (Braker and Tiedje 2003)	0.4	*Pseudomonas putida*
clade I *nosZ*	(95°C-15 s/65°C-30 s/72°C-30 s) x5[a] (95°C-15 s/60°C-30 s/72°C-30 s) x40	nosZ2F, nosZ2R (Henry, et al. 2004)	0.4	*Pseudomonas fluorescens*
clade II *nosZ*	(95°C-30 s/59°C-30 s/72°C-45 s) x5[a] (95°C-30 s/54°C-30 s/72°C-45 s/80°C-30 s) x40	nosZII-F, nosZII-R (Jones, et al. 2013)	1	*Dechloromonas denitrificans*

Table S4: Efficiencies the qPCR runs to quantify the target genes via qPCR and its transcripts via RT-qPCR.

Target gene	**Efficiency [%] of qPCR**	**Efficiency [%] of RT-qPCR**
16S rRNA	80.55	-
napA	71.26	72.79
narG	77.93	81.89
nirS	99.37	92.82
nirK	98.35	99.66
qnorB	88.57	77.57
cnorB	70.51	78.08
nosZ clade I	89.51	94.17
nosZ clade II	70.40	72.79

Table S5: Number of denitrification genes in complete genomes (downloaded from NCBI assembly) of the three genera *Dechloromonas*, *Azospira*, and *Sulfuritalea* to which ASVs were assigned to that increased significantly during the greatest period of nitrate reduction. The denitrification genes were detected with HMMER (Eddy 2011) using HMMs downloaded from FunGene (Fish, et al. 2013). Only hmmsearch hits with the gene specific domain accession, verified on NCBI conserved domain search (Marchler-Bauer, et al. 2016), are stated. Because *cnorB* and *qnorB* share the same domain accession, the sequences of the hmmsearch hits were incorporated in a phylogenetic tree of *norB* sequences (AJ507329-AJ507380) (Braker and Tiedje 2003) to differentiate betwenn *cnorB* and *qnorB* genes.

			Dechloromonas			***Azospira***		***Sulfuritalea***
			GCA_000519045.1	CP000089.1	CP031842.1	CP003153.1	AP021844.1	AP012547.1
gene	**KEGG**	**domain accession**	*agitata is5*	*aromatica RCB*	sp. HYN0024	*oryzae*	*sp 109*	*hydrogenivorans*
napA	K02567	PRK13532	1	1	1	1	0	1
narG	K00370	TIGR01580/COG5013	0	0	0	0	0	0
nirS	K15864	pfam02239/cl26549 & pfam13442/COG2010	2	3	2	3	3	3
nirK	K00368	cl31204	0	0	0	0	0	0
qnorB	K04561	cl00275	0	0	0	0	0	0
cnorB			1	1	1	1	1	0
clade I *nosZ*	K00367	PRK02888	0	0	0	0	0	0
calde II *nosZ*		TIGR04246	1	1	1	1	1	0

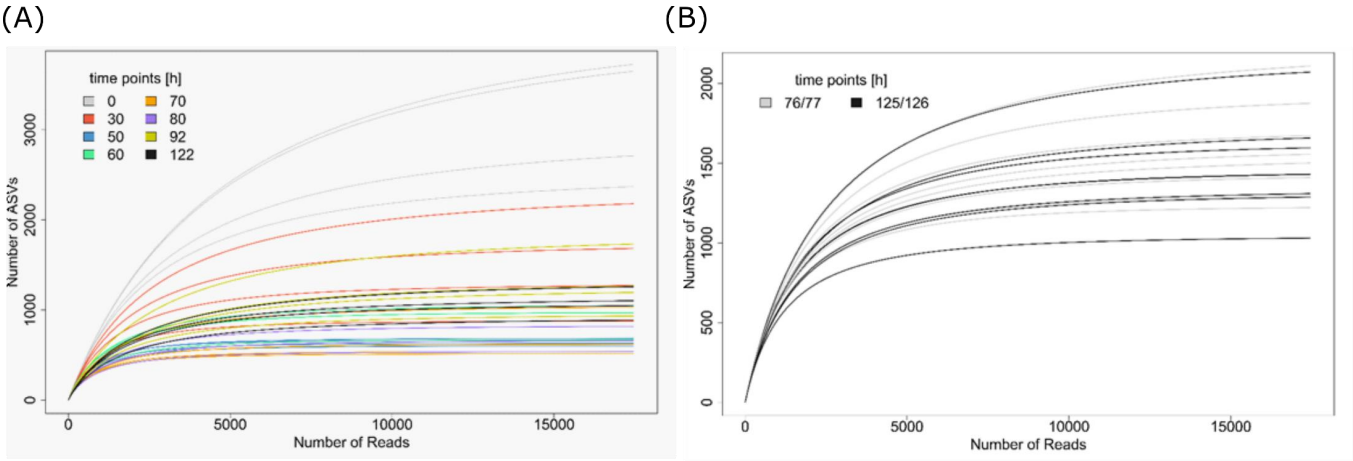

Figure S1: Rarefaction curves of (A) the hydrogen-treated samples and (B) the nitrogen-treated samples and untreated control.

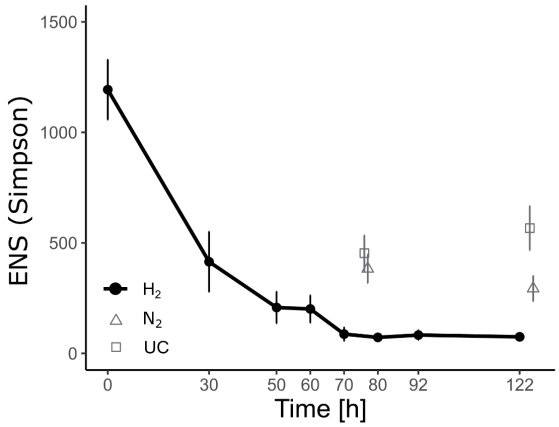

Figure S1: Changes in the effective number of species (ENS) calculated by dividing 1 by the complement of the Simpson index. The calculation of the alpha diversity is based on the 16S rRNA gene amplicon sequencing data. (n=4).

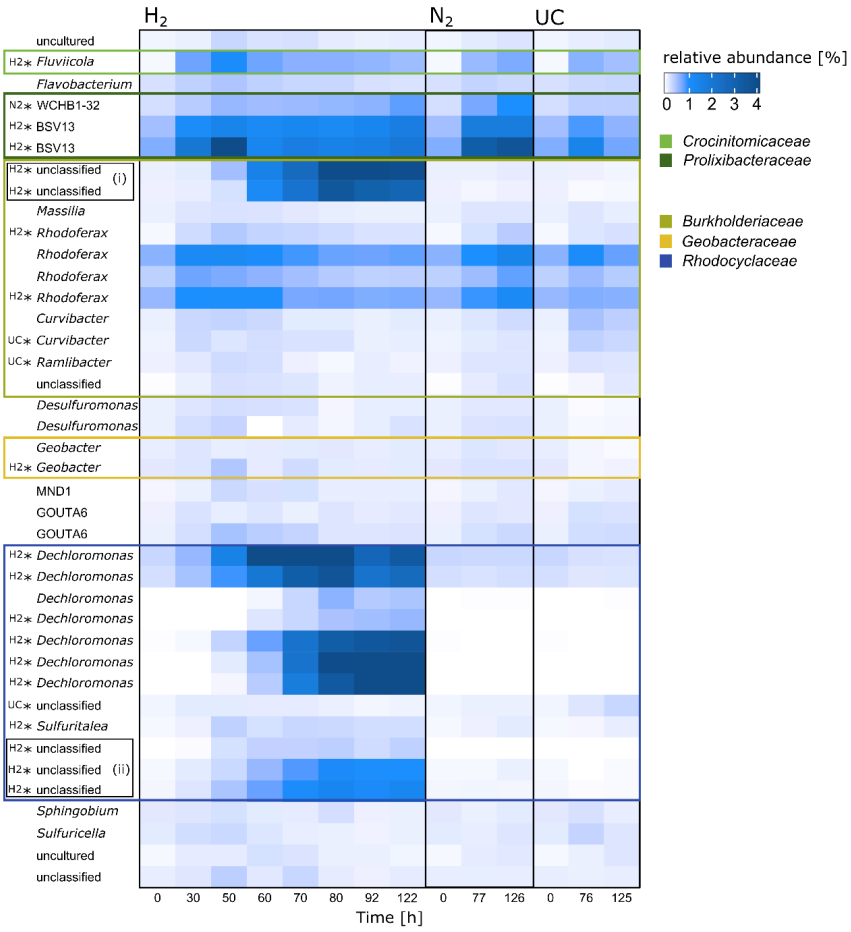
H2
N2
UC
uncultured
H2* Fluviicola
Flavobacterium
N2* WCHB1-32
H2* BSV13
H2* BSV13
H2* unclassified
H2* unclassified
(i)
Massilia
H2* Rhodoferax
Rhodoferax
Rhodoferax
H2* Rhodoferax
Curvibacter
UC* Curvibacter
UC* Ramlibacter
unclassified
Desulfuromonas
Desulfuromonas
Geobacter
H2* Geobacter
MND1
GOUTA6
GOUTA6
H2* Dechloromonas
H2* Dechloromonas
Dechloromonas
H2* Dechloromonas
H2* Dechloromonas
H2* Dechloromonas
H2* Dechloromonas
UC* unclassified
H2* Sulfuritalea
H2* unclassified
H2* unclassified
(ii)
H2* unclassified
Sphingobium
Sulfuricella
uncultured
unclassified
0 30 50 60 70 80 92 122 0 77 126 0 76 125
Time [h]
relative abundance [%]
0 1 2 3 4
Crocinitomicaceae
Prolixibacteraceae
Burkholderiaceae
Geobacteraceae
Rhodocyclaceae

Figure S3: Heatmap of the 40 most abundant ASVs in the hydrogen-treated microcosms belonging to the phyla *Proteobacteria* and *Bacteroidetes*. The families containing significantly increased ASVs over time (t1way) are framed and the respective ASVs are marked with an asterisk. The significantly increased unclassified ASVs can be assigned to the genera (i) *Massilia* and (ii) *Azospira/Rhodocyclus* according to nblast and phylogenetic trees (Figure S5). The shading is based on the mean relative abundance from four replicates.

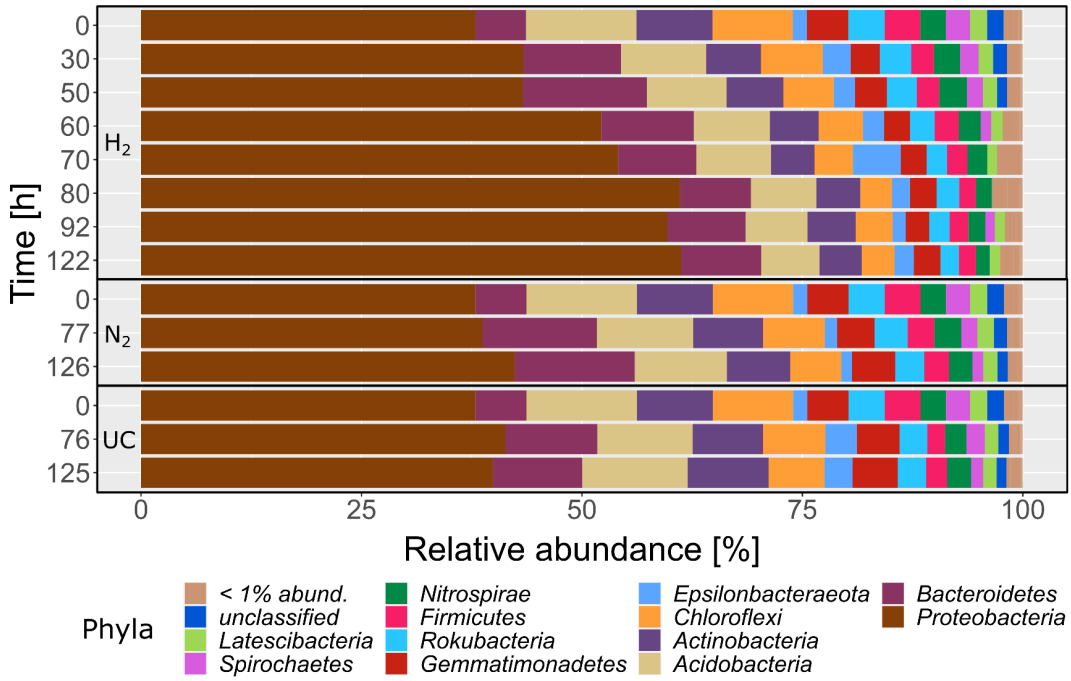

Figure S4: Changes in the bacterial community structure on the phylum level. The stacked bars represent mean relative abundances of four replicates.

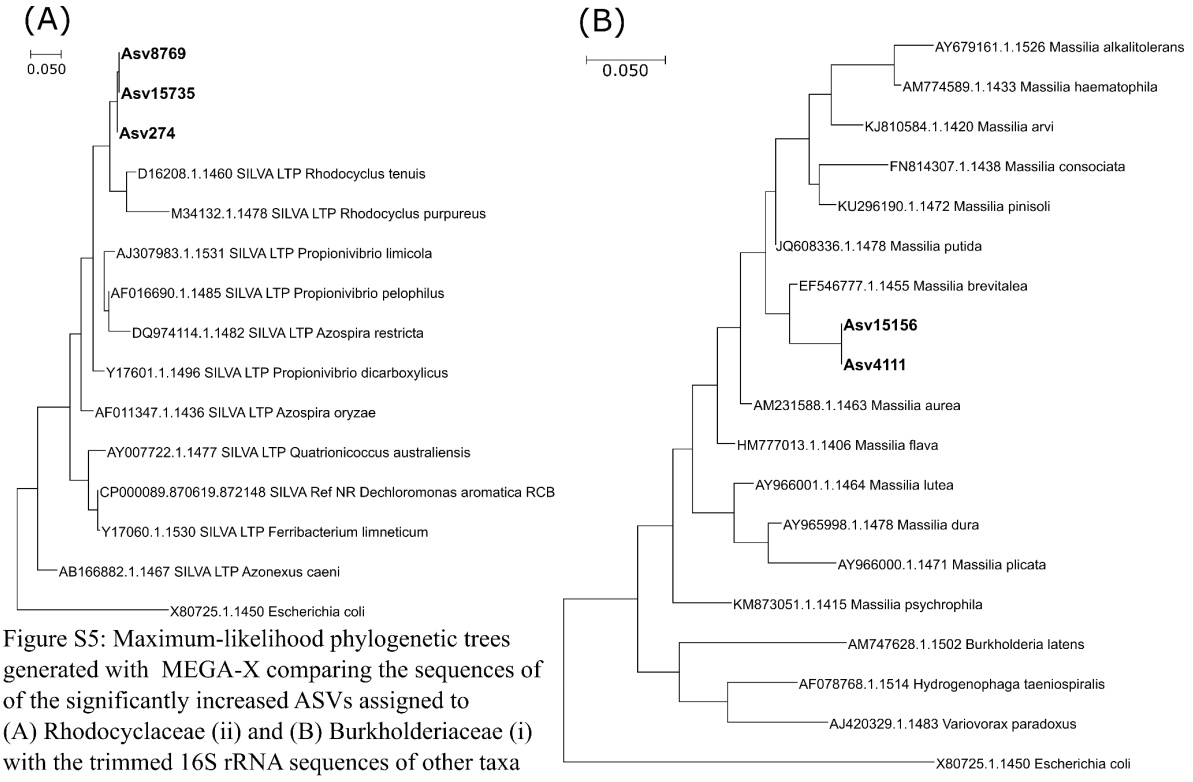

Figure S5: Maximum-likelihood phylogenetic trees generated with MEGA-X comparing the sequences of of the significantly increased ASVs assigned to (A) Rhodocyclaceae (ii) and (B) Burkholderiaceae (i) with the trimmed 16S rRNA sequences of other taxa from the respective families.

References:

Bach H-J, Tomanova J, Schloter M *et al.* Enumeration of total bacteria and bacteria with genes for proteolytic activity in pure cultures and in environmental samples by quantitative PCR mediated amplification. *Journal of Microbiological Methods* 2002;**49**: 235 - 45.

Bothe H, Ferguson S, Newton W. *Biology of the Nitrogen Cycle*: Elsevier Science, 2007.

Braker G, Fesefeldt A, Witzel KP. Development of PCR primer systems for amplification of nitrite reductase genes (nirK and nirS) to detect denitrifying bacteria in environmental samples. *Appl Environ Microbiol* 1998;**64**: 3769-75.

Braker G, Tiedje JM. Nitric oxide reductase (norB) genes from pure cultures and environmental samples. *Appl Environ Microbiol* 2003;**69**: 3476-83.

Bru D, Sarr A, Philippot L. Relative abundances of proteobacterial membrane-bound and periplasmic nitrate reductases in selected environments. *Appl Environ Microbiol* 2007;**73**: 5971-4.

Eddy SR. Accelerated Profile HMM Searches. *PLoS Comput Biol* 2011;**7**: e1002195-e.

Fish J, Chai B, Wang Q *et al.* FunGene: the functional gene pipeline and repository. *Frontiers in Microbiology* 2013;**4**: 291.

Henry S, Baudoin E, López-Gutiérrez JC *et al.* Quantification of denitrifying bacteria in soils by nirK gene targeted real-time PCR. *Journal of Microbiological Methods* 2004;**59**: 327-35.

Jones CM, Graf DR, Bru D *et al.* The unaccounted yet abundant nitrous oxide-reducing microbial community: a potential nitrous oxide sink. *ISME Journal* 2013;**7**: 417-26.

Marchler-Bauer A, Bo Y, Han L *et al.* CDD/SPARCLE: functional classification of proteins via subfamily domain architectures. *Nucleic Acids Research* 2016;**45**: D200-D3.

Michotey V, Méjean V, Bonin P. Comparison of Methods for Quantification of Cytochrome cd ₁-Denitrifying Bacteria in Environmental Marine Samples. *Appl Environ Microbiol* 2000;**66**: 1564.

Throbäck IN, Enwall K, Jarvis Å *et al.* Reassessing PCR primers targeting nirS, nirK and nosZ genes for community surveys of denitrifying bacteria with DGGE. *FEMS Microbiology Ecology* 2004.

Publication II

environmental microbiology

Environmental Microbiology (2022) **00**(00), 00–00 doi:10.1111/1462-2920.15921

Genotypic and phenotypic characterization of hydrogenotrophic denitrifiers

Clara Duffner,[1,2] **Susanne Kublik**,[2] **Bärbel Fösel**,[2] **Åsa Frostegård**,[3] **Michael Schloter**,[1,2] **Lars Bakken**[3] **and Stefanie Schulz**[2*]

[1]*Chair of Soil Science, TUM School of Life Sciences Weihenstephan, Technical University of Munich, Freising, Germany.*

[2]*Research Unit Comparative Microbiome Analysis, Helmholtz Zentrum München, Neuherberg, Germany.*

[3]*Department of Chemistry, Biotechnology and Food Sciences, Norwegian University of Life Sciences, Ås, Norway.*

Summary

Stimulating litho-autotrophic denitrification in aquifers with hydrogen is a promising strategy to remove excess NO_3^-, but it often entails accumulation of the cytotoxic intermediate NO_2^- and the greenhouse gas N_2O. To explore if these high NO_2^- and N_2O concentrations are caused by differences in the genomic composition, the regulation of gene transcription or the kinetics of the reductases involved, we isolated hydrogenotrophic denitrifiers from a polluted aquifer, performed whole-genome sequencing and investigated their phenotypes. We therefore assessed the kinetics of NO_2^-, NO, N_2O, N_2 and O_2 as they depleted O_2 and transitioned to denitrification with NO_3^- as the only electron acceptor and hydrogen as the electron donor. Isolates with a complete denitrification pathway, although differing intermediate accumulation, were closely related to *Dechloromonas denitrificans*, *Ferribacterium limneticum* or *Hydrogenophaga taeniospiralis*. High NO_2^- accumulation was associated with the reductases' kinetics. While available, electrons only flowed towards NO_3^- in the *narG*-containing *H. taeniospiralis* but flowed concurrently to all denitrification intermediates in the *napA*-containing *D. denitrificans* and *F. limneticum*. The denitrification regulator RegAB, present in the *napA* strains, may further secure low intermediate accumulation. High N_2O accumulation only occurred during the transition to denitrification and is thus likely caused by delayed N_2O reductase expression.

Received 19 October, 2021; revised 20 January, 2022; accepted 20 January, 2022. *For correspondence. E-mail stefanie.schulz@helmholtz-muenchen.de; Tel. +49 89 3187 3054.

Introduction

Denitrification is the stepwise reduction of nitrate (NO_3^-) to dinitrogen (N_2), via the three intermediates nitrite (NO_2^-), nitric oxide (NO) and nitrous oxide (N_2O) (Zumft, 1997). The process is mainly performed by facultative anaerobic organo-heterotrophic prokaryotes (Rivett *et al*., 2008), which use the pathway to sustain respiratory metabolism under oxygen (O_2) limiting conditions. Such organisms are widespread among bacterial and archaeal phyla, but many of these lack one to three of the four genes coding for the four steps of denitrification, thus having incomplete denitrification pathways (Shapleigh, 2013; Graf *et al*., 2014). While denitrification is not desirable in agricultural soils because it reduces the amounts of NO_3^- available to crops, the process is beneficial in groundwater (GW) and wastewater treatment systems, where it removes excess NO_3^- that would otherwise deteriorate the water quality as well as the downstream environment (Rivett *et al*., 2008). Deliberate stimulation of denitrification in aquifers has been proposed as a method to eliminate NO_3^-, to secure drinking water quality. This can be achieved by injecting water with dissolved organic carbon, but the downside is massive growth of organo-heterotrophic bacteria, hence high bacterial load in the water (Matějů *et al*., 1992). This problem can be minimized, however, by injecting hydrogen (H_2) instead of organic carbon, thus stimulating denitrification by organisms that utilize H_2 as an electron donor and CO_2 as a carbon source (Karanasios *et al*., 2010). The reason is that litho-autotrophic denitrification sustained by the electron donor H_2 only yields 0.22–0.37 g cells for each g NO_3^--N reduced (Lee and Rittmann, 2003; Ghafari *et al*., 2009), compared to 0.6–0.9 g cells reported for organo-heterotrophic denitrification (Ergas and Reuss, 2001).

The ability to use H_2 as an electron donor for respiratory metabolism is widespread and the application of H_2 and its stimulating effect on denitrification has been proven in several laboratory experiments, bioreactors

and in *in situ* studies (Schnobrich *et al*., 2007; Chaplin *et al*., 2009; Wu *et al*., 2018). The conditions for hydrogenotrophic denitrification are highly selective (anoxic, inorganic carbon, H_2 as the sole electron donor and NO_x as the terminal electron acceptors) (Karanasios *et al*., 2010) and only a limited number of bacteria with this metabolism have been isolated, including strains belonging to the genera *Acidovorax*, *Paracoccus*, *Acinetobacter* and *Pseudomonas* (Szekeres *et al*., 2002; Vasiliadou *et al*., 2006). Additionally, several genera, including *Rhodocyclus*, *Sulfuricurvum*, *Sulfuritalea*, *Hydrogenophaga*, *Ferribacterium* and *Dechloromonas*, have been detected in 16S rRNA gene-based community analyses of hydrogenotrophic environments (Zhang *et al*., 2009; Zhao *et al*., 2011; Kumar *et al*., 2018b; Duffner *et al*., 2021). A recent community analysis microcosm experiment with nitrate-polluted aquifer material by Duffner *et al*. (2021) confirmed the low diversity of hydrogenotrophic denitrifiers (HDs). Only six amplified sequence variants (ASVs) were assigned to the genus *Dechloromonas*, and another unclassified *Rhodocyclaceae* ASV increased significantly in relative abundance during the incubations under an H_2 atmosphere. Additionally, the study suggested species- or even strain-level differences in the hydrogenotrophic denitrifying ability of *Dechloromonas*. In such low diversity communities, the contribution of single taxa to the overall observed metabolic process is strong. Previous studies have revealed a possible accumulation of the cytotoxic intermediate NO_2^- and the greenhouse gas N_2O during lithotrophic denitrification with H_2. Analysing the persistent or transient intermediate accumulation of individual HDs is therefore of interest, both for a basic understanding of the functioning of these bacteria and for their application in nitrate remediation of aquifers. A study by Vasiliadou *et al*. (2006) quantified the denitrification derived NO_2^- of some HDs, but the strains tested (*Acinetobacter* sp., *Acidovorax* sp. and *Paracoccus* sp.) do not seem to be dominant in aquifers, and the study was limited to non-gaseous NO_3^- and NO_2^-.

The reasons for incomplete denitrification and transient accumulation of intermediates have been studied for heterotrophic denitrifiers, and there are indications that multiple factors play a role, such as the absence of genes encoding the denitrification reductases, transcriptional regulation and post-translational processes determined by environmental conditions (Liu *et al*., 2013; Lycus *et al*., 2017). Such information on the regulation of denitrification and accumulation of intermediates for hydrogenotrophic denitrification is still lacking. We therefore isolated HDs from aquifer material and characterized their genotypes and phenotypes. The genomes were sequenced and screened for genes involved in hydrogenotrophic denitrification, which code for different denitrification reductase types, Rubisco forms (II, IA, IC) (Badger and Bek, 2008), hydrogenase groups (Greening *et al*., 2016) and denitrification regulators. Additionally, the 'denitrification regulatory phenotypes (DRPs)', a method established by Bergaust *et al*. (2011), were determined under litho-autotrophic conditions with H_2 as the sole electron donor and under organo-heterotrophic conditions with low concentrations of mixed carbon sources. The former was analyzed during the transition from aerobic respiration to denitrification and with cells that were already adapted to denitrification. This was done to differentiate between delayed gene expression and differential electron flow to the different denitrification reductases causing intermediate accumulation. As a control group, three closely related isolates of complete HDs assigned to *D*. *denitrificans* and *F*. *limneticum*, which were lacking the ability to reduce a significant amount of NO_3^- with H_2 as electron donor were subjected to the same genotypic and phenotypic characterization.

Results

Bacterial community composition in the original materials and enrichments

The bacterial community composition in the original sediment and GW materials as well as in the enrichments were analyzed via 16S rRNA gene amplicon sequencing. The rarefaction curves of the enrichment setups from the first (EI) and second (EII) enrichment procedure were all reaching a plateau within the subsampled range, indicating sufficient sequencing depth (Fig. S3). The number of ASVs in the original sediment samples was comparable between EI (1342) and EII (1863). However, there was a large difference for the original GW samples, as 2338 ASVs were detected in EI compared with 1202 in EII. The number of ASVs was much lower in the enrichment cultures, resulting in 1102 (EI)/646 (EII) ASVs in the highly active SED/GW enrichment and 144 (EI)/181 (EII) ASVs in the GW enrichment with slower reduction rates (Fig. S1B). The subsequent transfers of the enrichments to fresh nitrate-rich medium for one replicate of each setup further reduced the number of ASVs. In the original sediment and GW material, *Rhodocyclaceae* ASVs made up less than 0.5% relative abundance. Due to the enrichment, the relative abundance of *Rhodocyclaceae* ASVs was increased up to 32.2% in the transferred GW ($GW_{(t)}$) and up to 25.6% in the transferred sediment/GW ($SED/GW_{(t)}$) setups of EII (Fig. S4B). In contrast, in EI, the major increase in relative abundance was detected for *Burkholderiaceae* ASVs, which made up 79.8% in the transferred mineral medium and GW ($MM/GW_{(t)}$) enrichment setup (Fig. S4A).

Phylogenetic classification of the isolates

After separating the isolates on agar plates and determining their taxonomy, 48% of all Sanger sequenced isolates in EI were assigned to the family *Burkholderiaceae* and only 4% to *Rhodocyclaceae* (equivalent to one isolate). Contrary in EII, most of the isolates (26%) were assigned to the family *Rhodocyclaceae*. Most obtained *Rhodocyclaceae* isolates clustered with the genera *Dechloromonas*, *Ferribacterium* and *Quatrionicoccus* in the phylogenetic tree (Fig. S2), whereas most *Burkholderiaceae* isolates clustered with the genera *Hydrogenophaga*, *Acidovorax* and *Rhodoferax*. In total, 45 isolates, including isolated strains of all obtained families, were tested for their ability to reduce NO_3^- with H_2, but only some genera of *Rhodocyclaceae* and *Burkholderiaceae* showed this ability (Table S3). Of those isolates, which could reduce NO_3^- with H_2, the isolates $F76_{(HD)}$, $F77_{(HD)}$, $F128_{(HD)}$, $F132_{(HD)}$, $D110_{(HD)}$, $D6_{(HD)}$, $H3_{(HD)}$ and $H2_{(HD)}$ (Fig. 1; Table S3) were selected for further genotypic and phenotypic characterization because they display a range of phylogenetically closely related and diverse genera. Additionally, the three isolates, D98, Q100 and Q9, which lacked the ability of hydrogenotrophic denitrification but were closely related to the other *Rhodocyclaceae* HDs, were characterized alongside as a control group.

Most sequenced genomes were assembled into a single contig that could be circularized (Table S6). Only Q100 and $H3_{(HD)}$ had one or two additional smaller contigs respectively, which may be plasmids (Table S5). The completeness was above 99.2% and the contamination below 0.95% for all 11 sequenced genomes (Table S6).

For a genome-based phylogenetic classification, the number of reference genomes was low, especially for the genera *Ferribacterium* and *Quatrionicoccus*, as no sequenced genomes were available at NCBI at the time of analysis (www.ncbi.nlm.nih.gov/genome, March 2021). The phylogenetic classification, therefore, was mostly based on 16S rRNA gene comparisons. Based on the data obtained using TYGS (Meier-Kolthoff and Göker, 2019) (Table S8), isolates $F76_{(HD)}$, $F77_{(HD)}$, $F128_{(HD)}$ and $F132_{(HD)}$ were closest related to *Ferribacterium limneticum* CdA-1. While $F132_{(HD)}$ and $F128_{(HD)}$ shared highly similar genomes, $F76_{(HD)}$ and $F77_{(HD)}$ had a 16S rRNA gene identity of 99.4%, but their dDDH values only reached 60.8%, which did not allow a clear assignment to the same species. $D110_{(HD)}$ and $D6_{(HD)}$ were closest related to *Dechloromonas denitrificans* ED1. Both genomes were similar, with a dDDH value of 89.2%. A detailed comparison of the two isolates with *D. denitrificans* ED1 revealed 97.8% identity of 16S rRNA genes, a dDDH value of 34.7% and differences in the G + C content of less than 0.2%. This does not allow a clear assignment of the two isolates to the species *D. denitrificans*. Isolates $H3_{(HD)}$ and $H2_{(HD)}$ were both closest related to *Hydrogenophaga taeniospiralis* 2K1 according to the 16S rRNA gene sequences. However, a dDDH value of 37.5% and a G + C content difference of 1.5% between $H2_{(HD)}$ and *H. taeniospiralis* 2K1 suggested that this isolate belonged to a different species.

The isolate D98 of the control group was closest related to *D. denitrificans* ED1. However, while D98 clustered with *D. denitrificans* ED1 in the 16S rRNA

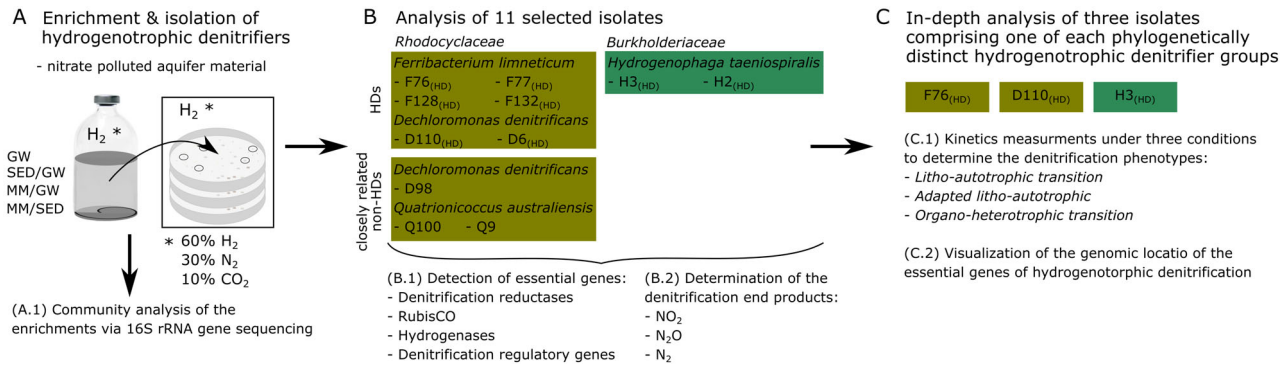

Fig. 1. Schematic overview of the experiments.
A. Initially, nitrate polluted aquifer material was incubated inside sealed vials in various setups with an H_2-containing atmosphere to enrich hydrogenotrophic denitrifiers and to isolate them on agar plates. (A.1) The community composition of the enrichments was additionally assessed by 16S rRNA gene amplicon sequencing.
B. Nine isolates of the families *Rhodocyclaceae* and two of the family *Burkholderiaceae* were selected for further (B.1) genotypic and (B.2) phenotypic analyses. Eight of the selected isolates were complete hydrogenotrophic denitrifiers (HDs) but the *Rhodocyclaceae* isolates also included three isolates which were closely related but were lacking the ability to denitrify with H_2 (non-HDs).
C. Finally, a sub-selection of three isolates, comprising one of each phylogenetically distinct hydrogenotrophic denitrifier groups ($F76_{(HD)}$, $D110_{(HD)}$, $H3_{(HD)}$) was analyzed in more depth. Therefore, (C.1) the denitrification phenotypes were determined under three different conditions and (C.2) the genomic location of hydrogenotrophic denitrifier genes was visualized.

gene-based phylogenetic tree (Fig. S6A), it clustered separately from all other isolated *Rhodocyclaceae* strains in the whole-genome sequence-based phylogenetic tree (Fig. S6B). The other two isolates of the control group, Q9 and Q100, were closest related to *Quatrionicoccus australiensis* Ben 117. The low dDDH values of 34.6% and 34.8% compared with the genome of *Q. australiensis* Ben 117 indicated that the isolates; however, belong to another species.

Phenotypes – intermediate accumulation during denitrification

The targeted isolation of bacteria revealed several complete HDs being capable of the complete reduction of NO_3^- to N_2 according to the endpoint analysis. These included eight isolates, which were assigned, based on their full 16S rRNA gene sequences, to the species *Ferribacterium limneticum* ($F76_{(HD)}$, $F77_{(HD)}$, $F128_{(HD)}$, $F132_{(HD)}$), *Dechloromonas denitrificans* ($D110_{(HD)}$, $D6_{(HD)}$) and *Hydrogenophaga taeniospiralis* ($H3_{(HD)}$, $H2_{(HD)}$) (Fig. 2A and B). Of the three closely related *Rhodocyclaceae* isolates (D98, Q100, Q9), which were analyzed as a control group, the two *Q. australiensis* isolates (Q100, Q9) reduced only NO_3^- to NO_2^-, while D98 did not reduce any nitrogen oxides (Fig. 2A and B). The pH at the endpoint measurements was on average significantly higher (0.11–0.18) in the incubations of the HDs compared with the non-inoculated incubations and the incubations with the isolates of the control group (lincon, $p \leq 0.009$) (Fig. S5A). The gas pressure was 0.125–0.151 bar lower in the incubations containing the HDs compared with the other incubations (lincon, $p \leq 0.009$) (Fig. S5B).

The DRPs were analyzed for a sub-selection of three HDs performing complete denitrification to N_2 ($F76_{(HD)}$, $D110_{(HD)}$ and $H3_{(HD)}$), which represent three phylogenetically distinct groups, under three conditions: *Litho-autotrophic transition*, *Adapted litho-autotrophic* and *Organo-heterotrophic transition* (Fig. 1). In the *Litho-autotrophic transition* experiment, the isolates $F76_{(HD)}$ and $D110_{(HD)}$, belonging to the family *Rhodocyclaceae*, displayed a continuous seamless transition to anaerobic respiration, i.e. the total electron flow continued to grow without any depression at the time of O_2 depletion (Fig. 3D and E). Furthermore, $F76_{(HD)}$ and $D110_{(HD)}$ initiated all denitrification steps simultaneously (Fig. 3A and B), as an electron flow was observed to all denitrification reductases from the onset of denitrification (Fig. 3D and E). The *H. taeniospiralis* isolate $H3_{(HD)}$ showed a similar seamless transition from aerobic respiration to NO_3^- reduction (no depression in total electron flow); however, the electron flow dropped substantially in response to NO_3^- depletion (Fig. 3F), which forced the cells to switch to nitrite reduction. The organism displayed a typical progressive onset of denitrification reactions (Liu *et al*., 2013) (Fig. 3C): initially, all electrons were flowing to NAR until all NO_3^- had been reduced to NO_2^-, before flowing to NIR, NOR and NOS (Fig. 3F). $F76_{(HD)}$ and $D110_{(HD)}$ differed significantly from $H3_{(HD)}$ in the O_2 concentration in the medium at the first appearance of NO: 6.9 μM (±0.37) O_2 for $F76_{(HD)}$, 8.1 μM (±1.75) O_2 for $D110_{(HD)}$ and 0.25 μM (±0.14) O_2 for $H3_{(HD)}$ (lincon, $p = 0.0127$) (Table 1 and S9). This contrast reflects the progressive onset of denitrification in $H3_{(HD)}$; however: in this strain, there was 8.3 μM (±1.6) O_2 in the liquid at the time when NO_2^- emerged. Thus, the three strains initiated anaerobic respiration at similar O_2 concentrations. Moreover, the relative growth rate (μ_{anoxic}/μ_{oxic}) was significantly lower for $H3_{(HD)}$ compared with $F76_{(HD)}$ (lincon, $p = 0.0121$) and $D110_{(HD)}$ (lincon, $p = 0.0343$) (Table 1 and S9). Even though $F76_{(HD)}$ and $D110_{(HD)}$ displayed a similar overall denitrification phenotype, they differed significantly in the transient NO_2^- accumulation of initial NO_3^- (lincon, $p = 0.0135$) (Table S9). $D110_{(HD)}$ accumulated on average 19.4% (±3.94) NO_2^- of the initial NO_3^-, whereas no NO_2^- accumulation was detected for $F76_{(HD)}$ (Table 1). Both, however, accumulated significantly less NO_2^- compared with 100% accumulated by the $H3_{(HD)}$ isolate (lincon, $p = 0.0124$) (Table 1 and S10). No significant differences between the three isolates were observed for the max. NO concentration in the medium and the maximum N_2O-N measured (t1way, $p = 0.24$ and 0.56) (Table S10). All isolates displayed a relatively high steady-state NO concentration, which ranged from 14.5–18.5 nM NO and a large variation in max. N_2O-N accumulation (Table 1).

In the *Organo-heterotrophic transition* experiment, we analyzed the DRPs with organic carbon as the electron donor and carbon source. The accumulated NO_2^- differed again significantly among the three isolates with the least NO_2^- accumulated in $F76_{(HD)}$ with 2.92% (±0.92), followed by $D110_{(HD)}$ with 9.54% (±0.81), and $H3_{(HD)}$ with 29.48% (±3.01) (Table 1). Especially for $H3_{(HD)}$, the transiently accumulated NO_2^- was significantly lower in the *Organo-heterotrophic transition* compared with the *Litho-autotrophic transition* experiment (t1way, $p = 0.0289$) (Table S11). Also, $D110_{(HD)}$ accumulated only approximately half of the NO_2^- measured during the H_2 transition experiment (Table 1). Contrary to the *Litho-autotrophic transition* experiments, the average max. steady-state NO differed significantly among the three isolates. It was significantly higher with 17.2 nM (±1.9) for isolate $H3_{(HD)}$, compared with 5.5 nM (±4.8) for $F76_{(HD)}$ (lincon, $p = 0.0212$) and 3.7 nM (±0.9) for $D110_{(HD)}$ (lincon, $p = 0.0004$) (Table S9). The max. accumulated N_2O-N was also significantly higher for isolate $H3_{(HD)}$ with 33.42% (±0.81) compared with 1.86%

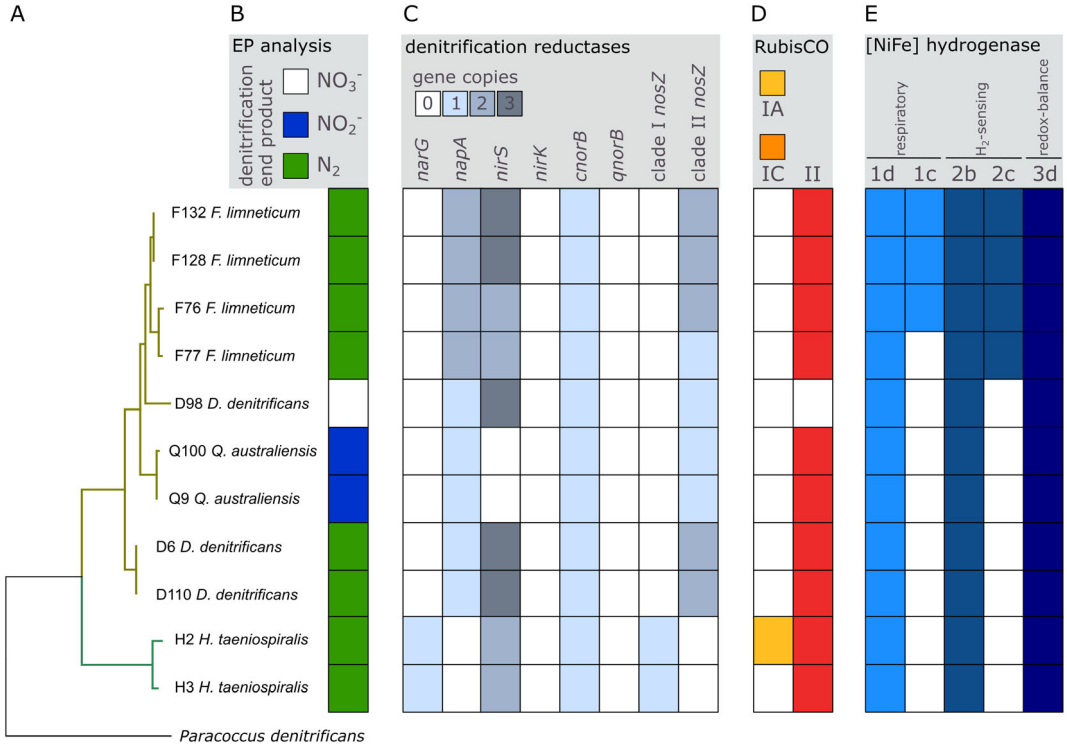

Fig. 2. (A) 16S rRNA gene-based maximum-likelihood phylogenetic tree of the 11 selected isolates from the genera *Rhodocyclaceae* (olive green) and *Burkholderiaceae* (dark green), as well as *Paracoccus denitrificans* (Y16927) as an outgroup. (B) Their denitrification end products were determined by measuring the changes in N-species after incubation in MM with H_2 as the sole electron donor and CO_2 as the sole carbon source. Furthermore, the type and copy number of (C) denitrification reductase, (D) RubisCO, and (E) hydrogenase genes detected in their sequenced genomes are displayed. White squares signify the absence of denitrification activity or the respective gene. Gas kinetics of the hydrogenotrophic denitrifier isolates (A) *F. limneticum* ($F76_{(HD)}$), (B) *D. denitrificans* ($D110_{(HD)}$) and (C) *H. taeniospiralis* ($H3_{(HD)}$) during the transition from aerobic respiration to denitrification in MM with H_2 as the sole electron donor are shown in the top panel. The period of denitrification is marked with a blue background, beginning at the appearance of detectable NO until all available nitrogen oxides had been reduced to N_2. [O_2], [NO_2^-], [NO], [N_2O] and [N_2] concentrations were quantified over time, while [NO_3^-] were extrapolated by subtracting the sum of N-oxides and N_2 from the initial [NO_3^-] concentration. The graphs are exemplary from one of several replicates, shown in Table 1. Calculated electron flow to the terminal oxidases (VeO_2) and the denitrification reductases (VeNAR/NAP, VeNIR, VeNOS) of isolates (D) $F76_{(HD)}$ ($n = 3$), (E) $D110_{(HD)}$ ($n = 6$), and (F) $H3_{(HD)}$ ($n = 6$) during the same experiment are shown in the bottom panel. The graphs show the average from several replicates (Table 1) and the standard deviations, which are large primarily due to temporal differences between replicate vials.

(±1.26) for $F76_{(HD)}$, and 0.82% (±1.49) for $D110_{(HD)}$ (both, lincon, $p \leq 0.0000$) (Table S9). However, it did not significantly differ from the N_2O-N accumulation in the H_2 transition experiment (Table S11). The concentration of dissolved O_2 at the appearance of detectable NO during the *Organo-heterotrophic transition* experiment was for isolates $F76_{(HD)}$ and $D110_{(HD)}$ approximately half of the average measured during the *Litho-autotrophic transition* experiment (t1way, both $p = 0.0289$) (Table 1 and S11).

In the *Adapted litho-autotrophic* experiment, the cells were already adapted to denitrification, i.e. equipped with a fully expressed denitrification proteome, with H_2 as the sole electron donor. In this experiment the max. accumulated NO_2^- still differed significantly among the three tested isolates. On average, $F76_{(HD)}$ transiently accumulated 0.02% (±0.01), $D110_{(HD)}$ 26.8% (±6.9) and $H3_{(HD)}$ 75.7% (±2.3) NO_2^- of the initial amount of NO_3^- added (Table 1). Unlike NO_2^-, which displayed a similar pattern in the *Adapted litho-autotrophic* and in the *Litho-autotrophic transition* experiment, the max. accumulated N_2O-N was much lower during the *Adapted litho-autotrophic* experiment (Table 1), even though the difference was again not significant due to the large variation among replicates.

During all three kinetics experiments, isolate $F76_{(HD)}$ displayed the least intermediate accumulation, followed by $D110_{(HD)}$, while $H3_{(HD)}$ displayed the largest intermediate accumulation, especially concerning that of NO_2^-.

Genotypes – genes of HDs

The hydrogenotrophic denitrifier isolates assigned to *F. limneticum* and *D. denitrificans* ($F76_{(HD)}$, $F77_{(HD)}$, $F128_{(HD)}$, $F132_{(HD)}$, $D110_{(HD)}$, $D6_{(HD)}$), were characterized by *napA* nitrate reductase genes and clade II *nosZ*

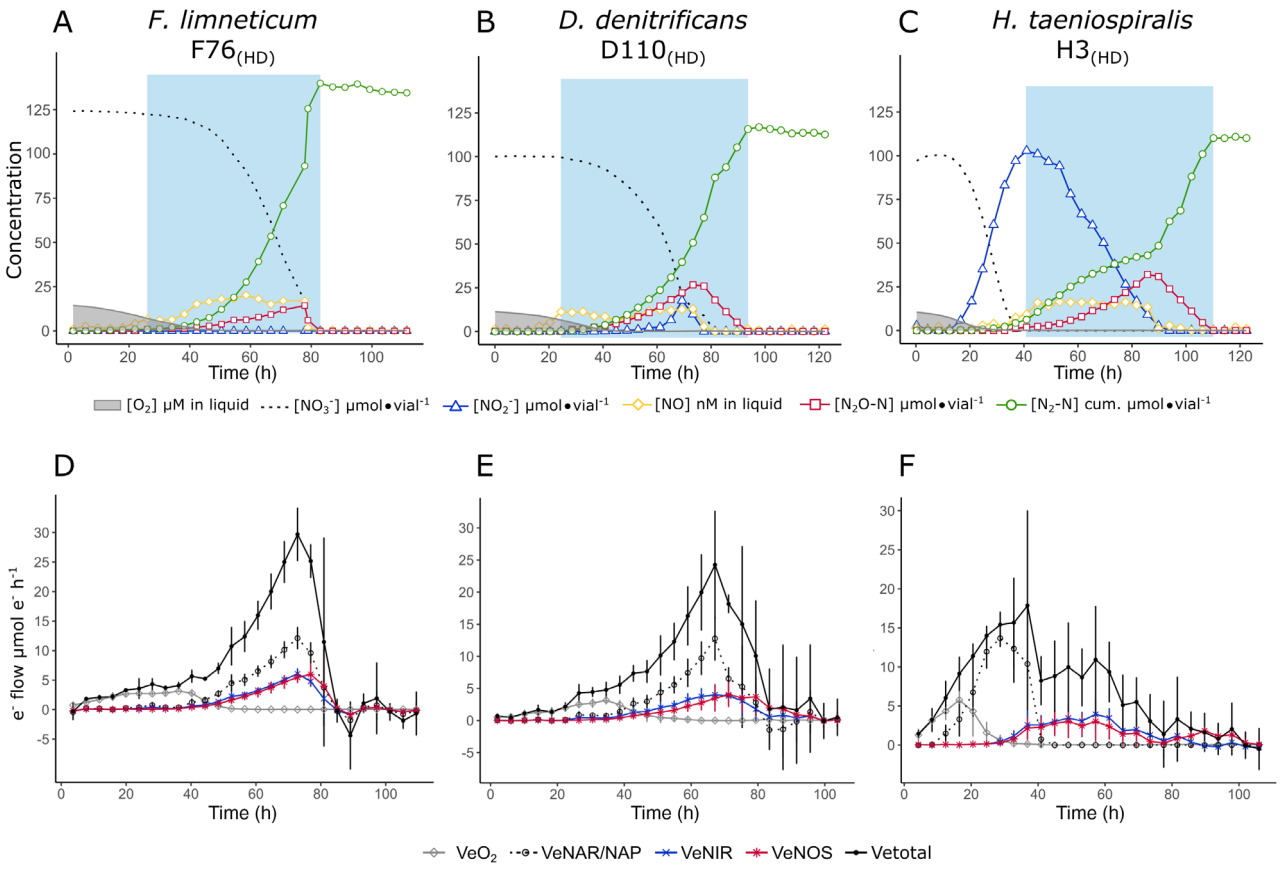

Fig. 3. Gas kinetics of the hydrogenotrophic denitrifier isolates (A) *F. limneticum* ($F76_{(HD)}$), (B) *D. denitrificans* ($D110_{(HD)}$) and (C) *H. taeniospiralis* ($H3_{(HD)}$) during the transition from aerobic respiration to denitrification in MM with H_2 as the sole electron donor are shown in the top panel. The period of denitrification is marked with a blue background, beginning at the appearance of detectable NO until all available nitrogen oxides had been reduced to N_2. [O_2], [NO_2^-], [NO], [N_2O] and [N_2] concentrations were quantified over time, while [NO_3^-] were extrapolated by subtracting the sum of N-oxides and N_2 from the initial [NO_3^-] concentration. The graphs are exemplary from one of several replicates, shown in Table 1. Calculated electron flow to the terminal oxidases (VeO_2) and the denitrification reductases (VeNAR/NAP, VeNIR, VeNOS) of isolates (D) $F76_{(HD)}$ ($n = 3$), (E) $D110_{(HD)}$ ($n = 6$), and (F) $H3_{(HD)}$ ($n = 6$) during the same experiment are shown in the bottom panel. The graphs show the average and standard deviation from several replicates, which are large primarily due to temporal differences between replicate vials.

nitrous oxide reductase genes (Fig. 2C). In contrast, the isolates assigned to *H. taeniospiralis* ($H3_{(HD)}$, $H2_{(HD)}$) harboured *narG* and clade I *nosZ* genes. All of them harboured *nirS* and *cnorB* rather than *nirK* and *qnorB* genes. For carbon assimilation, all complete hydrogenotrophic denitrifier isolates were equipped with a form II Rubisco gene (*cbbM*) (Fig. 2D), and several [NiFe]-hydrogenase genes (Fig. 2E) for H_2 oxidation. These hydrogenase genes comprised at least one group 1d respiratory hydrogenase gene, one group 2b H_2-sensing hydrogenase gene and one group 3d redox-balancing hydrogenase gene per genome. The *F. limneticum* isolates $F76_{(HD)}$, $F128_{(HD)}$ and $F132_{(HD)}$ additionally contained a group 1c respiratory hydrogenase gene and those isolates plus $F77_{(HD)}$, also harboured a group 2c H_2-sensing hydrogenase gene. All analyzed hydrogenotrophic denitrifier genomes contained the O_2-responsive regulator gene *fixL*, but the *D. denitrificans* and *F. limneticum* isolates, in contrast to the *H. taeniospiralis* isolates, were missing the two-component counterpart *fixJ* (Table S12). Instead, the genomes of the *Rhodocyclaceae* isolates contained one or multiple gene copies of the redox-sensing two-component system RegAB, which was not detected in the genomes of the two *H. taeniospiralis* isolates.

The location of these genes involved in hydrogenotrophic denitrification was analyzed for the genomes of the sub-selection, whose denitrification kinetics were also determined (Fig. 1). The analyzed genes were not confined to a certain region in either of the three genomes (Fig. S7). The denitrification operons in the genomes of $F76_{(HD)}$ and $D110_{(HD)}$ were less coherent compared with the genome of $H3_{(HD)}$. For example, one *nap* operon in $F76_{(HD)}$ and $D110_{(HD)}$ was fragmented into *napABC*, *napGH* and *napF* respectively. An extra *nap* operon in the $F76_{(HD)}$ genome was arranged as

Table 1. Basic characteristics of the denitrification phenotypes of the complete hydrogenotrophic denitrifiers *F. limneticum* ($F76_{(HD)}$), *D. denitrificans* ($D110_{(HD)}$) and *H. taeniospiralis* ($H3_{(HD)}$), as aerobically grown cells switched to denitrification while respiring H_2 only (*Litho-autotrophic transition*) or organic carbon only (*Organo-heterotrophic Transition*), and as the anaerobically H_2-respiring cells were given a second dose of NO_3^- and H_2 (*Adapted litho-autotrophic*).

Isolate	μ_{oxic}	μ_{anoxic}	μ_{anoxic}/μ_{oxic}	O_2 (μM) in liquid --> NO_2^-	O_2 (μM) in liquid --> NO	max. NO_2^- (% of initial NO_3^-)	max. NO (nM) in liquid	max. N_2O-N (% of initial NO_3^-)	*n*
Litho-autotrophic transition									
$F76_{(HD)}$	0.12 (±0.03)	0.10 (±0.01)	0.88 (±0.15)	nd[a]	6.9 (±0.4)	nd[a]	17.8 (±3.1)	7.1 (±4.6)	3
$D110_{(HD)}$	0.11 (±0.02)	0.10 (±0.02)	0.92 (±0.24)	1.5 (±1.4)	8.1 (±1.8)	19.4 (±3.9)	14.5 (±2.7)	13.3 (±11.3)	6
$H3_{(HD)}$	0.13 (±0.03)	0.03 (±0.01)	0.21 (±0.06)	8.3 (±1.6)	0.3 (±0.1)	100.1 (±13.7)	18.5 (±3.5)	18.3 (±15.5)	6
Adapted litho-autotrophic									
$F76_{(HD)}$	–	–	–	–	–	nd[a]	9.1 (±3.4)	2.4 (±4.1)	6
$D110_{(HD)}$	–	–	–	–	–	26.8 (±6.9)	16.1 (±4.3)	0.8 (±1.4)	3
$H3_{(HD)}$	–	–	–	–	–	75.7 (±2.3)	13.6 (±2.4)	0.01 (±0)	3
Organo-heterotrophic transition									
$F76_{(HD)}$	0.28 (±0.05)	0.16 (±0.04)	0.58 (±0.06)	10.3 (±0.6)	2.7 (±1.7)	2.9 (±0.9)	5.5 (±4.8)	1.9 (±1.3)	4
$D110_{(HD)}$	0.37 (±0.06)	0.29 (±0.06)	0.79 (±0.03)	8.2 (± 1.3)	1.7 (±0.8)	9.5 (±0.8)	3.7 (±0.9)	0.8 (±1.5)	4
$H3_{(HD)}$	0.18 (±0.10)	0.05 (±0.02)	0.35 (±0.20)	10.4 (±1.4)	0.3 (±0.1)	29.5 (±3.0)	17.2 (±1.9)	33.4 (±0.8)	4

napDAGHB. The *nar* genes of $H3_{(HD)}$, however, were organized all together as *narKGHJV*. Each analyzed genome contained multiple *nirS* gene copies in proximity, except for one *nirS* copy in the $D110_{(HD)}$ genome. Also, multiple copies of the accessory gene *nirM*, coding for cytochrome c551, were spread in all three genomes. The genes *norC* and *norB* clustered together close to *nirQ*, a synonym for *norQ*. While the *nos* operon genes of $H3_{(HD)}$ were located consecutively as *nosZ DFYL*, they were scattered among other genes in $F76_{(HD)}$ and $D110_{(HD)}$ (Fig. S7A and B). The *nos* genes of $F76_{(HD)}$ and $D110_{(HD)}$ were both accompanied by *regA*/*regB* genes.

Some of the above-specified genes were lacking in the genomes of the control group (D98, Q100, Q9). The two *Q. australiensis* isolates (Q100, Q9), which only reduced NO_3^- partly to NO_2^-, did not harbour any nitrite reductase gene, and D98, most closely related to *D. denitrificans*, did not harbour a RubisCO gene.

Discussion

Within this work bacteria that could denitrify with H_2 were isolated and characterized. The aim was to identify HDs with differing accumulation of intermediates, including NO_2^-, NO and N_2O, as well as to detect coherence between denitrification phenotypes, genetic properties and genome arrangement. The focus was on the genera *Dechloromonas* and its close relatives *Ferribacterium* and *Quatrionicoccus* from the family *Rhodocyclaceae*, as they had increased significantly in relative abundance in a recent microcosm experiment where H_2 was applied to stimulate lithotrophic denitrification with the aquifer material from the same location as used in this study (Duffner *et al*., 2021). The genus *Dechloromonas* has also been observed to thrive in other H_2-based environments, such as bioreactors (Zhang *et al*., 2009; Zhao *et al*., 2011) and microcosm experiments with GW and crushed rock material from a pristine aquifer (Kumar *et al*., 2018b). In the same experiments, the genus *Hydrogenophaga* was also detected. Indeed, in our study's second isolation, a large proportion of the isolates were assigned to the *Dechloromonas*, *Ferribacterium* and *Quatrionicoccus*, while in the first isolation, *Burkholderiaceae* isolates, mainly from the genera *Hydrogenophaga* and *Acidovorax*, were dominant. The different outcome could be due to high mineral nutrient concentrations in the MM that was used for the first isolation or due to the different sampling time points because seasonal differences in the bacterial community composition of aquifers are well-known (Chik *et al*., 2020). The multiple isolation of *D. denitrificans* and close relatives during the second isolation support their importance in hydrogenotrophic denitrification in oxic, nitrate-polluted oligotrophic aquifers (Duffner *et al*., 2021). While it is unclear which species prevails under which conditions, both *Dechloromonas* (and close relatives) and *Hydrogenophaga* obviously play an important role in hydrogenotrophic denitrification.

The significantly higher reduction in overpressure in the incubations with the HDs during the endpoint analysis compared to the control incubations confirms that the added H_2 and CO_2 were consumed by hydrogenotrophic bacteria. The increase in pH in the same incubations further indicates that denitrification occurred because denitrification uses protons to reduce NO_2^- to N_2 gas, increasing pH (Karanasios *et al*., 2010). The four isolates assigned to *F. limneticum* could all reduce NO_3^- to N_2 with H_2 as the electron donor, which was also the case for the closely related $D110_{(HD)}$ and $D6_{(HD)}$, belonging to the species *D. denitrificans*. The third group of complete HDs comprised the *Burkholderiaceae* isolates $H3_{(HD)}$ and $H2_{(HD)}$. While the first belonged to the species *H. taeniospiralis*, $H2_{(HD)}$ could be considered another species, based on the G + C content difference above 1%.

Genes for hydrogenotrophic denitrification

The genes coding for the dissimilatory nitrate reductase and nitrous oxide reductase differed between the *Rhodocyclaceae* isolates ($F76_{(HD)}$, $F77_{(HD)}$, $F128_{(HD)}$, $F132_{(HD)}$, $D110_{(HD)}$, $D6_{(HD)}$), which harboured *napA* and clade II *nosZ*, and the *Burkholderiaceae* isolates ($H3_{(HD)}$, $H2_{(HD)}$), which were characterized by *narG* and clade I *nosZ* genes. In conclusion, all complete HDs possessed denitrification reductases for all four steps, a form II Rubisco gene and three [NiFe] hydrogenase genes (group 1d, 2b and 3d). Thus, these genes are likely a prerequisite for hydrogenotrophic denitrification.

All detected hydrogenase genes in the analyzed hydrogenotrophic denitrifier genomes belonged to the [NiFe] class, which include the most common hydrogenases in bacteria (Vignais and Billoud, 2007). They harboured the O_2 tolerant group 1d respiratory [NiFe] hydrogenase (Greening *et al*., 2016), which is characteristic of many facultative anaerobic bacteria due to their frequent contact with O_2. Besides the respiratory hydrogenases, H_2-sensing and redox-balancing hydrogenases (Greening *et al*., 2016) were also detected. Of these, group 2b H_2-sensing [NiFe] hydrogenase controls hydrogenase expression, while the group 3d [NiFe] hydrogenase interconverts electrons between H_2 and NAD to adjust the redox state (Greening *et al*., 2016). Interestingly, only the *F. limneticum* isolates' genomes possessed extra hydrogenase genes (groups 1c and 2c). Moreover, CO_2 assimilation is an essential process of autotrophic hydrogenotrophic denitrification. Badger and Bek (2008) found that *Proteobacteria* may contain one or multiple RubisCO genes of the forms IA, IC and II, functioning at different concentrations of CO_2 and O_2. All investigated HDs possessed a form II Rubisco gene, which encodes a RubisCO version adapted to conditions with medium to high CO_2 and low or no O_2 (Badger and Bek, 2008). Thus, this is the only form that can assimilate CO_2 under anoxic conditions as encountered in the incubations.

Contrary to the findings of Yin *et al*. (2010), the genes of hydrogenotrophic denitrification did not cluster in close genome locations. Thus, their presence seems necessary, while their genomic location may vary. A plausible explanation for this observation is that operon proximity only occurs for operons whose encoding processes consistently work together, unlike denitrification, H_2 oxidation and CO_2 assimilation, which also function in combination with other metabolic pathways.

The closely related *Rhodocyclaceae* isolates, which lacked the ability to denitrify with H_2 (D98, Q100, Q9), lacked one of the mentioned genes which are likely a prerequisite of hydrogenotrophic denitrification: Q100 and Q9 lacked nitrite reductase gene, and D98 lacked a RubisCO gene. Additionally, D98 deviated phylogenetically from isolates $D110_{(HD)}$ and $D6_{(HD)}$, implying that D98 belonged to another species. The finding that all hydrogenotrophic denitrifying *Rhodocyclaceae* isolates either belonged to the species *D. denitrificans* or *F. limneticum*, and that the two isolates belonging to *Q. australiensis* and D98 of a so far not described species were incapable of hydrogenotrophic denitrification supports the finding of Duffner *et al*. (2021) that the ability for hydrogenotrophic denitrification among the family *Rhodocyclaceae* is species-specific.

Different hydrogenotrophic DRPs

Our data revealed that the *H. taeniospiralis* isolate $H3_{(HD)}$ differed significantly in multiple characteristics from the phenotypes of the *F. limneticum* isolate $F76_{(HD)}$ and the *D. denitrificans* isolate $D110_{(HD)}$. The most distinctive difference for isolate $H3_{(HD)}$ was the complete accumulation of NO_2^- until all NO_3^- had been reduced before continuing with further reduction steps, whereas isolates $F76_{(HD)}$ and $D110_{(HD)}$ initiated all denitrification steps simultaneously. This DRP of $H3_{(HD)}$ with a progressive onset of denitrification was also observed in several *Thauera* strains studied by Liu *et al*. (2013) as well as in another *Hydrogenophaga*, and a *Polaromonas* isolate studied by Lycus *et al*. (2017), with carbon as the electron donor. Like isolate $H3_{(HD)}$, the latter two are known to carry a *nar* gene, while isolates with the opposite phenotype, $F76_{(HD)}$ and $D110_{(HD)}$, harboured *nap* genes. Such a coherence between this distinct phenotype and the type of nitrate reductase has also been observed in recent studies by Gao *et al*. (2021) and Mania *et al*. (2020) for denitrifying *Bradyrhizobium* isolates. They also found that denitrifying *napA*-harbouring bradyrhizobia prefer N_2O reduction over NO_3^- reduction, while no such preference was detected in *narG*-carriers. This indicates that the electron pathway to the membrane-bound cytoplasmic nitrate reductase NarG competes better for electrons than the pathway to the periplasmic nitrate reductase NapA. The latter obtains electrons from NapC, a membrane-bound c-type cytochrome receiving electrons from the membrane-associated quinol pool, while NarG obtains electrons directly from the membrane-associated quinol pool (Shapleigh, 2013). The strong competition for electrons by the NarG pathway may prevent other denitrification reductases from receiving electrons when NO_3^- is still available, resulting in substantial NO_2^- accumulation like measured for $H3_{(HD)}$. The observation, that the transient NO_2^- accumulation did not differ significantly between the *Litho-autotrophic transition* and *Adapted litho-autotrophic* experiment for all tested isolates, further reasserts the hypothesis that the difference in NO_2^-

accumulation was due to differential electron flow rather than to differential gene expression. However, the occurrence of a *narG* gene cannot be the sole factor leading to 100% transient NO_2^- accumulation, as some *narG*-carrying bacteria, such as a *Pseudomonas* isolate in the study of Lycus *et al*. (2017), did not show any NO_2^- accumulation during denitrification with carbon. This could possibly be due to regulation at the transcriptional level (low transcription of *narG*). Contrary to transient NO_2^- accumulation, transient N_2O accumulation was on average considerably lower when the isolates were already equipped with a denitrification proteome (adapted to denitrification) compared with the transition phase, indicating that delayed *nos* gene expression caused most N_2O accumulation during the transition from aerobic respiration to denitrification. There was, however, considerable variation in transient N_2O accumulation between replicate experiments, also observed by Liu *et al*. (2013) with *Thauera* strains performing heterotrophic denitrification. The type of nitrous oxide reductase may influence the amount of N_2O accumulation as clade II NosZ enzymes have higher apparent N_2O affinity, higher biomass yield, and a more energy-efficient translocation mechanism compared with clade I NosZ (Yoon *et al*., 2016). Isolate $H3_{(HD)}$ also differed in this regard from $F76_{(HD)}$ and $D110_{(HD)}$, as it contained clade I *nosZ*, while the other tested strains harboured clade II.

The three analyzed HDs displayed a seamless transition from aerobic respiration to denitrification, i.e. without a substantial depression in electron flow rate at the transition from oxic to anoxic conditions. This was the case both with H_2 and carbon as the electron donor, implying that all cells, or at least the largest fraction of the cells, switched to denitrification due to anoxia unlike a phenomenon termed bet-hedging, observed by Lycus *et al*. (2017) for some denitrifying soil isolates. However, a drop in the total electron flow was observed in $H3_{(HD)}$ after nitrate depletion. This could either indicate that the organism expressed too little nitrite reductase to sustain the same high respiratory metabolism as during nitrate reduction or that only a fraction of the cells expressed nitrite reductase.

The denitrification phenotypes of $F76_{(HD)}$ and $D110_{(HD)}$ differed significantly between the oxic–anoxic transition under *Litho-autotrophic* and *Organo-heterotrophic* conditions. Litho-autotrophy led to an earlier onset of denitrification, as NO was detected at a significantly higher O_2 concentration. Also, both the oxic and anoxic growth rates were lower during the *Litho-autotrophic* compared to the *Organo-heterotrophic transition* experiment. Autotrophic growth requires much more energy to assimilate CO_2 (Albina *et al*., 2019) compared to heterotrophic growth. Consequently, cells grown on H_2 and CO_2 may switch earlier to denitrification to avoid entrapment in anoxia (Hassan *et al*., 2014). This difference in the O_2 concentration at the initiation of denitrification was not observed in $H3_{(HD)}$. However, the onset of NO_3^- reduction to NO_2^- occurred long before NO was detected, wherefore the estimated growth rate of $H3_{(HD)}$ was likely mostly based on NO_3^- reduction to NO_2^-. In the isolates $F76_{(HD)}$ and $D110_{(HD)}$ autotrophy additionally led to less balanced denitrification with higher transient accumulation of NO_2^-, NO and N_2O, indicating an influence of the electron donor H_2 on the proportionate expression of the respective reductase genes. In isolate $H3_{(HD)}$ this was only visible in the transient NO_2^- accumulation, which was significantly lower during *Organo-heterotrophic transition*.

The transcriptional regulation of denitrification differs largely among denitrifiers; however, the range of diversity is unknown as the regulation has mostly been studied in model organisms (e.g. *Paracoccus denitrificans*) (Gaimster *et al*., 2017; Lycus *et al*., 2017). Denitrification regulation comprises a network of regulators responding to intra- and extracellular signals such as NO, O_2, NO_3^- and NO_2^- concentrations as well as pH (Gaimster *et al*., 2017). An important sensor of decreasing O_2 concentrations and activator of denitrification is the RegAB redox-sensing two-component system, which was detected in all *Rhodocyclaceae* isolates. The *H. taeniospiralis* isolates; however, seemed to rely on the O_2-sensing two-component system FixLJ as their genomes harboured both genes. While FixL is directly activated by O_2 (Spiro, 2012), the membrane-associated RegB kinase indirectly responds to decreasing O_2 concentration as it is regulated by the redox state of the ubiquinone pool by non-catalytic equilibrium binding of ubiquinone (Wu and Bauer, 2010). The direct sensing of the ubiquinone redox state inside the denitrification respiratory membrane by RegAB may enable its carrier to react faster to changes in the electron availability inside the denitrification respiratory membrane and thus regulate the electron flow more efficiently. This could be a factor leading to a more balanced phenotype observed in the isolates $F76_{(HD)}$ and $D110_{(HD)}$ compared with $H3_{(HD)}$. In isolate $F76_{(HD)}$ extra hydrogenase genes were detected which may be connected to the even lower intermediate accumulation observed in $F76_{(HD)}$ compared with $D110_{(HD)}$.

Experimental procedures

Enrichment and isolation of HDs

Enrichment. Sediment and GW were sampled from a highly NO_3^- polluted oxic aquifer in the Hohenthann region in Southeast Germany (GPS: 48°42′01.2″N, 12°00′10.2″E). Location and sampling methods are

described in Duffner *et al*. (2021). Samples were stored at 4°C for 1 day until the enrichment incubations started. The used mineral medium (MM) was based on the 'multipurpose mineral medium' described by Widdel and Bak (1992). It contained separately autoclaved basal medium (without sulphate), 30 mM $NaHCO_3$ and 1.5–2 mM $NaNO_3$, as well as filter-sterilized 0.2% (vol./vol.) trace element solution SL-10 (Widdel and Pfennig, 1981; Widdel *et al*., 1983), 0.1% (vol./vol.) selenite tungsten solution (Widdel and Bak, 1992) and 0.1% (vol./vol.) vitamin solution (Balch *et al*., 1979). After autoclaving, all other components were added to the basal medium, and the pH was adjusted to 7.2 with 1 M HCl.

Approximately 100 ml of either only GW, sediment and groundwater (SED/GW), MM and groundwater (MM/GW) or MM and sediment (MM/SED), containing approximately 1.3 mM (70 mg L^{-1}) $NaNO_3$, were incubated inside 200 ml vials sealed with a rubber septum and an aluminium crimp cap. The crimped vials were sparged with a gas mixture containing 60% H_2, 10% CO_2 and 30% N_2 at an approximate flow rate of 100 ml min^{-1}, until the O_2 content in the outflowing air was 0% according to a digital oximeter (Greisinger Electronic, Germany) (~0.5 mM $H_{2(aq)}$, 14°C). The sparged enrichments were incubated at 14°C–20°C, while samples were taken every 2–5 days to monitor the NO_3^- and NO_2^- concentrations spectrophotometrically. NO_3^- was quantified according to Velghe and Claeys (1985), and NO_2^- according to Tsikas *et al*. (1997). Once all NO_3^- and NO_2^- had been reduced, which took between 6 and 46 days depending on the initial material (Fig. S1B), isolation from the enrichments was initiated. For one replicate per treatment 10% (vol./vol.) were transferred to fresh MM or 0.2 μm filtered/autoclaved GW once all NO_3^- had been reduced. This was done three times before the isolation.

Bacterial community analysis of the enrichments. Two milliliters (SED/GW, MM/SED) or 10 ml (GW, MM/GW) of the final enrichments were pelleted and frozen for bacterial community analysis. Additionally, original sediment and the material collected on a 0.22 μm filter of 3 L GW of each sampling was analyzed. DNA was extracted using the NucleoSpin Soil Kit (Macherey Nagel, Germany) with buffer SL2 and 30 s at 5.5 m s^{-1} bead beating. A negative extraction control was run alongside the samples. The 16S rRNA gene amplicon sequencing library preparation, the Illumina MiSeq sequencing and data processing were conducted as described in Duffner *et al*. (2021), with the exception that the primer pair 515F (Parada *et al*., 2016) and 806R (Apprill *et al*., 2015) suggested by the Earth Microbiome Project (V4 region), was used (Walters *et al*., 2016). The demultiplexed reads were processed using the QIIME2 and the DADA2 plugin (Bolyen *et al*., 2019), setting the N-terminal trimming to 10 bp and the C-terminal trimming to 270 bp for the forward and to 200 bp for the reverse reads. After denoising (Table S1), on average 70.6% of the reads remained for the enrichments, whereas only 53.1% of the reads remained for the original sediment and GW samples. Singleton reads from domains other than bacteria, and ASVs with more than nine reads in the negative extraction control were removed. The datasets were subsampled to the minimum number of reads per sample, 35 921 (EI) and 28 584 (EII), using the vegan package (v.2.5–7) (Oksanen *et al*., 2019) included in the R project (v.4.0.3) (Team, 2019). The rarefaction curves were generated using the vegan package, and the stacked bar plots with the phyloseq package (v.1.34.0) (McMurdie and Holmes, 2013). The amplicon sequences have been deposited in the Sequence Read Archive repository under the BioSample accession numbers SAMN19613689–SAMN19613703 as part of the BioProject PRJNA727717.

Isolation. The enrichments were serially diluted (10^{-2}–10^{-4}) upon depletion of the given nitrate. 100 μl of the dilutions were plated on MM agar plates, prepared with 1.5% (wt./vol.) purified agar (Oxoid Thermo Fisher, USA), under a laminar flow. The agar plates were incubated in anoxic pots flushed for approximately 1 h with the H_2-containing gas mixture. The anoxic pots were incubated for approximately 6 weeks at 14°C–20°C. In total 300 colonies were picked and secured in a colony library on agar plates. A large portion of the grown colonies was less than 0.5 mm in diameter, white/transparent and circular with a smooth edge, similar to the colony morphology of *Dechloromonas denitrificans* (Horn *et al*., 2005). For phylogenetic identification of the isolates, a colony PCR was performed targeting the full 16S rRNA gene (described in Table S2). Forty-five isolates (Table S3; Fig. S2), including strains of the species *Dechloromonas denitrificans*, *Ferribacterium limneticum*, *Quatrionicoccus australiensis* and *Hydrogenophaga taeniospiralis*, were inoculated in MM with the same H_2 atmosphere as described above and tested for their ability to reduce NO_3^- while being incubated at 20°C for 5 days. Ten isolates could reduce at least 35% of the initial NO_3^- within the given time (Table S3). Thereof eight were used for further phenotypic and genotypic characterization. They are marked as HD (hydrogenotrophic denitrifier) hereafter. These isolates included four strains assigned to *F. limneticum* ($F76_{(HD)}$, $F77_{(HD)}$, $F128_{(HD)}$, $F132_{(HD)}$), two isolates assigned to *D. denitrificans* ($D110_{(HD)}$, $D6_{(HD)}$) and two isolates assigned to *H. taeniospiralis* ($H3_{(HD)}$, $H2_{(HD)}$) (Fig. 1). Additionally, three close relatives of *D. denitrificans* and *F. limneticum* (D98, Q100, Q9) without

denitrifying ability with H_2 were characterized as a control group.

Difference between EI and EII. The enrichment and isolation procedure was performed twice, termed EI and EII, to increase the number of isolates from the family *Rhodocyclaceae*. For EI groundwater and sediment was sampled on February 20th 2019, and for EII on October 18th 2019. For EI, two replicates were prepared for each setup (GW, SED/GW, MM/GW, MM/SED), whereas four replicates were prepared for each setup of EII (GW, SED/GW). A difference was that the enrichment setups with MM were omitted for EII, and the agar plates contained only 10% of the mineral and vitamin mixtures described above. Also, during EII the enrichments were transferred to 0.2 μm filtered and autoclaved GW instead of fresh MM like during EI. Details of the enrichment and isolation procedure of HDs are given in Fig. S1 and Table S4.

Sequencing and analysis of the isolates' genomes

The 11 selected isolates (Fig. 1) were grown in R2A medium aerobically at 30°C for 2–4 days up to late exponential phase and harvested to reach approximately 4.5×10^9 cells, as recommended by the QIAGEN Genomic-tip (20/G) procedure (QIAGEN, Germany) protocol. This anion-exchange-based DNA extraction method, ensuring minimal fragmentation, was performed according to the manufacturer's protocol. The obtained high-quality DNA was sheared to 9–14 kb long fragments and quantified using a fragment analyzer (Agilent Technologies, USA) and the large fragment DNF-492 Kit (Agilent Technologies). With a maximum total expected genome size of 33 Mb, multiplexed microbial libraries were generated with the SMRTbell Express Template Prep Kit 2.0 Part Number 101-696-100 v.6 (March 2020) (PacBio, USA) without size selection. The libraries were sequenced using PacBio SMRT cells with the Sequel System and 3.0 chemistry. The genomes were assembled by the HGAP4 pipeline (SMRT Link: 8.0.0.80529, PacBio) with a seed coverage of 30 (Table S5). The genome sequences were circularized using the Circlator software (Hunt *et al*., 2015), and the genome sequence quality was assessed with the CheckM software (Parks *et al*., 2015) (Table S6). The circularized genomes were annotated with Prokka (version 1.13) (Seemann, 2014) using a similarity e-value cut-off of $1e^{-05}$.

The taxonomy of the genomes was determined by the Type Strain Genome Server (TYGS), the successor of the Genome-to-Genome Distance Calculator, in August 2020 (Meier-Kolthoff and Göker, 2019; Meier-Kolthoff *et al*., 2021). Instead of using a restricted number of marker proteins, TYGS computes genome-scale phylogeny and infers species boundaries from closest type genome sequences. It thereby also calculates the digital DNA–DNA hybridisation (dDDH) and G + C content difference between two isolates and the closest type strain genomes, which was described as a more reliable method compared to average nucleotide identity for example (Meier-Kolthoff and Göker, 2019). Furthermore, the complete 16S rRNA gene sequences were extracted and the percentage identity with the most similar 16S RNA gene sequence was calculated. The species delineation for dDDH has been set as 70% (Meier-Kolthoff and Göker, 2019). The G + C content difference is also an indicator of phylogeny because it rarely exceeds 1% within species (Meier-Kolthoff *et al*., 2014). For 16S rRNA gene comparison, species delineation ranges between 97% and 98.5% in the literature, as there is no universal agreement on the species boundaries (Janda and Abbott, 2007).

Further focus was given on the identification of genes potentially involved in hydrogenotrophic denitrification, such as denitrification reductases (*napA*, *narG*, *nirS*, *nirK*, *qnorB*, *cnorB*, clade I and clade II *nosZ*), RubisCO, hydrogenase and denitrification regulatory genes (*fixL*, *fixJ*, *ntcA*, *nnr*, *regA*, *regB*, *narX*, *narL*, *narQ*, *narP*, *norR*, *nsrR*, *dnrD*, *dnrN*) (see Supplementary Materials 2).

For a sub-selection, including one isolate of each phylogenetically distinct hydrogenotrophic denitrifier group ($F76_{(HD)}$, $D110_{(HD)}$, $H3_{(HD)}$) (Fig. 1), the circular genomes were visualized using the DNAPlotter software (Carver *et al*., 2008) showing the location of the important hydrogenotrophic denitrifier genes. If these were in proximity, their gene neighbourhood was additionally plotted using Gene Graphics (Harrison *et al*., 2018).

The genome sequences with the BioSample accessions SAMN19030600–SAMN19030611 are deposited at NCBI under the BioProject PRJNA727717.

Analyses of the denitrification phenotypes

Incubation system. A robotized incubation system was used for all analyses of the denitrification endpoints and denitrification kinetics. The system, described in detail by Molstad *et al*. (2007) and Molstad *et al*. (2016), hosts up to 30 parallel stirred batch cultures (120 ml serum vials with Teflon coated magnetic bars, crimp sealed with butyl rubber membranes) in a water bath with constant temperature (18°C in our experiments). At intervals, the system samples the headspace by piercing the butyl rubber septa and drawing the sample by a peristaltic pump into injection loops. After injection, the pump is reversed, returning a volume of He (equal to the volume drawn) into the vial. The gas chromatographic system [CP4900 microGC, Varian (now Agilent Technologies)] measures O_2, N_2, N_2O, CO_2 and CH_4 with thermal conductivity

detectors, and a chemoluminescence NOx analyzer (Model 200A, Advanced Pollution Instrumentation, USA) is used to measure NO. Measurements of standard gas mixtures (25 ppmv NO in N_2, 150 ppmv N_2O and 1% CO_2 in He, 21% O_2 in N_2) alongside the incubations were used for calibration and capture dilution of the headspace gases and leakage (see Molstad *et al*., 2007 for details). A spreadsheet developed by Bakken (2021) was used to convert the chromatography output into gas concentrations in the headspace and in the liquid, and the rate of production/consumption of each gas for every time interval between two samples. For the incubations with H_2 in the headspace, there was a significant reduction of the headspace pressure, despite the system's return of He at each sampling, due to the consumption of both H_2 and CO_2. This necessitated inclusion of pressure depression into calculating the gas concentrations. Therefore, the kinetics and in particular the mass balances for these incubations were not as accurately determined as is described in Molstad *et al*. (2007). NO_3^- and NO_2^- liquid concentrations were determined as described in Lycus *et al*. (2017), in small liquid samples taken manually throughout the incubations.

Endpoint analysis. First, the denitrification end products of all 11 selected isolates (eight HDs and three control strains) were determined by an endpoint analysis, essentially as described by Lycus *et al*. (2017). The cultures were incubated anoxically in the presence of NO_3^-, NO_2^- and N_2O, which allowed us to determine if they had complete or only partial denitrification pathways and if they were able to convert all available electron acceptors to N_2 with H_2 as the sole electron donor. The endpoint analyses were performed in triplicate for all 11 isolates. Approximately 1 ml pre-culture at an optical density (OD_{600}) of 0.3 was centrifuged at 4400*g* for 5 min, washed twice with 1 ml MM and dispersed in 1 ml MM. Since $F77_{(HD)}$ did not grow aerobically in liquid culture, it had to be scratched from R2A agar plates and washed in MM (as the others). The washed inocula were injected into 120 ml vials with 50 ml MM containing 1.5 mM $NaNO_3$ and 0.5 mM $NaNO_2$. After He-flushing, the vials were injected with 40 ml H_2 $vial^{-1}$, 20 ml CO_2 $vial^{-1}$ and 1.4 ml N_2O $vial^{-1}$ ($\sim$50 μmol N_2O $vial^{-1}$). The resulting overpressure of approximately 725 mbar (C9555 pressure metre, Comark Instruments, UK) was not released, and the vials were incubated for a minimum of 10 days at 18°C and 120 rpm. First, the pressure in the vials was quantified, the pressure was then released, and the headspace gases were measured twice in the robotized incubation system. Furthermore, NO_3^- and NO_2^- concentrations were determined, and the pH was measured directly after opening each vial. The experiment included additional control vials with inoculum but without H_2 to check for potential denitrification by carry-over carbon. The cultures were streaked onto R2A plates before and after incubation to check for cell viability and contamination.

Denitrification kinetics. The kinetics were investigated for the sub-selection of strains including $F76_{(HD)}$, $D110_{(HD)}$ and $H3_{(HD)}$. The first two experiments investigated the DRPs of cells that were raised under strict oxic conditions (to avoid the synthesis of denitrification enzymes), and monitored for O_2, NO_2^-, NO, N_2O and N_2 as the batch cultures depleted O_2, switched to anaerobic respiration and converted NO_3^- to N_2. These transition experiments were conducted with cells growing litho-autotrophically (H_2, CO_2, no organic carbon) and with cells growing organo-heterotrophically (only organic carbon provided), thus in the following, we will call the two experiments *Litho-autotrophic transition* and *Organo-heterotrophic transition* respectively. The DRP revealed by these transition experiments effectively confounds the effects of regulation at the transcriptional and metabolic level. To inspect the regulation at the metabolic level for litho-autotrophic denitrification, we conducted a third experiment where we continued to monitor the *Litho-autotrophic transition* experiment vials after adding a new dose of $NaNO_3$. In the following, we will call this experiment *Adapted litho-autotrophic*.

Litho-autotrophic transition: Liquid pre-cultures were grown aerobically in the most suitable complex organic medium (R2A for $F76_{(HD)}$ and $D110_{(HD)}$, and 20% TSB for $H3_{(HD)}$; Table S7) to secure high cell density for the inoculation. When these had reached mid/late exponential phase, 20–50 ml of the culture was centrifuged at 8000*g* for 10 min, washed twice with 20 ml MM (to remove organic compounds) and finally dispersed in MM. The washed cells were used to inoculate the 120 ml vials (1 ml per vial) containing 50 ml MM with 2 mM $NaNO_3$. After He-flushing and the injection of 40 ml H_2 $vial^{-1}$ and 20 ml CO_2 $vial^{-1}$, the vials were placed in the robotized incubation system, where the overpressure was released before 0.6 ml O_2 gas was injected ($\sim$26.5 μmol O_2 $vial^{-1}$). The headspace gases were measured at 4 h intervals, and the experiment lasted ≥120 h. The initial NO_3^- concentration was determined, and NO_2^- was measured throughout the incubation, more frequently during its accumulation.

Organo-heterotrophic transition: This experiment was similar to the *Litho-autotrophic transition* experiment. The differences were that the washing of the inocula (1 ml pre-culture, $OD_{600} = 0.1$) was omitted, complex organic liquid media were used (R2A for $F76_{(HD)}$, $D110_{(HD)}$, and 20% TSB for $H3_{(HD)}$; Table S7) and the anoxic atmosphere contained only Helium as no H_2 and CO_2 gas

was injected to the headspace. Thus, CO_2 fixation and lithotrophic denitrification were excluded.

Adapted litho-autotrophic: At the end of the *Litho-autotrophic transition* experiments, the vials were re-flushed with He, injected with 40 ml H_2 $vial^{-1}$, 20 ml CO_2 $vial^{-1}$ (but no O_2) and 1 ml 0.1 M $NaNO_3$ (=100 μmol $vial^{-1}$, 2 mM in the liquid). The pressure was released, and the vials were monitored for NO_2^-, NO, N_2O and N_2 in the robotized incubation system until all NO_3^- had been recovered as N_2.

Control vials with the same setup but without inoculum were measured alongside the bacterial incubations to check for contamination and gas leakage. All experiments were performed with a minimum of three replicate (*n* stated in Table 1) for each isolate.

Because NO_2^- was measured manually at different time points than the gases, the concentrations at the time points of the gas sampling were estimated by interpolation, using the SRS1 Cubic Spline Software (http://www.srs1software.com). Additionally, the electron flow (μmol e^- h^{-1}) to terminal oxidases and the denitrification reductases (NAR/NAP, NIR, NOR, NOS) was calculated based on the gross rates of each step in denitrification. The graphs were compiled in R project (v.4.0.1) with the ggplot2 package (Wickham, 2016). Due to the small number of replicates, a robust one-way analysis of variance with trimmed means (t1way function) and the post hoc test lincon from the package WRS2 (Mair and Wilcox, 2019) was used to detect statistically significant differences in the basic denitrification phenotype characteristics between the three analyzed isolates and kinetics experiments. The *p*-values were adjusted for each experiment or experimental comparison with a Benjamini and Hochberg ('BH') correction (Benjamini and Hochberg, 1995). Adjusted *p*-values <0.05 were considered significant.

Conclusion

We isolated and characterized prevailing complete HDs, which belong to the species *F. limneticum*, *D. denitrificans* and *H. taeniospiralis*. The presence of all denitrification reductase genes, a form II RubisCO gene and a minimum of three [NiFe]-hydrogenase genes were identified as common features to denitrify with H_2 as electron donor and CO_2 as carbon source. The results indicated that under ideal conditions without an electron donor limitation and sufficient nutrients and vitamins available, a difference in transient NO_2^- accumulation can be attributed to a stronger electron flow to the nitrate reductase NarG than NapA rather than sequential gene expression. If hydrogenotrophic denitrifying communities are dominated by *napA* carrying bacteria, e.g. of the species *F. limneticum* and *D. denitrificans*, we would thus expect less NO_2^- accumulation compared with communities dominated by *narG*-carrying bacteria e.g. of *H. taeniospiralis*. Furthermore, the genome analysis indicated that the phenotypes with less transient NO_2^- accumulation were associated with the RegAB two-component system, which could improve the regulation of electron flow inside the denitrification respiratory membrane. As detected in the *F. limneticum* isolates, additional hydrogenase genes may have a similar effect and thereby minimize intermediate accumulation further. Based on the obtained data, the next step is to develop ways enabling targeted stimulation of complete HDs with the least intermediate accumulation.

Acknowledgements

Clara Duffner received funding by Deutsche Forschungsgemeinschaft (DFG) through TUM International Graduate School of Science and Engineering (IGSSE), GSC 81. We would like to thank the Nitrogen Group from NMBU for welcoming Clara Duffner as a guest researcher and for all the help and guidance she received from all members of the group. Also, we would like to thank Franz Buegger (Helmholtz Centre Munich) for his help in setting up the gas system and Gabriele Barthel (Helmholtz Centre Munich) for her insights on cultivating litho-autotrophic bacteria anaerobically.

References

Albina, P., Durban, N., Bertron, A., Albrecht, A., Robinet, J.-C., and Erable, B. (2019) Influence of hydrogen electron donor, alkaline pH, and high nitrate concentrations on microbial denitrification: a review. *Int J Mol Sci* **20**: 5163.

Apprill, A., McNally, S., Parsons, R., and Weber, L. (2015) Minor revision to V4 region SSU rRNA 806R gene primer greatly increases detection of SAR11 bacterioplankton. *Aquat Microb Ecol* **75**: 129–137.

Badger, M.R., and Bek, E.J. (2008) Multiple Rubisco forms in proteobacteria: their functional significance in relation to CO_2 acquisition by the CBB cycle. *J Exp Bot* **59**: 1525–1541.

Bakken, L. (2021) Spreadsheet for Gas Kinetics in Batch Cultures: KINCALC.

Balch, W.E., Fox, G.E., Magrum, L.J., Woese, C.R., and Wolfe, R.S. (1979) Methanogens: reevaluation of a unique biological group. *Microbiol Rev* **43**: 260–296.

Benjamini, Y., and Hochberg, Y. (1995) Controlling the false discovery rate: a practical and powerful approach to multiple testing. *J R Stat Soc B Methodol* **57**: 289–300.

Bergaust, L., Bakken, L.R., and Frostegård, Å. (2011) Denitrification regulatory phenotype, a new term for the characterization of denitrifying bacteria. *Biochem Soc Trans* **39**: 207–212.

Bolyen, E., Rideout, J.R., Dillon, M.R., Bokulich, N.A., Abnet, C.C., Al-Ghalith, G.A., *et al*. (2019) Reproducible, interactive, scalable and extensible microbiome data science using QIIME 2. *Nat Biotechnol* **37**: 852–857.

Carver, T., Thomson, N., Bleasby, A., Berriman, M., and Parkhill, J. (2008) DNAPlotter: circular and linear interactive genome visualization. *Bioinformatics* **25**: 119–120.

Chaplin, B.P., Schnobrich, M.R., Widdowson, M., Semmens, M.J., and Novak, P.J. (2009) Stimulating in situ hydrogenotrophic denitrification with membrane-delivered hydrogen under passive and pumped groundwater conditions. *J Environ Eng* **135**: 666–676.

Chik, A.H.S., Emelko, M.B., Anderson, W.B., O'Sullivan, K. E., Savio, D., Farnleitner, A.H., *et al*. (2020) Evaluation of groundwater bacterial community composition to inform waterborne pathogen vulnerability assessments. *Sci Total Environ* **743**: 140472.

Duffner, C., Holzapfel, S., Wunderlich, A., Einsiedl, F., Schloter, M., and Schulz, S. (2021) *Dechloromonas* and close relatives prevail hydrogenotrophic denitrification in stimulated microcosms with oxic aquifer material. *FEMS Microbiol Ecol* **97**: fiab004.

Ergas, S.J., and Reuss, A.F. (2001) Hydrogenotrophic denitrification of drinking water using a hollow fibre membrane bioreactor. *J Water Supply: Res Technol-Aqua* **50**: 161–171.

Gaimster, H., Alston, M., Richardson, D.J., Gates, A.J., and Rowley, G. (2017) Transcriptional and environmental control of bacterial denitrification and N_2O emissions. *FEMS Microbiol Lett* **365**: 1–8.

Gao, Y., Mania, D., Mousavi, S.A., Lycus, P., Arntzen, M.Ø., Woliy, K., *et al*. (2021) Competition for electrons favours N_2O reduction in denitrifying Bradyrhizobium isolates. *Environ Microbiol* **23**: 2244–2259.

Ghafari, S., Hasan, M., and Aroua, M.K. (2009) Effect of carbon dioxide and bicarbonate as inorganic carbon sources on growth and adaptation of autohydrogenotrophic denitrifying bacteria. *J Hazard Mater* **162**: 1507–1513.

Graf, D.R.H., Jones, C.M., and Hallin, S. (2014) Intergenomic comparisons highlight modularity of the denitrification pathway and underpin the importance of community structure for N_2O emissions. *PLoS One* **9**: 1–20.

Greening, C., Biswas, A., Carere, C.R., Jackson, C.J., Taylor, M.C., Stott, M.B., *et al*. (2016) Genomic and metagenomic surveys of hydrogenase distribution indicate H_2 is a widely utilised energy source for microbial growth and survival. *ISME J* **10**: 761–777.

Harrison, K.J., Crécy-Lagard, V.D., and Zallot, R. (2018) Gene graphics: a genomic neighborhood data visualization web application. *Bioinformatics (Oxford, England)* **34**: 1406–1408.

Hassan, J., Bergaust, L.L., Wheat, I.D., and Bakken, L.R. (2014) Low probability of initiating *nirS* transcription explains observed gas kinetics and growth of bacteria switching from aerobic respiration to denitrification. *PLoS Comput Biol* **10**: e1003933.

Horn, M.A., Ihssen, J., Matthies, C., Schramm, A., Acker, G., and Drake, H.L. (2005) *Dechloromonas denitrificans* sp. nov., *Flavobacterium denitrificans* sp. nov., *Paenibacillus anaericanus* sp. nov. and *Paenibacillus terrae* strain MH72, N_2O-producing bacteria isolated from the gut of the earthworm *Aporrectodea caliginosa*. *Int J Syst Evol Microbiol* **55**: 1255–1265.

Hunt, M., Silva, N.D., Otto, T.D., Parkhill, J., Keane, J.A., and Harris, S.R. (2015) Circlator: automated circularization of genome assemblies using long sequencing reads. *Genome Biol* **16**: 294.

Janda, J.M., and Abbott, S.L. (2007) 16S rRNA gene sequencing for bacterial identification in the diagnostic laboratory: pluses, perils, and pitfalls. *J Clin Microbiol* **45**: 2761–2764.

Karanasios, K.A., Vasiliadou, I.A., Pavlou, S., and Vayenas, D.V. (2010) Hydrogenotrophic denitrification of potable water: a review. *J Hazard Mater* **180**: 20–37.

Kumar, S., Herrmann, M., Blohm, A., Hilke, I., Frosch, T., Trumbore, S.E., and Küsel, K. (2018b) Thiosulfate- and hydrogen-driven autotrophic denitrification by a microbial consortium enriched from groundwater of an oligotrophic limestone aquifer. *FEMS Microbiol Ecol* **94**: fiy141.

Lee, K.-C., and Rittmann, B.E. (2003) Effects of pH and precipitation on autohydrogenotrophic denitrification using the hollow-fiber membrane-biofilm reactor. *Water Res* **37**: 1551–1556.

Liu, B., Mao, Y., Bergaust, L., Bakken, L.R., and Frostegård, Å. (2013) Strains in the genus *Thauera* exhibit remarkably different denitrification regulatory phenotypes. *Environ Microbiol* **15**: 2816–2828.

Lycus, P., Lovise Bøthun, K., Bergaust, L., Peele Shapleigh, J., Reier Bakken, L., and Frostegård, Å. (2017) Phenotypic and genotypic richness of denitrifiers revealed by a novel isolation strategy. *ISME J* **11**: 2219–2232.

Mair, P., and Wilcox, R. (2019) Robust statistical methods in R using the WRS2 package. *Behav Res Methods* **52**: 464–488.

Mania, D., Woliy, K., Degefu, T., and Frostegård, å. (2020) A common mechanism for efficient N_2O reduction in diverse isolates of nodule-forming bradyrhizobia. *Environ Microbiol* **22**: 17–31.

Matějů, V., Čižinská, S., Krejčí, J., and Janoch, T. (1992) Biological water denitrification—A review. *Enzyme Microb Technol* **14**: 170–183.

McMurdie, P.J., and Holmes, S. (2013) phyloseq: an R package for reproducible interactive analysis and graphics of microbiome census data. *PLoS One* **8**: e61217.

Meier-Kolthoff, J.P., Carbasse, J.S., Peinado-Olarte, R.L., and Göker, M. (2021) TYGS and LPSN: a database tandem for fast and reliable genome-based classification and nomenclature of prokaryotes. *Nucleic Acids Res* **50**: D801–D807.

Meier-Kolthoff, J.P., and Göker, M. (2019) TYGS is an automated high-throughput platform for state-of-the-art genome-based taxonomy. *Nat Commun* **10**: 2182.

Meier-Kolthoff, J.P., Klenk, H.-P., and Göker, M. (2014) Taxonomic use of DNA G+C content and DNA–DNA hybridization in the genomic age. *Int J Syst Evol Microbiol* **64**: 352–356.

Molstad, L., Dörsch, P., and Bakken, L.R. (2007) Robotized incubation system for monitoring gases (O_2, NO, N_2O N_2) in denitrifying cultures. *J Microbiol Methods* **71**: 202–211.

Molstad, L., Dörsch, P. & Bakken, L.R. (2016) Improved robotized incubation system for gas kinetics in batch cultures. Researchgate.

Oksanen, J., Blanchet, F.G., Friendly, M., Kindt, R., Legendre, P., McGlinn, D. *et al*. (2019) vegan: Community Ecology Package.

Parada, A.E., Needham, D.M., and Fuhrman, J.A. (2016) Every base matters: assessing small subunit rRNA primers for marine microbiomes with mock communities, time series and global field samples. *Environ Microbiol* **18**: 1403–1414.

Parks, D.H., Imelfort, M., Skennerton, C.T., Hugenholtz, P., and Tyson, G.W. (2015) CheckM: assessing the quality of microbial genomes recovered from isolates, single cells, and metagenomes. *Genome Res* **25**: 1043–1055.

R Core Team. (2019) *R: A Language and Environment for Statistical Computing*: Vienna, Austria: *R Foundation for Statistical Computing*.

Rivett, M.O., Buss, S.R., Morgan, P., Smith, J.W.N., and Bemment, C.D. (2008) Nitrate attenuation in groundwater: a review of biogeochemical controlling processes. *Water Res* **42**: 4215–4232.

Schnobrich, M.R., Chaplin, B.P., Semmens, M.J., and Novak, P.J. (2007) Stimulating hydrogenotrophic denitrification in simulated groundwater containing high dissolved oxygen and nitrate concentrations. *Water Res* **41**: 1869–1876.

Seemann, T. (2014) Prokka: rapid prokaryotic genome annotation. *Bioinformatics* **30**: 2068–2069.

Shapleigh, J. (2013) *The Prokaryotes: Prokaryotic Physiology and Biochemistry*. Berlin, Heidelberg: Springer.

Spiro, S. (2012) Nitrous oxide production and consumption: regulation of gene expression by gas-sensitive transcription factors. *Philos Trans R Soc B: Biol Sci* **367**: 1213–1225.

Szekeres, S., Kiss, I., Kalman, M., and Soares, M.I.M. (2002) Microbial population in a hydrogen-dependent denitrification reactor. *Water Res* **36**: 4088–4094.

Tsikas, D., Gutzki, F.-M., Rossa, S., Bauer, H., Neumann, C., Dockendorff, K., *et al*. (1997) Measurement of nitrite and nitrate in biological fluids by gas chromatography–mass spectrometry and by the Griess assay: problems with the Griess assay—solutions by gas chromatography–mass spectrometry. *Anal Biochem* **244**: 208–220.

Vasiliadou, I.A., Siozios, S., Papadas, I.T., Bourtzis, K., Pavlou, S., and Vayenas, D.V. (2006) Kinetics of pure cultures of hydrogen-oxidizing denitrifying bacteria and modeling of the interactions among them in mixed cultures. *Biotechnol Bioeng* **95**: 513–525.

Velghe, N., and Claeys, A. (1985) Rapid spectrophotometric determination of nitrate in mineral waters with resorcinol. *Analyst* **110**: 313–314.

Vignais, P.M., and Billoud, B. (2007) Occurrence, classification, and biological function of hydrogenases: an overview. *Chem Rev* **107**: 4206–4272.

Walters, W., Hyde, E.R., Berg-Lyons, D., Ackermann, G., Humphrey, G., Parada, A., *et al*. (2016) Improved bacterial 16S rRNA gene (V4 and V4-5) and fungal internal transcribed spacer marker gene primers for microbial community surveys. *mSystems* **1**: e00009-00015.

Wickham, H. (2016) *ggplot2: Elegant Graphics for Data Analysis*. New York: Springer-Verlag.

Widdel, F., and Bak, F. (1992) Gram-negative mesophilic sulfate-reducing bacteria. In *The Prokaryotes: A Handbook on the Biology of Bacteria: Ecophysiology, Isolation, Identification, Applications*, Balows, A., Trüper, H.G., Dworkin, M., Harder, W., and Schleifer, K.-H. (eds). Springer New York: New York, NY, pp. 3352–3378.

Widdel, F., Kohring, G.-W., and Mayer, F. (1983) Studies on dissimilatory sulfate-reducing bacteria that decompose fatty acids. *Arch Microbiol* **134**: 286–294.

Widdel, F., and Pfennig, N. (1981) Studies on dissimilatory sulfate-reducing bacteria that decompose fatty acids. *Arch Microbiol* **129**: 395–400.

Wu, J., and Bauer, C.E. (2010) RegB kinase activity is controlled in part by monitoring the ratio of oxidized to reduced ubiquinones in the ubiquinone pool. *mBio* **1**: e00272-00210.

Wu, J., Yin, Y., and Wang, J. (2018) Hydrogen-based membrane biofilm reactors for nitrate removal from water and wastewater. *Int J Hydrogen Energy* **43**: 1–15.

Yin, Y., Zhang, H., Olman, V., and Xu, Y. (2010) Genomic arrangement of bacterial operons is constrained by biological pathways encoded in the genome. *Proc Natl Acad Sci U S A* **107**: 6310–6315.

Yoon, S., Nissen, S., Park, D., Sanford, R.A., and Löffler, F. E. (2016) Nitrous oxide reduction kinetics distinguish bacteria harboring clade I NosZ from those harboring clade II NosZ. *Appl Environ Microbiol* **82**: 3793–3800.

Zhang, Y., Zhong, F., Xia, S., Wang, X., and Li, J. (2009) Autohydrogenotrophic denitrification of drinking water using a polyvinyl chloride hollow fiber membrane biofilm reactor. *J Hazard Mater* **170**: 203–209.

Zhao, H.P., Van Ginkel, S., Tang, Y., Kang, D.-W., Rittmann, B., and Krajmalnik-Brown, R. (2011) Interactions between perchlorate and nitrate reductions in the biofilm of a hydrogen-based membrane biofilm reactor. *Environ Sci Technol* **45**: 10155–10162.

Zumft, W.G. (1997) Cell biology and molecular basis of denitrification. *Microbiol Mol Biol Rev* **61**: 533–616.

Supporting Information

Additional Supporting Information may be found in the online version of this article at the publisher's web-site:

Appendix S1: Supplementary Information.

Publication II Supplementary Materials

SUPPLEMENTARY MATERIALS

Genotypic and Phenotypic Characterisation of Hydrogenotrophic Denitrifiers

Clara Duffner[1,2], Susanne Kublik[2], Bärbel Fösel[2], Åsa Frostegård[3], Michael Schloter[1,2], Lars Bakken[3], Stefanie Schulz[2]*

[1] Chair of Soil Science, TUM School of Life Sciences Weihenstephan, Technical University of Munich, Freising, Germany, [2] Research Unit Comparative Microbiome Analysis, Helmholtz Centre Munich, Neuherberg, Germany, [3] Department of Chemistry, Biotechnology and Food Sciences, Norwegian University of Life Sciences, Ås, Norway.

***Corresponding author:** Phone: +49 89 3187 3054; Address: Research Unit Comparative Microbiome Analysis (HMGU), Ingolstädter Landstr. 1, 85764 Neuherberg; E-Mail: stefanie.schulz@helmholtz-muenchen.de

One sentence summary: Isolation and characterisation of the complete hydrogenotrophic denitrifiers *Ferribacterium limneticum*, *Dechloromonas denitrificans*, and *Hydrogenophaga taeniospiralis* with a focus on intermediate accumulation during denitrification.

Keywords: genome sequencing, denitrification phenotype, denitrification reductases, RubisCO, hydrogenases

List of Figures:

List of Tables:

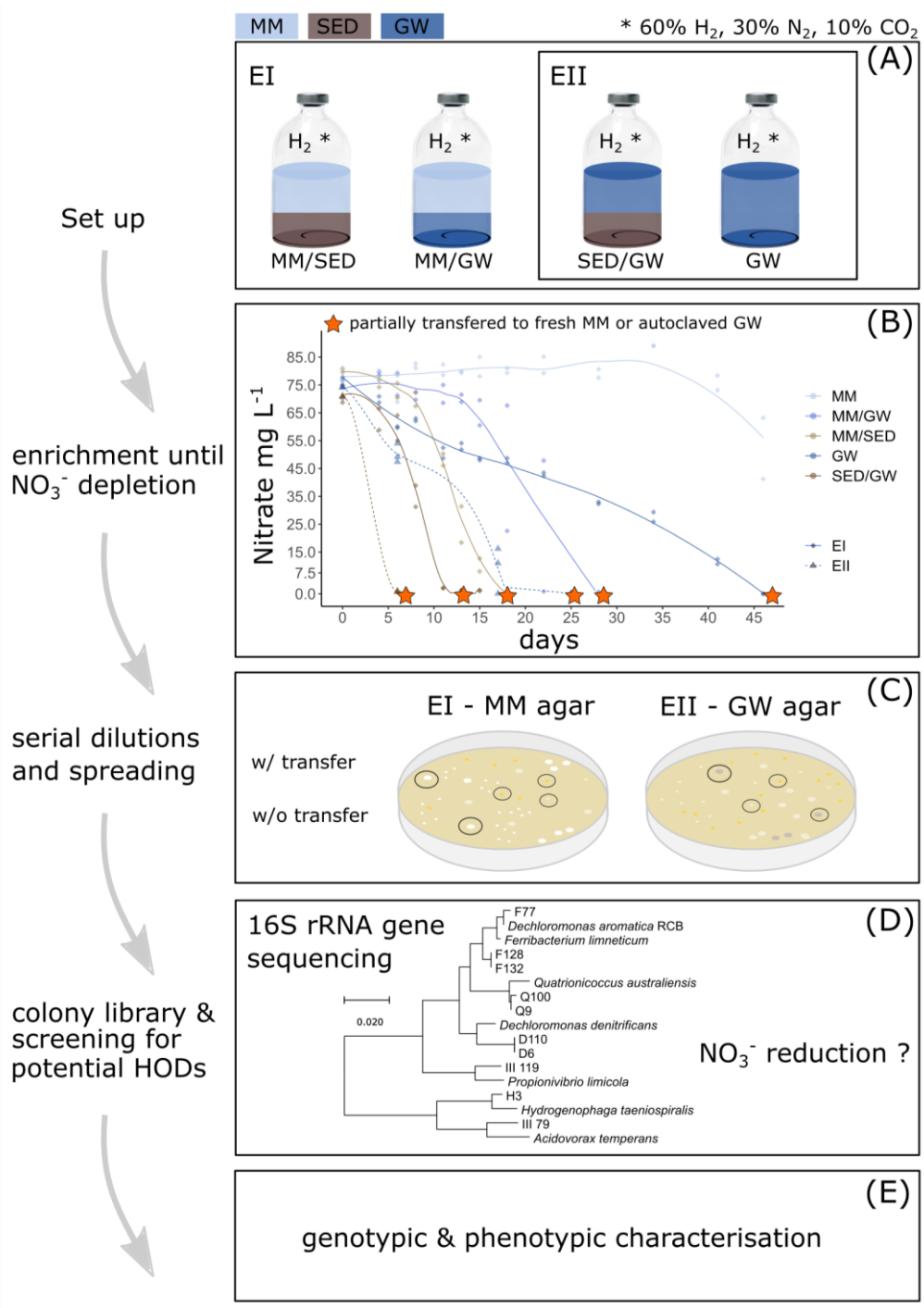

Figure S1: Schematic overview of the targeted isolation of hydrogenotrophic denitrifiers from groundwater and sediment material obtained from a nitrate polluted oxic aquifer. (A) The first isolation (EI) included enrichment setups containing mineral medium inoculated with sediment (MM/SED) or groundwater (MM/GW), as well as solely groundwater (GW), and a mix of sediment and groundwater (SED/GW). The second isolation (EII) contained only GW and SED/GW enrichments. (B) Once the initial 75 mg L^{-1} nitrate had been reduced, (C) serial dilutions of the enrichments were plated onto MM or GW agar plates. For each enrichment set up one replicate was transferred to fresh MM or autoclaved GW and again serial dilutions were plated respectively once the nitrate had been reduced. Colonies (of various morphologies) were picked and conserved within a colony library. (D) The colonies were screened via full length 16S rRNA gene Sanger Sequencing and the taxonomy was provisionally assigned by nblast. Isolates belonging to the families *Rhodocylaceae* and *Burkholderiaceae* were further classified in their phylogenetic relationship by generating maximum-likelihood phylogenetic trees. Differing isolates were screened for their ability to reduce nitrate. Finally, a selection of 11 isolates, including potential hydrogenotrophic denitrifiers and some close relatives, were characterised for their denitrification genotype and phenotype.

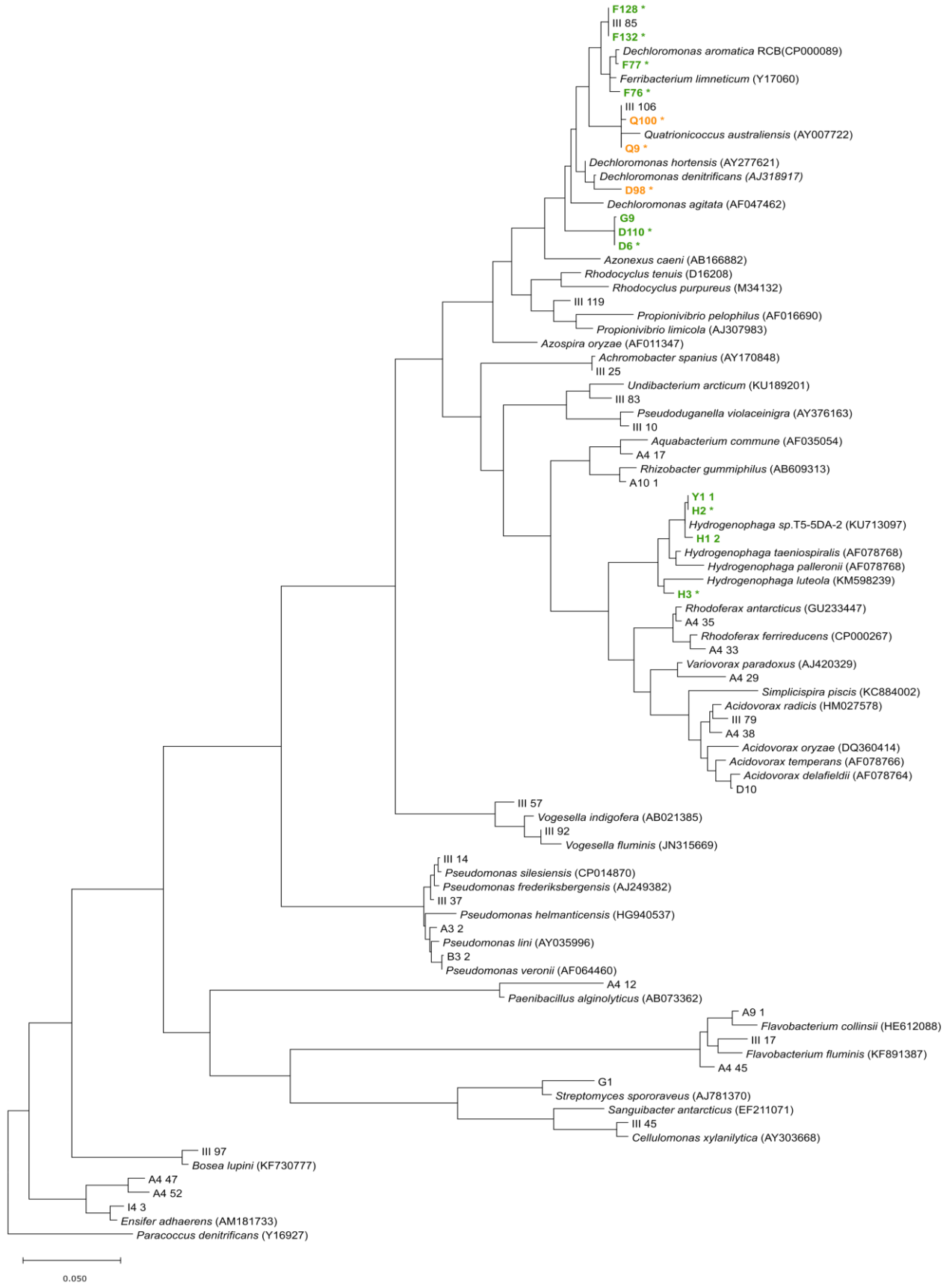

Figure S2: Maximum-likelihood phylogenetic tree based on the full 16S rRNA gene sequences of obtained isolates, as well as 16S rRNA gene sequences of related taxa downloaded from the LTP SILVA database (Quast *et al.*, 2012). The isolates included in the tree were tested for their ability to reduce nitrate with H_2 as the sole electron donor. Isolates which were able to reduce at least 50 % of the initial nitrate within 5 days are marked in green. Of those a selection (marked with an asterisk) was further phenotypically and genotypically characterised. The isolates marked in orange with an asterisk were characterised alongside to elucidate genetic traits which hinder these close relatives to denitrify with H_2.

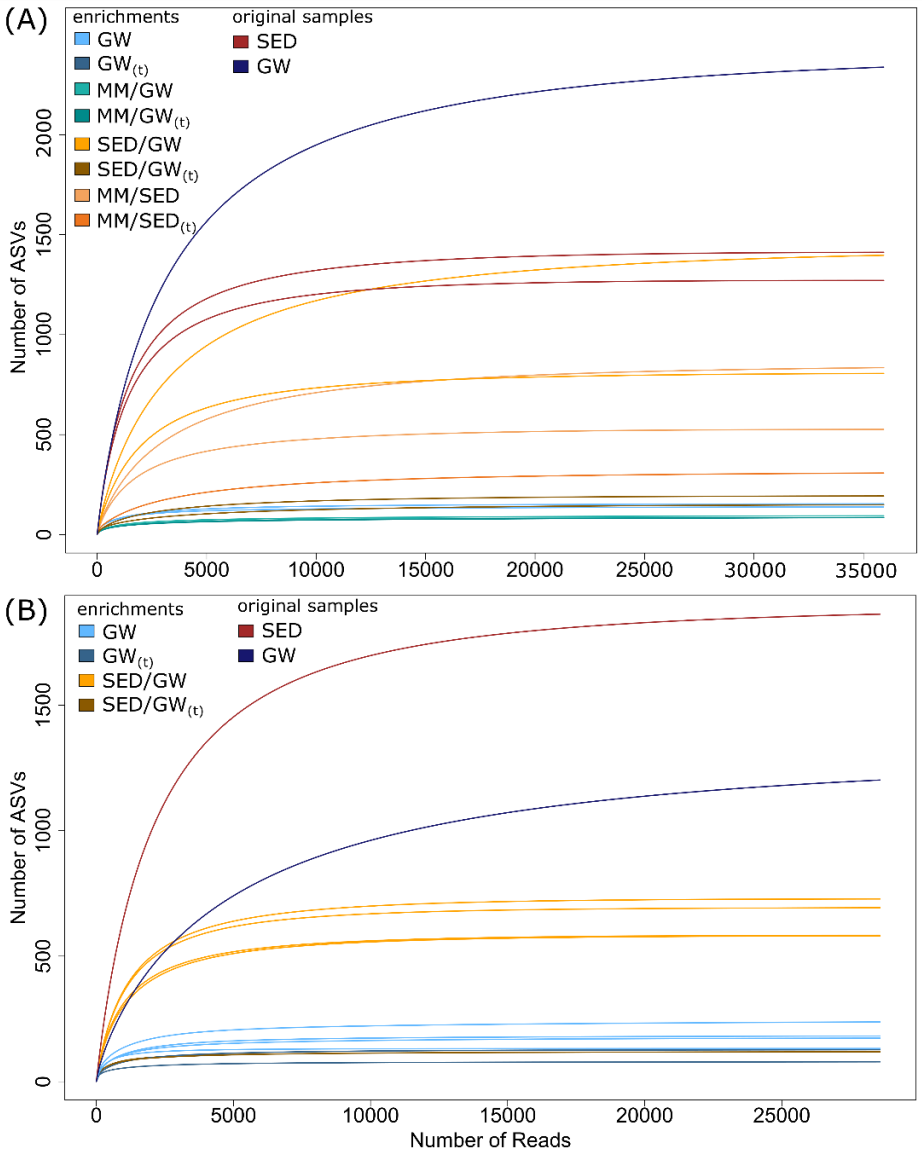

Figure S3: Rarefaction curves of the enrichments of (A) EI and (B) EII.

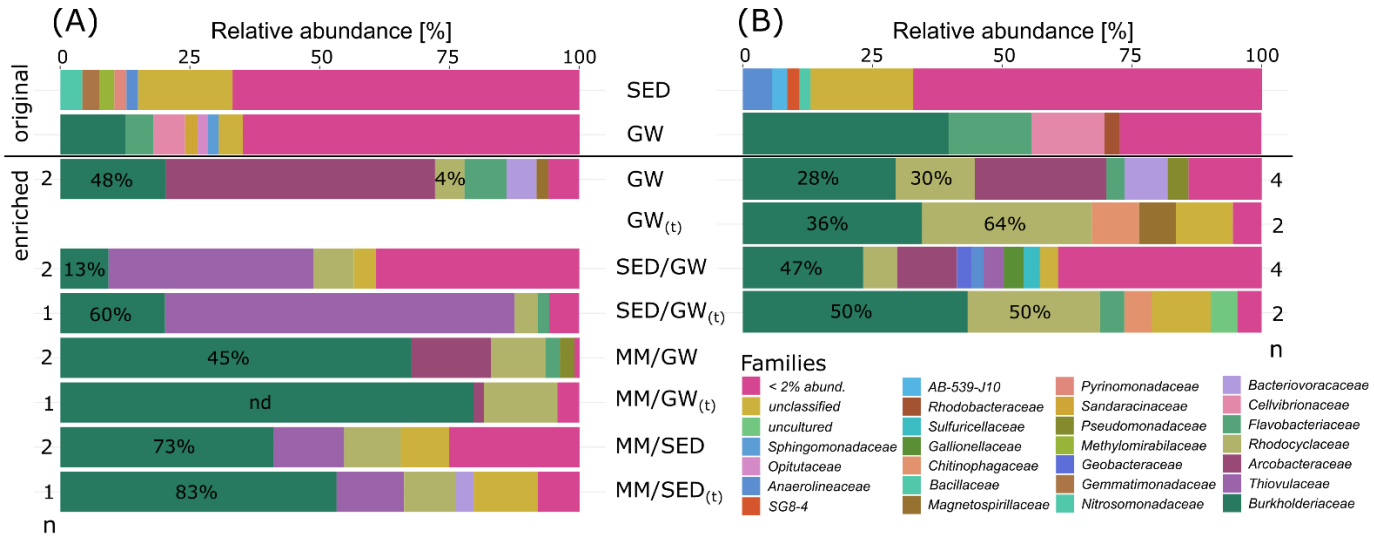

Figure S4: Relative abundances of the families detected in the original sediment (SED) and groundwater (GW) samples (top), as well as in the anoxic enrichments with H_2 atmosphere (bottom) of the isolations (A) EI and (B) EII based on 16S rRNA gene amplicon sequencing. Samples were taken before dilution plating. The relative abundances are the mean of n number of replicates, which are specified on the edges of the graphs. The percentage on the stacked bar plot segments of *Rhodocyclaceae* and *Burkholderiaceae* show the percentage of screened colonies belonging to the respective family according to 16S rRNA gene Sanger Sequencing.

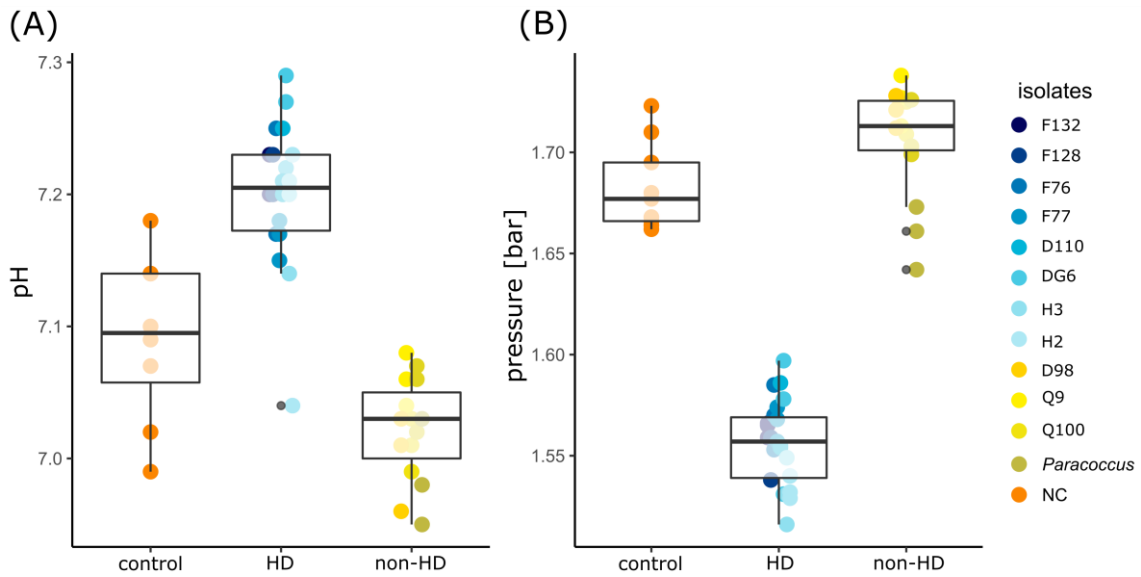

Figure S5: Boxplots showing the difference in (A) pH and (B) gas pressure at the endpoint measurement between the control incubations without inoculum, the hydrogenotrophic denitrifier (HD) incubations and the incubations of other isolates which did not perform hydrogenotrophic denitrification (non-HD). Pairwise comparison indicated that the HD incubations had a significantly higher pH and lower pressure compared to nonHOD and control incubations (lincon, both p = < 0.009). The control incubations also differed significantly from the nonHOD incubations, as their pressure was significantly higher (lincon, p = < 0.005).

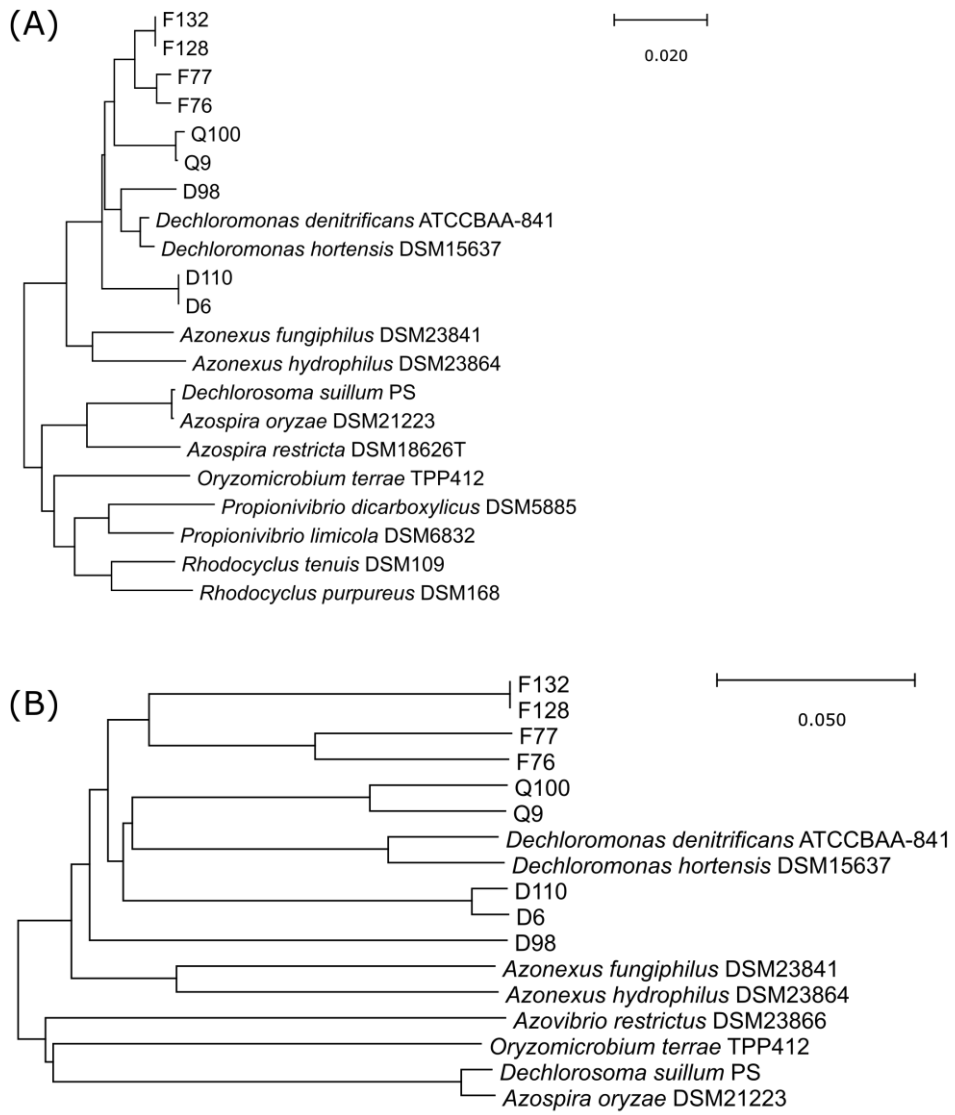

Figure S6: (A) 16S rRNA gene-based and (B) whole genome sequence-based phylogenetic trees of the *Rhodocyclaceae* isolates and related type strains generated by TyGS (Meier-Kolthoff & Göker, 2019) using default parameters.

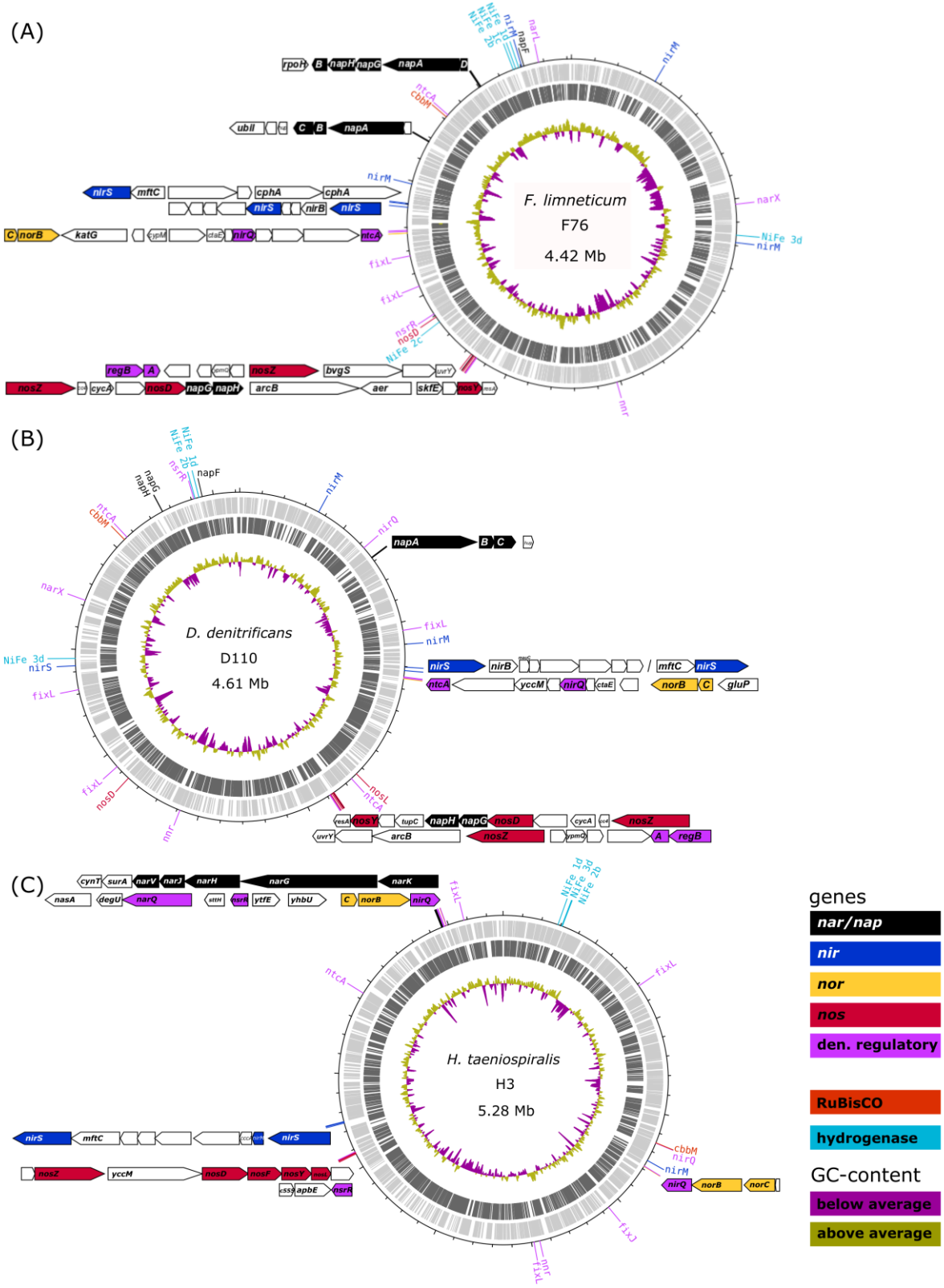

Figure S7: Location of the denitrification genes (nar/nap, nir, nor, nos), denitrification regulatory genes (fixL/fixJ, ntcA, nnr, regB/regA, narX, narL, narQ, nirQ, norR, nsrR), Rubisco gene (cbbM), and hydrogenase genes (NiFe groups 1d, 1c, 2b, 2c, 3d) within the genomes of the sub-selected hydrogenotrophic denitrifiers (A) *F. limneticum* ($F76_{(HD)}$), (B) *D. denitrificans* ($D110_{(HD)}$), and (C) *H. taeniospiralis* ($H3_{(HD)}$). The gene neighbourhood is shown when the above-mentioned genes are in proximity. The light grey outer track shows the genes of the forward strand while the dark grey track shows the genes of the reverse strand. The G+C content across the genome is depicted in the innermost track.

Table S1: Quality control statistics output from Qiime2 for the amplicon sequencing of the enrichments and the original sediment and groundwater samples. It shows the loss of reads of each sample after filtering, denoising, merging of reads, and removal of chimeric reads.

			# of reads					
	sample	type	input	filtered	denoised	merged	non-chimeric	% left after denoising
EI	MM/GW	enriched	170255	151212	151212	142455	134660	79.09
	MM/GW	enriched	138705	123494	123494	118211	105240	75.87
	MM/SED	enriched	137877	118198	118198	95530	87304	63.32
	MM/SED	enriched	98845	74359	74359	53325	51494	52.10
	SED/GW	enriched	134682	94998	94998	58979	56320	41.82
	SED/GW	enriched	157371	134843	134843	106938	97031	61.66
	GW	enriched	89561	80846	80846	77994	66018	73.71
	GW	enriched	127088	114780	114780	109994	97635	76.82
	MM/GW(t)	enriched	202571	172758	172758	155301	147651	72.89
	MM/SED(t)	enriched	105045	91084	91084	80516	73017	69.51
	SED/GW(t)	enriched	58098	52252	52252	48147	46547	80.12
	SED/GW(t)	enriched	89771	81286	81286	77339	70710	78.77
	SED	original	87330	75287	75287	50866	49049	56.17
	SED	original	85283	74452	74452	52490	49344	57.86
	GW	original	209333	176600	176600	116681	91042	43.49
	MM	control	1480	1286	1286	1189	953	64.39
	MM	control	9968	8728	8728	8585	6631	66.52
	NE	control	41177	36030	36030	35142	27055	65.70
	PCR NTC	control	287	216	216	177	177	61.67
EII	SED/GW	enriched	108213	95561	89202	76481	72109	66.64
	SED/GW	enriched	118032	105331	99278	87448	81326	68.9
	SED/GW	enriched	95833	84749	79330	68774	64662	67.47
	SED/GW	enriched	110182	98545	92980	81652	77580	70.41
	GW	enriched	123390	112748	112009	109281	101247	82.05
	GW	enriched	107896	94195	92730	87559	67360	62.43
	GW	enriched	114244	103811	102881	99386	91130	79.77
	GW	enriched	95434	86496	85745	82477	74390	77.95
	SED/GW(t)	enriched	96464	86814	86004	83358	67142	69.6
	SED/GW(t)	enriched	95072	85809	85530	84483	80467	84.64
	GW(t)	enriched	133782	118672	117705	113039	89926	67.22
	GW(t)	enriched	116211	102489	102052	99006	83886	72.18
	SED	original	178713	155496	140567	102656	93877	52.53
	GW	original	201093	180141	169979	147851	111421	55.41
	NE	control	2135	1370	1327	1200	1159	54.29
	PCR NTC	control	14827	13324	13256	12646	12265	82.72

Table S2: For each colony PCR one colony was added to the PCR reaction mixture and the PCR was run under the described conditions. Further, the amplified DNA was purified using the Nucleo-Spin Gel and PCR Clean-up Kit (Macherey-Nagel, Germany), and Sanger sequenced with the BigDye Terminator v3.1 sequencing chemistry on an ABI 3730 capillary sequencers (Thermo Fisher, USA). The sequencing chromatograms were manually checked, and the merged forward and reverse reads were taxonomically assigned by aligning the sequences against the rRNA/ITS databases of the nucleotide Basic Local Alignment Search Tool (nblast) (NCBI: https://blast.ncbi.nlm.nih.gov/Blast.cgi, version 2.10.0). Additionally, maximum-likelihood phylogenetic trees were generated with MEGA-X (Kumar et al., 2018) using the default settings to differentiate the phylogeny of the obtained isolates.

PCR reaction mixture	Cycling conditions
1X PCR buffer	1x 94 °C 10 min.
0.2 mM dNTPs	94 °C 1 min.
1.5 mM MgCl2	30x 56 °C 1 min.
2 mg/mL BSA	72 °C 1.5 min.
0.2 µM 27f forward primer	1x 72 °C 5 min.
0.2 µM 1492r reverse primer	
3 U Taq DNA polymerase	
1 colony	
50 µL total volume	

Table S3: Percentage of reduced NO_3^- within five days by 45 selected isolates growing in mineral medium with an anoxic H_2/CO_2 atmosphere. The 11 isolates selected for detailed phenotypic and genotypic analysis are marked in grey and an abbreviation is given.

isolation	setup	ID	abbreviation	family (GTDB Taxonomy)	nblast hit	% NO_3 reduced
EI	GW	G6	$D6_{(HD)}$	*Rhodocyclaceae*	*Dechloromonas denitrificans*	99.3
EEII	GW	III 110	$D110_{(HD)}$	*Rhodocyclaceae*	*Dechloromonas denitrificans*	99.2
EEII	GW	III 77	$F77_{(HD)}$	*Rhodocyclaceae*	*Ferribacterium limneticum*	99.2
EEII	GW	III 76	$F76_{(HD)}$	*Rhodocyclaceae*	*Ferribacterium limneticum*	88.3
EI	MM/SED	LT3	$H3_{(HD)}$	*Burkholderiaceae*	*Hydrogenophaga taeniosoiralis*	80.6
EI	MM/SED	Y1.1		*Burkholderiaceae*	*Hydrogenophaga sp. T5-5DA-2*	75.8
EI	MM/SED	LT2	$H2_{(HD)}$	*Burkholderiaceae*	*Hydrogenophaga taeniosoiralis*	74
EI	MM/GW	H1.2		*Burkholderiaceae*	*Hydrogenophaga taeniosoiralis*	72.5
EEII	$GW_{(t)}$	III 128	$F128_{(HD)}$	*Rhodocyclaceae*	*Ferribacterium limneticum*	35.9
EEII	$GW_{(t)}$	III 132	$F132_{(HD)}$	*Rhodocyclaceae*	*Ferribacterium limneticum*	35.3
EEII	GW	III 85		*Rhodocyclaceae*	*Ferribacterium limneticum*	26.7
EEII	GW	III 97		*Beijerinckiaceae*	*Bosea lupini*	19.3
EI	MM/GW	B3.2		*Pseudomonadaceae*	*Pseudomonas veronii*	19.3
EEII	GW	III 106		*Rhodocyclaceae*	*Quatrionicoccus australiensis*	17.4
EEII	GW	III 92		*Chromobacteriaceae*	*Vogesella fluminis*	14.9
EEII	GW	III 79		*Burkholderiaceae*	*Acidovorax radicis*	13.1
EI	$MM/SED_{(t)}$	A4 38		*Burkholderiaceae*	*Acidovorax defluvii*	12.8
EEII	GW	III 83		*Burkholderiaceae*	*Undibacterium arcticum*	12.5
EEII	SED/GW	III 30		*Cellulomonadaceae*	*Cellulomonas soli*	10.6
EEII	SED	III 45		*Cellulomonadaceae*	*Cellulomonas xylanilytica*	10.6
EI	SED/GW	A10.1		*Burkholderiaceae*	*Rhizobacter gummiphilus*	9.8
EI	$SED/GW_{(t)}$	A4.29		*Burkholderiaceae*	*Variovorax paradoxus*	8.9
EEII	GW	III 57		*Chromobacteriaceae*	*Vogesella indigofera*	8.8
EI	GW	A4.47		*Rhizobiaceae*	*Rhizobium selenitreducens*	8.3
EEII	SED/GW	III 25		*Burkholderiaceae*	*Achromobacter spanius*	8.2
EEII	SED/GW	III 17		*Flavobacteriaceae*	*Flavobacterium fluminis*	7.6
EEII	SED/GW	III 14		*Pseudomonadaceae*	*Pseudomonas silesiensis*	6.9
EEII	$SED/GW_{(t)}$	III 119		*Rhodocyclaceae*	*Propionivibrio militaris*	6.9
EI	MM/SED	A3.2		*Pseudomonadaceae*	*Pseudomonas lini*	6.5
EI	SED/GW	G1		*Streptomycetaceae*	*Streptomyces spororaveus*	5.7
EI	$MM/SED_{(t)}$	C6.1		*Burkholderiaceae*	*Uncultured Comamonadaceae*	5.5
EEII	SED/GW	III 10		*Burkholderiaceae*	*Pseudoduganella violaceinigra*	5.1
EI	$SED/GW_{(t)}$	I4.3		*Rhizobiaceae*	*Ensifer adhaerens strain NBRC 100388*	4.6
EI	$MM/SED_{(t)}$	A4.35		*Burkholderiaceae*	*Rhodoferax antarcticus*	4
EI	SED/GW	A9.1		*Flavobacteriaceae*	*Flavobacterium collinsii*	3.8
EEII	SED/GW	III 37		*Pseudomonadaceae*	*Pseudomonas frederiksbergensis*	3.2
EI	GW	A4.52		*Rhizobiaceae*	*Agrobacterium rubi*	2.2
EI	GW	D10		*Burkholderiaceae*	*Acidovorax delafieldii*	1.6
EI	MM/SED	A4 17		*Burkholderiaceae*	*Aquabacterium commune*	1.3
EI	SED/GW	A4.12		*Paenibacillaceae*	*Paenibacillus alginolyticus*	0.3
EEII	GW	III 100	Q100	*Rhodocyclaceae*	*Quatrionicoccus australiensis*	0.2
EEII	GW	III 98	D98	*Rhodocyclaceae*	*Dechloromonas denitrificans*	0
EI	$MM/SED_{(t)}$	A4.33		*Burkholderiaceae*	*Rhodoferax ferrireducens*	0
EI	GW	A4.45		*Flavobacteriaceae*	*Flavobacterium succinicans*	0
EI	GW	D9	Q9	*Rhodocyclaceae*	*Quatrionicoccus australiensis*	0

Table S4: Enrichment setups from the first (EI) and second (EII) isolation. The serial dilutions of EI enrichments were plated onto mineral medium agar plates and the serial dilutions of EII enrichments were plated onto agar plates prepared from 1/10 mineral medium (10 % of the original salts, trace elements, and vitamins) and from filtered (0.2 µm) and autoclaved groundwater (GW*). The plates were all prepared with 1.5 % (w/v) purified agar.

enrichment	set up	replicates	GW [ml]	SED [ml]	MM [ml]	agar plates
EI	GW	2	80	-	-	MM
	SED/GW	2	85	15	-	
	MM/GW	2	8	-	72	
	MM/SED	2	-	8	72	
EII	GW	4	100	-	-	GW*,
	SED/GW	4	85	15	-	1/10 MM

Table S5: SMRT® link software (PacBio, USA) assembly parameters and polished assembly results of the isolates sequenced with the PacBio single-molecule real-time technology.

	SMRT Link assembly parameters			Polished Assembly			
ID	seed coverage	application	expected genome size [Mb]	# of contigs	max contig length [bp]	mean coverage	plasmid length [bp]
F132$_{(HD)}$	30	HGAP4	4.5	1	4215942	320	
F128$_{(HD)}$	30	HGAP4	4.5	1	4215797	580	
F76$_{(HD)}$	30	HGAP4	4.5	1	4419139	259	
F77$_{(HD)}$	30	HGAP4	4.5	1	4150051	712	
D6$_{(HD)}$	30	HGAP4	4.24	1	4580459	233	
D110$_{(HD)}$	30	HGAP4	4.24	1	4619273	511	
H3$_{(HD)}$	30	HGAP4	5.28	3	5275671	206	5700, 2750
H2$_{(HD)}$	30	HGAP4	5.28	1	5668326	311	
Q100	30	HGAP4	4.2	2	4168471	363	145710
Q9	30	HGAP4	4.24	1	4171110	276	
D98	30	HGAP4	4.24	1	3457400	591	

Table S6: Number of circularized contigs determined with the Circlator software (Hunt *et al.*, 2015) and the completeness, contamination, GC-content, as well as the genome size calculated by the CheckM software (Parks *et al.*, 2015) are stated.

	Circlator	CheckM			
ID	circularized contigs	Completeness [%]	Contamination [%]	GC-content	Genome size [Mb]
F132$_{(HD)}$	(1/1)	99.61	0.50	0.60	4.22
F128$_{(HD)}$	(1/1)	99.61	0.50	0.60	4.22
F76$_{(HD)}$	(1/1)	99.21	0.03	0.60	4.42
F77$_{(HD)}$	(1/1)	98.74	0.34	0.60	4.15
D6$_{(HD)}$	(1/1)	99.61	0.43	0.62	4.58
D110$_{(HD)}$	(1/1)	99.84	0.36	0.62	4.62
H3$_{(HD)}$	(1/3)	99.61	0.93	0.67	5.28
H2$_{(HD)}$	(1/1)	99.61	0.56	0.65	5.67
Q100	(2/2)	99.37	0.19	0.61	4.31
Q9	(1/1)	99.84	0.19	0.61	4.17
D98	(1/1)	99.84	0.05	0.59	3.46

Table S7: Preferred carbon medium and maximum OD_{600} reached during aerobic growth by the 11 selected isolates.

ID	preferred carbon medium	max OD_{600} reached during aerobic growth
F132(HD)	R2A	0.219
F128(HD)	R2A	0.172
F76(HD)	R2A	0.14
F77(HD)	no aerobic growth in carbon medium	
D6(HD)	R2A	0.216
D110(HD)	R2A	0.168
H3(HD)	20 % TSB	1.554
H2(HD)	20 % TSB	0.63
Q100	R2A	0.449
Q9	R2A	0.221
D98	R2A	0.124

Table S8: Closest known relatives of the 11 sequenced isolates determined with the Type Strain Genome Server (Meier-Kolthoff & Göker, 2019) based on the 16S rRNA gene (bold). The whole-genome sequence-based comparison shows the computed digital DNA-DNA-hybridization and G+C content difference among the 11 isolates and compared to whole-genome sequenced relatives. However, the taxonomy could not be determined based on the whole-genome sequence for neither of the sequenced isolates because all whole-genome sequenced relatives were too distant.

16S rRNA gene-based			Whole genome sequence-based				
Query strain	Subject strain	identity [%]	Query strain	Subject strain	dDDH [%]	CI [%]	G+C content difference [%]
F132(HD)	***F. limneticum*** (Y17060)	98.95	F132(HD)	*D. hortensis* DSM 15637	32.1	(28.7 - 35.7)	1.57
F132(HD)	F128(HD)	100	F132(HD)	F128(HD)	100	(100 - 100)	0
F128(HD)	***F. limneticum*** (Y17060)	98.95	F128(HD)	*D. hortensis* DSM 15637	32.1	(28.7 - 35.7)	1.57
F76(HD)	***F. limneticum*** (Y17060)	99.15	F76(HD)	*D. denitrificans* ATCC BAA-841	31.9	(28.6 - 35.5)	1.76
F76(HD)	F77(HD)	99.41	F76(HD)	F77(HD)	60.8	(57.1 - 64.4)	0.2
F77(HD)	***F. limneticum*** (Y17060)	99.21	F77(HD)	*D. hortensis* DSM 15637	32.8	(29.4 - 36.4)	1.28
D6(HD)	***D. denitrificans*** (AJ318917)	97.77	D6(HD)	*D. denitrificans* ATCC BAA-841	34.7	(31.3 - 38.2)	0.02
D6(HD)	D110(HD)	100	D6(HD)	D110(HD)	89.2	(85.9 - 91.9)	0.12
D110(HD)	***D. denitrificans*** (AJ318917)	97.77	D110(HD)	*D. denitrificans* ATCC BAA-841	34.7	(31.4 - 38.3)	0.1
H3(HD)	***H. taeniospiralis*** (AF078768)	99.67	H3(HD)	*H. taeniospiralis* NBRC 102512	71.6	(67.6 - 75.2)	0.12
H2(HD)	H3(HD)	99.01	H2(HD)	H3(HD)	37.8	(34.4 - 41.3)	1.62
H2(HD)	***H. taeniospiralis*** (AF078768)	99.34	H2(HD)	*H. taeniospiralis* NBRC 102512	37.5	(34.2 - 41.0)	1.5
Q100	***Q. australiensis*** (AY007722)	98.91	Q100	*D. denitrificans* ATCC BAA-841	34.8	(31.4 - 38.3)	0.28
Q100	Q9	99.8	Q100	Q9	65.4	(61.6 - 69.0)	0.18
Q9	***Q. australiensis*** (AY007722)	99.12	Q9	*D. denitrificans* ATCC BAA-841	34.6	(31.2 - 38.2)	0.46
D98	***D. denitrificans*** (AJ318917)	98.62	D98	*D. denitrificans* ATCC BAA-841	31.6	(28.3 - 35.2)	3.04
D98	F132	97.9	D98	Q9	30	(26.6 - 33.6)	2.58

Table S9: Pairwise comparison (lincon test) between the three isolates of each denitrification phenotype (DP) characteristic determined for the three kinetics experiments where significant differences occurred according to the one-way analysis of variance (Table S8). P-values < 0.05 are considered significant (marked with an *).

experiment	DP characteristics	isolate1		isolate2	CI (lower)	CI (upper)	p-value
Autotrophic transition	max. NO_2 (% of initial NO_3)	$D110_{(HD)}$	vs.	$F76_{(HD)}$	4.96	33.78	**0.0135***
		$D110_{(HD)}$	vs.	$H3_{(HD)}$	-126.28	-35.23	**0.0124***
		$F76_{(HD)}$	vs.	$H3_{(HD)}$	-150.26	-49.99	**0.0124***
	O_2 [µM] --> NO	$D110_{(HD)}$	vs.	$F76_{(HD)}$	-3.54	4.90	0.5956
		$D110_{(HD)}$	vs.	$H3_{(HD)}$	3.20	12.39	**0.0127***
		$F76_{(HD)}$	vs.	$H3_{(HD)}$	3.45	10.78	**0.0127***
	μ_{anoxic}	$D110_{(HD)}$	vs.	$F76_{(HD)}$	-0.07	0.05	0.6473
		$D110_{(HD)}$	vs.	$H3_{(HD)}$	-0.00	0.12	**0.0448 ***
		$F76_{(HD)}$	vs.	$H3_{(HD)}$	0.023	0.11	**0.0155 ***
	μ_{anoxic}/μ_{oxic}	$D110_{(HD)}$	vs.	$F76_{(HD)}$	-0.63	0.23	0.1678
		$D110_{(HD)}$	vs.	$H3_{(HD)}$	0.03	0.93	**0.0343***
		$F76_{(HD)}$	vs.	$H3_{(HD)}$	0.34	1.02	**0.0121***
Heterotrophic transition	max. NO_2 (% of initial NO_3)	$D110_{(HD)}$	vs.	$F76_{(HD)}$	3.96	9.29	**0.0023***
		$D110_{(HD)}$	vs.	$H3_{(HD)}$	-30.05	-9.82	**0.0049***
		$F76_{(HD)}$	vs.	$H3_{(HD)}$	-36.46	-16.67	**0.0045***
	max. NO [nM]	$D110_{(HD)}$	vs.	$F76_{(HD)}$	-11.99	8.53	0.5234
		$D110_{(HD)}$	vs.	$H3_{(HD)}$	-17.27	-9.63	**0.0004***
		$F76_{(HD)}$	vs.	$H3_{(HD)}$	-21.38	-2.06	**0.0212***
	max. N_2O-N (% of initial NO_3)	$D110_{(HD)}$	vs.	$F76_{(HD)}$	-4.19	2.09	0.3255
		$D110_{(HD)}$	vs.	$H3_{(HD)}$	-35.58	-29.63	**0.0000***
		$F76_{(HD)}$	vs.	$H3_{(HD)}$	-34.07	-29.04	**0.0000***
	μ_{anoxic}	$D110_{(HD)}$	vs.	$F76_{(HD)}$	-0.03	0.29	**0.0389 ***
		$D110_{(HD)}$	vs.	$H3_{(HD)}$	0.05	0.43	**0.0389 ***
		$F76_{(HD)}$	vs.	$H3_{(HD)}$	0.00	0.22	**0.0389 ***
	μ_{anoxic}/μ_{oxic}	$D110_{(HD)}$	vs.	$F76_{(HD)}$	0.05	0.36	**0.0264***
		$D110_{(HD)}$	vs.	$H3_{(HD)}$	-0.04	0.69	0.0561
		$F76_{(HD)}$	vs.	$H3_{(HD)}$	-0.20	0.44	0.2001

Table S10: One-way analysis of variance (t1way) of the denitrification phenotype characteristics between the three isolates ($F76_{(HD)}$, $D110_{(HD)}$, $H3_{(HD)}$) during each kinetics experiment. The p-values were adjusted for each experiment with a Benjamini & Hochberg ('BH') correction. Adjusted p-values < 0.05 are considered significant (marked with an *).

experiment	parameters	p-value	p-value (adj.)
Litho-autotrophic transition	max. NO_2 (% of initial NO_3^-)	0.0034	**0.0088 ***
	max. NO [nM]	0.2103	0.2366
	max. N_2O-N (% of initial NO_3^-)	0.5330	0.5643
	O_2 [µM] in liquid --> NO_2^-	0.0013	**0.0056 ***
	O_2 [µM] in liquid --> NO	0.0016	**0.0056 ***
	μ_{oxic}	0.7960	0.7960
	μ_{anoxic}	0.0066	**0.0141 ***
	μ_{anoxic}/μ_{oxic}	0.0019	**0.0056 ***
Adapted litho-autotrophic	max. NO_2 (% of initial NO_3)	0.0091	**0.0169 ***
	max. NO [nM]	0.1541	0.2003
	max. N_2O-N (% of initial NO_3)	0.5810	0.5810
Organo-heterotrophic transition	max. NO_2 (% of initial NO_3)	0.0006	**0.0026 ***
	max. NO [nM]	0.0003	**0.0017 ***
	max. N_2O-N (% of initial NO_3)	0.0000	**0.0000 ***
	O_2 [µM] in liquid --> NO_2^-	0.2081	0.2366
	O_2 [µM] in liquid --> NO	0.0381	0.0550
	μ_{oxic}	0.1218	0.1687
	μ_{anoxic}	0.0094	**0.0168 ***
	μ_{anoxic}/μ_{oxic}	0.0126	**0.0205 ***

Table S11: One-way analysis of variance (t1way) of the denitrification phenotype (DP) characteristics between the *Autotrophic transition* and *Adapted autotrophic*, as well as the *Autotrophic transition* and *Heterotrophic transition* kinetics experiments for each characterised isolate. The p-values were adjusted for each experimental comparison with a Benjamini & Hochberg ('BH') correction. Adjusted p-values < 0.05 are considered significant (marked with an *).

experiment	DP characteristics	isolate	p-value	p-value (adj.)
Litho-autotrophic transition vs. *Adapted litho-autotrophic*	max. NO_2 (% of initial NO_3)	$F76_{(HD)}$	0.0778	0.2198
		$D110_{(HD)}$	0.3390	0.3814
		$H3_{(HD)}$	0.0856	0.2198
	max. NO [nM]	$F76_{(HD)}$	0.0185	0.1661
		$D110_{(HD)}$	0.5908	0.5908
		$H3_{(HD)}$	0.1017	0.2198
	max. N_2O-N (% of initial NO_3)	$F76_{(HD)}$	0.1376	0.2198
		$D110_{(HD)}$	0.1910	0.2455
		$H3_{(HD)}$	0.1465	0.2198
Litho-autotrophic transition vs. *Organo-heterotrophic transition*	max. NO_2 (% of initial NO_3)	$F76_{(HD)}$	0.0315	0.0674
		$D110_{(HD)}$	0.0446	0.0836
		$H3_{(HD)}$	0.0096	**0.0289***
	max. NO [nM]	$F76_{(HD)}$	0.0093	**0.0289***
		$D110_{(HD)}$	0.0001	**0.0016***
		$H3_{(HD)}$	0.6546	0.6546
	max. N_2O-N (% of initial NO_3)	$F76_{(HD)}$	0.1774	0.2390
		$D110_{(HD)}$	0.1912	0.2390
		$H3_{(HD)}$	0.3782	0.4364
	O_2 [µM] in liquid --> NO_2^-	$F76_{(HD)}$	nd[a]	
		$D110_{(HD)}$	0.0024	**0.0274 ***
		$H3_{(HD)}$	0.1551	0.2230
	O_2 [µM] --> NO	$F76_{(HD)}$	0.0074	**0.0289***
		$D110_{(HD)}$	0.0051	**0.0289***
		$H3_{(HD)}$	0.1686	0.2390
	μ_{oxic}	$F76_{(HD)}$	0.0150	**0.0346 ***
		$D110_{(HD)}$	0.0104	**0.0343 ***
		$H3_{(HD)}$	0.4501	0.4930
	μ_{anoxic}	$F76_{(HD)}$	0.0753	0.1236
		$D110_{(HD)}$	0.0137	**0.0348 ***
		$H3_{(HD)}$	0.1399	0.2145
	μ_{anoxic}/μ_{oxic}	$F76_{(HD)}$	0.0150	**0.0374***
		$D110_{(HD)}$	0.6322	0.6546
		$H3_{(HD)}$	0.0652	0.1087

Table S12: Occurrence and copy number of genes involved in the regulation of denitrification which were annotated by prokka (Seemann, 2014) in the isolates' genomes. Hydrogenotrophic denitrifiers are marked with (HD). No clear pattern in denitrification regulatory genes differentiates the HD from the non-HD isolates.

	O_2 responsive regulator		global regulator		redox sensing		NO_3^-/NO_2^- sensing				NO sensing	
ID	*fixL*	*fixJ*	*ntcA*	*nnr*	*regA*	*regB*	*narX*	*narL*	*narQ*	*narP*	*norR*	*nsrR*
F132$_{(HD)}$	3	-	1	1	1	1	1	-	-	-	-	1
F128$_{(HD)}$	3	-	1	1	1	1	1	-	-	-	-	1
F76$_{(HD)}$	2	-	2	1	1	1	1	1	-	-	-	1
F77$_{(HD)}$	2	-	2	1	1	1	1	-	-	-	-	1
D6$_{(HD)}$	2	-	3	1	1	1	1	-	-	-	-	1
D110$_{(HD)}$	3	-	3	1	1	1	1	-	-	-	-	1
H3$_{(HD)}$	3	1	1	1	-	-	-	-	1	-	-	2
H2$_{(HD)}$	3	4	1	1	-	-	1	1	2	-	-	3
Q100	4	-	2	1	2	1	1	1	-	-	-	1
Q9	4	1	3	1	3	2	1	1	-	-	-	1
D98	3	-	1	1	1	1	1	-	-	-	-	-

References:

Hunt M, Silva ND, Otto TD, Parkhill J, Keane JA & Harris SR (2015) Circlator: automated circularization of genome assemblies using long sequencing reads. *Genome Biology* **16**: 294.

Kumar S, Stecher G, Li M, Knyaz C & Tamura K (2018) MEGA X: Molecular Evolutionary Genetics Analysis across Computing Platforms. *Mol Biol Evol* **35**: 1547-1549.

Meier-Kolthoff JP & Göker M (2019) TYGS is an automated high-throughput platform for state-of-the-art genome-based taxonomy. *Nature Communications* **10**: 2182.

Parks DH, Imelfort M, Skennerton CT, Hugenholtz P & Tyson GW (2015) CheckM: assessing the quality of microbial genomes recovered from isolates, single cells, and metagenomes. *Genome Res* **25**: 1043-1055.

Quast C, Pruesse E, Yilmaz P, Gerken J, Schweer T, Yarza P, Peplies J & Glöckner FO (2012) The SILVA ribosomal RNA gene database project: improved data processing and web-based tools. *Nucleic Acids Research* **41**: D590-D596.

Seemann T (2014) Prokka: rapid prokaryotic genome annotation. *Bioinformatics* **30**: 2068-2069.

SUPPLEMENTARY MATERIALS 2

Genotypic and Phenotypic Characterisation of Hydrogenotrophic Denitrifiers

Clara Duffner[1,2], Susanne Kublik[2], Bärbel Fösel[2], Åsa Frostegård[3], Michael Schloter[1,2], Lars Bakken[3], Stefanie Schulz[2]

[1] Chair of Soil Science, TUM School of Life Sciences Weihenstephan, Technical University of Munich, Freising, Germany, [2] Research Unit Comparative Microbiome Analysis, Helmholtz Centre Munich, Neuherberg, Germany, [3] Department of Chemistry, Biotechnology and Food Sciences, Norwegian University of Life Sciences, Ås, Norway.

***Corresponding author:** Phone: +49 89 3187 3054; E-Mail: stefanie.schulz@helmholtz-muenchen.de

One sentence summary: Isolation and characterisation, with a focus on intermediate accumulation during denitrification, of the complete hydrogenotrophic denitrifiers *Ferribacterium limneticum*, *Dechloromonas denitrificans*, and *Hydrogenophaga taeniospiralis*.

Keywords: genome sequencing, denitrification phenotype, denitrification reductases, Rubisco, hydrogenases

Detection and classification of denitrification reductase, hydrogenase, and Rubisco genes:

Denitrification reductase genes including the respective gene-specific domain listed in table S2-1, verified by a search against the conserved domain database (Lu *et al.*, 2020), were further considered. Also, clade I *nosZ* (domain accession PRK02888) could thereby be differentiated from clade II *nosZ* (domain accession TIGR04246). The *norB* annotated genes were differentiated by incorporating the annotated sequences in a maximum-likelihood phylogenetic tree (MEGA-X, Kumar *et al.* (2018)) with classified *cnorB* and *qnorB* sequences (Genbank AJ507329-AJ507380) from Braker & Tiedje (2003). The Rubisco genes were identified by Hidden Markov Model (HMM) search (HMMER 3.3, http://hmmer.org/) with the Pfam HMMs PF00016 (large subunit) and PF00101 (small subunit). The hits were verified and classified (form IA, IC, II) by determining their position within a maximum-likelihood tree (MEGA-X, Kumar *et al.* (2018)) generated with the amino acid sequences of the HMM hits and the Rubisco partial sequences from Alfreider *et al.* (2012) (GenBank JF414941–JF415078). For the detection and classification of hydrogenase genes, the [NiFe]-, [FeFe]-, and [Fe]-hydrogenase sequences, including information on the hydrogenase group and subgroup, utilized by Greening *et al.* (2015), were downloaded from NCBI. An HMM for each metal-centre type hydrogenase was built with HMMER 3.3 and used to search hydrogenase genes in the genomes of the isolates. Furthermore, the downloaded hydrogenase

sequences were reduced in quantity to generate maximum-likelihood trees (MEGA-X, Kumar *et al.* (2018)) including the HMM search hits from the isolates genomes. The gene sequences of the isolates which clustered with the known hydrogenase genes were seen as potential hydrogenases, and their position also indicated the group and subgroup they belong to. These results were verified by manual revision of the L1/L2 metal centre motifs specific to the respective hydrogenase group/subgroup shown in Table 2 of Greening *et al.* (2015).

Table S2-1: KEGG numbers and domain accessions of the denitrification reductase genes.

gene	KEGG	domain accession (CDD)
napA	K02567	PRK13532
narG	K00370	TIGR01580 or COG5013
nirS	K15864	pfam02239 or cl26549 & pfam13442 or COG2010
nirK	K00368	TIGR02376 (superfamily cl31204)
qnorB *cnorB*	K04561	cl00275
clade I *nosZ*	K00367	PRK02888
clade II *nosZ*		TIGR04246

Alfreider A, Schirmer M & Vogt C (2012) Diversity and expression of different forms of RubisCO genes in polluted groundwater under different redox conditions. *FEMS Microbiology Ecology* **79**: 649-660.
Braker G & Tiedje JM (2003) Nitric oxide reductase (norB) genes from pure cultures and environmental samples. *Appl Environ Microbiol* **69**: 3476-3483.
Greening C, Biswas A, Carere CR, Jackson CJ, Taylor MC, Stott MB, Cook GM & Morales SE (2015) Genomic and metagenomic surveys of hydrogenase distribution indicate H2 is a widely utilised energy source for microbial growth and survival. *The Isme Journal* **10**: 761.
Kumar S, Stecher G, Li M, Knyaz C & Tamura K (2018) MEGA X: Molecular Evolutionary Genetics Analysis across Computing Platforms. *Mol Biol Evol* **35**: 1547-1549.
Lu S, Wang J, Chitsaz F*, et al.* (2020) CDD/SPARCLE: the conserved domain database in 2020. *Nucleic acids research* **48**: D265-D268.

Publication III

frontiers in Microbiology

PERSPECTIVE
published: 04 March 2021
doi: 10.3389/fmicb.2021.610437

Strategies to Overcome Intermediate Accumulation During *in situ* Nitrate Remediation in Groundwater by Hydrogenotrophic Denitrification

Clara Duffner[1,2], Anja Wunderlich[3], Michael Schloter[1,2], Stefanie Schulz[2] and Florian Einsiedl[3]**

[1] Chair of Soil Science, TUM School of Life Sciences Weihenstephan, Technical University of Munich, Freising, Germany, [2] Research Unit Comparative Microbiome Analysis, Helmholtz Center Munich, Neuherberg, Germany, [3] Chair of Hydrogeology, TUM Department of Civil, Geo and Environmental Engineering, Technical University of Munich, Munich, Germany

Bioremediation of polluted groundwater is one of the most difficult actions in environmental science. Nonetheless, the clean-up of nitrate polluted groundwater may become increasingly important as nitrate concentrations frequently exceed the EU drinking water limit of 50 mg L^{-1}, largely due to intensification of agriculture and food production. Denitrifiers are natural catalysts that can reduce increasing nitrogen loading of aquatic ecosystems. Porous aquifers with high nitrate loading are largely electron donor limited and additionally, high dissolved oxygen concentrations are known to reduce the efficiency of denitrification. Therefore, denitrification lag times (time prior to commencement of microbial nitrate reduction) up to decades were determined for such groundwater systems. The stimulation of autotrophic denitrifiers by the injection of hydrogen into nitrate polluted regional groundwater systems may represent a promising remediation strategy for such environments. However, besides high costs other drawbacks, such as the transient or lasting accumulation of the cytotoxic intermediate nitrite or the formation of the potent greenhouse gas nitrous oxide, have been described. In this article, we detect causes of incomplete denitrification, which include environmental factors and physiological characteristics of the underlying bacteria and provide possible mitigation approaches.

Keywords: nitrate pollution, hydrogen-oxidizing denitrification, nitrite accumulation, bioremediation, abiotic nitrite reduction

OPEN ACCESS

Edited by:
Hyung-Sool Lee,
University of Waterloo, Canada

Reviewed by:
Daniele Cecconet,
University of Pavia, Italy
Haihan Zhang,
Xi'an University of Architecture and Technology, China

***Correspondence:**
Florian Einsiedl
f.einsiedl@tum.de
Michael Schloter
schloter@helmholtz-muenchen.de

Specialty section:
This article was submitted to Microbiotechnology, a section of the journal Frontiers in Microbiology

Received: *02 November 2020*
Accepted: *15 February 2021*
Published: *04 March 2021*

Citation:
Duffner C, Wunderlich A, Schloter M, Schulz S and Einsiedl F (2021) Strategies to Overcome Intermediate Accumulation During in situ Nitrate Remediation in Groundwater by Hydrogenotrophic Denitrification. Front. Microbiol. 12:610437. doi: 10.3389/fmicb.2021.610437

INTRODUCTION

Increased amounts of reactive nitrogen (Nr) and severe anthropogenic intervention in the global nitrogen cycle induce climatic change, cause biodiversity losses, and pose direct and indirect risks to human health (Fields, 2004; Galloway et al., 2008). In groundwater, the main Nr species is dissolved nitrate (NO_3^-) which leaches into the groundwater due to excessive use of chemical and organic fertilizers as well as leaking sewage (Zhu et al., 2019; Wild et al., 2020). The resulting NO_3^- pollution of groundwater has been a severe global environmental problem since the 1970s (Rivett et al., 2008). Because groundwater infiltrates into rivers, lakes, and subsequently into coastal areas these ecosystems suffer from Nr-based eutrophication leading to toxic algal blooms and consequently

anoxic "dead-zones" (Fields, 2004; Galloway et al., 2008) when natural attenuation processes fall short. A prominent example for coastal eutrophication is the Baltic Sea (Murray et al., 2019). The effect of eutrophication on urban lakes is also severe, as total-N and NO_3^--N are one of the primary factors determining the algal community composition (Zhang et al., 2021). Additionally, in many regions where groundwater is used as a drinking water resource, NO_3^- concentrations above the WHO recommended maximum of 50 mg L^{-1} require costly *ex situ* methods of NO_3^- removal (Karanasios et al., 2010) or blending with less polluted water to ensure drinking water quality.

Denitrification, includes four main redox reactions from NO_3^- (redox state + V), via nitrite (NO_2^-), nitric oxide (NO), and nitrous oxide (N_2O) to atmospheric nitrogen (N_2, redox state 0), each catalyzed by a different metalloenzyme (Bothe et al., 2007). Since the first reduction step from NO_3^- to NO_2^- is also performed in other metabolic pathways and gaseous N_2O gas can already leave the ecosystem, in a strict sense denitrification includes only NO_2^- and NO respiration (Zumft, 1997). Nonetheless, because NO_3^- remediation aims at safely removing nitrogen from highly polluted aquatic systems, without releasing the greenhouse gas N_2O, in this work complete denitrification signifies the reduction of NO_3^- to N_2. Only when the oxygen (O_2) concentration falls below $\sim$ 0.08–0.256 mg L^{-1} (Lycus et al., 2017) denitrification becomes energetically favorable and is initiated through precisely coordinated regulation. An exception are aerobic denitrifiers which may utilize O_2 and NO_3^- simultaneously as electron acceptors, likely favorable in environments with fluctuating O_2 concentrations and sufficient reduced carbon (Ji et al., 2015). Denitrification is known to occur in groundwater bodies (Korom, 1992). However, in some aquifers, none, or only little microbial available electron donors are present resulting in high dissolved O_2 concentrations. Under these conditions, the intrinsic capacity for denitrification is low, whereby it will take years to decades (denitrification lag times) until the O_2 is depleted and biotic NO_3^- reduction commences (Wassenaar, 1995; Wild et al., 2018).

Creating conditions favoring denitrification and supplementation with an electron donor presents a strategy for small-scale *in situ* NO_3^- remediation (**Figure 1**). Hydrogen (H_2) was proven to be a promising electron donor in multiple NO_3^- removal applications (Liessens et al., 1992; Chaplin et al., 2009; Karanasios et al., 2010). The risk of bio-clogging in aquifers due to H_2 is lower compared to added dissolved carbon (Baveye et al., 1998) because the growth of autotrophic hydrogenotrophic denitrifiers is limited compared to heterotrophic denitrifiers in aquatic systems (Ergas and Reuss, 2001). Also, no by-products which would require further purification are formed during the oxidation of H_2 to water (Lee and Rittmann, 2002). The possibility of local off-grid H_2 production using wind or solar energy (Ulleberg et al., 2010; Onwe et al., 2020) provides another advantage. Drinking water sources and critical natural resources could be protected locally without building up elaborate infrastructure for a cost-effective long-term operation. Another way that allows for "clean" remediation of numerous environmental contaminants in groundwater is provided by bio-electrochemical systems which may supply bacteria directly with electrons, as discussed in the review by Cecconet et al. (2020).

Several studies have attempted to stimulate hydrogenotrophic denitrification in closed systems (Haugen et al., 2002; Chaplin et al., 2009; Kumar et al., 2018; Duffner et al., 2021), columns, bioreactors (Liessens et al., 1992; Chang et al., 1999; Haugen et al., 2002; Lee and Rittmann, 2002; Schnobrich et al., 2007) as well as *in situ* (Chaplin et al., 2009). However, transient NO_2^- accumulation and/or incomplete denitrification has been reported in most of the batch and flow-through experiments. The H_2 concentration was shown to be an influential factor determining complete denitrification because several flow-through experiments were able to reach an effluent NO_3^- concentration below 1 mg NO_3^--N/L and NO_2^- concentration below detection limit by increasing the H_2 pressure (Haugen et al., 2002; Lee and Rittmann, 2002; Schnobrich et al., 2007). Other chemo-physical parameters which influence the denitrification efficiency are pH (Li et al., 2017), carbon dioxide (CO_2) availability, NO_3^- and O_2 concentrations, as well as the water flow velocity (Ergas and Reuss, 2001; Haugen et al., 2002). The pH optimum of hydrogenotrophic denitrification is between 7.6 and 8.6 (Karanasios et al., 2010). Increased pH above 8.6 can inhibit the process (Lee and Rittmann, 2003) and generally NO_2^- accumulation increases with increasing pH (Lim et al., 2018). On the other side at pH 6.5 or lower the maturation of the nitrous oxide reductase is inhibited resulting in significant N_2O accumulation (Liu et al., 2014). H_2 injection may strip CO_2 from groundwater, altering the CO_2 availability and as a result also the pH. Thus, these parameters must be closely monitored. Additionally, the composition of the denitrifier community may determine whether denitrification is complete.

In the following sections, we will discuss the effects of H_2 application on groundwater limited by atmospheric pressure and the influence of the hydrogenotrophic denitrifier community composition on the outcome of NO_3^- remediation. These factors have been already discussed in literature as major drivers of hydrogenotrophic denitrification. We discuss their impact on NO_3^- remediation in groundwater and how they can be controlled to foster complete denitrification. Additionally, we discuss combining the H_2 amendment with the injection of Fe(II)-containing nano-sized minerals that stimulate abiotic NO_2^- reduction to N_2O and could thereby prevent NO_2^- accumulation.

FOSTERING COMPLETE DENITRIFICATION – HYDROGEN CONCENTRATION AS A MAJOR TRIGGER

The dissolved H_2 concentration in groundwater is the most important factor determining hydrogenotrophic denitrification efficiency at a neutral pH. Chang et al. (1999) observed that at a dissolved H_2 concentration below 0.1 mg L^{-1} the nitrate reductase is inhibited while the nitrite reductase is inhibited already below 0.2 mg L^{-1}. As the nitrite reductase responds

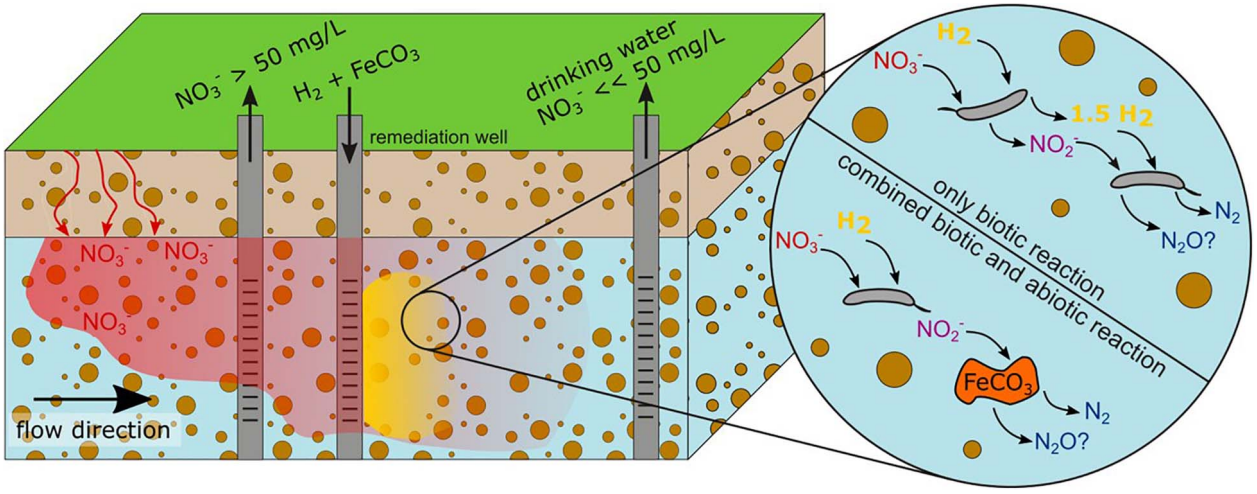

FIGURE 1 | Concept of local *in situ* NO_3^- remediation. The addition of H_2 into an aquifer through a remediation well generates an anoxic H_2-rich zone (yellow) where hydrogenotrophic denitrification is stimulated. Further downstream groundwater with NO_3^- levels below the WHO recommended maximum of 50 mg L^{-1} could be obtained. Complementation with Fe(II)-containing minerals (e.g., siderite $FeCO_3$), injected in the anoxic, H_2-rich zone, could foster complete denitrification by abiotic reduction of the intermediate NO_2^-.

even more sensitive to low dissolved H_2 concentrations than the nitrate reductase, NO_2^- accumulation in groundwater because of H_2 limitation is likely. Optimal H_2 concentrations for complete nitrogen removal are between 0.4 and 0.8 mg L^{-1} H_2 (Karanasios et al., 2011). Successful hydrogenotrophic denitrification with H_2 concentration of 1.4 mg L^{-1}, slightly below its maximum solubility of 1.6 mg L^{-1} (20°C, aqueous medium), have also been described in literature (Karanasios et al., 2010).

The dissolved H_2 concentration in closed bottles with a headspace and a water phase can be determined easily as it is homogenous and proportional to the partial pressure of the headspace gas at a constant temperature according to Henry's law. However, in settings with a continuous water flow, such as in bioreactors or in an aquifer, it is difficult to determine the dissolved H_2 concentrations. Most H_2 is consumed directly inside the biofilm that is growing on the H_2 releasing membrane and additionally local conditions change continuously due to the groundwater flow (Haugen et al., 2002; Lee and Rittmann, 2002). The required H_2 gas supply pressure to achieve locally sufficiently high dissolved hydrogen concentrations for complete denitrification also differs depending on the NO_3^- and O_2 concentrations, as well as the water flow velocity (Haugen et al., 2002; Lee and Rittmann, 2002). Increasing the H_2 gas supply pressure was the determining factor in several continuous flow reactor experiments to achieve complete NO_3^- and NO_2^- reduction (Haugen et al., 2002; Lee and Rittmann, 2002; Schnobrich et al., 2007). To the best of our knowledge, in the only *in situ* experiment on hydrogenotrophic denitrification even an increase in the H_2 lumen pressure from 1.68 atm to 2.36 atm could not resolve that only approximately half of the NO_3^- was reduced to NO_2^-, but not further to N_2O or N_2 (Chaplin et al., 2009). As the lightest molecule, the diffusion coefficient of H_2 in water is large, making it more difficult to obtain sufficiently high dissolved H_2 concentration *in situ* compared to a closed system such as a bioreactor. Its high diffusion and the bacterial biofilm formation decrease the H_2 mobility and its zone of influence needed for efficient NO_3^- removal. The denitrification activity is known to be largest in a biofilm of medium thickness and decreases when the biofilm further thickens (Chu and Wang, 2013). Thus, a large area of gas exchange accommodating as many bacteria as possible would be advantageous. A promising method to deliver gas over a large surface area are hollow-fiber membranes, e.g., made of gas-permeable silicon tubes (Ho et al., 2001).

In conclusion, it is important to determine the required local dissolved H_2 concentration at the membrane water interface under consideration of the water flow velocity, as well as dissolved O_2 and NO_3^- concentrations and the respective gas pressure needed to achieve this. Considering these difficulties of achieving sufficiently high dissolved H_2 concentrations, initial *in situ* NO_3^- remediation trials should focus on aquifers with high NO_3^- pollution and innate low O_2 concentrations so that only little H_2 is utilized to react with the remaining O_2.

FOSTERING COMPLETE DENITRIFICATION – THE ROLE OF GENOMIC AND PHENOTYPIC PLASTICITY OF DENITRIFIERS

Disparity between the genetic potential and the observed denitrification phenotypes, for example lacking N_2O reduction despite the presence of a nitrous oxide reductase gene (*nosZ*), has been observed in several denitrifiers (Lycus et al., 2017). One possible explanation thereof is, that a functioning electron transfer coupled to proton translocation during denitrification (**Figure 2A**) requires several other

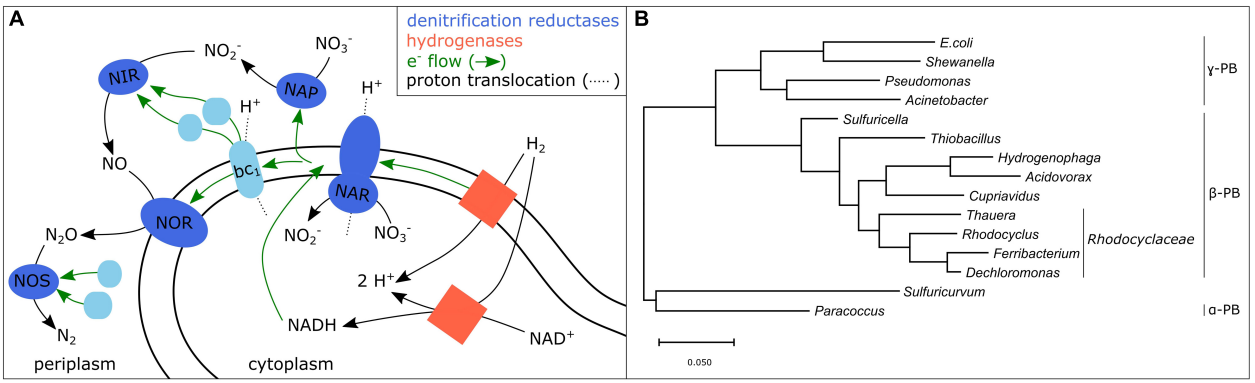

FIGURE 2 | (A) Scheme of a potential electron transport chain of hydrogenotrophic denitrifiers based on Bothe et al. (2007) and Matassa et al. (2015). Hydrogenases, membrane-bound or soluble, transfer electrons to ubiquinone (not depicted) which delivers electrons within the cell membrane to the membrane bound denitrification reductases NAR and NOR and to the cytochrome bc_1 complex. The later delivers electrons via two other redox-active proteins to the periplasmic denitrification reductases NAP, NIR, and NOS. **(B)** Phylogenetic tree of genera which include autotrophic bacteria detected in hydrogenotrophic denitrifying systems (PB, *Proteobacteria*; Karanasios et al., 2010; Kumar et al., 2018; Wu et al., 2018).

proteins besides the reductases which ultimately influence the phenotypic outcome. These proteins include electron carriers, regulatory proteins, chaperonins, as well as proteins involved in metal processing, which together manage the maturation and finely coordinated regulation of the denitrification reductases (Philippot, 2002; Bothe et al., 2007). The genes encoding these proteins are arranged in gene clusters of which only few are conserved in all or most bacterial and archaeal genomes (Philippot, 2002). The disparities may have arisen due to several evolutionary drivers including horizontal gene transfer, convergent evolution of different structural types, as well as gene duplication and loss (Jones et al., 2008). The prediction of denitrification phenotypes based on genome sequences is in many cases still impossible, likely because of the divergence of gene cluster organization and the organization of those clusters in the genome. Additionally, the denitrification reductases compete for electrons from the electron transport chain (Albina et al., 2019). Some denitrification reductases are known to be stronger competitors (e.g., *narG*) than others (e.g., *napA*) (Gao et al., 2020) and the competition may even be additionally influenced by environmental factors such as pH (Albina et al., 2019).

Recent studies on heterotrophic pure cultures of denitrifiers (Bergaust et al., 2011; Liu et al., 2013; Lycus et al., 2017; Mania et al., 2020) revealed a vast phenotypic and genotypic diversity when investigating the difference in denitrification characteristics, termed "Denitrification Regulatory Phenotypes" (DRP). The phenotypic differences were visible in the O_2 concentration at the onset of denitrification, the performed reduction steps, the electron flow rates to the individual denitrification reductases and resulting intermediate accumulation. Such differences were also observed in pure cultures of hydrogenotrophic denitrifiers (Vasiliadou et al., 2006). For example, while an *Acinetobacter* strain was accumulating 84.1% of the initial NO_3^- as NO_2^- with 1.37 mg L^{-1} dissolved H_2, strains belonging to the genera *Acidovorax* and *Paracoccus* did not show any NO_2^- accumulation (Vasiliadou et al., 2006).

Main taxa of the hydrogenotrophic denitrifier community, such as *Acidovorax*, *Paracoccus*, *Acinetobacter*, *Pseudomonas*, *Paracoccus*, *Rhodocyclus*, *Hydrogenophaga*, *Sulfuritalea*, and *Dechloromonas*, are well known from literature (Karanasios et al., 2010; Wu et al., 2018; Duffner et al., 2021) (**Figure 2B**). However, the results on DRPs show that phylogeny does not help to detect efficient hydrogenotrophic denitrifiers. Thus, the microbiological analysis must go beyond phylogeny and rather decipher the denitrification characteristics of hydrogenotrophic denitrifiers to identify intermediate accumulation and required parameters under which the former can be prevented. These required parameters include the previously stated such as minimal dissolved H_2 concentration, maximum O_2 concentration, dissolved CO_2 availability, as well as the influence of biofilm formation and flow velocity. Once this data is available on widespread and efficient hydrogenotrophic denitrifiers, simple community analyses of site-specific hydrogenotrophic enrichment cultures could help to assess whether the native bacteria are able to perform complete denitrification and which conditions these bacteria require.

Generally, environmental conditions such as electron donor/electron acceptor interaction, which is highly affected by transversal dispersion in groundwater (Rolle et al., 2009), and dissolved carbon availability (Kraft et al., 2014) shape the bacterial community composition and the dominating metabolic pathways. In phylogenetically diverse microbial communities shifts in environmental conditions can change metabolic activities, while individual taxa do not have a notable influence. This is also true for denitrifying communities which have been described for example in bulk soil, where the degree of functional redundancy is high (Regan et al., 2017). Conversely, in less diverse bacterial communities, such as hydrogenotrophic denitrifiers (Karanasios et al., 2010; Duffner et al., 2021), the genotypic and phenotypic characteristics of individual taxa influence the dominating metabolic pathway more significantly, which makes the investigation of pure

cultures even more relevant to understand hydrogenotrophic denitrification.

FOSTERING COMPLETE DENITRIFICATION – COMBINING BIOTIC DENITRIFICATION WITH IRON-BASED ABIOTIC NITRITE REDUCTION

Microbial catalyzed reduction of oxidized nitrogen species is not the only environmental process of NO_3^- remediation. Abiotic reduction of NO_2^- by iron Fe(II), termed chemo-denitrification, is also known to occur under environmentally relevant conditions (Jones et al., 2015; Buchwald et al., 2016; Grabb et al., 2017). The reduction of NO_2^- is catalyzed mainly by Fe(II) located on mineral surfaces while aqueous Fe(II) reacts much slower (Buchwald et al., 2016). Among the reactive Fe(II)-containing minerals are siderite ($FeCO_{3(s)}$) (Rakshit et al., 2008), magnetite (Fe_3O_4) (Dhakal et al., 2013; Margalef-Marti et al., 2020), pyrite (FeS_2), pyrrhotite ($Fe_{(1-x)}S$), and biotite (Margalef-Marti et al., 2020). Fe(II)-containing minerals react rapidly with NO_2^- and the reaction may be much faster than abiotic NO_3^- reduction (Dhakal et al., 2013). This preference for NO_2^- over NO_3^- reduction makes Fe(II)-containing minerals a beneficial additive to counteract the accumulation of NO_2^-. Supplementation with Fe(II)-containing minerals alongside H_2 injection thus presents a possible method to foster complete denitrification by sustaining NO_2^- and NO reduction and leaving more dissolved H_2 to microbial denitrification.

An important factor contributing to the reactivity may be the mineral size of Fe(II)-containing minerals. Nano-sized but not macro-sized magnetite lead to complete NO_3^- reduction to N_2 in an experiment by Margalef-Marti et al. (2020) due to greater surface area and Fe(II) availability. Additionally, nano-sized minerals have a wider range of distribution when injected into an aquifer. However, in order to prevent the exergonic oxidation of Fe(II) with dissolved O_2 the nano-colloids should be injected directly with the H_2 into the anaerobic plume *in situ*.

While reducing NO_2^- accumulation, the addition of Fe(II)-containing minerals may increase accumulation of the gaseous intermediates NO and N_2O, which was demonstrated by isotope measurements and the calculated isotopic offsets between NO_2^- and N_2O. These showed that much of the NO_2^- consumed was not directly accounted for as N_2O and likely accumulated as NO (Jones et al., 2015; Margalef-Marti et al., 2020). The complementation with H_2 injection to stimulate hydrogenotrophic denitrifiers is therefore necessary and the effect of Fe(II)-containing minerals on the physiological characteristics of the underlying bacteria must also be examined. In this regard, Fe(II)-containing minerals may also be used as electron donors by numerous autotrophic denitrifiers (Otero et al., 2009; Jones et al., 2015; Hernández-del Amo et al., 2018; Margalef-Marti et al., 2020). As a result the abiotic reduction of NO_2^- with Fe(II) may occur alongside microbial denitrification, the two processes are even interconnected (Melton et al., 2014) and may catalyze NO_3^- remediation. In the study of Margalef-Marti et al. (2020) magnetite nano-particles alone rapidly reduced NO_2^- to N_2O but the addition of a microbial inoculum stimulated complete reduction to N_2. Lithoautotrophic NO_3^--dependent pyrite oxidation has been detected as the predominant denitrification process in a carbon-limited aquifer (Schwientek et al., 2008; Otero et al., 2009), thus the responsible bacteria are likely widespread. Even though NO_3^--dependent Fe(II) oxidation is an energetically favorable metabolism at neutral pH, most NO_3^- reducing Fe(II)-oxidizing bacteria require an additional electron donor or organic carbon for growth (Weber et al., 2006; Melton et al., 2014). These findings indicate that apart from the abiotic reduction, introducing a second electron donor to stimulate denitrification potentially increases the bacterial diversity making the enriched denitrifying community likely more resilient (Girvan et al., 2005).

Even though the injection of nano-sized particles to contaminated sites is already applied in some countries, concerns remain, including unknown long-term effects, transformation and ecotoxicity (Crane and Scott, 2012). For example, adverse effects of nano-sized iron on the biomass and activity of soil microbial communities under stress have been determined (Anza et al., 2019). Additionally, nano-sized particles or reaction products may react rapidly with sediment leading to clogging of the reactive zone and forcing the groundwater to bypass (Strutz et al., 2016). Therefore, before such nano-sized particles can be applied *in situ*, their long-term behavior in the investigated aquifer type must be determined.

SUMMARY AND OUTLOOK

Fostering complete hydrogenotrophic denitrification *in situ* can only be achieved by combining multiple approaches. First, it is important to determine and estimate a set of aquifer parameters in a NO_3^- polluted groundwater to decide whether NO_3^- remediation by H_2 injection is feasible under the given hydrogeological conditions. These parameters include pH, organic and inorganic carbon contents, dissolved O_2 concentrations and NO_3^- concentrations, the groundwater flow velocity, potential biofilm formation, and the transversal dispersion. For example, when treating groundwater, pH shifts below 6.5 or above 8 may lead to an accumulation of NO_2^- and make the NO_3^- polluted aquifer unsuitable for bioremediation. Therefore, clean-up strategies of NO_3^- polluted aquifers may only be sustainable in groundwater with sufficient inorganic carbon which is able to buffer pH changes. Second, hydrogen-enhanced denitrification requires an effective H_2 transfer into the aquifer which must be adapted considering the previously stated parameters to ensure locally sufficiently high H_2 concentrations. Third, the denitrification phenotypes of dominant hydrogenotrophic denitrifiers must be understood

in depth. Hence the native bacterial community in the aquifer can be screened for complete hydrogenotrophic denitrifiers with little intermediate accumulation by amplicon sequencing approaches. Thus, one can determine whether the community is beneficial for complete denitrification or whether bacterial augmentation is necessary. Since these bacteria are generally low abundant in oxic groundwater, it is advised to enrich hydrogenotrophic denitrifiers under selective conditions before the screening.

Being a sequential process, it is difficult to avoid transient NO_2^- accumulation during denitrification completely, especially *in situ*. When almost all dissolved O_2 is reduced in groundwater an amendment with Fe(II)-containing minerals could thus aid the denitrifiers if periods of NO_2^- accumulation occur and could potentially diversify the denitrifying community by providing an additional electron donor. Our analysis shows that remediation strategies of NO_3^- polluted groundwater may be feasible in inorganic rich shallow groundwater systems that are characterized by low O_2 concentrations, low organic carbon concentrations, but high NO_3^- concentrations.

DATA AVAILABILITY STATEMENT

The original contributions presented in the study are included in the article/supplementary material, further inquiries can be directed to the corresponding author/s.

AUTHOR CONTRIBUTIONS

FE and MS developed the project idea and secured necessary funding to support the work of this manuscript. CD conceived and prepared the first draft of this manuscript. AW, SS, FE, and MS critically reviewed the draft. All authors contributed to the article and approved the submitted version.

FUNDING

CD received funding by Deutsche Forschungsgemeinschaft (DFG) through TUM International Graduate School of Science and Engineering (IGSSE), GSC 81.

REFERENCES

Albina, P., Durban, N., Bertron, A., Albrecht, A., Robinet, J. C., and Erable, B. (2019). Influence of hydrogen electron donor, alkaline pH, and high nitrate concentrations on microbial denitrification: a review. *Int. J. Mol. Sci*. 20:5163. doi: 10.3390/ijms20205163

Anza, M., Salazar, O., Epelde, L., Alkorta, I., and Garbisu, C. (2019). The application of nanoscale zero-valent iron promotes soil remediation while negatively affecting soil microbial biomass and activity. *Front. Environ. Sci*. 7:19. doi: 10.3389/fenvs.2019.00019

Baveye, P., Vandevivere, P., Hoyle, B. L., DeLeo, P. C., and de Lozada, D. S. (1998). Environmental impact and mechanisms of the biological clogging of saturated soils and aquifer materials. *Crit. Rev .Environ. Sci. Technol*. 28, 123–191. doi: 10.1080/10643389891254197

Bergaust, L., Bakken, L. R., and Frostegård, Å (2011). Denitrification regulatory phenotype, a new term for the characterization of denitrifying bacteria. *Biochem. Soc. Trans*. 39, 207–212. doi: 10.1042/bst0390207

Bothe, H., Ferguson, S., and Newton, W. (2007). *Biology of the Nitrogen Cycle*. Amsterdam: Elsevier Science.

Buchwald, C., Grabb, K., Hansel, C. M., and Wankel, S. D. (2016). Constraining the role of iron in environmental nitrogen transformations: dual stable isotope systematics of abiotic NO2– reduction by Fe(II) and its production of N2O. *Geochim. Cosmochim. Acta* 186, 1–12. doi: 10.1016/j.gca.2016.04.041

Cecconet, D., Sabba, F., Devecseri, M., Callegari, A., and Capodaglio, A. G. (2020). In situ groundwater remediation with bioelectrochemical systems: a critical review and future perspectives. *Environ. Int*. 137:105550. doi: 10.1016/j.envint.2020.105550

Chang, C. C., Tseng, S. K., and Huang, H. K. (1999). Hydrogenotrophic denitrification with immobilized *Alcaligenes eutrophus* for drinking water treatment. *Bioresour. Technol*. 69, 53–58. doi: 10.1016/s0960-8524(98)00168-0

Chaplin, B. P., Schnobrich, M. R., Widdowson, M., Semmens, M. J., and Novak, P. J. (2009). Stimulating in situ hydrogenotrophic denitrification with membrane-delivered hydrogen under passive and pumped groundwater conditions. *J. Environ. Eng*. 135, 666–676. doi: 10.1061/(asce)ee.1943-7870.0000021

Chu, L., and Wang, J. (2013). Denitrification performance and biofilm characteristics using biodegradable polymers PCL as carriers and carbon source. *Chemosphere* 91, 1310–1316. doi: 10.1016/j.chemosphere.2013.02.064

Crane, R. A., and Scott, T. B. (2012). Nanoscale zero-valent iron: future prospects for an emerging water treatment technology. *J. Hazard. Mater*. 21, 112–125. doi: 10.1016/j.jhazmat.2011.11.073

Dhakal, P., Matocha, C. J., Huggins, F. E., and Vandiviere, M. M. (2013). Nitrite reactivity with magnetite. *Environ. Sci. Technol*. 47, 6206–6213. doi: 10.1021/es304011w

Duffner, C., Holzapfel, S., Wunderlich, A., Einsiedl, F., Schloter, M., and Schulz, S. (2021). *Dechloromonas* and close relatives prevail hydrogenotrophic denitrification in stimulated microcosms with oxic aquifer material. *FEMS Microbiol. Ecol*. Epub ahead of print

Ergas, S. J., and Reuss, A. F. (2001). Hydrogenotrophic denitrification of drinking water using a hollow fibre membrane bioreactor. *J. Water Supply Res. Technol. Aqua* 50, 161–171. doi: 10.2166/aqua.2001.0015

Fields, S. (2004). Global nitrogen: cycling out of control. *Environ. Health Perspect*. 112, 556–563.

Galloway, J. N., Townsend, A. R., Erisman, J. W., Bekunda, M., Cai, Z., Freney, J. R., et al. (2008). Transformation of the nitrogen cycle: recent trends, questions, and potential solutions. *Science* 320, 889–892. doi: 10.1126/science.1136674

Gao, Y., Mania, D., Mousavi, S., Lycus, P., Arntzen, M., Woliy, K., et al. (2020). Competition for electrons favors N2O reduction in denitrifying *Bradyrhizobium* isolates. *bioRxiv [Preprint]*

Girvan, M. S., Campbell, C. D., Killham, K., Prosser, J. I., and Glover, L. A. (2005). Bacterial diversity promotes community stability and functional resilience after perturbation. *Environ. Microbiol*. 7, 301–313. doi: 10.1111/j.1462-2920.2005.00695.x

Grabb, K. C., Buchwald, C., Hansel, C. M., and Wankel, S. D. (2017). A dual nitrite isotopic investigation of chemodenitrification by mineral-associated Fe(II) and its production of nitrous oxide. *Geochim. Cosmochim. Acta* 196, 388–402. doi: 10.1016/j.gca.2016.10.026

Haugen, K. S., Semmens, M. J., and Novak, P. J. (2002). A novel in situ technology for the treatment of nitrate contaminated groundwater. *Water Res*. 36, 3497–3506. doi: 10.1016/s0043-1354(02)00043-x

Hernández-del Amo, E., Menció, A., Gich, F., Mas-Pla, J., and Bañeras, L. (2018). Isotope and microbiome data provide complementary information to identify natural nitrate attenuation processes in groundwater. *Sci. Total Environ*. 61, 579–591. doi: 10.1016/j.scitotenv.2017.09.018

Ho, C. M., Tseng, S. K., and Chang, Y. J. (2001). Autotrophic denitrification via a novel membrane-attached biofilm reactor. *Lett. Appl. Microbiol*. 33, 201–205. doi: 10.1046/j.1472-765x.2001.00984.x

Ji, B., Yang, K., Zhu, L., Jiang, Y., Wang, H., Zhou, J., et al. (2015). Aerobic denitrification: a review of important advances of the last 30 years. *Biotechnol. Bioprocess Eng.* 20, 643–651. doi: 10.1007/s12257-015-0009-0

Jones, C. M., Stres, B., Rosenquist, M., and Hallin, S. (2008). Phylogenetic analysis of nitrite, nitric oxide, and nitrous oxide respiratory enzymes reveal a complex evolutionary history for denitrification. *Mol. Biol. Evol.* 25, 1955–1966. doi: 10.1093/molbev/msn146

Jones, L. C., Peters, B., Lezama Pacheco, J. S., Casciotti, K. L., and Fendorf, S. (2015). Stable isotopes and iron oxide mineral products as markers of chemodenitrification. *Environ. Sci. Technol.* 49, 3444–3452. doi: 10.1021/es504862x

Karanasios, K. A., Michailides, M. K., Vasiliadou, I. A., Pavlou, S., and Vayenas, D. V. (2011). Potable water hydrogenotrophic denitrification in packed-bed bioreactors coupled with a solar-electrolysis hydrogen production system. *Desalination Water Treat.* 33, 86–96. doi: 10.5004/dwt.2011.2614

Karanasios, K. A., Vasiliadou, I. A., Pavlou, S., and Vayenas, D. V. (2010). Hydrogenotrophic denitrification of potable water: a review. *J. Hazard. Mater.* 180, 20–37. doi: 10.1016/j.jhazmat.2010.04.090

Korom, S. F. (1992). Natural denitrification in the saturated zone: a review. *Water Resour. Res.* 28, 1657–1668. doi: 10.1029/92wr00252

Kraft, B., Tegetmeyer, H. E., Sharma, R., Klotz, M. G., Ferdelman, T. G., Hettich, R. L., et al. (2014). The environmental controls that govern the end product of bacterial nitrate respiration. *Science* 345, 676–679. doi: 10.1126/science.1254070

Kumar, S., Herrmann, M., Blohm, A., Hilke, I., Frosch, T., Trumbore, S. E., et al. (2018). Thiosulfate- and hydrogen-driven autotrophic denitrification by a microbial consortium enriched from groundwater of an oligotrophic limestone aquifer. *FEMS Microbiol. Ecol.* 94:fiy141.

Lee, K. C., and Rittmann, B. E. (2002). Applying a novel autohydrogenotrophic hollow-fiber membrane biofilm reactor for denitrification of drinking water. *Water Res.* 36, 2040–2052. doi: 10.1016/s0043-1354(01)00425-0

Lee, K. C., and Rittmann, B. E. (2003). Effects of pH and precipitation on autohydrogenotrophic denitrification using the hollow-fiber membrane-biofilm reactor. *Water Res.* 37, 1551–1556. doi: 10.1016/s0043-1354(02)00519-5

Li, P., Wang, Y., Zuo, J., Wang, R., Zhao, J., and Du, Y. (2017). Nitrogen removal and N2O accumulation during hydrogenotrophic denitrification: influence of environmental factors and microbial community characteristics. *Environ. Sci. Technol.* 51, 870–879. doi: 10.1021/acs.est.6b00071

Liessens, J., Vanbrabant, J., De Vos, P., Kersters, K., and Verstraete, W. (1992). Mixed culture hydrogenotrophic nitrate reduction in drinking water. *Micro. Ecol.* 24, 271–290. doi: 10.1007/bf00167786

Lim, N. Y. N., Frostegård, Å, and Bakken, L. R. (2018). Nitrite kinetics during anoxia: the role of abiotic reactions versus microbial reduction. *Soil Biol. Biochem.* 119, 203–209. doi: 10.1016/j.soilbio.2018.01.006

Liu, B., Frostegård, Å, and Bakken, L. R. (2014). Impaired reduction of N2O to N2 in acid soils is due to a posttranscriptional interference with the expression of nosZ. *mBio* 5, e01383–14.

Liu, B., Mao, Y., Bergaust, L., Bakken, L. R., and Frostegård, Å (2013). Strains in the genus *Thauera* exhibit remarkably different denitrification regulatory phenotypes. *Environ. Microbiol.* 15, 2816–2828.

Lycus, P., Lovise Bøthun, K., Bergaust, L., Peele Shapleigh, J., Reier Bakken, L., and Frostegård, Å (2017). Phenotypic and genotypic richness of denitrifiers revealed by a novel isolation strategy. *ISME J.* 11, 2219–2232. doi: 10.1038/ismej.2017.82

Mania, D., Woliy, K., Degefu, T., and Frostegård, Å (2020). A common mechanism for efficient N2O reduction in diverse isolates of nodule-forming bradyrhizobia. *Environ. Microbiol.* 22, 17–31.

Margalef-Marti, R., Carrey, R., Benito, J. A., Marti, V., Soler, A., and Otero, N. (2020). Nitrate and nitrite reduction by ferrous iron minerals in polluted groundwater: isotopic characterization of batch experiments. *Chem. Geol.* 548:119691. doi: 10.1016/j.chemgeo.2020.119691

Matassa, S., Boon, N., and Verstraete, W. (2015). Resource recovery from used water: The manufacturing abilities of hydrogen-oxidizing bacteria. *Water Res.* 68, 467–478. doi: 10.1016/j.watres.2014.10.028

Melton, E. D., Swanner, E. D., Behrens, S., Schmidt, C., and Kappler, A. (2014). The interplay of microbially mediated and abiotic reactions in the biogeochemical Fe cycle. *Nat. Rev. Microbiol.* 12, 797–808. doi: 10.1038/nrmicro3347

Murray, C. J., Müller-Karulis, B., Carstensen, J., Conley, D. J., Gustafsson, B. G., and Andersen, J. H. (2019). Past, present and future eutrophication status of the Baltic Sea. *Front. Mar. Sci.* 6:2. doi: 10.3389/fmars.2019.00002

Onwe, C. A., Rodley, D., and Reynolds, S. (2020). Modelling and simulation tool for off-grid PV-hydrogen energy system. *Int. J. Sustain. Energy* 39, 1–20. doi: 10.1080/14786451.2019.1617711

Otero, N., Torrentó, C., Soler, A., Menció, A., and Mas-Pla, J. (2009). Monitoring groundwater nitrate attenuation in a regional system coupling hydrogeology with multi-isotopic methods: the case of Plana de Vic. (Osona, Spain). *Agric. Ecosyst. Environ.* 133, 103–113. doi: 10.1016/j.agee.2009.05.007

Philippot, L. (2002). Denitrifying genes in bacterial and archaeal genomes. *Biochim. Biophys. Acta* 1577, 355–376. doi: 10.1016/s0167-4781(02)00420-7

Rakshit, S., Matocha, C. J., and Coyne, M. S. (2008). Nitrite reduction by siderite. *Soil Sci. Soc. Am. J.* 72, 1070–1077. doi: 10.2136/sssaj2007.0296

Regan, K., Stempfhuber, B., Schloter, M., Rasche, F., Prati, D., Philippot, L., et al. (2017). Spatial and temporal dynamics of nitrogen fixing, nitrifying and denitrifying microbes in an unfertilized grassland soil. *Soil. Biol. Biochem.* 109, 214–226. doi: 10.1016/j.soilbio.2016.11.011

Rivett, M. O., Buss, S. R., Morgan, P., Smith, J. W. N., and Bemment, C. D. (2008). Nitrate attenuation in groundwater: a review of biogeochemical controlling processes. *Water Res.* 42, 4215–4232. doi: 10.1016/j.watres.2008.07.020

Rolle, M., Eberhardt, C., Chiogna, G., Cirpka, O. A., and Grathwohl, P. (2009). Enhancement of dilution and transverse reactive mixing in porous media: experiments and model-based interpretation. *J. Contam. Hydrol.* 110, 130–142. doi: 10.1016/j.jconhyd.2009.10.003

Schnobrich, M. R., Chaplin, B. P., Semmens, M. J., and Novak, P. J. (2007). Stimulating hydrogenotrophic denitrification in simulated groundwater containing high dissolved oxygen and nitrate concentrations. *Water Res.* 41, 1869–1876. doi: 10.1016/j.watres.2007.01.044

Schwientek, M., Einsiedl, F., Stichler, W., Stögbauer, A., Strauss, H., and Maloszewski, P. (2008). Evidence for denitrification regulated by pyrite oxidation in a heterogeneous porous groundwater system. *Chem. Geol.* 255, 60–67. doi: 10.1016/j.chemgeo.2008.06.005

Strutz, T. J., Hornbruch, G., Dahmke, A., and Köber, R. (2016). Influence of permeability on nanoscale zero-valent iron particle transport in saturated homogeneous and heterogeneous porous media. *Environ. Sci. Pollut. Res.* 23, 17200–17209. doi: 10.1007/s11356-016-6814-y

Ulleberg, Ø, Nakken, T., and Eté, A. (2010). The wind/hydrogen demonstration system at Utsira in Norway: evaluation of system performance using operational data and updated hydrogen energy system modeling tools. *Int. J. Hydrogen Energy* 35, 1841–1852. doi: 10.1016/j.ijhydene.2009.10.077

Vasiliadou, I. A., Siozios, S., Papadas, I. T., Bourtzis, K., Pavlou, S., and Vayenas, D. V. (2006). Kinetics of pure cultures of hydrogen-oxidizing denitrifying bacteria and modeling of the interactions among them in mixed cultures. *Biotechnol. Bioeng.* 95, 513–525. doi: 10.1002/bit.21031

Wassenaar, L. I. (1995). Evaluation of the origin and fate of nitrate in the abbotsford aquifer using the isotopes of15N and18O in NO3–. *Appl. Geochem.* 10, 391–405. doi: 10.1016/0883-2927(95)00013-a

Weber, K. A., Achenbach, L. A., and Coates, J. D. (2006). Microorganisms pumping iron: anaerobic microbial iron oxidation and reduction. *Nat. Rev. Microbiol.* 4, 752–764. doi: 10.1038/nrmicro1490

Wild, L., Mayer, B., and Einsiedl, F. (2018). Decadal delays in groundwater recovery from nitrate contamination caused by low O2 reduction rates. *Water Resour. Res.* 54, 9996–10012. doi: 10.1029/2018wr023396

Wild, L. M., Rein, A., and Einsiedl, F. (2020). Monte Carlo simulations as a decision support to interpret δ15N values of nitrate in groundwater. *Groundwater* 58, 571–582. doi: 10.1111/gwat.12936

Wu, J., Yin, Y., and Wang, J. (2018). Hydrogen-based membrane biofilm reactors for nitrate removal from water and wastewater. *Int. J. Hydrogen Energy* 43, 1–15. doi: 10.1016/j.ijhydene.2017.10.178

Zhang, H., Zong, R., He, H., Liu, K., Yan, M., Miao, Y., et al. (2021). Biogeographic distribution patterns of algal community in different urban lakes in China: insights into the dynamics and co-existence. *J. Environ. Sci*. 100, 216–227. doi: 10.1016/j.jes.2020.07.024

Zhu, A., Chen, J., Gao, L., Shimizu, Y., Liang, D., Yi, M., et al. (2019). Combined microbial and isotopic signature approach to identify nitrate sources and transformation processes in groundwater. *Chemosphere* 228, 721–734. doi: 10.1016/j.chemosphere.2019.04.163

Zumft, W. G. (1997). Cell biology and molecular basis of denitrification. *Microbiol. Mol. Biol. Rev*. 61, 533–616. doi: 10.1128/.61.4.533-616.1997

Conflict of Interest: The authors declare that the research was conducted in the absence of any commercial or financial relationships that could be construed as a potential conflict of interest.